THE ROLE OF PROTEIN POST-TRANSLATIONAL MODIFICATIONS IN PROTEIN-RNA INTERACTIONS AND RNP ASSEMBLIES

EDITED BY: Roberto Giambruno, Dorothee Dormann, Nicolas Lux Fawzi and Ewa Anna Grzybowska

PUBLISHED IN: Frontiers in Molecular Biosciences

frontiers Research Topics

frontiers

ISSN 1664-8714
ISBN 978-2-88974-369-8
DOI 10.3389/978-2-88974-369-8

About Frontiers

Frontiers is more than just an open-access publisher of scholarly articles: it is a pioneering approach to the world of academia, radically improving the way scholarly research is managed. The grand vision of Frontiers is a world where all people have an equal opportunity to seek, share and generate knowledge. Frontiers provides immediate and permanent online open access to all its publications, but this alone is not enough to realize our grand goals.

Frontiers Journal Series

The Frontiers Journal Series is a multi-tier and interdisciplinary set of open-access, online journals, promising a paradigm shift from the current review, selection and dissemination processes in academic publishing. All Frontiers journals are driven by researchers for researchers; therefore, they constitute a service to the scholarly community. At the same time, the Frontiers Journal Series operates on a revolutionary invention, the tiered publishing system, initially addressing specific communities of scholars, and gradually climbing up to broader public understanding, thus serving the interests of the lay society, too.

Dedication to Quality

Each Frontiers article is a landmark of the highest quality, thanks to genuinely collaborative interactions between authors and review editors, who include some of the world's best academicians. Research must be certified by peers before entering a stream of knowledge that may eventually reach the public - and shape society; therefore, Frontiers only applies the most rigorous and unbiased reviews.
Frontiers revolutionizes research publishing by freely delivering the most outstanding research, evaluated with no bias from both the academic and social point of view. By applying the most advanced information technologies, Frontiers is catapulting scholarly publishing into a new generation.

What are Frontiers Research Topics?

Frontiers Research Topics are very popular trademarks of the Frontiers Journals Series: they are collections of at least ten articles, all centered on a particular subject. With their unique mix of varied contributions from Original Research to Review Articles, Frontiers Research Topics unify the most influential researchers, the latest key findings and historical advances in a hot research area! Find out more on how to host your own Frontiers Research Topic or contribute to one as an author by contacting the Frontiers Editorial Office: frontiersin.org/about/contact

THE ROLE OF PROTEIN POST-TRANSLATIONAL MODIFICATIONS IN PROTEIN-RNA INTERACTIONS AND RNP ASSEMBLIES

Topic Editors:
Roberto Giambruno, Center for Genomic Science, Italian Institute of Technology (IIT), Italy
Dorothee Dormann, Johannes Gutenberg University Mainz, Germany
Nicolas Lux Fawzi, Brown University, United States
Ewa Anna Grzybowska, Maria Sklodowska-Curie National Research Institute of Oncology, Poland

Dr. Nicolas Lux Fawzi is a member of the Scientific Advisory Board of Dewpoint Therapeutics LLC. All other Topic Editors declare no competing interests with regards to the Research Topic.

Citation: Giambruno, R., Dormann, D., Fawzi, N. L., Grzybowska, E. A., eds. (2022). The Role of Protein Post-Translational Modifications in Protein-RNA Interactions and RNP Assemblies. Lausanne: Frontiers Media SA. doi: 10.3389/978-2-88974-369-8

Table of Contents

frontiers in Molecular Biosciences

EDITORIAL
published: 04 January 2022
doi: 10.3389/fmolb.2021.831810

Editorial: The Role of Protein Post-Translational Modifications in Protein-RNA Interactions and RNP Assemblies

Roberto Giambruno[1]*, *Ewa A. Grzybowska*[2], *Nicolas L. Fawzi*[3] and *Dorothee Dormann*[4,5]

[1]Center for Genomic Science, Italian Institute of Technology (IIT), Milano, Italy, [2]Maria Sklodowska-Curie National Research Institute of Oncology, Warsaw, Poland, [3]Brown University, Providence, RI, United States, [4]Biocenter, Johannes Gutenberg University Mainz, Mainz, Germany, [5]Institute of Molecular Biology (IMB), Mainz, Germany

Keywords: PTMs (post-translational modifications), RNA-protein interactions, RNP granules, phase separation, intrinsically disordered region (IDR)

Editorial on the Research Topic

The Role of Protein Post-Translational Modifications in Protein-RNA Interactions and RNP Assemblies

RNA binding proteins (RBPs) are crucial regulators that participate in almost every cellular function by contributing to key biological processes such as transcription, translation, RNA splicing and RNA transport (Gerstberger et al., 2014). Posttranslational modifications (PTMs) control different aspects of RBPs, in particular their cellular localization; their stability and turnover; the ability of RBPs to bind to RNA and other proteins; and the propensity of RBPs to undergo liquid-liquid phase separation (LLPS). The most well characterized PTMs of RBPs are phosphorylation, methylation, acetylation, sumoylation and ubiquitinylation. The first four of these PTMs have been mainly linked to the regulation of RBPs cellular distribution and interactions, while ubiquitinylation is mainly involved in protein degradation and turnover (Sternburg et al., 2022). Recently, all of these PTMs have been described to regulate the LLPS behavior of RBPs and the consequent formation of membraneless-organelles (MLOs), such as stress granules (SGs) or other ribonucleoprotein (RNP) granules (Wiedner and Giudice, 2021).

The goal of our research topic is to highlight how PTMs regulate RNA-protein interactions, protein-protein interactions, LLPS of RBPs, and RNP granule formation and dynamics, as well as how altered PTM patterns on RBPs can be linked to human diseases.

The review by Velázquez-Cruz et al. summarizes the impact that PTMs have on several mammalian RBPs and how an aberrant PTM profile causes an alteration of physiological processes leading to diseases, such as cancer and neurodegenerative disorders. In particular, alterations of the PTM profile or mutations in post-translationally modified amino acids in RBPs like trans-activating response element DNA-binding protein of 43 kDa (TDP-43), fused in sarcoma (FUS) and heterogeneous nuclear ribonucleoprotein A and B type (hnRNP-A/B) are linked to neurodegenerative disorders, such as amyotrophic lateral sclerosis (ALS), as summarized by Farina et al. This aspect has also been covered in a review by Clarke et al. of biochemical and functional characterization of heterogeneous nuclear ribonucleoprotein A1 (hnRNPA1), belonging to the hnRNP-A/B subfamily, in both physiological conditions and neurodegenerative diseases; and how PTMs modulate hnRNPA1 molecular functions.

Among the numerous PTMs reported so far, arginine methylation, phosphorylation and sumoylation seem to play major roles in the regulation of RBP activities and in particular on their RNA-binding properties. This last aspect is extremely relevant but at the same time challenging

Edited and reviewed by:
André P. Gerber,
University of Surrey, United Kingdom

****Correspondence:***
Roberto Giambruno
giambrun84@gmail.com
roberto.giambruno@iit.it

Specialty section:
This article was submitted to RNA Networks and Biology, a section of the journal Frontiers in Molecular Biosciences

Received: *08 December 2021*
Accepted: *14 December 2021*
Published: *04 January 2022*

Citation:
Giambruno R, Grzybowska EA, Fawzi NL and Dormann D (2022) Editorial: The Role of Protein Post-Translational Modifications in Protein-RNA Interactions and RNP Assemblies. Front. Mol. Biosci. 8:831810. doi: 10.3389/fmolb.2021.831810

because the current quantitative affinity purification processes, both protein- and RNA-centric strategies, are biased in the assessment of the interactions of a specific RBP and its respective targets, as reviewed by Vieira-Vieira and Selbach. To overcome this challenge, Maniaci et al., used an alternative quantitative proteomic approach that is based on orthogonal organic phase separation (OOPS) (Queiroz et al., 2019) to profile global effects on RNA-protein interaction dynamics exerted by the modulation of protein arginine methyltransferase (PRMT) activity, revealing differences caused by an altered arginine methylation pattern of RBPs. The role of PRMTs in RBP binding activities has also been reported in pathogenic kinetoplastids, as summarized by Campagnaro et al. The authors suggest that the activity of PRMTs can be pharmacologically inhibited paving the way to repurposing these drugs and the development of novel anti-parasite strategies.

Arginine methylation is also a key regulator of phase transition and RNP granules dynamics (Hofweber and Dormann, 2019). *In vitro* studies have demonstrated that arginine methylation often reduces RBP phase separation; however, in the germ line arginine methylation promotes the formation of RNP condensates, as reviewed by Schisa and Elaswad. Thus, there might be a discrepancy between *in vitro* and *in vivo* results that can be explained by the presence of additional factors or other PTMs (and hence a PTM crosstalk) in eukaryotic cells. Indeed, phosphorylation and arginine methylation can be juxtaposed on the same RBP and can have a synergistic or antagonistic effect in the regulation of RBP phase separation. Along these lines, Lenard et al. discovered that the serine-arginine protein kinase 1 (SRPK1) phosphorylates the cold-inducible RNA-binding protein (CIRBP) in the RG/RGG regions, thus impairing arginine methylation of RGG/RG motifs and suppressing CIRBP LLPS. At the same time, arginine methylation of CIRBP RG/RGG regions precludes any phosphorylation event by SRPK1. Hence, LLPS of CIRBP is co-regulated by both phosphorylation and methylation of the same CIRBP region.

Similarly, sumoylation is known to regulate LLPS of RBPs and in particular the formation of different MLOs, including P-bodies, nucleoli and stress granules, as reviewed by Keiten-Schmitz et al. In addition, the SUMO pathway has a crucial role in the disassembly of stress granules through the activation of the SUMO-targeted ubiquitin ligase (StUbl) pathway. As summarized by the authors, the StUbl pathway contrasts the formation of aberrant stress granules observed in neurodegenerative disorders, such as ALS, opening new perspectives for the understanding and cure of these diseases.

Overall, the articles collected in this Research Topic highlight the impact that PTMs have on RBP interactions and functions. In addition, they shed light on the crosstalk between different PTMs that finely regulate the generation and disassembly of RBP condensates. These aspects can be relevant for the future development of therapeutic strategies aimed at regulating aberrant LLPS of RBPs that are strongly linked to neurodegenerative disorders.

AUTHOR CONTRIBUTIONS

All authors listed have made a substantial, direct, and intellectual contribution to the work and approved it for publication.

REFERENCES

Gerstberger, S., Hafner, M., and Tuschl, T. (2014). A Census of Human RNA-Binding Proteins. *Nat. Rev. Genet.* 15, 829–845. doi:10.1038/nrg3813

Hofweber, M., and Dormann, D. (2019). Friend or Foe-Post-Translational Modifications as Regulators of Phase Separation and RNP Granule Dynamics. *J. Biol. Chem.* 294, 7137–7150. doi:10.1074/jbc.tm118.001189

Queiroz, R. M. L., Smith, T., Villanueva, E., Marti-Solano, M., Monti, M., Pizzinga, M., et al. (2019). Comprehensive Identification of RNA-Protein Interactions in Any Organism Using Orthogonal Organic Phase Separation (OOPS). *Nat. Biotechnol.* 37, 169–178. doi:10.1038/s41587-018-0001-2

Sternburg, E. L., Gruijs da Silva, L. A., and Dormann, D. (2022). Post-Translational Modifications on RNA-Binding Proteins: Accelerators, Brakes, or Passengers in Neurodegeneration? *Trends Biochem. Sci.* 47 (1), 6–22. doi:10.1016/j.tibs.2021.07.004

Wiedner, H. J., and Giudice, J. (2021). It's Not Just a Phase: Function and Characteristics of RNA-Binding Proteins in Phase Separation. *Nat. Struct. Mol. Biol.* 28, 465–473. doi:10.1038/s41594-021-00601-w

Conflict of Interest: NLF is a member of the Scientific Advisory Board of Dewpoint Therapeutics LLC.

The remaining authors declare that the research was conducted in the absence of any commercial or financial relationships that could be construed as a potential conflict of interest.

frontiers in Molecular Biosciences

MINI REVIEW
published: 08 April 2021
doi: 10.3389/fmolb.2021.658020

An Emerging Role for Post-translational Modifications in Regulating RNP Condensates in the Germ Line

Jennifer A. Schisa and Mohamed T. Elaswad*

Department of Biology, Central Michigan University, Mount Pleasant, MI, United States

RNA-binding proteins undergo regulated phase transitions in an array of cell types. The phase separation of RNA-binding proteins, and subsequent formation of RNP condensates or granules, occurs during physiological conditions and can also be induced by stress. Some RNP granules have roles in post-transcriptionally regulating mRNAs, and mutations that prevent the condensation of RNA-binding proteins can reduce an organism's fitness. The reversible and multivalent interactions among RNP granule components can result in RNP complexes that transition among diffuse and condensed states, the latter of which can be pathological; for example, in neurons solid RNP aggregates contribute to disease states such as amyotrophic lateral sclerosis (ALS), and the dysregulation of RNP granules in human germ cells may be involved in Fragile X-associated primary ovarian insufficiency. Thus, regulating the assembly of mRNAs and RNA-binding proteins into discrete granules appears to provide important functions at both cellular and physiological levels. Here we review our current understanding of the role of post-translational modifications (PTMs) in regulating the condensation of RNA-binding proteins in the germ line. We compare and contrast the *in vitro* evidence that methylation inhibits phase separation of RNA binding proteins, with the extent to which these results apply to the *in vivo* germ line environment of several model systems. We also focus on the role of phosphorylation in modulating the dynamics of RNP granules in the germ line. Finally, we consider the gaps that exist in our understanding of the role of PTMs in regulating germ line RNP granules.

Keywords: RNP granules, phase transition, germ line, methylation, phosphorylation, condensate

OPEN ACCESS

Edited by:
Nicolas Lux Fawzi,
Brown University, United States

Reviewed by:
Dustin Updike,
Mount Desert Island Biological Laboratory, United States
Florence Besse,
INSERM U1091 Institut de biologie de Valrose, France
Richard Freiman,
Brown University, United States

****Correspondence:***
Jennifer A. Schisa
schis1j@cmich.edu

Specialty section:
This article was submitted to Protein and RNA Networks, a section of the journal Frontiers in Molecular Biosciences

Received: *24 January 2021*
Accepted: *19 March 2021*
Published: *08 April 2021*

Citation:
Schisa JA and Elaswad MT (2021) An Emerging Role for Post-translational Modifications in Regulating RNP Condensates in the Germ Line. Front. Mol. Biosci. 8:658020. doi: 10.3389/fmolb.2021.658020

INTRODUCTION

Phase separation is an important principle of cellular organization. Many types of membraneless organelles (MLOs) assemble through the process of liquid-liquid phase separation. Some of the best studied MLOs in the cytoplasm are ribonucleoprotein (RNP) granules composed of RNA and RNA binding proteins, such as stress granules and processing bodies. Much of our understanding of phase separation to date has come from *in vitro* studies. From such studies, we now understand that phase separation is driven mainly by weak interactions between multivalent protein interaction domains or intrinsically disordered low complexity domains (LCDs)

(Kato et al., 2012; Li et al., 2012). Since multivalent interaction motifs and the short linear motifs in intrinsically disordered regions and LCDs are often post-translationally modified (Xie et al., 2007; Bah and Forman-Kay, 2016; Chong and Forman-Kay, 2016), in hindsight it is not surprising that post-translational modifications (PTMs) have been revealed as important regulators of phase separation (Itakura et al., 2018; Rhoads et al., 2018). While a diverse array of PTMs can modulate condensates, in this review we focus on the best-studied paradigms: methylation and phosphorylation.

PTMs can alter the chemical properties of amino acids, such as the steric properties, bulkiness, or charge state. For example, when Arginine (Arg) is methylated, bulkiness is increased, and the distribution of charge and hydrophobicity is altered which affects intermolecular interactions and phase separation. Phosphorylation of Tyr or Ser introduces a negative charge which can either promote or inhibit phase separation (Monahan et al., 2017; Wang et al., 2018); thus, PTMs can weaken or enhance multivalent interactions between phase-separated macromolecules. PTMs can also recruit protein into, or exclude protein from, the condensate (Hofweber and Dormann, 2019). Thus, PTMs can modulate the assembly and disassembly of liquid-like RNP granules, and transitions from the liquid state to gel- or solid-like states.

Condensation of RNA binding proteins and RNA in the germ line of many organisms results in germ granules (Voronina et al., 2011). A variety of terms are used to describe the array of germ granules found across different species which can be confusing but are described in several resources (**Table 1** and Schisa, 2012). While some germ granule proteins exhibit liquid-like properties, such as the PGL-1 granules in *C. elegans* embryos (Brangwynne et al., 2009), other types of germ granules such as the Balbiani body in *Xenopus* oocytes have solid-like properties (Boke et al., 2016; Woodruff et al., 2018). Careful examination has revealed multiple phases within germ granules; for example, the germ granules of early *C. elegans* embryos include a liquid-like phase of PGL proteins, and a gel phase of MEG-3 protein that appears to have a scaffolding role in the assembly of germ granules (Putnam et al., 2019). An increasing number of examples of PTMs modulating the assembly of germ granules have been documented over the past two decades. Building upon our understanding from *in vitro* studies, these *in vivo* experiments are revealing both conserved and complex roles of PTMs in regulating condensates of RNA binding proteins in the germ line that are associated with critical germ line functions. This review will focus on our understanding of how methylation and phosphorylation regulate germ line RNP condensates across invertebrate and vertebrate model systems.

ROLE OF METHYLATION

Methylation Inhibits Condensate Assembly in *in vitro* Studies

Methylation is a key regulator of phase transitions and RNP granule dynamics. Within many RNP granules are proteins with RGG or RG-rich motifs, and the Arginine residues in these motifs are often methylated by protein arginine methyltransferase (PRMT) enzymes (Bedford and Clarke, 2009). In general, Arg-methylation is considered a less dynamic modification, in how it impacts target proteins, than others such as phosphorylation and acetylation (Fackelmayer, 2005). In *in vitro* studies methylation of Arg weakens intermolecular interactions and thus inhibits phase separation of RNA binding proteins. For example, droplets of the N-terminal RGG-rich domain of the conserved nuage protein Ddx4/Vasa are destabilized by Arg-methylation (Nott et al., 2015). Methylation of recombinant or purified FUS protein, the protein that phase separates into granules in amyotrophic lateral sclerosis (ALS) mutations, similarly reduces liquid-liquid de-mixing (Qamar et al., 2018; Hofweber and Dormann, 2019). Since no examples have shown Arg-methylation to promote condensation *in vitro*, it has been suggested that this PTM is a general inhibitor of Arg-aromatic (π) interactions that reduces phase separations (Hofweber and Dormann, 2019). However, *ex vivo* studies reveal a more complex effect of methylation on phase separation (**Figure 1A**). Some experiments align with *in vitro* results showing Arg-methylation suppresses RNP granule formation. Treatments of cultured U2OS cells that increase the methylation of Ras-GAP SH3-binding protein (G3BP1) repress the assembly of stress granules (Tsai et al., 2016). However, there is also evidence for Arg-methylation promoting RNP granule assembly. When methylation of the Lsm4 protein, RAP55A, is decreased, the localization of RAP55A to P bodies is inhibited in cell culture (Matsumoto et al., 2012), and similarly, recruitment of unmethylated CIRP to stress granules is blocked (De Leeuw et al., 2007). Overall, many *in vitro* and *ex vivo* examples highlight a role for Arg-methylation in controlling the dynamics of RNP granules; however, these results do not address the extent to which this regulation occurs *in vivo* or in the germ line. To date, studies in three model systems all demonstrate a role for Arg-methylation in promoting phase separation of RNA binding proteins in the germ line, opposite of the role seen *in vitro* (**Figure 1B**).

Methylation Promotes Condensate Assembly in the Germ Line

In *Drosophila*, components of the methylosome regulate RNA binding proteins in multiple MLOs of the female germ line (**Figure 1B**). Capsuleen (Csul), also known as Dart5, is the homolog of the methyltransferase PRMT5. In *dart5/csul* mutant egg chambers the condensation of Tudor, Vasa, and Maelstrom into perinuclear granules of the nurse cell nuage is diminished, suggesting methylation normally promotes condensation of these proteins in the *Drosophila* female germ line (Gonsalvez et al., 2006; Anne et al., 2007). The Capsuleen-Valois methylosome complex also has a role in assembly of the pole plasm of *Drosophila* oocytes. The localization of Tudor and the Sm proteins, SmB and SD3, to the posterior pole plasm requires the methylation of Arg residues (Anne et al., 2007; Anne, 2010). The consequence of blocked methylation and disrupted nuage and pole plasm assembly in *dart5/csul* mutants is a grandchildless phenotype, where embryos of mutant females completely lack pole cells

TABLE 1 | Summary of germ line RNP condensates described in this review.

Species	Germ granule/RNP condensate	Description
All	Germ granule	Refers collectively to the electron-dense, RNP granules in vertebrate and invertebrate germ lines, often given a specific name in a species.
Drosophila		
	Nuage	Perinuclear, small Vasa-positive granules in nurse cells of ovary, and in several stages of spermatogenesis.
	Pole plasm	Posterior cytoplasm of the oocyte that contains polar granules; it is necessary and sufficient for the induction of germ cells.
	piNG body (piRNA nuage giant body)	Granules, larger than nuage, that appear late during spermatogenesis; granules contain several components of the piRNA pathway.
C. elegans		
	P granule	Germ granules in adult germ cells and germ cell precursors (P lineage) of embryo; perinuclear during most of development.
Mouse		
	Chromatoid body	Nuage component of mammalian spermatogenic cells; condensed form detected after completion of meiosis; contains similar proteins as germ granules in female germ cells, e.g., mouse Vasa homolog.
	Cajal body	Non-membraneous nuclear organelle; site of spliceosome maturation.
	Stress granule	RNP granules induced by heat stress; detected in spermatogonia and preleptotene and early pachytene spermatocytes.
	Oocyte aggregate	A subcortical RNP aggregate in germinal vesicle-stage oocytes, contains maternal mRNAs, and P body proteins.
Zebrafish		
	Balbiani body	Structure in zebrafish (and other) oocytes analogous to the mitochondrial cloud.
Xenopus		
	Oocyte aggregate	Patches of XStau1 in the vegetal subcortical region of Stage VI oocytes and eggs.

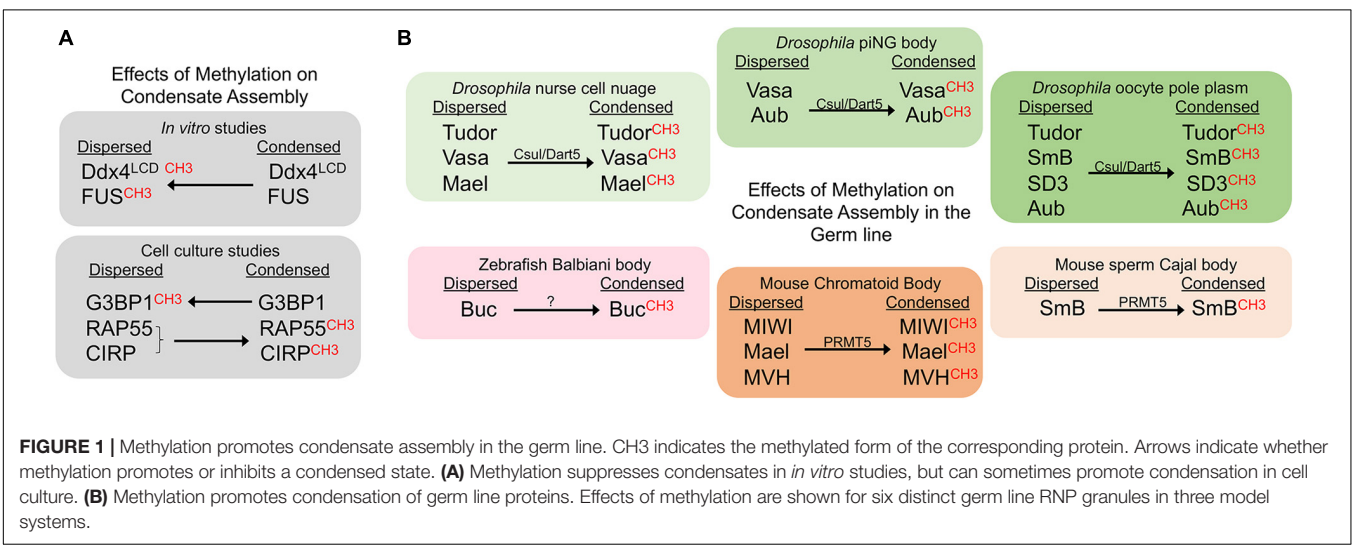

FIGURE 1 | Methylation promotes condensate assembly in the germ line. CH3 indicates the methylated form of the corresponding protein. Arrows indicate whether methylation promotes or inhibits a condensed state. **(A)** Methylation suppresses condensates in *in vitro* studies, but can sometimes promote condensation in cell culture. **(B)** Methylation promotes condensation of germ line proteins. Effects of methylation are shown for six distinct germ line RNP granules in three model systems.

and develop into agametic, sterile adults (Gonsalvez et al., 2006; Anne et al., 2007). Csul also methylates the Piwi protein Aubergine (Aub), which is required for Aub to bind Tudor and to promote the assembly of pole plasm in the developing oocyte (Kirino et al., 2010).

A role for methylation has also been identified in *Drosophila* primary spermatocytes, where a novel condensate called the piRNA nuage giant body (piNG-body) is enriched for Vasa, Aub, Argonaute 3, and Tudor (Kibanov et al., 2011). In spermatocytes lacking Csul/PRMT5, unmethylated Vasa and Aub fail to condense into the piNG-body; only small Vasa-positive nuage granules, and unlocalized Aub signals are detected. At the same time, the piRNA pathway is disrupted, and male sterility occurs. Thus, methylation by PRMT5 appears to be essential for piNG-body assembly and normal development of the male germ line.

Methylation of Ddx4/Vasa is widely conserved from planar worms to humans (Rouhana et al., 2012); thus, it will be interesting to determine if Arg-methylation also promotes assembly of Vasa granules in systems beyond *Drosophila*. It is notable that these *in vivo* germ line studies show an opposite effect of methylation as compared to *in vitro* studies, where PRMT1-dependent methylation disrupts the phase separation of Ddx4 (Nott

et al., 2015). This difference seems likely to be due to the fact *in vitro* studies generally involve only one or a few purified RBPs while the *in vivo* environment is much more complex.

Piwi-tudor domain protein interactions promote the assembly of germ granules not only in *Drosophila*, but also in mouse (Arkov and Ramos, 2010). *In vitro* studies show that Tudor proteins recognize methylarginine marks on mouse Piwi proteins to drive their localization to cytoplasmic foci (Vagin et al., 2009). In cell culture, treatment with an inhibitor of methyltransferases abolishes interactions between Tdrd1 and the mouse Piwi protein, MILI, suggesting that Arg-methylation and Tudor binding promote assembly of piRNA pathway components into nuage (Vagin et al., 2009). Moreover, immunoprecipitation studies show Tdrd6 interacts with the mouse Piwi proteins Miwi and Mili *in vivo*, and Miwi is methylated by PRMT5 and binds Tdrd6 in a symmetrical dimethylarginine methylation (sDMA)-dependent manner (Vasileva et al., 2009; Kirino et al., 2010). In *tdrd6-/-* testes the RNA binding proteins Mael, Miwi, and Mouse Vasa homolog (MVH)/Ddx4 fail to condense into the normal chromatoid bodies (the nuage in mouse spermatogenic cells) (Vasileva et al., 2009). The defects in condensation are accompanied by a lack of elongated spermatids and sperm. Given the proposed role for chromatoid bodies as storage sites during spermatid differentiation, their aberrant architecture and absence of condensed Mael, Miwi, and MVH in chromatoid bodies may directly impact spermatid differentiation (Vasileva et al., 2009). PRMT5 also methylates the SmB splicing protein in mouse spermatocytes. When Arg-methylation is abrogated via mutation of Tdrd6, the assembly of spliceosomes is impaired in primary spermatocytes, resulting in a decreased number of Cajal bodies, the nuclear membraneless condensates where spliceosome maturation occurs (Akpınar et al., 2017). Thus, methylation promotes condensation in both cytoplasmic and nuclear compartments of the mouse male germ line.

In the zebrafish model system methylation appears to promote the condensation of a solid-like germ granule, the Balbiani body. The germ plasm in early embryos originates from the Balbiani body in the oocyte (Kloc et al., 2004). A role for Tudor6 (Tdrd6) has been shown in modulating the aggregation of Buckyball (Buc), the organizer of the Balbiani body (Roovers et al., 2018). Tdrd6a and Tdrd6c interact with Buc via its three symmetrically dimethylated arginines. The three arginines of Buc are required for Buc to condense into a mature Balbiani body in oocytes, and to form germ plasm in embryos. The importance of Arg-methylation in promoting this phase transition to a solid condensate is further underscored by the observation that deleting the three arginines of Buc has a more severe phenotype than a *tdrd6a* mutant, with defects in germ cell formation and embryonic development (Roovers et al., 2018). It will be interesting to determine if methylation also modulates condensation of germ granule proteins in the adult germ cells or embryonic primordial germ cells where Tdrd7 has a role in maintaining the integrity of the germ granule protein Vasa (Strasser et al., 2008). The recent discovery of a role for PRMT5 in the methylation of Zili and Vasa in the zebrafish gonad should allow researchers to address whether methylation has any role in modulating condensation of Zili, Vasa, or other granule components (Zhu et al., 2019).

No studies to date have identified regulation of RNP condensates by methylation in the *C. elegans* germ line. However, Arg-methylation of the *C. elegans* RG proteins PGL-1/-3 by the PRMT1 homolog EPG-11 results in decreased phase separation *in vitro* (Zhang et al., 2018). In addition, in *C. elegans* embryos, where the primordial germ cells localize PGL-1/-3 to germ granules, EPG-11 destabilizes PGL-1/-3 aggregates from somatic blastomeres via methylation of the PGL-1/-3 RGG repeats (Li et al., 2013). It remains to be determined if this example of an inhibition of condensation by methylation will be extended to the worm germ line in future studies. In any event, the experiments in the fly, fish, and mouse germ lines clearly indicate differences from how methylation modulates phase separation *in vitro* and highlight the necessity of additional *in vivo* studies. Biochemical approaches to further study Ddx4/Vasa may be especially valuable due its broad conservation. Employing a high-resolution mass spectrometry approach to profile PRMT substrates may also be useful, as has been successful in other contexts (Shishkova et al., 2017).

ROLE OF PHOSPHORYLATION

Phosphorylation Can Promote or Inhibit Condensate Assembly *in vitro*

Phosphorylation is a common PTM that is implicated in the regulation of RNP granule dynamics. Phosphorylation is a rapid and reversible process by which proteins acquire negatively charged PO_4 groups that alter their intramolecular interactions and consequently impact phase separation (Hofweber and Dormann, 2019). Multivalent interactions among serine and tyrosine residues are especially prominent in the LCDs and intrinsically disordered regions (IDRs) of RNA binding proteins in granules. In *in vitro* studies phosphorylation sometimes promotes, and other times suppresses, phase separation of RNA binding proteins (Hofweber and Dormann, 2019). For example, phase separation of FUS is blocked when FUS is phosphorylated by the DNA-dependent protein kinase (Monahan et al., 2017; Murray et al., 2017; Luo et al., 2018). In contrast, phosphomimetic S48E substitution in the N-terminal domain of TDP-43 (TAR DNA– binding protein of 43 kDa) blocks the phosphorylation of TDP-43 by Casein Kinase 1 (CK1), and leads to reduced liquid-liquid phase separation of TDP-43 *in vitro* (Kametani et al., 2009; Wang et al., 2018; Hofweber and Dormann, 2019). Phosphorylation also promotes the condensation of Tau, a neuron-specific microtubule-associated protein (Ambadipudi et al., 2017). Similar to the varied effects of phosphorylation in *in vitro* studies (**Figure 2A**), cell culture experiments also reveal both inhibitory and stimulatory roles of phosphorylation on condensation of stress granule proteins (Hofweber and Dormann, 2019). It is not yet clear how well the *in vitro* and *ex vivo* studies translate to more complex environments of *in vivo* tissues and organisms. However, the studies highlighted below elucidate a growing role for

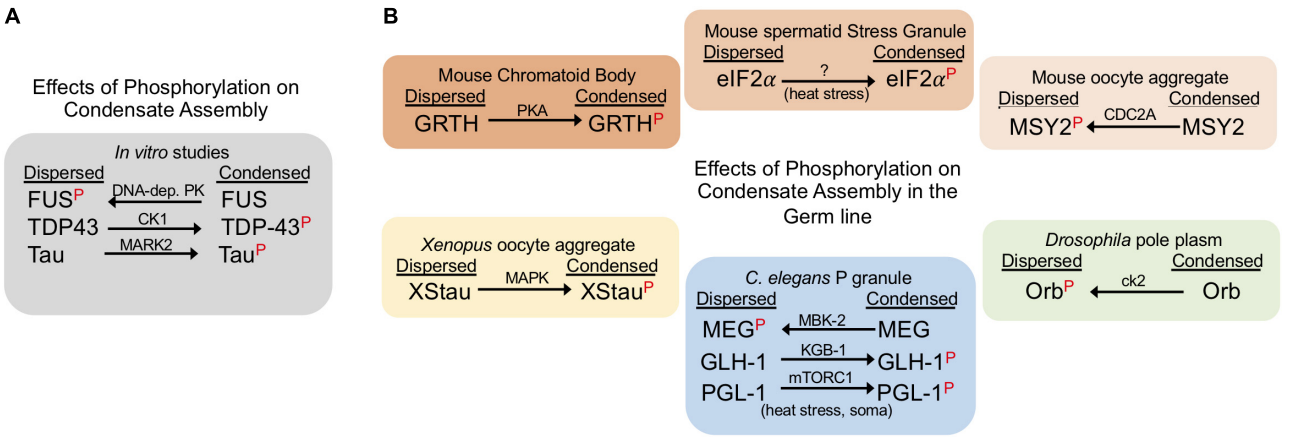

FIGURE 2 | Phosphorylation can suppress or promote condensate assembly. The red P indicates the phosphorylated form of the corresponding protein. Arrows indicate whether phosphorylation drives a dispersed or condensed state; kinase names are above each arrow. **(A)** Phosphorylation has varying effects on phase separation in *in vitro* studies. **(B)** Phosphorylation negatively and positively regulates RNP condensates in the germ line. The effects of phosphorylation are shown for proteins in six distinct germ line RNP granules in three model systems. Note: phosphorylation of the *C. elegans* P granule protein PGL-1 during heat stress conditions promotes condensates in somatic cells, outside of the germline.

phosphorylation in regulating the assembly and disassembly of germ granules in invertebrate and vertebrate systems.

Phosphorylation Can Promote or Inhibit Condensate Assembly in the Germ Line

Studies of *C. elegans* germ cells reveal insights into the complex roles of phosphorylation in regulating RNP granule assembly (**Figure 2B**). MBK-2, the *C. elegans* DYRK3 kinase homolog, and the PP2A$^{PPTR-1/2}$ phosphatase are key players in mediating the dynamics of PGL-1, an RGG protein in germ granules (Seydoux, 2018). Phosphorylation of MEG-1 and MEG-3 (maternal-effect germline defective) proteins by MBK-2 promotes disassembly of PGL-1 granules in zygotes (Wippich et al., 2013). This action is balanced by PPTR-1 and PPTR-2 which have redundant phosphatase functions to dephosphorylate MEG proteins and stabilize PGL-1 granule formation (Wang et al., 2014). In addition to contributing to P granule regulation, the MEG proteins are required for fertility; however, how regulated phosphorylation impacts fertility is not yet clear (Wang et al., 2014). A contrasting example of phosphorylation in *C. elegans* is the Ddx4/Vasa homolog GLH-1 which is phosphorylated by the KGB-1 MAP kinase (Orsborn et al., 2007). In the *kgb-1* knockout the localization of GLH-1 to discrete P granules is partially disrupted, suggesting that KGB-1 normally promotes condensation of GLH-1 via phosphorylation. When GLH-1 is not phosphorylated by KGB-1, elevated levels of GLH-1 protein are detected in the gonad, as well as over-proliferation of germ cells, and a high level of sterility. A second example of phosphorylation promoting condensation of P granules has been described outside of germ cells. mTORC1-mediated phosphorylation of PGL-1/-3 during mild heat-stress promotes the assembly of PGL-1/-3 granules in somatic blastomeres of early embryos (Zhang et al., 2018).

In the *Drosophila* germ line, phosphorylation has been shown to inhibit protein condensation. Orb, the cytoplasmic polyadenylation element binding protein (CPEB) homolog, regulates the translation of target mRNAs in *Drosophila* ovaries and is phosphorylated by casein kinase II (ck2) (Wong et al., 2011). When ck2 activity is compromised, Orb transitions from a diffuse state in oocytes into condensed sponge body-like granules, implicating phosphorylation in inhibiting Orb condensation (Wong et al., 2011). Deducing the precise consequence of ectopic Orb condensates in *ck2* mutants is not straightforward; however, the phenotype of both *orb* and *ck2* mutants includes dorsal-ventral defects during oogenesis. Interestingly, several examples demonstrate that phosphorylation does not always affect protein condensation. The *Drosophila* Pan Gu (PNG) kinase directly phosphorylates two de-capping activator proteins Trailer hitch (TRAL)/RAP55 and Me31B/RCK; however, the dispersal of TRAL granules is not affected during *in vitro* egg activation (Hara et al., 2018). In addition, the phosphorylation of maelstrom (Mael) by polo kinase is not required for its localization to nuage puncta in ovaries (Pek et al., 2012).

Multiple examples in both female and male germ lines of vertebrates demonstrate a role for phosphorylation in regulating protein condensation. In the female mouse germ line, MSY2 is one of several RNA-binding proteins that condense into transient, RNA-containing aggregates in fully grown oocytes but later decondense during oocyte maturation (Flemr et al., 2010). Phosphorylation of MSY2 by CDC2A occurs during oocyte maturation concomitant with its de-condensation, suggesting that phosphorylation may inhibit MSY2 condensation (Medvedev et al., 2008). In contrast, in the male mouse germ line, when Gonadotropin-regulated testicular RNA helicase (GRTH) is not phosphorylated by Protein Kinase A (PKA), GRTH localization to the chromatoid body (CB) is impaired, the CB is reduced in size, testis size is reduced due to germ cell apoptosis, and spermatogenesis arrests at the round spermatid stage (Sheng et al., 2006; Kavarthapu et al., 2019). Phosphorylation of eIF2α by GCN2 also appears to promote its condensation into stress

granules in male spermatids in response to temperature stress (Kim et al., 2012; Yoon et al., 2017). In *Xenopus* oocytes, Staufen proteins (XStau1 and XStau2) are phosphorylated via the MAP Kinase pathway during meiotic maturation (Allison et al., 2004). Phosphorylated XStau1 appears to transition from small aggregates concentrated locally in the vicinity of the ER, to larger aggregates less localized to the ER, suggesting phosphorylation promotes condensation of XStau1 which may impact its association with the ER network (Allison et al., 2004). It is not yet clear how phosphorylation modifies XStau1 function.

Overall, the role of phosphorylation in modulating phase transitions in the germ line has been understudied to date. Dozens of RNA binding proteins have been characterized as components of P granules in *C. elegans*, and of polar granules and nuage in *Drosophila* (Updike and Strome, 2010; Kato and Nakamura, 2012). It will be interesting to determine the extent to which phosphorylation regulates condensation of these proteins. For example, the *C. elegans* MPK-1 ERK (extracellular signal-regulated kinase) controls seven different processes in the adult germ line, including germ cell apoptosis and oocyte maturation (Lee et al., 2007). Genomic approaches have identified 30 ERK substrates including several RNA binding proteins, some of which are P granule proteins (Arur et al., 2009). Future studies should be able to address if ERK modulates condensation of any of its protein substrates.

PERSPECTIVES

The germ line has distinct functions from the soma, including the need to accurately transmit genetic information between generations and the requirement of pluripotency. The germ line may also have unique requirements in regulating gene expression, as large pools of maternal mRNAs accumulate in oocytes, many of which are non-translating until after fertilization. Germ line RNP condensates can facilitate post-transcriptional gene regulation of mRNA, and the prevailing theory is that such gene regulation is advantageous for rapid gene activation post-fertilization. PTMs afford some of the fastest changes to protein function that are also reversible and avoid *de novo* nuclear activities. Since RNP condensates are very dynamic complexes, these advantages may begin to answer why PTMs have evolved as an important regulator of germ line RNP condensates.

In comparison to the many examples of PTMs modulating phase transitions *in vitro* and in cell culture, there are notably fewer documented cases in the germ line. This discrepancy may simply reflect the challenge of studying PTMs *in vivo*, with the expectation that additional examples will be identified in the future. Alternatively, the relatively low number of examples may be due to alternative mechanisms regulating condensates in the germ line, with a smaller relative role for PTMs. This review highlights one major difference between *in vitro* studies that demonstrate a role for methylation in reducing phase separation, and germ line studies that show a role in promoting condensation of RNA binding proteins. In particular, the example of Ddx4/Vasa is striking. The formation of liquid droplets of the disordered N-terminal domain of Ddx4 is suppressed by asymmetric demethylation via PRMT1 expression in bacterial cells (Nott et al., 2015). In contrast, the methylation of Vasa by Dart5/Csul in *Drosophila* promotes the assembly of nuage granules in nurse cells and of piNG bodies in spermatocytes (Kibanov et al., 2011). The explanation for these opposite effects may simply be a more complex *in vivo* environment in the germ line, but probing this difference could be helpful in understanding the limitations of applying *in vitro* findings to the germ line. Another instance of context-specific effects of PTMs can be seen in the *C. elegans* embryo. MBK-2 phosphorylation of the MEG proteins drives disassembly of P granules, including the PGL-1 protein (Wang et al., 2014); however, phosphorylation of PGL-1 by mTORC1 stimulates the assembly of ectopic P granules in somatic blastomeres during heat stress (Zhang et al., 2018). These differences highlight our incomplete understanding of the role of PTMs in regulating phase separation.

One important consideration not yet discussed is the combinatorial nature of PTMs in modulating the assembly of granules. RNA binding proteins are often both phosphorylated and methylated, suggesting these two types of PTMs can be either synergistic or antagonistic (Bah and Forman-Kay, 2016). In addition, other PTMs such as O-linked GlcNAc modification and lysine acetylation have been shown to interact with phosphorylation in *in vitro* assays. For example, acetylation of Tau on Lys-321 prevents phosphorylation of a downstream Ser residue, and results in decreased aggregation of Tau filaments (Carlomagno et al., 2017). In regards to the germ line, few combinatorial PTMs of RNA binding proteins have been identified to date. However, the *C. elegans* PGL-1 protein is methylated by EPG-11 which inhibits PGL-1 aggregation into granules *in vitro*, and may act similarly in somatic blastomeres of the early embryo (Li et al., 2013; Zhang et al., 2018). The de-condensation of PGL-1 in somatic blastomeres can be balanced during heat stress when phosphorylation of PGL-1 by mTORC1 accelerates phase separations, resulting in ectopic somatic granules (Zhang et al., 2018). It remains to be seen if RNP condensates in the germ line proper are similarly modulated by combinations of PTMs.

Another interesting avenue to pursue is the extent to which stress conditions trigger PTMs that regulate RNP condensates in the germ line. Heat stress, extended meiotic arrest, starvation, hypoxia, and osmotic stress can induce the assembly of large RNP condensates in the germ line; however, PTMs have not been identified as regulators of any of these stress-induced granules to date (Schisa, 2014). *In vitro* studies, on the other hand, show that certain stresses lead to phosphorylation of FUS in addition to its constitutive Arg-methylation (Rhoads et al., 2018). During environmental stresses, stress granule formation is stimulated by a combination of phosphorylation and *O*-GlcNAcylation on Ser/Thr residues; however, the precise cause and effect relationship between these combinations of PTMs and phase transitions remains incompletely understood (Hofweber and Dormann, 2019).

Another unresolved question is whether RNP condensates in germ cells are bona fide phase-separated structures. To address this, time-lapse microscopy could be useful to determine the behavior of fusing droplets *in vivo*. FRAP studies may

also be helpful; however, fast FRAP recovery is not sufficient to demonstrate phase separation (Alberti et al., 2019). The use of super-resolution microscopy is a relatively new tool that may be useful in mapping phase diagrams to determine concentration dependent thresholds for assembly (Patel et al., 2015; Rai et al., 2018). Another approach being developed to assess viscosity and porosity of condensates is the use of genetically encoded nanoparticles (GEMS) as microrheology probes (Alberti et al., 2019). One challenge to the field with investigations of the physical properties of *in vivo* germ line condensates is distinguishing whether genetic perturbations that affect function do so due to altered condensation or independently of condensation alterations.

We have a good appreciation that the dysregulation of protein folding and condensation can result in human disease, as is well-exemplified by multiple neurodegenerative diseases, for example, ectopic aggregates containing TDP-43 and FUS in ALS. Germ cells share several attributes with neurons such as being post-mitotic and differentiated, and relying on regulation of gene expression post-transcriptionally, e.g., the synaptic ends of axons are a distance from nuclei, and maturing oocytes have large stores of maternal mRNAs. Certain stresses and mutations cause increased condensation of RNA binding proteins in *C. elegans* and *Drosophila* germ lines. In some cases, the condensates are liquid-like and reversible and have been hypothesized to be protective (Jud et al., 2008; Shimada et al., 2011; Hubstenberger et al., 2013); while in other cases, such as the *cgh-1 (tn691)* germ line at restrictive temperature, RNA binding proteins condense into sheet-like structures with immobile pools of protein (Hubstenberger et al., 2013; Langerak et al., 2019). The *cgh-1 (tn691)* phenotype also includes oogenesis defects, increased germ line apoptosis, and embryonic lethality; therefore, the pleiotropic nature of the defects makes it impossible to assess if the condensation of RNA binding proteins into solid structures contributes directly to the infertility (Navarro et al., 2001; Audhya et al., 2005). It will be of interest for future studies to find approaches to address the cause and effect relationships between condensate regulation and gamete development/function in the germ line.

AUTHOR CONTRIBUTIONS

JS contributed writing and editing of the manuscript and prepared the figures. ME contributed writing of the manuscript. Both authors contributed to the article and approved the submitted version.

FUNDING

JS is funded by the National Institutes of General Medical Sciences 2R15GM109337.

ACKNOWLEDGMENTS

The authors thank Dr. Xantha Karp and lab members for helpful feedback on the manuscript.

REFERENCES

Akpınar, M., Lesche, M., Fanourgakis, G., Fu, J., Anasstasiadis, K., Dahl, A., et al. (2017). TDRD6 mediates early steps of spliceosome maturation in primary spermatocytes. *PLoS Genet.* 13:e1006660. doi: 10.1371/journal.pgen.1006660

Alberti, S., Gladfelter, A., and Mittag, T. (2019). Considerations and challenges in studying liquid-liquid phase separation and biomolecular condensates. *Cell* 176, 419–434. doi: 10.1016/j.cell.2018.12.035

Allison, R., Czaplinski, K., Git, A., Adegbenro, E., Stennard, F., Houliston, E., et al. (2004). Two distinct Staufen isoforms in *Xenopus* are vegetally localized during oogenesis. *RNA* 10, 1751–1763. doi: 10.1261/rna.7450204

Ambadipudi, S., Biernat, J., Riedel, D., Mandelkow, E., and Zweckstetter, M. (2017). Liquid-liquid phase separation of the microtubule-binding repeats of the Alzheimer-related protein Tau. *Nat. Commun.* 8:275. doi: 10.1038/s41467-017-00480-0

Anne, J. (2010). Arginine methylation of SmB is required for *Drosophila* germ cell development. *Development* 137, 2819–2828. doi: 10.1242/dev.052944

Anne, J., Ollo, R., Ephrussi, A., and Mechler, B. M. (2007). Arginine methyltransferase Capsuléen is essential for methylation of spliceosomal Sm proteins and germ cell formation in *Drosophila*. *Development* 134, 137–146. doi: 10.1242/dev.02687

Arkov, A. L., and Ramos, A. (2010). Building RNA-protein granules: insight from the germline. *Trends Cell Biol.* 20, 482–490. doi: 10.1016/j.tcb.2010.05.004

Arur, S., Ohmachi, M., Nayak, S., Hayes, M., Miranda, A., Hay, A., et al. (2009). Multiple ERK substrates execute single biological processes in *Caenorhabditis elegans* germ-line development. *Proc. Natl. Acad. Sci. U.S.A.* 106, 4776–4781. doi: 10.1073/pnas.0812285106

Audhya, A., Hyndman, F., McLeod, I. X., Maddox, A. S., Yates, J. R. III, Desai, A., et al. (2005). A complex containing the Sm protein CAR-1 and the RNA helicase CGH-1 is required for embryonic cytokinesis in *Caenorhabditis elegans*. *J. Cell Biol.* 171, 267–279. doi: 10.1083/jcb.200506124

Bah, A., and Forman-Kay, J. D. (2016). Modulation of intrinsically disordered protein function by post-translational modifications. *J. Biol. Chem.* 291, 6696–6705. doi: 10.1074/jbc.R115.695056

Bedford, M. T., and Clarke, S. G. (2009). Protein Arginine Methylation in Mammals: who. What, and why. *Mol. Cell* 33, 1–13. doi: 10.1016/j.molcel.2008.12.013

Boke, E., Ruer, M., Wühr, M., Coughlin, M., Lemaitre, R., Gygi, S. P., et al. (2016). Amyloid-like self-assembly of a cellular compartment. *Cell* 166, 637–650. doi: 10.1016/j.cell.2016.06.051

Brangwynne, C. P., Eckmann, C. R., Courson, D. S., Rybarska, A., Hoege, C., Gharakhani, J., et al. (2009). Germline P granules are liquid droplets that localize by controlled dissolution/condensation. *Science* 324, 1729–1732. doi: 10.1126/science.1172046

Carlomagno, Y., Chung, D. C., Yue, M., Castanedes-Casey, M., Madden, B. J., Dunmore, J., et al. (2017). An Acetylation–phosphorylation switch that regulates tau aggregation propensity and function. *J. Biol. Chem.* 292, 15277–15286. doi: 10.1074/jbc.M117.794602

Chong, P. A., and Forman-Kay, J. D. (2016). Liquid–liquid phase separation in cellular signaling systems. *Curr. Opin. Struct. Biol.* 41, 180–186. doi: 10.1016/j.sbi.2016.08.001

De Leeuw, F., Zhang, T., Wauquier, C., Huez, G., Kruys, V., and Gueydan, C. (2007). The cold-inducible RNA-binding protein migrates from the nucleus to cytoplasmic stress granules by a methylation-dependent mechanism and acts as a translational repressor. *Exp. Cell Res.* 313, 4130–4144. doi: 10.1016/j.yexcr.2007.09.017

Fackelmayer, F. O. (2005). Protein arginine methyltransferases: guardians of the arg? *Trends Biochem. Sci.* 30, 666–671. doi: 10.1016/j.tibs.2005.10.002

Flemr, M., Ma, J., Schultz, R. M., and Svoboda, P. (2010). P-body loss is concomitant with formation of a messenger RNA storage domain in mouse oocytes. *Biol. Reprod.* 82, 1008–1017. doi: 10.1095/biolreprod.109.082057

Gonsalvez, G. B., Rajendra, T. K., Tian, L., and Matera, A. G. (2006). The Sm-protein methyltransferase, Dart5, is essential for germ-cell specification and maintenance. *Curr. Biol.* 16, 1077–1089. doi: 10.1016/j.cub.2006.04.037

Hara, M., Lourido, S., Petrova, B., Lou, H. J., Von Stetina, J. R., Kashevsky, H., et al. (2018). Identification of PNG kinase substrates uncovers interactions with the translational repressor TRAL in the oocyte-to-embryo transition. *ELife* 7:e33150. doi: 10.7554/eLife.33150

Hofweber, M., and Dormann, D. (2019). Friend or foe-post-translational modifications as regulators of phase separation and RNP granule dynamics. *J. Biol. Chem.* 294, 7137–7150. doi: 10.1074/jbc.TM118.001189

Hubstenberger, A., Noble, S. L., Cameron, C., and Evans, T. C. (2013). Translation repressors, an RNA helicase, and developmental cues control RNP phase transitions during early development. *Dev. Cell* 27, 161–173. doi: 10.1016/j.devcel.2013.09.024

Itakura, A. K., Futia, R. A., and Jarosz, D. F. (2018). It pays to be in phase. *Biochemistry* 57, 2520–2529. doi: 10.1021/acs.biochem.8b00205

Jud, M. C., Czerwinski, M. J., Wood, M. P., Young, R. A., Gallo, C. M., Bickel, J. S., et al. (2008). Large P body-like RNPs form in C. elegans oocytes in response to arrested ovulation, heat shock, osmotic stress and anoxia and are regulated by the major sperm protein pathway. *Dev. Biol.* 318, 38–51. doi: 10.1016/j.ydbio.2008.02.059

Kametani, F., Nonaka, T., Suzuki, T., Arai, T., Dohmae, N., Akiyama, H., et al. (2009). Identification of casein kinase-1 phosphorylation sites on TDP-43. *Biochem. Biophys. Res. Commun.* 382, 405–409. doi: 10.1016/j.bbrc.2009.03.038

Kato, M., Han, T. W., Xie, S., Shi, K., Du, X., Wu, L. C., et al. (2012). Cell-free formation of RNA granules: low complexity sequence domains form dynamic fibers within hydrogels. *Cell* 149, 753–767. doi: 10.1016/j.cell.2012.04.017

Kato, Y., and Nakamura, A. (2012). Roles of cytoplasmic RNP granules in intracellular RNA localization and translational control in the *Drosophila oocyte*. *Dev. Grow. Differ.* 54, 19–31. doi: 10.1111/j.1440-169X.2011.01314.x

Kavarthapu, R., Anbazhagan, R., Raju, M., Morris, C. H. T., Pickel, J., and Dufau, M. L. (2019). Targeted knock-in mice with a human mutation in GRTH/DDX25 reveals the essential role of phosphorylated GRTH in spermatid development during spermatogenesis. *Hum. Mol. Genet.* 28, 2561–2572. doi: 10.1093/hmg/ddz079

Kibanov, M. V., Egorova, K. S., Ryazansky, S. S., Sokolova, O. A., Kotov, A. A., Olenkina, O. M., et al. (2011). A novel organelle, the piNG-body, in the nuage of *Drosophila* male germ cells is associated with piRNA-mediated gene silencing. *Mol. Biol. Cell* 22, 3410–3419. doi: 10.1091/mbc.E11-02-0168

Kim, B., Cooke, H. J., and Rhee, K. (2012). DAZL is essential for stress granule formation implicated in germ cell survival upon heat stress. *Development* 139, 568–578. doi: 10.1242/dev.075846

Kirino, Y., Vourekas, A., Sayed, N., De Lima Alves, F., Thomson, T., Lasko, P., et al. (2010). Arginine methylation of aubergine mediates tudor binding and germ plasm localization. *RNA* 16, 70–78. doi: 10.1261/rna.1869710

Kloc, M., Bilinski, S., and Etkin, L. D. (2004). The Balbiani body and germ cell determinants: 150 years later. *Curr. Top. Dev. Biol.* 59, 1–36. doi: 10.1016/S0070-2153(04)59001-4

Langerak, S., Trombley, A., Patterson, J. R., Leroux, D., Couch, A., Wood, M. P., et al. (2019). Remodeling of the endoplasmic reticulum in *Caenorhabditis elegans* oocytes is regulated by CGH-1. *Genesis* 57:e23267. doi: 10.1002/dvg.23267

Lee, M. H., Ohmachi, M., Arur, S., Nayak, S., Francis, R., Church, D., et al. (2007). Multiple functions and dynamic activation of MPK-1 extracellular signal-regulated kinase signaling in *Caenorhabditis elegans* germline development. *Genetics* 177, 2039–2062. doi: 10.1534/genetics.107.081356

Li, P., Banjade, S., Cheng, H. C., Kim, S., Chen, B., Guo, L., et al. (2012). Phase transitions in the assembly of multivalent signalling proteins. *Nature* 483, 336–340. doi: 10.1038/nature10879

Li, S., Yang, P., Tian, E., and Zhang, H. (2013). Arginine methylation modulates autophagic degradation of PGL granules in *C.elegans*. *Mol. Cell* 52, 421–433. doi: 10.1016/j.molcel.2013.09.014

Luo, F., Gui, X., Zhou, H., Gu, J., Li, Y., Liu, X., et al. (2018). Atomic structures of FUS LC domain segments reveal bases for reversible amyloid fibril formation. *Nat. Struct. Mol. Biol.* 25, 341–346. doi: 10.1038/s41594-018-0050-8

Matsumoto, K., Nakayama, H., Yoshimura, M., Masuda, A., Dohmae, N., Matsumoto, S., et al. (2012). PRMT1 is required for RAP55 to localize to processing bodies. *RNA Biol.* 9, 610–623. doi: 10.4161/rna.19527

Medvedev, S., Yang, J., Hecht, N. B., and Schultz, R. M. (2008). CDC2A (CDK1)-mediated phosphorylation of MSY2 triggers maternal mRNA degradation during mouse oocyte maturation. *Dev. Biol.* 321, 205–215. doi: 10.1016/j.ydbio.2008.06.016

Monahan, Z., Ryan, V. H., Janke, A. M., Burke, K. A., Rhoads, S. N., Zerze, G. H., et al. (2017). Phosphorylation of the FUS low−complexity domain disrupts phase separation, aggregation, and toxicity. *EMBO J.* 36, 2951–2967. doi: 10.15252/embj.201696394

Murray, D. T., Kato, M., Lin, Y., Thurber, K. R., Hung, I., McKnight, S. L., et al. (2017). Structure of FUS protein fibrils and its relevance to self-assembly and phase separation of low-complexity domains. *Cell* 171, 615–627.e16. doi: 10.1016/j.cell.2017.08.048

Navarro, R. E., Shim, E. Y., Kohara, Y., Singson, A., and Blackwell, T. K. (2001). Cgh-1, a conserved predicted RNA helicase required for gametogenesis and protection from physiological germline apoptosis in *C. elegans*. *Development* 128, 3221–3232.

Nott, T. J., Petsalaki, E., Farber, P., Jervis, D., Fussner, E., Plochowietz, A., et al. (2015). Phase transition of a disordered nuage protein generates environmentally responsive membraneless organelles. *Mol. Cell* 57, 936–947. doi: 10.1016/j.molcel.2015.01.013

Orsborn, A. M., Li, W., McEwen, T. J., Mizuno, T., Kuzmin, E., Matsumoto, K., et al. (2007). GLH-1, the *C. elegans P granule* protein, is controlled by the JNK KGB-1 and by the COP9 subunit CSN-5. *Development* 134, 3383–3392. doi: 10.1242/dev.005181

Patel, A., Lee, H. O., Jawerth, L., Maharana, S., Jahnel, M., Hein, M. Y., et al. (2015). A Liquid-to-Solid phase transition of the ALS protein FUS accelerated by disease mutation. *Cell* 162, 1066–1077. doi: 10.1016/j.cell.2015.07.047

Pek, J. W., Ng, B. F., and Kai, T. (2012). Polo-mediated phosphorylation of maelstrom regulates oocyte determination during oogenesis in drosophila. *Development (Cambridge)* 139, 4505–4513. doi: 10.1242/dev.082867

Putnam, A., Cassani, M., Smith, J., and Seydoux, G. (2019). A gel phase promotes condensation of liquid *P granules* in *C. elegans embryos*. *Nat. Struct. Mol. Biol.* 26, 220–226. doi: 10.1038/s41594-019-0193-2

Qamar, S., Wang, G. Z., Randle, S. J., Ruggeri, F. S., Varela, J. A., Lin, J. Q., et al. (2018). FUS phase separation is modulated by a molecular chaperone and methylation of arginine cation-π interactions. *Cell* 173, 720–734.e15. doi: 10.1016/j.cell.2018.03.056

Rai, D., Dey, S., and Ray, K. (2018). A method for estimating relative changes in the synaptic density in *Drosophila* central nervous system. *BMC Neurosci.* 19:30. doi: 10.1186/s12868-018-0430-3

Rhoads, S. N., Monahan, Z. T., Yee, D. S., and Shewmaker, F. P. (2018). The role of post-translational modifications on prion-like aggregation and liquid-phase separation of FUS. *Int. J. Mol. Sci.* 19:886. doi: 10.3390/ijms19030886

Roovers, E. F., Kaaij, L. J. T., Redl, S., Bronkhorst, A. W., Wiebrands, K., de Jesus Domingues, A. M., et al. (2018). Tdrd6a regulates the aggregation of Buc into functional subcellular compartments that drive germ cell specification. *Dev. Cell* 46, 285–301.e9. doi: 10.1016/j.devcel.2018.07.009

Rouhana, L., Vieira, A. P., Roberts-Galbrait, R. H., and Newmark, P. A. (2012). PRMT5 and the role of symmetrical dimethylarginine in chromatoid bodies of planarian stem cells. *Development* 139, 1083–1094. doi: 10.1242/dev.076182

Schisa, J. A. (2012). New insights into the regulation of RNP granule assembly in oocytes. *Int. Rev. Cell Mol. Biol.* 295, 233–289. doi: 10.1016/B978-0-12-394306-4.00013-7

Schisa, J. A. (2014). Effects of stress and aging on ribonucleoprotein assembly and function in the germ line. *WIREs RNA* 5, 231–246. doi: 10.1002/wrna.1204

Seydoux, G. (2018). The P granules of *C. elegans*: a genetic model for the study of RNA–protein condensates. *J. Mol. Biol.* 430, 4702–4710. doi: 10.1016/j.jmb.2018.08.007

Sheng, Y., Tsai-Morris, C. H., Gutti, R., Maeda, Y., and Dufau, M. L. (2006). Gonadotropin-regulated testicular RNA helicase (GRTH/Ddx25) is a transport protein involved in gene-specific mRNA export and protein translation during spermatogenesis. *J. Biol. Chem.* 281, 35048–35056. doi: 10.1074/jbc.M605086200

Shimada, Y., Burn, K. M., Niwa, R., and Cooley, L. (2011). Reversible response of protein localization and microtubule organization to nutrient stress during *Drosophila* early oogenesis. *Dev. Biol.* 355, 250–262. doi: 10.1016/j.ydbio.2011.04.022

Shishkova, E., Zeng, H., Liu, F., Kwiecien, N. W., Hebert, A. S., Coon, J. J., et al. (2017). Global mapping of CARM1 substrates defines enzyme specificity and substrate recognition. *Nat. Commun.* 24:15571. doi: 10.1038/ncomms15571

Strasser, M. J., Mackenzie, N. C., Dumstrei, K., Nakkrasae, L. I., Stebler, J., and Raz, E. (2008). Control over the morphology and segregation of Zebrafish germ cell granules during embryonic development. *BMC Dev. Biol.* 8:58. doi: 10.1186/1471-213X-8-58

Tsai, W. C., Gayatri, S., Reineke, L. C., Sbardella, G., Bedford, M. T., and Lloyd, R. E. (2016). Arginine demethylation of G3BP1 promotes stress granule assembly. *J. Biol. Chem.* 291, 22671–22685. doi: 10.1074/jbc.M116.739573

Updike, D., and Strome, S. (2010). P granule assembly and function in *Caenorhabditis elegans* germ cells. *J. Androl.* 31, 53–60. doi: 10.2164/jandrol.109.008292

Vagin, V. V., Wohlschlegel, J., Qu, J., Jonsson, Z., Huang, X., Chuma, S., et al. (2009). Proteomic analysis of murine Piwi proteins reveals a role for arginine methylation in specifying interaction with Tudor family members. *Genes Dev.* 23, 1749–1762. doi: 10.1101/gad.1814809

Vasileva, A., Tiedau, D., Firooznia, A., Müller-Reichert, T., and Jessberger, R. (2009). Tdrd6 is required for spermiogenesis, chromatoid body architecture, and regulation of miRNA expression. *Curr. Biol.* 19, 630–639. doi: 10.1016/j.cub.2009.02.047

Voronina, E., Seydoux, G., Sassone-Corsi, P., and Nagamori, I. (2011). RNA granules in germ cells. *Cold Spring Harb. Perspect. Biol.* 3:a002774. doi: 10.1101/cshperspect.a002774

Wang, A., Conicella, A. E., Schmidt, H. B., Martin, E. W., Rhoads, S. N., Reeb, A. N., et al. (2018). A single N-terminal phosphomimic disrupts TDP-43 polymerization, phase separation, and RNA splicing. *EMBO J.* 37, 1–18. doi: 10.15252/embj.201797452

Wang, J. T., Smith, J., Chen, B. C., Schmidt, H., Rasoloson, D., Paix, A., et al. (2014). Regulation of RNA granule dynamics by phosphorylation of serine-rich, intrinsically disordered proteins in *C. elegans*. *ELife* 3:e04591. doi: 10.7554/eLife.04591

Wippich, F., Bodenmiller, B., Trajkovska, M. G., Wanka, S., Aebersold, R., and Pelkmans, L. (2013). Dual specificity kinase DYRK3 couples stress granule condensation/ dissolution to mTORC1 signaling. *Cell* 152, 791–805. doi: 10.1016/j.cell.2013.01.033

Wong, L. C., Costa, A., McLeod, I., Sarkeshik, A., Yates, J., Kyin, S., et al. (2011). The functioning of the drosophila CPEB protein orb is regulated by phosphorylation and requires casein kinase 2 activity. *PLoS One* 6:e24355. doi: 10.1371/journal.pone.0024355

Woodruff, J. B., Hyman, A. A., and Boke, E. (2018). Organization and function of non-dynamic biomolecular condensates. *Trends Biochem. Sci.* 43, 81–94. doi: 10.1016/j.tibs.2017.11.005

Xie, H., Vucetic, S., Iakoucheva, L. M., Oldfield, C. J., Dunker, A. K., Uversky, V. N., et al. (2007). Functional anthology of intrinsic disorder. 1. Biological processes and functions of proteins with long disordered regions. *J. Proteome Res.* 6, 1882–1898. doi: 10.1021/pr060392u

Yoon, J., Park, K., Hwang, D. S., and Rhee, K. (2017). Importance of eIF2α phosphorylation as a protective mechanism against heat stress in mouse male germ cells. *Mol. Reprod. Dev.* 84, 265–274. doi: 10.1002/mrd.22778

Zhang, G., Wang, Z., Du, Z., and Zhang, H. (2018). mTOR regulates phase separation of PGL granules to modulate their autophagic degradation. *Cell* 174, 1492–1506.e22. doi: 10.1016/j.cell.2018.08.006

Zhu, J., Zhang, D., Liu, X., Yu, G., Cai, X., Xu, C., et al. (2019). zebrafish prmt5 arginine methyltransferase is essential for germ cell development (Development (Cambridge)(2019) 146 (dev179572) doi: 10.1242/dev.179572)

Conflict of Interest: The authors declare that the research was conducted in the absence of any commercial or financial relationships that could be construed as a potential conflict of interest.

frontiers in Molecular Biosciences

REVIEW
published: 12 April 2021
doi: 10.3389/fmolb.2021.659610

A Comprehensive Analysis of the Role of hnRNP A1 Function and Dysfunction in the Pathogenesis of Neurodegenerative Disease

*Joseph P. Clarke[1,2], Patricia A. Thibault[2,3], Hannah E. Salapa[2,3] and Michael C. Levin[1,2,3,4]**

[1] Department of Health Sciences, College of Medicine, University of Saskatchewan, Saskatoon, SK, Canada, [2] Office of the Saskatchewan Multiple Sclerosis Clinical Research Chair, University of Saskatchewan, Saskatoon, SK, Canada, [3] Division of Neurology, Department of Medicine, University of Saskatchewan, Saskatoon, SK, Canada, [4] Department of Anatomy, Physiology and Pharmacology, University of Saskatchewan, Saskatoon, SK, Canada

OPEN ACCESS

Edited by:
Nicolas Lux Fawzi, Brown University, United States

Reviewed by:
Hong Joo Kim, St. Jude Children's Research Hospital, United States
Erik Martin, St. Jude Children's Research Hospital, United States

***Correspondence:**
Michael C. Levin
Michael.levin@usask.ca

Specialty section:
This article was submitted to Protein and RNA Networks, a section of the journal Frontiers in Molecular Biosciences

Received: *27 January 2021*
Accepted: *15 March 2021*
Published: *12 April 2021*

Citation:
Clarke JP, Thibault PA, Salapa HE and Levin MC (2021) A Comprehensive Analysis of the Role of hnRNP A1 Function and Dysfunction in the Pathogenesis of Neurodegenerative Disease. Front. Mol. Biosci. 8:659610. doi: 10.3389/fmolb.2021.659610

Heterogeneous nuclear ribonucleoprotein A1 (hnRNP A1) is a member of the hnRNP family of conserved proteins that is involved in RNA transcription, pre-mRNA splicing, mRNA transport, protein translation, microRNA processing, telomere maintenance and the regulation of transcription factor activity. HnRNP A1 is ubiquitously, yet differentially, expressed in many cell types, and due to post-translational modifications, can vary in its molecular function. While a plethora of knowledge is known about the function and dysfunction of hnRNP A1 in diseases other than neurodegenerative disease (e.g., cancer), numerous studies in amyotrophic lateral sclerosis, frontotemporal lobar degeneration, multiple sclerosis, spinal muscular atrophy, Alzheimer's disease, and Huntington's disease have found that the dysregulation of hnRNP A1 may contribute to disease pathogenesis. How hnRNP A1 mechanistically contributes to these diseases, and whether mutations and/or altered post-translational modifications contribute to pathogenesis, however, is currently under investigation. The aim of this comprehensive review is to first describe the background of hnRNP A1, including its structure, biological functions in RNA metabolism and the post-translational modifications known to modify its function. With this knowledge, the review then describes the influence of hnRNP A1 in neurodegenerative disease, and how its dysfunction may contribute the pathogenesis.

Keywords: RNA binding protein, hnRNP A1, post-translational modifications, RNA metabolism, neurodegenerative diseases

INTRODUCTION

The molecular mechanisms that define neurodegenerative diseases are as diverse and complex as the diseases themselves. While core mechanisms are shared by all cells (e.g., RNA metabolism, protein translation, ATP production, cytoskeletal growth), the downstream effects of changes in these mechanisms vary across neurodegenerative diseases. Pathological perturbations in cellular pathways that may be a major component of one neurodegenerative disease may not underlie

others. Despite mechanistic heterogeneity, however, several commonalities have been identified to help understand neurodegenerative disease pathophysiology. Prominent observations shared amongst neurodegenerative diseases, including Alzheimer's, Parkinson's, and Huntington's are the toxic accumulation of misfolded, insoluble protein inclusions within the cytoplasm or nucleus (Chung et al., 2018). While the toxic accumulation of proteins has been observed for decades in these neurologic diseases, current research has further expanded upon this phenomenon to include new toxic protein targets in several neurodegenerative conditions. Interestingly, several of these protein targets have been identified as RNA binding proteins (RBPs), which contribute significantly to RNA metabolism (i.e., RNA transcription, pre-mRNA splicing, mRNA transport, translation, sequestration, and degradation). This has led to the hypothesis that neurodegenerative disease is a result of altered RNA metabolism and its downstream consequences [reviewed in Liu et al. (2017)].

The heterogeneous nuclear ribonucleoproteins (hnRNPs) have become an intriguing target in neurodegenerative disease research as they are RBPs and several of them are mechanistically linked to pathophysiology (Kashima et al., 2007; Chen et al., 2008; Kim et al., 2013; Cho et al., 2014; Dombert et al., 2014; Moursy et al., 2014; Borreca et al., 2016). HnRNPs are the most abundantly expressed RBPs in mammalian cells, constituting of approximately 20 major types of proteins, and play a major role in all facets of RNA metabolism, especially RNA splicing (Beyer et al., 1977; Pinol-Roma et al., 1988; Dreyfuss et al., 1993). Additionally, within subgroups, hnRNPs share similar structural properties, such as the hnRNP(A/B) subfamily, which includes hnRNP A1, A2/B1, A3 and A0 (hnRNP A1 is focused upon and discussed in this review), however, between subgroups structural properties can differ significantly, which is reviewed in detail (Geuens et al., 2016). For example, hnRNP A1 and hnRNP A2/B1 utilize two RNA recognition motifs (RRMs) for RNA binding, both found in their N-termini, while the hnRNP family member hnRNP K utilizes three K homology (KH) domains, two found in the N-terminus and one in the C-terminus (Geuens et al., 2016). Additional structural differences occur amongst the hnRNPs, including re-organization of similar domains within the N- and C- termini, and/or the inclusion of different domains for added functions such as DNA/RNA binding and protein interaction (Geuens et al., 2016). Together, the intricate structural properties of each hnRNP dictate their individual cellular targets and functions.

In this review we describe hnRNP A1, initially focusing upon its structure and what is known about its cellular functionality. Throughout, we interweave the effects of post-translational modifications (PTMs) on hnRNP A1 and how they have been shown to regulate hnRNP A1 function. We then describe the involvement of hnRNP A1 in the pathogenesis of different neurodegenerative diseases, with an aim to highlight the many open questions about the role, regulation, and effects of PTMs on hnRNP A1 in disease pathogenesis.

HnRNP A1: STRUCTURAL CHARACTERIZATION AND ROLE IN LIQUID-LIQUID PHASE SEPARATION

Genetics, Molecular Structure, and Functional Regions of hnRNP A1

The hnRNP A1 gene (Ensembl symbol ENSG00000135486) is located on chromosome 12q13.13 and has two main characterized isoforms, hnRNP A1-A (isoform A, 320 amino acids, NM_002136.4→NP_002127.1) and hnRNP A1-B (isoform B, 372 amino acids, NM_031157.4→NP_112420.1), with hnRNP A1-A being 20 times more abundantly expressed, especially in neuronal cells (**Figure 1A**; Kamma et al., 1995). Like other members of the hnRNP(A/B) subfamily, both hnRNP A1 isoforms are similarly divided into two main structural portion: an N-terminal portion that includes two RRMs, and a C-terminal portion known as the prion-like domain (PrLD), which mediates cellular compartmentalization, protein-protein interaction, and RNA-binding (**Figure 1B**; He and Smith, 2009). Protein crystallization of the N-terminal portion of hnRNP A1 shows the two RRMs arranged in tandem and composed of four β-sheets adjoined by two α-helices, in a structure composed of β1α1β2β3α2β4 (Shamoo et al., 1997). The β-sheet surfaces, opposite the α-helices, primarily interact with RNA via amino acid stretches containing predominantly aromatic residues, with two conserved phenylalanine (Phe) residues, Phe17 and Phe59, being necessary for RNA binding (Merrill et al., 1988; Jones et al., 2001). The RRMs are each approximately 90 amino acids long and participate in general and specific RNA and messenger RNA (mRNA) binding through a docking platform, rather than a crevice, allowing for a high degree of RNA accessibility (Gorlach et al., 1992). Although both RRMs share a high degree of homology (∼35% identical and ∼60% similar), they are not redundant and operate as functionally distinct domains, able to bind to distinct RNAs and mRNAs (Casas-Finet et al., 1993; Mayeda et al., 1998). Their sequence binding specificity, however, is similar, as hnRNP A1 prefers to bind to AU-rich elements (AREs), or UAGGGA(U)-motifs present in the 3′-untranslated regions (3′-UTR) of messenger RNA transcripts (Hamilton et al., 1993; Burd and Dreyfuss, 1994; Shamoo et al., 1997).

Biochemical and Biological Characterization of Functional Regions of hnRNP A1

Biochemical characterization of the C-terminus of hnRNP A1 has shown that hnRNP A1 includes an Arginine-Glycine-Glycine domain (RGG domain), a glycine-rich, PrLD, and a 38-amino acid, nuclear localization/export sequence (NLS/NES), referred to as M9 (**Figure 1B**). The RGG domain of hnRNP A1 has been shown to influence RNA binding specificity and strength, G-quadruplex DNA binding and unfolding, and in mediating protein-protein interactions (Nadler et al., 1991; Cartegni et al., 1996; Fisette et al., 2010; Hudson et al., 2014). The PrLD is a low complexity domain that promotes both the liquid-liquid phase separation (LLPS) and the self-associative fibrillization

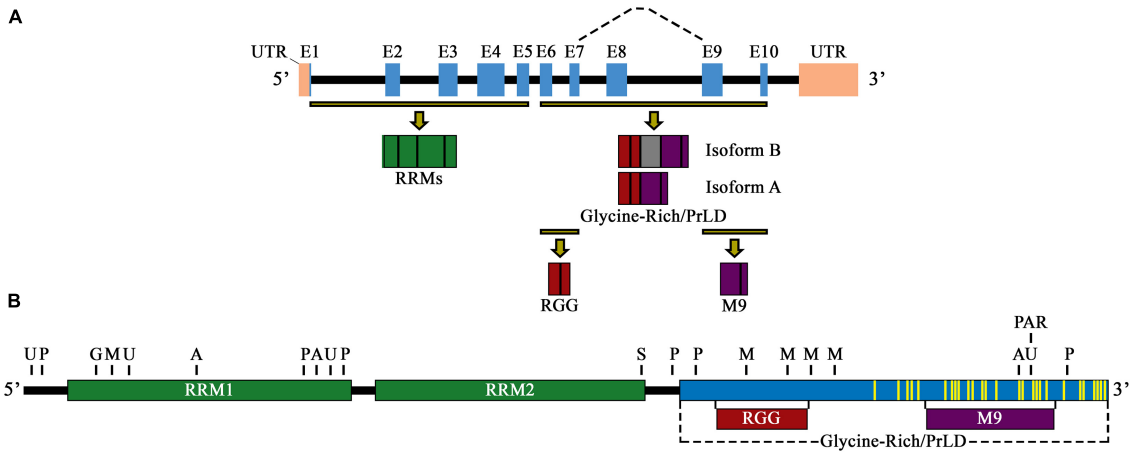

FIGURE 1 | (A) Schematic illustration of the primary pre-mRNA transcript and alternative mRNA splicing of hnRNP A1. Exons are labeled E1–E10 and are highlighted by blue boxes. Black boxes indicate introns, and pink boxes are UTRs. Highlighted exon fractions (yellow-black lines) that form the N-terminal and C-terminal regions of hnRNP A1 are illustrated in green (RRM1 and RRM2) and a combination of red (RGG domain) and purple (M9 sequence), forming the glycine-rich/PrLD domain, respectively. The dashed line represents the main spliced region of hnRNP A1, with inclusion of E8 (gray box) constituting isoform B, and its exclusion constituting isoform A. **(B)** Schematic illustration of the primary protein structure and functional domains of hnRNP A1 isoform A. RRM1 and RRM1 are signified by green boxes, and the glycine-rich/PrLD domain by a blue box. Highlighted protein fractions that form the RGG domain (red box) and the M9 sequence (purple box) are noted and are in the glycine-rich/PrLD domain relative to their placement underneath. PTM sites of ubiquitination (U), phosphorylation (P), O-GlcNAcylation (G), acetylation (A), sumoylation (S), methylation (M), and PARylation (PAR) are noted above the protein illustration (selectively representative; refer to Table 1 for full list of PTM locations).Yellow lines delineate mutations sites found in hnRNP A1 that have been published and are associated with the neurodegenerative diseases ALS/FTLD and MS.

propensity of hnRNP A1, as studies on the hnRNP(A/B) subfamily homolog hnRNP A2/B1 show this domain contains a steric-zipper motif that can potentially forms the spine of an amyloid fibril through two self-complementary β-sheets (Kim et al., 2013; Molliex et al., 2015; Xiang et al., 2015; Franzmann and Alberti, 2019).

The role of the hnRNP A1 PrLD in LLPS is important because it processes metastable de-mixing of proteins and/or RNA thought to be mediated by transient and diverse multivalent interactions (Molliex et al., 2015; Shin et al., 2017; Bracha et al., 2018; Gomes and Shorter, 2019). Briefly, LLPS enables the formation of biologically relevant intracellular assemblies of macromolecules in non-membrane-bound cellular compartments, referred to as membraneless organelles, such as stress granules (SGs), processing bodies, nuclear paraspeckles, Cajal bodies, nuclear stress bodies, the centrosome, and the nucleolus (Hyman et al., 2014; Molliex et al., 2015; Zaslavsky et al., 2018; Gomes and Shorter, 2019). Thought to be most important to neurodegeneration, SGs have been shown to assemble via LLPS in response to environmental stressors, and sequester and protect cytoplasmic mRNAs, proteins, and stalled translation complexes (Protter and Parker, 2016; Youn et al., 2019). However, it must be noted that these functions have been challenged recently utilizing high power, single molecule live-cell imaging techniques (Wilbertz et al., 2019). SGs also indirectly promote the specific translation of stress pathway proteins that are involved in mitigating the cell stress effect by limiting global cellular translation (Protter and Parker, 2016; Youn et al., 2019). Once the stressor has been removed, SGs disassemble and release their sequestered components. Current research suggests that alterations in RBP LLPS, thought to occur due to mutations that affect protein-protein interactions, can influence the formation and stability of SGs, and can promote neurodegeneration (Molliex et al., 2015; Protter and Parker, 2016; Gomes and Shorter, 2019; Youn et al., 2019). An evolving theory with hnRNP A1 is that it can inadvertently self-associate, either due to mutation, an adverse PTMs or due to a lack of RNA binding, and may indirectly induce LLPS of other PrLD-containing proteins, many of which are found in SGs (e.g., Ras-GTPase-Activating Protein SH3-Domain-Binding Protein, G3BP1; TAR-DNA binding protein-43, TDP-43; Fused In Sarcoma, FUS; and T-Cell-Restricted Intracellular Antigen-1, TIA1), thereby catalyzing SG assemblies independent of cell stress signaling (Hyman et al., 2014; Molliex et al., 2015; Protter and Parker, 2016; Markmiller et al., 2018; Youn et al., 2019). Recent studies give support to this idea, as PrLD mutations in hnRNP A1 can lead to its aggregation, and subfamily homolog hnRNP A2/B1 LLPS and aggregation are prevented *in vitro* with RNA binding (Kim et al., 2013; Lee and Levin, 2014; Molliex et al., 2015; Ryan et al., 2020).

Finally, the M9 sequence mediates the nuclear import and export of hnRNP A1, however, the amino acid sequences that mediate both functions are indistinguishable within M9 (Michael et al., 1995). Studies have shown that hnRNP A1 nucleocytoplasmic import is mediated by a cytoplasmic interaction with the transport receptors Transportin 1 and 2 (TNPO1/2), both β-karyopherin family proteins, resulting in hnRNP A1 import from the cytoplasm to the nucleus (Rebane et al., 2004; Allemand et al., 2005). This is an active process that requires the utilization of the RanGTP/RanGDP gradient at the

nucleopore, and the nucleopore complex (NPC) (Rebane et al., 2004). In addition to mediating hnRNP A1 nucleocytoplasmic transport, TNPO1 has also been shown recently to be a molecular chaperone of hnRNP A1 and has been demonstrated to prevent and reverse hnRNP A1 aggregation (Guo et al., 2018). Nuclear export, however, is not as well understood, as its export is not mediated by exportin 1 transport and is thought to be controlled by PTMs of hnRNP A1 (Lichtenstein et al., 2001; Roy et al., 2014).

HnRNP A1 FUNCTION AND POST-TRANSLATIONAL MODIFICATIONS

PTMs play a significant role in the functional diversity of hnRNP A1. HnRNP A1 undergoes phosphorylation, sumoylation, ubiquitination, PARylation, acetylation, methylation, and *O*-linked and *N*-linked β-N-acetylglucosaminylation (*O*-GlcNAcylation/*N*-GlcNAcylation), and all affect the location and functionality of hnRNP A1 (**Figure 1B** and **Table 1**). Since cellular location partially defines the function and activity of hnRNP A1, these effects are inextricably intertwined. Importantly, many of these modifications have been identified and characterized in the context of cancer biology and/or general stress responses, rather than in neurons or neurodegenerative disease, leaving us with important, unanswered questions and several avenues for future exploration.

HnRNP A1 is considered a key component of the response to cellular stresses, and neuronal dysfunction and loss in neurodegenerative disease is mediated in part by cellular stress. The activities of hnRNP A1 in regulating RNA metabolism are likely to be its major function in responding to cell stress – altered RNA binding and modulation of alternative splicing, altered transportation to the cytoplasm with mRNAs, and a shift to facilitating cellular translation to cap-independent translation from internal ribosomal entry sites (IRESs). The majority of characterized PTMs are shown to regulate these hnRNP A1 activities and are broadly characterized in the context of canonical cellular stressors: heat shock, low-dose ultraviolet irradiation, osmotic and oxidative stress, and external signaling factor stimulation. From these, we can extrapolate outcomes in response to other inputs and stressors, including protein aggregate accumulation or chronic inflammation that are associated with neurodegenerative disease.

HnRNP A1 and Transcription

Initial reports described hnRNP A1 as a DNA binding protein that influences RNA transcription through its binding to promoters, whereby its interaction either suppressed or activated transcription, depending on the gene of interest (**Figure 2A**; Lau et al., 2000; Campillos et al., 2003; Chen et al., 2003; Das et al., 2004; Xia, 2005). The mechanisms how hnRNP A1 affects transcriptional regulation are predominantly divided between two lines of evidence. Firstly, it has been shown that hnRNP A1 regulates promoter suppression by mediating the activity of transcriptional factors through protein-protein interactions with its PrLD domain (Hay et al., 2001). Other studies have shown that hnRNP A1 regulates promoter activation by binding to and destabilizing G-quadruplex structures within the promoters of genes (Takimoto et al., 1993; Fukuda et al., 2002; Paramasivam et al., 2009). This latter effect depends upon recognition of the RGG domain and subsequent binding to G-quadruplex DNA by interacting with loop nucleotides of the G-quadruplex structure (Paramasivam et al., 2009; Ghosh and Singh, 2018; Liu and Xu, 2018). This interaction then allows the RRMs of hnRNP A1 to destabilize the G-quadruplex structure and stabilize the unfolded form of the DNA through its interaction with single-stranded DNA (Paramasivam et al., 2009; Ghosh and Singh, 2018; Liu and Xu, 2018).

Dysregulated cellular senescence is also implicated in the progression of several neurodegenerative disorders [reviewed in Kritsilis et al. (2018) and Martinez-Cue and Rueda (2020)], and global hnRNP A1 knockdown results in cellular senescence (Shimada et al., 2009), as indicated in its role in cell cycle progression and senescence. Transcription of oncogenes, like Kirsten Rat Sarcoma Viral Proto-Oncogene (*KRAS)* and Transformer 2 Beta Homolog (*TRA2B),* are promoted by hnRNP A1 binding to a G-quadruplex structure in the genes' promoters, utilizing hnRNP A1 DNA binding activity (Paramasivam et al., 2009; Nishikawa et al., 2019). Promotion of *KRAS* transcription has recently been shown to be regulated by the cell stress response regulator poly (ADP-ribose) polymerase (PARP-1), which itself PARylates hnRNP A1 (discussed below), although the impact of hnRNP A1 PARylation on *KRAS* transcription, and the function of KRAS expression in the context of oxidative stress are currently unclear (**Table 1**) (Duan et al., 2019; Cinque et al., 2020). Additionally, hnRNP A1 stabilizes *SIRT1* mRNA (Wang et al., 2016); increased abundance of its protein product Sirtuin/SIRT1 prevents progression to cellular senescence, but also de-acetylates hnRNP A1 protein, which negatively regulates oncogenic cell proliferation by modulating alternative splicing of pro-survival mRNAs like *PKM* (**Table 1**) (Yang et al., 2019). Since both de-acetylation and acetylation at different sites on hnRNP A1 result in similar consequences (see **Table 1**), the regulation of cellular senescence and proliferation by hnRNP A1 by these processes may require additional experimental exploration.

HnRNP A1 and Telomeres

Further insights into hnRNP A1/DNA interactions have shown that hnRNP A1 also affects telomeric metabolism, in a multifaceted mechanism (**Figure 2B**). Firstly, hnRNP A1 helps destabilize the G-rich extension at the 3′ telomeric end through interactions with its RRMs to promote the association of telomerase (Ghosh and Singh, 2018). Additionally, hnRNP A1 binds to the single-stranded DNA and RNA component of telomerase and promotes its activation at the telomere (Wang et al., 2019). HnRNP A1 also promotes the Shelterin protein complex capping of telomeres through its binding with DNA-dependent protein kinase catalytic subunit (DNA-PKcs) (**Table 1**). HnRNP A1 is a direct substrate for DNA-PKcs, and phosphorylated hnRNP A1 promotes Shelterin complex formation by initially promoting the association of protection

TABLE 1 | Post-translational modifications of hnRNP A1.

	Amino acid location	Mediator	Consequence of PTM
Phosphorylation	Serine 4	S6K2	Decreased IRES RNA binding, increased IRES translation (Roy et al., 2014)
	Serine 6	VRK1	Increased telomerase activation (Choi et al., 2012)
		S6K2	Decreased IRES RNA binding, increased IRES translation (Roy et al., 2014)
	Threonine 51	PERK	Destabilization of hnRNP A1 protein (Koo et al., 2016)
	Serine 95	DNA-PKcs	Reduced RNA binding (Sui et al., 2015)
	Serine 192	DNA-PKcs MNK1	Regulation of splicing activity (van der Houven van Oordt et al., 2000; Buxade et al., 2005; Guil et al., 2006; Ziaei et al., 2012; Sui et al., 2015)
	Serine 199	AKT	Decreased IRES RNA binding, translocation to cytoplasm (Martin et al., 2011)
	Serines 310-312	MNK1, MNK2	Reduced TNPO1 interaction resulting in cytoplasmic accumulation (Allemand et al., 2005) Increased cytoplasmic retention with canonical stressors, but not with T-cell activation (van der Houven van Oordt et al., 2000; Buxade et al., 2005; Guil et al., 2006; Ziaei et al., 2012) Facilitates interaction with stress granules under canonical stressors (Guil et al., 2006)
Methylation	Arginine 31	PRMT3	Asymmetrical di-methylation Reduced RNA binding, permitting increased translation of the mRNA (Hsu et al., 2018)
	Arginine 218, Arginine 225	PRMT5	Symmetrical di-methylation Increased IRES-mediated translation from HIV and HTLV-1 viruses (Gao et al., 2017; Barrera et al., 2020) Decreased RNA binding activity
	Arginine 206, Arginine 218, Arginine 225, Arginine 232	PRMT1	Asymmetrical di-methylation Reduction in ITAF activity (Wall and Lewis, 2017)
Ubiquitination	Lysine 3, Lysine 8, Lysine 15	TRAF6	K63-linked ubiquitination Induction of alternative splicing (Fang et al., 2017)
	Lysine 183, **Lysine 298**[a]	SPSB1 with Elongins B & C and Cullins 2 & 5	Unconventional K29-linked ubiquitination Induction of alternative splicing (Wang et al., 2017) Some cytoplasmic accumulation Reduced RNA binding
	unknown	USP7, USP5	De-ubiquitination of hnRNP A1, results in hnRNP A1 protein stabilization (Vashistha et al., 2020; Zhang et al., 2020)
Acetylation	Lysine 3, Lysine 52, Lysine 87	*unknown*	De-acetylation by SIRT1 results in reduced cellular proliferation (Yang et al., 2019)
Sumo-ylation	Lysine 183	Ubc9[a]	Re-shuttling to the nucleus from the cytoplasm after mRNA transport. Requires prior phosphorylation on Ser4/6 and the binding of 14-3-3 protein (Roy et al., 2014)
β-N-acetyl-glucosamin-ylation	Serine 22	OGT[a]	Increased interaction with TNPO1 and enhanced nuclear localization (Hart et al., 2011; Roth and Khalaila, 2017)
PAR-ylation	**Lysine 298**[a]	PARP1	Promotes hnRNP A1 cytoplasmic localization to stress granules (Duan et al., 2019) Increases association with TDP-43 (Duan et al., 2019)

Amino acid numbering is based upon hnRNP A1 isoform A.
[a] *Putative.*
[b] *Bolded residues are in the hnRNP A1 M9 nuclear localization sequence.*
S6K2, ribosomal protein S6 kinase 2; VRK1, vaccinia-Related Kinase 1; PERK, eukaryotic translation initiation factor 2 alpha kinase 3; DNA-PKcs, DNA-dependent protein kinase catalytic subunit; MNK1/2 MAP, kinase signal-integrating kinase 1; AKT, protein kinase B; PRMT1/3/5, protein arginine methyltransferase; TRAF6, TNF receptor-associated factor 6; SPSB1, SplA/Ryanodine receptor domain and SOCS box containing 1; USP5/7, ubiquitin specific peptidase; Ubc9 SUMO, conjugating enzyme; OGT, O-linked N-Acetylglucosamine (GlcNAc) transferase; PARP-1, poly(ADP-Ribose) polymerase 1.

of telomeres 1 (POT1) protein to telomeres, that then associates with other Shelterin proteins to form a complex (**Figure 2B** and **Table 1**; Sui et al., 2015).

Phosphorylation is also key to how hnRNP A1 modulates telomerase activity during cell cycle progression. HnRNP A1 binds both G-quadruplex telomere DNA and telomere repeat-containing RNA (TERRA), as well as telomerase itself, and further modifies the balance between telomerase regulatory molecules RPA (replication protein A) and POT1 (**Table 1**; Fiset and Chabot, 2001; Flynn et al., 2011; Choi et al., 2012; Redon et al., 2013; Ghosh and Singh, 2018). HnRNP A1 has been found to have both negative and positive effects on telomerase activity and telomere length (Redon et al., 2013); some of this has been shown to be due to its phosphorylation. In G2/M phase cells, hnRNP A1 is phosphorylated at the SQ motif of Ser95 and Ser192 by DNA-PKcs, and at Ser6 by vaccinia-related kinase 1 (VRK1) (**Table 1**; Choi et al., 2012; Sui et al., 2015); VRK1-mediated phosphorylation appears to result in hnRNP A1 promoting telomerase activity, while phosphorylation by DNA-PKcs instead promotes hnRNP A1-mediated protection of telomeres from stimulating DNA damage responses (**Table 1**).

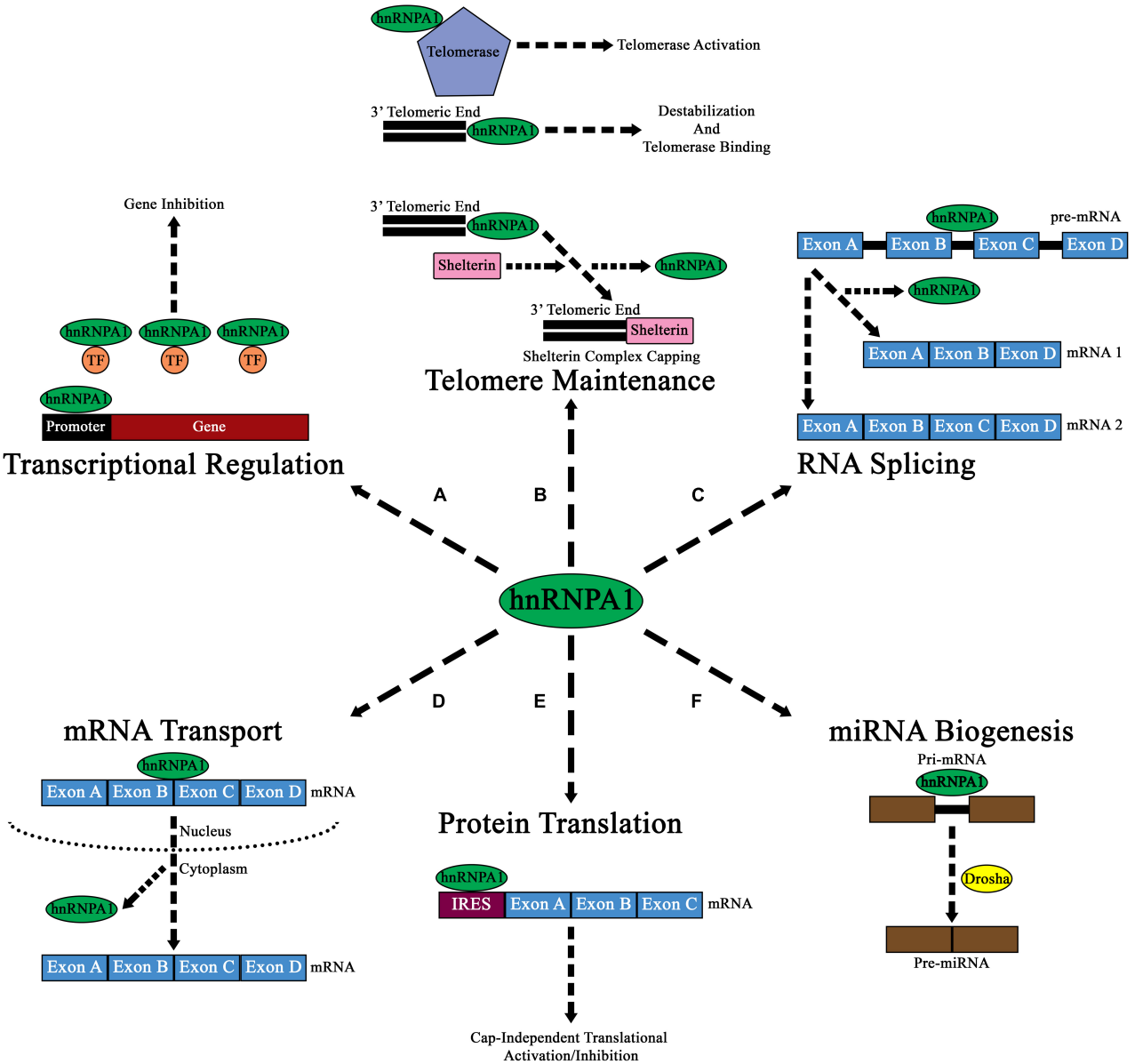

FIGURE 2 | Diagram of the major cellular functions of hnRNP A1. **(A)** Nuclear hnRNP A1 can regulate transcriptional expression by either promoter regulation, or by binding and sequestering transcription factors (TF; orange circles). **(B)** hnRNP A1 can also regulate telomeric elongation and capping either via telomerase binding and activation, direct 3' telomeric end binding, or by aiding in the binding of Shelterin complex proteins. The results of these interactions are to prevent NHEJ and telomere degradation. **(C)** Pre-mRNA splicing is a major component of hnRNP A1 nuclear function, and its binding can result in the formation of various mRNA isoforms from a single pre-mRNA transcript. **(D)** mRNA transport from the nucleus to the cytoplasm has been shown to be a major function of hnRNP A1, where hnRNP A1 directs mRNA to ribosomes for cap-dependen translation. **(E)** In addition to directing mRNA to ribosomes for cap-dependent mRNA translation in the cytoplasm, hnRNP A1 can also bind to IRES elements within mRNA and influence cap-independent translational activation or inhibition. **(F)** hnRNP A1 has been shown to influence the nuclear formation of pre-miRNAs from pri-miRNAs. While the exact mechanism of how hnRNPA1 affects this pathway is unknown, it is theorized that hnRNP A1 may influence Drosha (yellow circle) binding to pri-miRNA.

In this instance, phosphorylated hnRNP A1 functions in a pro-survival mechanism that prevents the unique structure of DNA telomeres exposed during the G2/M phase of cell cycle progression from aberrantly triggering DNA damage responses and cell death. Overall, the regulation of hnRNP A1 by several kinases affect cell survival through cell cycle progression. Its direct impact on neurodegenerative disease, however, remains to be explored.

HnRNP A1 and RNA Splicing

In addition to affecting RNA transcription and telomeric metabolism, hnRNP A1 plays a significant role in RNA splicing

(**Figure 2C**). HnRNP A1 is an essential component of the spliceosome, where it contributes to both constitutive and alternative mRNA splicing. HnRNP A1 acts as a negative *cis* splicing element, binding to either exonic splicing silencer (ESS) elements, or to intronic splicing silencer (ISS) elements found within pre-mRNA, leading to blocked exon recognition or promotion of exon exclusion in mRNA (Han et al., 2005). In neurodegenerative diseases, it has been theorized that altered hnRNP A1 binding to ESS or ISS elements within pre-mRNA may lead to pathogenesis. As described later in this review, altered splicing activity of hnRNP A1 to targets such as *SMN2*, *APP*, *TAU*, *MAG,* and even its own pre-mRNA, may lead to neurodegeneration.

The splicing process of hnRNP A1 is tightly regulated by a variety of PTMs that generally disrupt hnRNP A1 RNA binding activity – a common theme for controlling hnRNP A1 function – resulting in alternative splicing of hnRNP A1-regulated mRNAs. This has been characterized in the context of viral mRNAs as well as host mRNAs, and through a variety of stimuli. An early characterization utilized the Adenovirus E1A mRNA as a splicing reporter, identifying that activation of p38-MAPK through osmotic and UV stressors resulted in hnRNP A1 phosphorylation and alternative splicing of the viral mRNA (**Table 1**; van der Houven van Oordt et al., 2000). This also results in accumulation of hnRNP A1 in the cytoplasm, another common theme of the effects of PTMs of hnRNP A1 (van der Houven van Oordt et al., 2000). Later works indicate that it is likely MAP kinase signal-integrating kinase 1 (MNK1), a downstream kinase, that carries out p38-MAPK-stimualted phosphorylation (**Table 1**; Buxade et al., 2005; Guil et al., 2006; Ziaei et al., 2012).

HnRNP A1 alternative splicing activity has also been shown to be regulated by ribosomal protein S6 kinase 2 (S6K2) phosphorylation of hnRNP A1 Ser6 in cancer (discussed below) (**Table 1**; Sun et al., 2017). Non-canonical ubiquitination of hnRNP A1, however, has also been characterized as a regulator for hnRNP A1-mediated alternative splicing. Wang et al. determined that the adaptor protein SplA/Ryanodine receptor domain and SOCS box containing 1 (SPSB1) coordinates K29-linked ubiquitination of hnRNP A1 in response to EGF stimulation at Lys183 and Lys298 requires the Elongin B/C-Cullin 2/5 E3 ubiquitin ligase complexes (**Table 1**; Wang et al., 2017). This unusual ubiquitination reduces hnRNP A1 affinity for RNA and permits alternative splicing of rac family small GTPase 1 *(RAC1)* mRNA to the *RAC1B* isoform, as well as family with sequence similarity 13 member B (*FAM13B),* muscleblind like splicing regulator 1 *(MBNL1),* and RNA binding motif protein 10 *(RBM10)* (Wang et al., 2017). The *b* splice isoform of the Rac1 protein is associated with increased motility in cancer cells, while FAM13B function remains poorly characterized, and Rbm10 and MBNL1 are themselves both important regulators of mRNA splicing (Wang et al., 2017; Bergsma et al., 2018). In parallel, Fang et al. characterized hnRNP A1 in response to Toll-like receptor (TLR) signaling due sensing pathogen-associated molecules like bacterial lipopolysaccharides (Fang et al., 2017). This inflammatory signal stimulates TNF Receptor-Associated Factor 6 (TRAF6), an E3 ligase that is also a transducer of TLR signaling to ubiquitinate the RRM1 region of hnRNP A1 with K63-linkages, again resulting in reduced RNA binding to facilitate alternative splicing of many mRNAs (Fang et al., 2017). Overall, PTMs of hnRNP A1 that impact its splicing activities cause hnRNP A1 to release its protective binding at non-canonical exons, allowing alternative splicing using those exons and producing alternate forms of select mRNAs.

HnRNP A1, RNA Trafficking and Translation

HnRNP A1, however, can also affect mRNA translation, as it is an internal ribosome entry site (IRES)-trans activating factor (ITAF) that binds IRES sequences, and regulates ribosomal entry and/or transcript reading (Bonnal et al., 2005; Jo et al., 2008; Martin et al., 2011). Specifically, studies have shown that hnRNP A1 can regulate the IRES dependent translation of mRNAs that encode proteins related to apoptosis and proliferation (Bonnal et al., 2005; Lewis et al., 2007; Jo et al., 2008; Martin et al., 2011; Damiano et al., 2013).

HnRNP A1 has been identified to act as an IRES *trans*-activating factor (ITAF) to many cellular IRES containing mRNAs, including mRNAs for oncogenes and cell cycle regulators like Myc Proto-Oncogene Protein (c-Myc), Cyclin D, B-cell lymphoma-extra-large (BCL-XL), fibroblast growth factor 2 (FGF-2), and X-linked inhibitor of apoptosis (XIAP) (Bonnal et al., 2005; Martin et al., 2011; Roy et al., 2014). Cellular switching to IRES-mediated (cap-independent) translation can be initiated in response to cellular stressors, during cell cycle progression or growth signaling, or under aberrant signaling conditions like oncogenesis, and functions to permit production of select proteins while global cap-dependent translation is halted (Godet et al., 2019; Yang and Wang, 2019). HnRNP A1 binding to IRES sequences in mRNAs is thought to facilitate trafficking of the mRNAs to the cytoplasm, where subsequent phosphorylation of hnRNP A1 results in the protein releasing the IRES, allowing cap-independent translation to initiate (Martin et al., 2011; Roy et al., 2014; Sun et al., 2017). As an example, FGF2 stimulates the kinase S6K2 to phosphorylate Ser6 of RNA-bound hnRNP A1 in the nucleus, driving association with nuclear RNA export factor 1 (NXF1) and transport from the nucleus with IRES-containing mRNAs like *BCL-XL* and *XIAP* (**Table 1**; Roy et al., 2014). After cytoplasmic release of the mRNAs, the 14-3-3 protein binds phosphorylated hnRNP A1 and acts as an adaptor for an unknown Small Ubiquitin Like Modifier (SUMO) E3 ligase; SUMOylated hnRNP A1 then efficiently returns to the nucleus (Roy et al., 2014). Several other kinases have been implicated in similar regulation [e.g., protein kinase B (PKB; AKT), MNKs; see **Table 1**], and it is likely that different kinases carry out this phosphorylation dependent upon the stressor or stimulus (Martin et al., 2011; Roy et al., 2014; Sun et al., 2017). Particularly, S6K2 expression is associated with response to growth factor signaling and tumorigenesis, and its phosphorylation of hnRNP A1 at Ser4 and Ser6 may be aberrant in differentiated cells (Roy et al., 2014; Sun et al., 2017).

Protein arginine (Arg) methyltransferase PRMT5 also regulates hnRNP A1 promotion of IRES-dependent translation

of both HIV and HTLV-1 viral RNAs, and several cellular mRNAs through symmetrical di-methylation at Arg218 and Arg225 of hnRNP A1 (**Table 1**; Gao et al., 2017; Barrera et al., 2020). Methylation at these sites appears to have a similar impact as phosphorylation, resulting in decreased RNA binding and freeing IRES RNA structures to permit assembly of translation initiation factors (Gao et al., 2017; Barrera et al., 2020); methylation at Arg31 by PRMT3 has a similar effect, reducing hnRNP A1 binding to the cellular ATP binding cassette subfamily G member 2 (*ABCG2)* mRNA and increasing its protein abundance (Hsu et al., 2018). It is not clear from these studies whether these methylation events occur in the nucleus or cytoplasm, as the subcellular localization of PRMTs are highly variable (Tang et al., 1998; Frankel and Clarke, 2000; Rho et al., 2001; Lee et al., 2005; Meyer et al., 2007; Herrmann et al., 2009). Nonetheless, it is likely that PRMT5 methylation occurs in the cytoplasm, as decreased RNA binding in the nucleus would affect mRNA transport to the cytoplasm, where the assembly of translational machinery occurs. Alternatively, asymmetrical methylation of hnRNP A1 by PRTM1 at Arg206, 218, 225, and 232 has been shown to reduce IRES-mediated translation (**Table 1**; Wall and Lewis, 2017). When Hartel et al. screened the human "methylome" by a combination of biochemical methods with and without PRTM1 knockdown, they identified a switch in methylation of hnRNP A1 Arg206, from asymmetrical to symmetrical methylation, and suggest that this may be evidence of mutually antagonistic activities of PRTM1 and PRTM5 in regulating hnRNP A1 ITAF activity (**Table 1**; Hartel et al., 2019).

HnRNP A1 also modulates translation through binding in the 3′ UTR of mRNAs – this function was originally defined by hnRNP A1 binding in AU-rich elements (AREs) in mRNAs and reducing translation activity of the mRNAs. The mRNA for the inflammatory cytokine TNFα contains an ARE, as do many other cytokines' mRNAs; particularly, *TNF* has been shown to be bound, and its translation suppressed, by hnRNP A1. Buxadé et al. carefully defined the mechanism by which suppression is lifted and found that mRNA circularization brings 3′-bound translational regulatory factors into proximity to the translation initiation complex, permitting activated MNK1 to mono-phosphorylate hnRNP A1 at one of Ser310, Ser311, or Ser312 (**Table 1**; Buxade et al., 2005). Phosphorylation of hnRNP A1 in this poly-serine tract (comprised of Ser308-313, and Ser316) causes it to release the *TNF* mRNA, and de-repress its translation (**Table 1**; Buxade et al., 2005). Canonical stress-induced MNK1-mediated phosphorylation of hnRNP A1 also requires hnRNP A1 RNA-binding activity (**Table 1**). This suggests that hnRNP A1 is itself a better MNK1 substrate when bound to RNA; RNA-bound hnRNP A1 is also a better substrate for DNA-PKcs-mediated phosphorylation, although this latter activity may be predominantly associated with hnRNP A1 splicing activity (Zhang et al., 2004). While the key players may change depending upon stimulus, the core mechanism is likely common across hnRNP A1-regulated mRNA translational suppression.

HnRNP A1 Cellular Localization

HnRNP A1 also functions to transport mRNAs from the nucleus to the cytoplasm (**Figure 2D**) and affects mRNA translation (**Figure 2E**). The majority of characterized PTMs that regulate hnRNP A1 localization do so directly in the context of the protein's DNA or RNA-regulating functions. Particularly, several of the modifications that affect hnRNP A1 translation-modulating activities are driven by cellular stress responses and promote translocation to the cytoplasm. PARylation of hnRNP A1 by PARP-1 has been recently identified to occur in neurons in response to stress; PARP-1 activation broadly promotes SG formation, and PARylation of hnRNP A1 results in its nuclear depletion and increased accumulation in SGs (**Table 1**; Duan et al., 2019). Interestingly, Duan et al. note that hnRNP A1 has a putative PAR binding site between RRM1 and RRM2; while they find that hnRNP A1 PARylation and this site are both required for interaction with TDP-43 (another protein widely involved in neurodegenerative disease) in SGs, they do not define whether this may affect hnRNP A1 self-interaction (**Table 1**; Duan et al., 2019). In addition, unlike most of the research described above, Duan et al. monitor resolution of the stress response, finding that increased PARylation of hnRNP A1 results in delayed SG disassembly (Duan et al., 2019). This outcome provides a link between cellular stressors, PTMs of hnRNP A1, and a dysregulated stress response that could lead to long-term pathology.

In contrast, *O*-GlcNAcylation appears to modulate hnRNP A1 localization in the brief window where it is not interacting with or regulating RNA metabolism and appears to play a role in restoring hnRNP A1 nuclear localization. Roth and Khalaila have identified a single *O*-GlcNAc modification at Ser22 and demonstrate that *O*-GlcNAcylation increases hnRNP A1 association with TNPO1, the nuclear transport protein that returns hnRNP A1 to the nucleus to resume regulation of RNA production (**Table 1**; Roth and Khalaila, 2017). They do not define a cellular stimulus that promotes this modification but note that phosphorylation and *O*-GlcNAcylation can function antagonistically, such that *O*-GlcNAcylation may be potentiated by some of the hnRNP A1 phosphorylation states described above as a means of restoring hnRNP A1 nuclear localization and cellular homeostasis (Hart et al., 2011; Roth and Khalaila, 2017). Interestingly, SUMOylation in response to 14-3-3 binding of phosphorylated hnRNP A1 described above seems to serve the same or a similar purpose, marking RNA-depleted hnRNP A1 for return to the nucleus (**Table 1**; Roy et al., 2014).

Separately, increased MNK1 activity has been shown to promote hnRNP A1 localization to the cytoplasm during cellular senescence, although it is not yet clear whether MNK1 directly phosphorylates hnRNP A1 to facilitate this (**Table 1**; Ziaei et al., 2012). However, MNK1 has been shown to phosphorylate hnRNP A1 in NIH3T3s, and specifically at Ser192 and Ser310-311-312 in activated T-cells (**Table 1**; van der Houven van Oordt et al., 2000; Buxade et al., 2005). Additionally, activity of p38 MAP kinase (an upstream activator of MNK1) has resulted in hnRNP A1 phosphorylation and localization to the cytoplasm during cell stress (discussed above) and senescence (**Table 1**). Again, it is not clear whether p38 MAPK directly phosphorylates hnRNP A1, but overall activation of the MAPK signaling cascade seems to result in hnRNP A1 phosphorylation, translocation to the cytoplasm, and promotion of cellular senescence (Shimada et al., 2009).

A large proportion of the modifications described above should result in temporary alterations to hnRNP A1 function, including mRNA splicing, transport, and translation. These data provide the first means to resolve these responses and restore homeostatic function, and it is likely that dysregulation of these resolution processes can themselves be pathological.

HnRNP A1 Stability and Other Functions

Turnover of hnRNP A1 protein is mediated by ubiquitination, like much of the mammalian proteome. Wen et al. have recently identified a long non-coding RNA, *ANCR*, that prevents ubiquitination of hnRNP A1, resulting in its stabilization, but whether *ANCR* prevents ubiquitination or promotes de-ubiquitination of hnRNP A1, and by what mechanisms, is unknown (Wen et al., 2020). Zhang et al. and Vashistha et al. have separately characterized two de-ubiquitinating enzymes [Ubiquitin Specific Peptidase 5 and 7 (USP5 and USP7), respectively] that remove classical K48-linked ubiquitin degradation markers and prevent hnRNP A1 degradation; both of these studies were done in the context of oncogenesis and chemotherapy resistance, and indicate a role of stabilized hnRNP A1 in cellular survival (**Table 1**; Vashistha et al., 2020; Zhang et al., 2020). In contrast, Koo et al. have found that eukaryotic translation initiation factor 2 alpha kinase 3 (PERK)-mediated phosphorylation of hnRNP A1 at Thr51 results in hnRNP A1 degradation in response to endoplasmic reticulum stress (e.g., exposure to tunicamycin or thapsigargin), although the mechanism of this destabilization is not understood (**Table 1**; Koo et al., 2016). HnRNP A1 regulates the processing of at least two known microRNAs (miRNAs), pri-miR-18a and pri-Let-7a, which themselves modulate mRNA stability and translation (**Figure 2F**). HnRNP A1 binds to primary miRNA (pri-mRNA) in the nucleus and is thought to promotes cleavage into pre-miRNA by promoting Drosha protein binding (Guil and Caceres, 2007; Michlewski and Caceres, 2010; Michlewski et al., 2010). Thus, when hnRNP A1 is depleted, the authors find a reduction in miR-18a processing and activity in hepatic stellate cells, broadly increasing the translation of several targets and promoting fibrotic signaling in the liver (Koo et al., 2016). Clearly, the consequence of global changes to hnRNP A1 abundance vary by cell type and stimulus; there is a large body of data from hnRNP A1 overexpression and knockdown experiments, but metrics of interest are rarely defined compared to hnRNP A1 abundance. However, a recent paper by Duan et al. (discussed above) uses PARylation inhibition to abrogate the effects of long-term hnRNP A1 overexpression in neuron-like cells, suggesting that long-term hnRNP A1 accumulation likely leads to cell stress signaling mediated by PARylation in a neuronal context (Duan et al., 2019).

HnRNP A1 AND NEURODEGENERATIVE DISEASES

A consequence of the toxic accumulation of proteins within the neuronal milieu of neurodegenerative disease is perturbation in RNA metabolism [reviewed in Liu et al. (2017)]. While the contribution of hnRNP A1 to the disturbance of RNA metabolism and its subsequent consequences has been characterized in cancer and viral immunology, the role of hnRNP A1 in altered RNA metabolism in neurodegenerative disease is less well understood. This lack of understanding is in part due to the complicated systemic nature of neurodegenerative diseases, where physical brain architecture, interactions with the immune system, and multiple glial cell types all contribute to disease progression, making modeling difficult. Identification of molecular players has historically begun with detection of associations between heritable or spontaneous mutations and disease, only then leading to careful characterization in animal models and cell culture. Studies in amyotrophic lateral sclerosis (ALS), frontotemporal lobar degeneration (FTLD), multiple sclerosis (MS), spinal muscular atrophy (SMA), Alzheimer's disease (AD) and Huntington's disease (HD) all show compelling evidence that suggests hnRNP A1 may influence neurodegenerative disease pathogenesis (**Table 2** and **Figure 3**). However, our understanding of the molecular mechanisms – including regulation by PTMs – by which hnRNP A1 contributes to these diseases remains incomplete.

Amyotrophic Lateral Sclerosis (ALS) and Frontotemporal Lobar Degeneration (FTLD)

Insights into ALS and FTLD have shown that genetic mutations and altered expression of hnRNP A1 may influence pathogenesis. Mutations in hnRNP A1 have been associated with forms of ALS and FTLD and have been suggested to affect hnRNP A1 insoluble protein aggregation. HnRNP A1 is hypothesized to promote insoluble protein aggregation through mutations found in its PrLD, resulting in alterations in protein-protein interactions, including self-association and fibrillization propensity. In a study on a family with multisystem proteinopathy (MSP), a rare syndrome that includes inclusion body myopathy with FTLD, Paget's disease of bone and ALS, the authors reported three distinct mutations in hnRNP A1, p.D262V, p.D262N and p.N267S (Kim et al., 2013). These mutations were found in the PrLD of hnRNP A1 and were shown to both increase the recruitment of hnRNP A1 to SGs and accelerate hnRNP A1 fibrillization and the formation of prionogenic protein accumulations, by both deregulating and accelerating the nucleation and polymerization process of hnRNP A1 (**Figure 3**; Kim et al., 2013).

The downstream effects of altered hnRNP A1 protein dynamics are still currently under investigation, but a prevailing theory is that SG biology is a likely target of dysregulation. This theory is supported by data that demonstrates that a genetic missense mutation in the PrLD of hnRNP A1 found in ALS patients (c.862.1018C > T/p.P288S) resulted in the cytoplasmic mislocalization of hnRNP A1 and the formation of cytoplasmic inclusions (**Figure 3**; Liu et al., 2016). The authors further showed that hnRNP A1 inclusions colocalized with SGs but did not elaborate further on the effect of hnRNP A1 inclusions on SG dynamics (**Figure 3**; Liu et al., 2016). Interestingly, these results were similarly replicated in a separate study where the

TABLE 2 | Proposed mutations and effects of hnRNP A1 dysfunction in neurodegenerative diseases.

Neurodegenerative Disease	Disease-associated mutations	Proposed hnRNP A1 altered function	Disease alteration
ALS/FTLD	[a] p.D262V	Nucleocytoplasmic transport	Prolonged LLPS leading to increased protein-protein interactions.
	p.D262N p.N267S	Nucleocytoplasmic transport	Increased cytoplasmic insoluble hnRNP A1 aggregation.
	p.P288S p.P288A	Nucleocytoplasmic transport	Altered SG dynamics, leading to stable and prolonged SG formation.
		RNA splicing	Altered interaction with TDP-43, leading to increased longer *hnRNP A1* splice variant formation.
SMA		RNA splicing	Formation of unstable and truncated SMN1 protein from *SMN2* RNA.
MS and HAM/TSP	[b] p.S252N	Nucleocytoplasmic transport	Antibodies produced by an immune response bind to hnRNPA1, sequestering it in the cytoplasm and leading to increased insoluble hnRNP A1 aggregation.
	p.S259G p.N265D	RNA splicing	Cytoplasmic mislocalization of hnRNPA1 leading to the dysregulation of spastin, spartin and paraplegin splicing.
	p.F263L p.F273L	Nucleocytoplasmic transport	Somatic mutations in hnRNP A1 lead to increased cytoplasmic retention and increased insoluble hnRNPA1 aggregation.
	p.P275S p.M276L p.K277N p.N280S p.F281L p.R284G p.S285G p.Y295C p.F296L p.P299L p.R300S p.N301D p.N301S p.S308P p.S313G p.Y314C p.Y314H p.G317D p.G317S p.R318G p.R319G p.F320L	RNA splicing	Altered *S-MAG/L-MAG* mRNA ratio, leading to an increase in *S-MAG* mRNA and protein expression. No direct evidence in MS, but data from EAE mice show a depletion in MAG protein in the spinal cord.
Alzheimer's disease		RNA splicing	Increased generation of longer *APP* splice variant, leading to increased amyloid-β formation.
		RNA splicing	Increased generation of *mRAGE* mRNA, leading to an increase in mRAGE expression.
		RNA splicing	Altered *4R-Tau/3R-Tau* mRNA ratio, leading to tauopathy.
Huntington's disease		mRNA stability	Increased expression of Drp1, leading to increased mitochondrial fragmentation and cell death.

[a] *Germline Mutations.*
[b] *Somatic Mutations.*

authors discovered the familial ALS genetic missense hnRNP A1 mutation p.P288A and described its propensity to also form cytoplasmic inclusions that colocalized with SGs (**Figure 3**; Naruse et al., 2018). Further, a current study under review has demonstrated that the p.P288A and p.D262V mutations, as well as newly found mutations p.G304Nfs*3, p.*321Eext*6 and p.*321Qext*6, have altered self-aggregation properties, undergo reduced LLPS, and in the case of p.P288A and p.D262V, attenuate both SG formation and dissociation properties (Beijer et al., 2021). A subset of these hnRNP A1 mutations introduce new potential phosphorylation sites that may aberrantly regulate hnRNP A1 functionality, contributing to disease (Blom et al., 1999, 2004).

As mentioned above, TDP-43 interacts with hnRNP A1 through its PrLD and influences the splicing activity of hnRNPA1, as well as modulates *HNRNP A1* mRNA splice

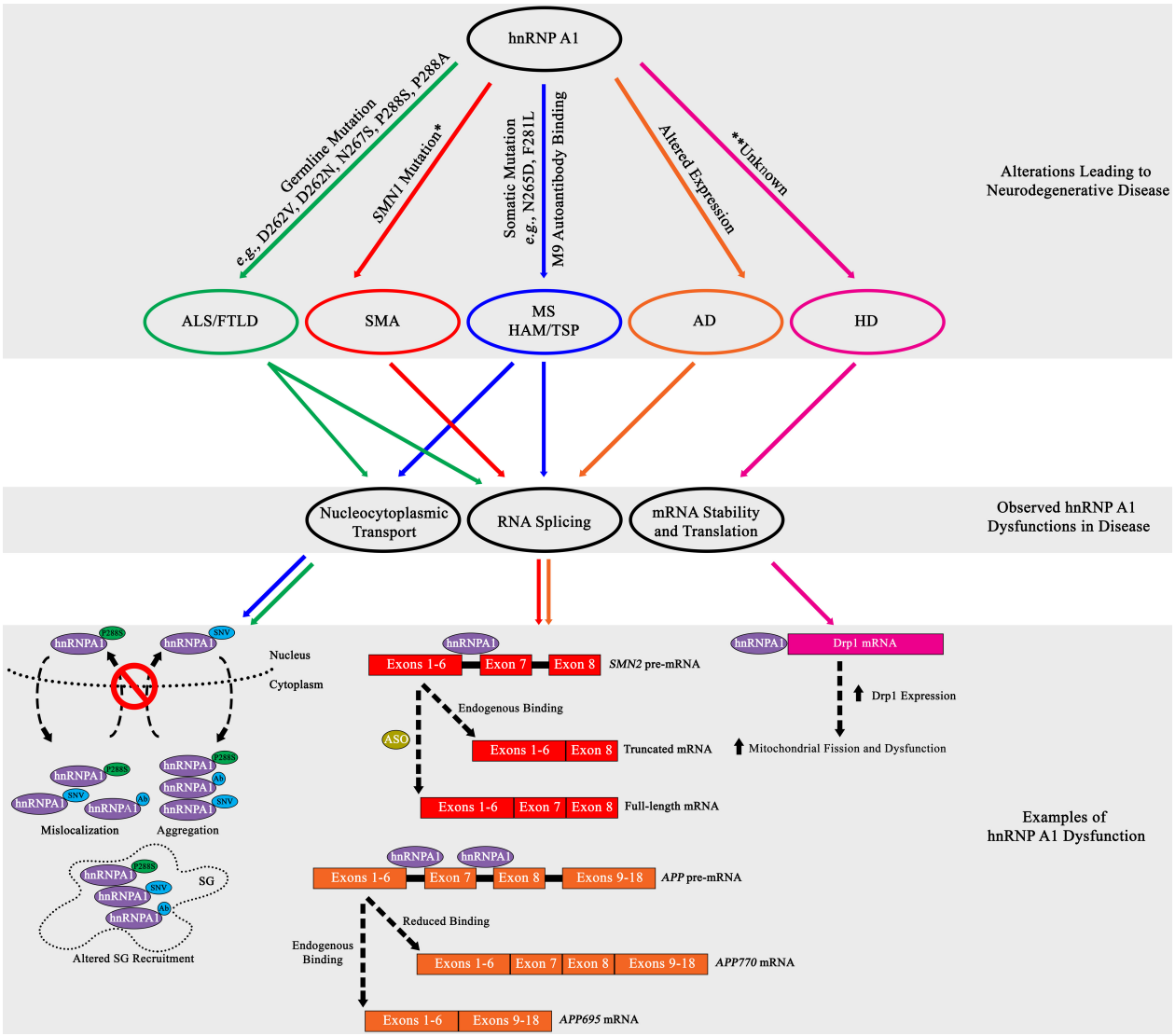

FIGURE 3 | Summary diagram of hnRNP A1 dysfunctional pathways leading to neurodegenerative disease pathogenesis. Top Grey Box: HnRNP A1 alterations that are disease specific (ALS/FTLD, green; SMA, red; MS and HAM/TSP, blue; AD, orange; HD, pink) lead to pathogenesis. Middle Gray Box: Commonly observed hnRNP A1 dysfunctions in neurodegenerative diseases are nucleocytoplasmic transport deficits (leading to protein mislocalization, aggregation and altered SG recruitment), dysregulated RNA splicing, and modification of target mRNA stability. Bottom Gray Box: Selectively highlighted examples of hnRNP A1 dysfunction in neurodegenerative disease. Each dysfunctional mechanism is colour coded for the disease it refers to. Refer to the individual neurodegenerative disease sections for more information. Ab = antibody. *Dysregulation of the SMN1 gene precedes the effects of hnRNP A1 splicing.

variant formation (Deshaies et al., 2018). Specifically, research has shown that depleting endogenous TDP-43 with siRNA in HeLa cells increases the retention of exon 7B in *HNRNP A1* mRNA, resulting in increased *HNRNP A1-B* isoform expression (Deshaies et al., 2018). The result of this increase was the generation of toxic cytoplasmic hnRNP A1 aggregates that were also comparable in size to those found in cells expressing the ALS hnRNP A1 mutation D262V (Deshaies et al., 2018). While this study focuses primarily on the effect of TDP-43 perturbation on altered hnRNP A1 dynamics, mutational alterations of hnRNP A1 might similarly influence TDP-43 interaction. Furthermore, since TDP-43 is suggested to affect both ALS and FTLD disease progression, it is possible that hnRNP A1 may play a similar role.

Spinal Muscular Atrophy (SMA)

The stringent regulation of survival of motor neuron 1 (*SMN1*) RNA splicing is essential to the survival of α-motor neurons in the anterior horn of the spinal cord and has been shown to be significantly influenced by hnRNP A1. Briefly, the homozygous loss, interruption, or autosomal recessive mutation in the *SMN1* gene culminates in the reduced expression of SMN1 protein, resulting in SMA progression (Lefebvre et al., 1995, 1997). While *SMN1* deficiency is partially compensated for by the

SMN2 gene, a near identical copy of the *SMN1* gene, *SMN2* cannot fully compensate for *SMN1* genetic loss (Lefebvre et al., 1995, 1997). Research has established that although *SMN2* is transcribed comparably to *SMN1*, a silent genetic mutation in *SMN2* (c.840C > T) transforms a 3′ splice site ESE element within exon 7 into an ESS element, resulting in the translation of an unstable, truncated SMN1 protein due to the majority of *SMN2* mRNA lacking exon 7 (Cartegni and Krainer, 2002; Kashima and Manley, 2003). Research has established that hnRNP A1 binds to the ESS element found in *SMN2*, influencing the exclusion of exon 7, leading to SMN1 deficiency and disease pathogenesis (**Figure 3**; Kashima et al., 2007; Doktor et al., 2011). Binding of hnRNP A1 has been theorized to either directly block the 3′ splice site, or after initial binding, propagate along the exon or along the RNA polypurine tract to inhibit spliceosomal recognition and recruitment (**Figure 3**; Doktor et al., 2011).

Additional research suggests that hnRNP A1 binds to an ISS element in *SMN2* RNA resulting in its alternative splicing (**Figure 3**; Beusch et al., 2017). While the regulatory effects of phosphorylation on hnRNP A1-mediated alternative splicing have been characterized for other mRNAs, *SMN2* has yet to be explored in this context. The authors of this study indicate that both RRMs of hnRNP A1 bind to an intron 7 bipartite ISS element in *SMN2* RNA, in a cumulative and directional manner, with RRM2 contacting a 5′ motif and RRM1 contacting a 3′ motif, resulting in exon 7 exclusion (Beusch et al., 2017). In parallel, another study treated SMA fibroblast cells with the histone deacetylase (HDAC) inhibitor valproic acid and showed a decrease in hnRNP A1 protein expression that coincided with an increase in exon 7 *SMN2* transcription (Harahap et al., 2012).

The studies presented above suggest that targeting hnRNP A1 alternative splicing activity may have therapeutic value. In this regard, to date the most successful research on improving the translation of stable, full-length SMN1 through hnRNP A1 mediation was observed in a series of studies that utilized anti-sense oligonucleotide (ASO) blocking of the bipartite ISS element, thus blocking hnRNP A1 binding, which showed an enhanced inclusion of *SMN2* exon 7 by approximately 90% (Hua et al., 2007, 2008). The collective information from these and associated studies has led to the development of Nusinersen (Spinraza®), an ASO treatment that was FDA approved in 2016 for the treatment of infantile- and later-onset SMA (Finkel et al., 2017; Mercuri et al., 2018).

Autoimmune Diseases of the Central Nervous System (CNS): Multiple Sclerosis (MS) and Human T-Lymphotropic Virus Type 1 (HTLV-1) Associated Myelopathy/Tropical Spastic Paraparesis (HAM/TSP)

Studies of MS and HAM/TSP have implicated hnRNP A1 dysfunction as a contributor to disease pathogenesis. Previously described as a predominantly demyelinating disease, MS is now considered both a disease of inflammatory-mediated demyelination and neurodegeneration (loss or damage to neurons and axons) (Peterson and Fujinami, 2007). These pathologic features are also present in HAM/TSP, which resembles progressive forms of MS clinically, but unlike MS, has been shown to be caused by infection with HTLV-1 (Jernigan et al., 2003; Lee et al., 2008, 2012).

Our lab showed that molecular mimicry contributed to the pathogenesis of HAM/TSP via cross-reactive antibodies between HTLV-1 and neuronal antigens. Specifically, we initially reported that IgG isolated from HAM/TSP patients and a monoclonal antibody (Mab) to HTLV-1 tax (the regulatory region of HTLV-1) stained neurons in human brains from healthy controls (Levin et al., 1998). This suggested that there was molecular mimicry between the viral and host proteins recognized by the antibodies. HAM/TSP IgG immunoreacted with a 33-38 kDa protein isolated from human neurons and the immunoreactive host protein was identified as hnRNP A1 by matrix assisted laser desorption ionization (MALDI) mass spectroscopy (NM). Further investigation revealed that both the tax Mab and HAM/TSP IgG immunoreacted with hnRNP A1 (Levin et al., 2002a; Lee S.M. et al., 2006). The epitope of the monoclonal antibody mapped to tax 346-353 (KHFRETEV) and that of HAM/TSP IgG within hnRNP A1-M9 (293-GQYFAKPRNQGG-304) (Levin et al., 2002b; Lee S.M. et al., 2006). The tax Mab also immunoreacted with the identical hnRNP A1-M9 epitope (Lee S.M. et al., 2006). Pre-absorption of the tax Mab with hnRNP A1 inhibited tax Mab staining for human neurons and immunoreactivity with hnRNP A1 by Western blot. Taken together, these data indicate molecular mimicry between hnRNP A1 and HTLV-1-tax. There was little primary sequence identity between the viral and host epitopes. This is common, considering that molecular mimicry due to immunologic cross-reactivity as shown by these and other data have increased biological significance compared with mimics defined by primary sequences (Oldstone, 1998; Albert and Inman, 1999; Gran et al., 1999; Lee and Levin, 2008). Indicative of anti-hnRNP A1 IgG's biological activity and potential pathogenicity, further studies showed that anti-hnRNP A1 antibodies inhibited neuronal firing using whole-cell current clamp recordings of individual rat neurons (*ex vivo*) and immunostaining immunoreactivity to hnRNP A1 was greatest in the corticospinal system of human brain (Levin et al., 2002a; Kalume et al., 2004).

With a close biological and pathological relationship between HAM/TSP and MS, it was hypothesized that MS patients might also develop autoantibodies to hnRNP A1. Our lab confirmed this in later studies, and further found that the immunodominant epitope of the autoimmune IgG response was specific for the M9 domain (**Figure 1B**; Lee et al., 2011; Levin et al., 2012, 2013; Douglas et al., 2013). It was also found that anti-hnRNP A1 antibodies entered neuronal cells through clathrin-mediated endocytosis in neuronal cell lines (Mohamed et al., 2002; Douglas et al., 2013) and exacerbated the nucleocytoplasmic mislocalization of hnRNP A1 in animal models of disease (**Figure 3**; Lee B.J. et al., 2006; Lee et al., 2011; Levin et al., 2012, 2013). Subsequent studies showed that *in vitro* neuronal cell lines exposed to anti-hnRNP A1 monoclonal antibodies, again overlapping the human immunodominant M9 epitope, developed: (Chung et al., 2018) increased markers of

neurodegeneration, apoptosis and reduced levels of ATP (Liu et al., 2017) changes in gene expression related to the clinical phenotype of progressive MS patients and (Kashima et al., 2007) mislocalization of hnRNP A1 from the nucleus to the cytoplasm (Douglas et al., 2013, 2016).

Observations in neurons of MS brains have shown the cytoplasmic mislocalization of hnRNP A1. We initially reported hnRNP A1 mislocalization from the nucleus to the cytoplasm, where it co-localized with SGs, in neurons of a brain from an MS patient with aggressive disease (Salapa et al., 2018). In a more recent study, we carried out a comprehensive analysis of over 2700 neurons examined from twelve MS compared to six healthy control brains showed nucleocytoplasmic mislocalization of hnRNP A1 and TDP−43 statistically distinguished MS from control cases (Salapa et al., 2020). There were also neurons in MS cases that displayed nuclear depletion of hnRNP A1 and TDP-43 (Salapa et al., 2020). Nuclear depletion is a marker of neuronal injury and death and was not present in the healthy controls (Salapa et al., 2020). These results were paralleled *in vivo* in mice with experimental autoimmune encephalomyelitis (EAE), an animal model of MS, where hnRNP A1 mislocalization and SG formation are observed in spinal cord neurons of EAE, but not naïve mice (Douglas et al., 2016; Lee et al., 2019; Libner et al., 2020). Additionally, in separate experiments with EAE-induced mice, anti-hnRNP A1 antibodies were injected into EAE mice upon presenting limp tail physiology, a clinical sign of initial disease progression in EAE (Douglas et al., 2016; Libner et al., 2020). In these studies, we observed an exacerbation of clinical phenotypes throughout the EAE time-course, and upon visualization of spinal cord motor neurons at all cord levels, found predominant localization of antibodies to ventral gray matter motor neurons, significant increases in neuronal hnRNP A1 mislocalization and SG formation in thoracic and lumbar regions, and significant neuronal cell loss in thoracic and lumbar motor neurons (Douglas et al., 2016; Libner et al., 2020). Furthermore, these mice also displayed spastic paraparesis, a common clinical feature of the progressive MS phenotype (Douglas et al., 2016; Libner et al., 2020). Throughout these experiments with tissue culture, animal models, and human tissues, we have found a common theme of hnRNP A1 mislocalization and association with induced SGs (**Figure 3**); other data demonstrates that this can be regulated by several PTMs in response to acute stressors, and so it remains to be seen how this is regulated under chronic inflammatory stress signaling.

While germline mutations in hnRNP A1 have not been described in the pathogenesis of MS, an accumulation of somatic mutations in hnRNP A1 were identified in lymphocytes of progressive MS patients. Specifically, experiments showed novel single nucleotide variants (SNVs) in hnRNP A1, in the PrLD domain (e.g., c.793A > G/N265D) and M9 sequence (e.g., c.841T > C/F281L) (Lee and Levin, 2014). Experimentally, it was shown that transfection of these hnRNP A1 mutants into neuronal-like cells influenced hnRNP A1 cytoplasmic mislocalization, SG formation, and binding to Transportin-1 (**Figure 3**; Lee and Levin, 2014; Salapa et al., 2018). While the specific mechanisms of how hnRNP A1 mutations contribute to dysfunction are currently unknown, results indicate an influence in altered SG biology, altered RNA metabolism and the induction of apoptosis (**Figure 3**). Overall, the discovery of somatic mutations in hnRNP A1 in MS supports a tripartite hypothesis, where an environmental trigger, in a genetically susceptible individual, causes an autoimmune response to CNS antigens that results in MS pathology (Lee and Levin, 2014).

As it is still mechanistically unknown how hnRNP A1 dysregulation leads to MS pathogenesis, some targets have been proposed. Recently, a study showed that hnRNP A1 contributes to myelin associated glycoprotein (MAG) RNA splicing by interacting with a motif in intron 12, immediately downstream of the 5′ splice site in exon 12 (Zearfoss et al., 2013). Molecularly, *MAG* mRNA can occur as two alternatively spliced isoforms, a shorter variant that includes exon 12 and contains a termination codon (*S-MAG*), and a longer variant where exon 12 is spliced out (*L-MAG*) (Quarles, 2007). The authors show that hnRNP A1 binding blocks 5′-splice site recognition in *MAG* pre-mRNA, inhibiting the inclusion of exon 12, thereby forming the *L-MAG* mRNA isoform (Zearfoss et al., 2013). They further confirmed this by reducing the expression of hnRNP A1 with siRNA and showed an increase in *MAG* exon 12 inclusion, producing more *S-MAG* isoform mRNA (Zearfoss et al., 2011). While a potential disruption in the S-MAG/L-MAG ratio has yet to be specified in MS, a study using the EAE mouse model observed a depletion in MAG protein levels in the spinal cord, resulting in an increase in PARP-1 cleavage, and an increase in apoptosis activation in glial and neuronal cells (Skundric et al., 2008). This cleavage abrogates the PARylation activity of PARP-1, preventing its ability to regulate hnRNP A1 accumulation in SGs (Blom et al., 2004; Duan et al., 2019). Additionally, antibodies toward MAG have been found in the CSF of MS patients, and MAG is thought to be a specific target of neuroinflammation, leading to its role in the dysregulation of axonal demyelination (Moller et al., 1989; Baig et al., 1991). Overall, these results suggest the control of *MAG* RNA splicing by hnRNP A1 may be an interesting target for further study, as well as present another avenue where hnRNP A1 dysregulation may influence MS pathogenesis.

Alzheimer's Disease

Alzheimer's disease (AD) is characterized by the formation of amyloid-β and Tau aggregates, leading to neuronal dysfunction and death. Current research suggests that hnRNP A1 may influence the formation of both amyloid-β and Tau aggregates. HnRNP A1 is theorized to affect amyloid-β formation through its effect on the alternative splicing of amyloid precursor protein (APP) pre-mRNA (Donev et al., 2007). Specifically, hnRNP A1 has been reported to influence the splice variation of pre-mRNA *APP* through binding to *Alu* RNA elements that are located on either side of exon 7 (Donev et al., 2007). The RNA transcribed from the *Alu* elements in the sense orientation contain a sequence of GCGGA that partially matches the high-affinity binding sequence of the RRM in hnRNP A1 (Donev et al., 2007). By binding to *Alu* elements, hnRNP A1 influences the alternative splicing of both exons 7 and 8, thereby affecting the generation of APP splice variants (**Figure 3**; Donev et al., 2007). Reduced expression of hnRNP A1, which has been observed in

neurons of AD patients, limits the production of *APP* mRNA with skipped exons 7 and 8 (*APP770* mRNA) (**Figure 3**; Donev et al., 2007). To remedy this, studies suggest treatment with estradiol may result in an increased expression of hnRNP A1, and the formation of spliced *APP* mRNA that produces lower levels of amyloid-β (*APP695* mRNA) (Donev et al., 2007; Villa et al., 2011). Additionally, cholinergic signaling may also play a role in controlling hnRNP A1 expression, and a loss of cholinergic neurons, as observed in AD, may contribute to hnRNP A1 down-regulation, and modified alternative splicing of *APP* mRNA (Berson et al., 2012). Interestingly, the effect of kinase inhibitors to prevent hnRNP A1-mediated alternative splicing on exclusion of exons 7 and 8 from *APP* mRNA has not been explored.

In addition to potentially influencing amyloid-β production, hnRNP A1 has also been reported to affect the splicing of the receptor for advanced glycation end-products (*RAGE*). Amyloid-β binding to membrane-bound RAGE leads to its improper activation, resulting in a chronic cellular immune response and dysfunction and death of neurons (Lue et al., 2001; Son et al., 2012). It has been shown that increased expression of hnRNP A1 is associated with changes in two splice variants of *RAGE*, including an increase in membrane RAGE expression, and a decrease in secretory RAGE expression in AD patients (Nozaki et al., 2007; Liu et al., 2015).

Another study indicates that hnRNP A1 influences AD by modulating *TAU* splicing. The authors show that hnRNP A1 promotes the formation of *3R-TAU* mRNA through the exclusion of exon 10 (Liu et al., 2020). Mechanistically, the authors suggest that hnRNP A1 inhibits the splicing of intron 9, but not intron 10, through a direct interaction with a 3′ splice site in exon 10 of *TAU* pre-mRNA, thus promoting the exclusion of exon 10 (Liu et al., 2020). Reduction in hnRNP A1 expression using siRNA led to an increase in both exon 10 inclusion in *TAU* pre-mRNA, leading to an increase in 4R-Tau protein expression (Liu et al., 2020). This study, however, only demonstrates a correlation between hnRNP A1 dysfunction and tauopathy modulation in AD, and further research is needed to ascertain whether this mechanism affects the pathogenesis of AD. Overall, the effect of phosphorylation or unconventional ubiquitination of hnRNP A1 on alternative splicing of these AD-associated mRNAs have not been characterized, but it is likely to be relevant since this could provide a means to modulate all three of these dysregulated mRNAs.

Huntington's Disease

Recently, hnRNP A1 been suggested to influence Huntington's disease (HD) through mitochondrial mechanisms. Current data shows that hnRNP A1 regulates the expression of dynamin-related protein 1 (Drp1), through an interaction with the 3′-UTR of *DRP1* mRNA (Park et al., 2015). Drp1 is a GTPase protein primarily located in the cytosol and is recruited to the mitochondria where it acts in a concert with other proteins to promote mitochondrial fission using GTPase hydrolysis (Shirendeb et al., 2012). This is important in HD because reports have shown that Drp1 expression is increased in the post-mortem brains of HD patients and data indicate that Drp1 dysfunction, caused by mHtt, may result in excessive mitochondrial fission and fragmentation (Song et al., 2011; Shirendeb et al., 2012; Guo et al., 2013). While the specifics of the hnRNP A1 and *DRP1* mRNA interaction are unknown, or whether hnRNP A1 influences *DRP1* mRNA splicing or stability, the data does show that hnRNP A1 does not significantly change the levels of *DRP1* mRNA, suggesting hnRNP A1 control of Drp1 does not affect the generation of *DRP1* pre-mRNA (Park et al., 2015). Furthermore, current data shows that downregulating hnRNP A1 with siRNA results in a significant decrease in Drp1 protein expression, while the opposite was observed with hnRNP A1 overexpression (**Figure 3**; Park et al., 2015). This suggests a pro-translational effect of hnRNP A1 on *DRP1*, although no IRES has been identified for *DRP1*. Morphologically, downregulation of hnRNP A1 resulted in increased mitochondrial fusion and decreased fragmentation, both indicators of mitochondrial dysfunction (Park et al., 2015). Additionally, 3-nitropropionic acid (3-NP) treatment, an inhibitor of mitochondrial complex II, paired with hnRNP A1 downregulation, leads to cell death and caspase activation inhibition, and there is subsequent recovery of mitochondrial membrane potential and ATP levels (Park et al., 2015). Based on these results, it is suggested that hnRNP A1 dysregulation, caused possibly by either overexpression or cell stress meditation, potentially causes the enhanced expression of Drp1, leading to mitochondrial dysfunction (**Figure 3**; Park et al., 2015). The specific mechanism of how this occurs, however, have not been reported, but further investigation of hnRNP A1 in HD would help elucidate its role in pathogenesis.

CONCLUSION

While hnRNP A1 has been studied for over 40 years, only recently has hnRNP A1 dysfunction been shown to contribute to the pathogenesis of neurodegenerative disease. The functional view of hnRNP A1 has evolved past its depiction as a protein primarily involved in RNA metabolism, to a protein involved in the specific regulation of many cellular processes that have important functions in health and disease. Research describing such functions as LLPS, membraneless organelle formation, and protein aggregation, have consistently shown that hnRNP A1 contributes significantly to both normal and perturbed function, and may play a greater role than once thought. The mechanisms that hnRNP A1 utilizes to regulate each function, however, are not completely understood, but ongoing and future research aim to clarify and augment current knowledge, with a goal to develop therapeutics. This is especially exemplified in current SMA research, where new knowledge on hnRNP A1 endogenous function has led to successful therapeutic development.

Adding to the complexity of hnRNP A1 in endogenous and perturbed molecular functions are PTMs. While there has been extensive characterization of the effects of myriad PTMs on hnRNP A1 function in cell survival and acute stress responses, research in the context of neurodegenerative disease has been lagging. Although neurodegenerative disease has not extensively been the focus of hnRNP A1 research to date, it is still reasonable

to theorize that PTMs may influence pathogenesis and may be an eventual target for disease therapeutics.

As there are still gaps in our understanding of hnRNP A1 regulation and dysfunction in neuronal health, continued research into the mechanisms and outcomes of hnRNP A1 dysfunction will help elucidate the contribution of hnRNP A1 in neurodegenerative disease and hopefully lead to therapies for improved outcomes.

AUTHOR CONTRIBUTIONS

JC designed the figures and tables, and was the primary writer of the manuscript. PT contributed to manuscript content and edited the manuscript. HS reviewed and edited the manuscript. ML reviewed and edited the manuscript, and approved the final version, including figures. All authors contributed to the article and approved the submitted version.

FUNDING

This research was funded by Saskatchewan Health Research Foundation (SHRF), Award #4244, and the Office of the Saskatchewan Multiple Sclerosis Research Chair, University of Saskatchewan.

REFERENCES

Albert, L. J., and Inman, R. D. (1999). Molecular mimicry and autoimmunity. *N. Engl. J. Med.* 341, 2068–2074.

Allemand, E., Guil, S., Myers, M., Moscat, J., Caceres, J. F., and Krainer, A. R. (2005). Regulation of heterogenous nuclear ribonucleoprotein A1 transport by phosphorylation in cells stressed by osmotic shock. *Proc. Natl. Acad. Sci. U S A.* 102, 3605–3610. doi: 10.1073/pnas.0409889102

Baig, S., Olsson, T., Yu-Ping, J., Hojeberg, B., Cruz, M., and Link, H. (1991). Multiple sclerosis: cells secreting antibodies against myelin-associated glycoprotein are present in cerebrospinal fluid. *Scand. J. Immunol.* 33, 73–79. doi: 10.1111/j.1365-3083.1991.tb02493.x

Barrera, A., Ramos, H., Vera-Otarola, J., Fernandez-Garcia, L., Angulo, J., Olguin, V., et al. (2020). Post-translational modifications of hnRNP A1 differentially modulate retroviral IRES-mediated translation initiation. *Nucleic Acids Res.* 48, 10479–10499. doi: 10.1093/nar/gkaa765

Beijer, D., Kim, H., Guo, L., O'Donovan, K., Mademan, I., Deconinck, T., et al. (2021). Defining the diversity of hnRNPA1 mutations in clinical phenotype and pathomechanism. *medRxiv* 330. Preprint.

Bergsma, A. J., van der Wal, E., Broeders, M., van der Ploeg, A. T., and Pim Pijnappel, W. W. M. (2018). Alternative Splicing in Genetic Diseases: Improved Diagnosis and Novel Treatment Options. *Int. Rev. Cell Mol. Biol.* 335, 85–141. doi: 10.1016/bs.ircmb.2017.07.008

Berson, A., Barbash, S., Shaltiel, G., Goll, Y., Hanin, G., Greenberg, D. S., et al. (2012). Cholinergic-associated loss of hnRNP-A/B in Alzheimer's disease impairs cortical splicing and cognitive function in mice. *EMBO Mol. Med.* 4, 730–742. doi: 10.1002/emmm.201100995

Beusch, I., Barraud, P., Moursy, A., Clery, A., and Allain, F. H. (2017). Tandem hnRNP A1 RNA recognition motifs act in concert to repress the splicing of survival motor neuron exon 7. *Elife* 6:e25736.

Beyer, A. L., Christensen, M. E., Walker, B. W., and LeStourgeon, W. M. (1977). Identification and characterization of the packaging proteins of core 40S hnRNP particles. *Cell* 11, 127–138. doi: 10.1016/0092-8674(77)90323-3

Blom, N., Gammeltoft, S., and Brunak, S. (1999). Sequence and structure-based prediction of eukaryotic protein phosphorylation sites. *J. Mol. Biol.* 294, 1351–1362. doi: 10.1006/jmbi.1999.3310

Blom, N., Sicheritz-Ponten, T., Gupta, R., Gammeltoft, S., and Brunak, S. (2004). Prediction of post-translational glycosylation and phosphorylation of proteins from the amino acid sequence. *Proteomics* 4, 1633–1649. doi: 10.1002/pmic.200300771

Bonnal, S., Pileur, F., Orsini, C., Parker, F., Pujol, F., Prats, A. C., et al. (2005). Heterogeneous nuclear ribonucleoprotein A1 is a novel internal ribosome entry site trans-acting factor that modulates alternative initiation of translation of the fibroblast growth factor 2 mRNA. *J. Biol. Chem.* 280, 4144–4153. doi: 10.1074/jbc.m411492200

Borreca, A., Gironi, K., Amadoro, G., and Ammassari-Teule, M. (2016). Opposite Dysregulation of Fragile-X Mental Retardation Protein and Heteronuclear Ribonucleoprotein C Protein Associates with Enhanced APP Translation in Alzheimer Disease. *Mol. Neurobiol.* 53, 3227–3234. doi: 10.1007/s12035-015-9229-8

Bracha, D., Walls, M. T., Wei, M. T., Zhu, L., Kurian, M., Avalos, J. L., et al. (2018). Mapping Local and Global Liquid Phase Behavior in Living Cells Using Photo-Oligomerizable Seeds. *Cell* 175, 1467–80e13.

Burd, C. G., and Dreyfuss, G. (1994). RNA binding specificity of hnRNP A1: significance of hnRNP A1 high-affinity binding sites in pre-mRNA splicing. *EMBO J.* 13, 1197–1204. doi: 10.1002/j.1460-2075.1994.tb06369.x

Buxade, M., Parra, J. L., Rousseau, S., Shpiro, N., Marquez, R., Morrice, N., et al. (2005). The Mnks are novel components in the control of TNF alpha biosynthesis and phosphorylate and regulate hnRNP A1. *Immunity* 23, 177–189. doi: 10.1016/j.immuni.2005.06.009

Campillos, M., Lamas, J. R., Garcia, M. A., Bullido, M. J., Valdivieso, F., and Vazquez, J. (2003). Specific interaction of heterogeneous nuclear ribonucleoprotein A1 with the -219T allelic form modulates APOE promoter activity. *Nucleic Acids Res.* 31, 3063–3070. doi: 10.1093/nar/gkg435

Cartegni, L., and Krainer, A. R. (2002). Disruption of an SF2/ASF-dependent exonic splicing enhancer in SMN2 causes spinal muscular atrophy in the absence of SMN1. *Nat. Genet.* 30, 377–384. doi: 10.1038/ng854

Cartegni, L., Maconi, M., Morandi, E., Cobianchi, F., Riva, S., and Biamonti, G. (1996). hnRNP A1 selectively interacts through its Gly-rich domain with different RNA-binding proteins. *J. Mol. Biol.* 259, 337–348. doi: 10.1006/jmbi.1996.0324

Casas-Finet, J. R., Smith, J. D. Jr., Kumar, A., Kim, J. G., Wilson, S. H., and Karpel, R. L. (1993). Mammalian heterogeneous ribonucleoprotein A1 and its constituent domains. Nucleic acid interaction, structural stability and self-association. *J. Mol. Biol.* 229, 873–889. doi: 10.1006/jmbi.1993.1093

Chen, H. H., Chang, J. G., Lu, R. M., Peng, T. Y., and Tarn, W. Y. (2008). The RNA binding protein hnRNP Q modulates the utilization of exon 7 in the survival motor neuron 2 (SMN2) gene. *Mol. Cell Biol.* 28, 6929–6938. doi: 10.1128/mcb.01332-08

Chen, H., Hewison, M., Hu, B., and Adams, J. S. (2003). Heterogeneous nuclear ribonucleoprotein (hnRNP) binding to hormone response elements: a cause of vitamin D resistance. *Proc. Natl. Acad. Sci. U S A.* 100, 6109–6114. doi: 10.1073/pnas.1031395100

Cho, S., Moon, H., Loh, T. J., Oh, H. K., Cho, S., Choy, H. E., et al. (2014). hnRNP M facilitates exon 7 inclusion of SMN2 pre-mRNA in spinal muscular atrophy by targeting an enhancer on exon 7. *Biochim. Biophys. Acta.* 1839, 306–315. doi: 10.1016/j.bbagrm.2014.02.006

Choi, Y. H., Lim, J. K., Jeong, M. W., and Kim, K. T. (2012). HnRNP A1 phosphorylated by VRK1 stimulates telomerase and its binding to telomeric DNA sequence. *Nucleic Acids Res.* 40, 8499–8518. doi: 10.1093/nar/gks634

Chung, C. G., Lee, H., and Lee, S. B. (2018). Mechanisms of protein toxicity in neurodegenerative diseases. *Cell Mol. Life Sci.* 75, 3159–3180. doi: 10.1007/s00018-018-2854-4

Cinque, G., Ferino, A., Pedersen, E. B., and Xodo, L. E. (2020). Role of Poly [ADP-ribose] Polymerase 1 in Activating the Kirsten ras (KRAS) Gene in Response to Oxidative Stress. *Int. J. Mol. Sci.* 21:6237. doi: 10.3390/ijms21176237

Damiano, F., Rochira, A., Tocci, R., Alemanno, S., Gnoni, A., and Siculella, L. (2013). hnRNP A1 mediates the activation of the IRES-dependent SREBP-1a mRNA translation in response to endoplasmic reticulum stress. *Biochem. J.* 449, 543–553. doi: 10.1042/bj20120906

Das, S., Ward, S. V., Markle, D., and Samuel, C. E. (2004). DNA damage-binding proteins and heterogeneous nuclear ribonucleoprotein A1 function as constitutive KCS element components of the interferon-inducible RNA-dependent protein kinase promoter. *J. Biol. Chem.* 279, 7313–7321. doi: 10.1074/jbc.m312585200

Deshaies, J. E., Shkreta, L., Moszczynski, A. J., Sidibe, H., Semmler, S., Fouillen, A., et al. (2018). TDP-43 regulates the alternative splicing of hnRNP A1 to yield an aggregation-prone variant in amyotrophic lateral sclerosis. *Brain* 141, 1320–1333. doi: 10.1093/brain/awy062

Doktor, T. K., Schroeder, L. D., Vested, A., Palmfeldt, J., Andersen, H. S., Gregersen, N., et al. (2011). SMN2 exon 7 splicing is inhibited by binding of hnRNP A1 to a common ESS motif that spans the 3' splice site. *Hum. Mutat.* 32, 220–230. doi: 10.1002/humu.21419

Dombert, B., Sivadasan, R., Simon, C. M., Jablonka, S., and Sendtner, M. (2014). Presynaptic localization of Smn and hnRNP R in axon terminals of embryonic and postnatal mouse motoneurons. *PLoS One* 9:e110846. doi: 10.1371/journal.pone.0110846

Donev, R., Newall, A., Thome, J., and Sheer, D. (2007). A role for SC35 and hnRNPA1 in the determination of amyloid precursor protein isoforms. *Mol. Psychiatry* 12, 681–690. doi: 10.1038/sj.mp.4001971

Douglas, J. N., Gardner, L. A., Salapa, H. E., and Levin, M. C. (2016). Antibodies to the RNA Binding Protein Heterogeneous Nuclear Ribonucleoprotein A1 Colocalize to Stress Granules Resulting in Altered RNA and Protein Levels in a Model of Neurodegeneration in Multiple Sclerosis. *J. Clin. Cell Immunol.* 7:402.

Douglas, J. N., Gardner, L., and Levin, M. (2013). Antibodies to an intracellular antigen penetrate neuronal cells and cause deleterious effects. *J. Clin. Cell Immunol.* 4, 1–7.

Dreyfuss, G., Matunis, M. J., Pinol-Roma, S., and Burd, C. G. (1993). hnRNP proteins and the biogenesis of mRNA. *Annu. Rev. Biochem.* 62, 289–321. doi: 10.1146/annurev.bi.62.070193.001445

Duan, Y., Du, A., Gu, J., Duan, G., Wang, C., Gui, X., et al. (2019). PARylation regulates stress granule dynamics, phase separation, and neurotoxicity of disease-related RNA-binding proteins. *Cell Res.* 29, 233–247. doi: 10.1038/s41422-019-0141-z

Fang, J., Bolanos, L. C., Choi, K., Liu, X., Christie, S., Akunuru, S., et al. (2017). Ubiquitination of hnRNPA1 by TRAF6 links chronic innate immune signaling with myelodysplasia. *Nat. Immunol.* 18, 236–245. doi: 10.1038/ni.3654

Finkel, R. S., Mercuri, E., Darras, B. T., Connolly, A. M., Kuntz, N. L., Kirschner, J., et al. (2017). Nusinersen versus Sham Control in Infantile-Onset Spinal Muscular Atrophy. *N. Engl. J. Med.* 377, 1723–1732. doi: 10.1056/nejmoa1702752

Fiset, S., and Chabot, B. (2001). hnRNP A1 may interact simultaneously with telomeric DNA and the human telomerase RNA in vitro. *Nucleic Acids Res.* 29, 2268–2275. doi: 10.1093/nar/29.11.2268

Fisette, J. F., Toutant, J., Dugre-Brisson, S., Desgroseillers, L., and Chabot, B. (2010). hnRNP A1 and hnRNP H can collaborate to modulate 5' splice site selection. *RNA* 16, 228–238. doi: 10.1261/rna.1890310

Flynn, R. L., Centore, R. C., O'Sullivan, R. J., Rai, R., Tse, A., Songyang, Z., et al. (2011). TERRA and hnRNPA1 orchestrate an RPA-to-POT1 switch on telomeric single-stranded DNA. *Nature* 471, 532–536. doi: 10.1038/nature09772

Frankel, A., and Clarke, S. (2000). PRMT3 is a distinct member of the protein arginine N-methyltransferase family. Conferral of substrate specificity by a zinc-finger domain. *J. Biol. Chem.* 275, 32974–32982. doi: 10.1074/jbc.m006445200

Franzmann, T. M., and Alberti, S. (2019). Prion-like low-complexity sequences: Key regulators of protein solubility and phase behavior. *J. Biol. Chem.* 294, 7128–7136. doi: 10.1074/jbc.tm118.001190

Fukuda, H., Katahira, M., Tsuchiya, N., Enokizono, Y., Sugimura, T., Nagao, M., et al. (2002). Unfolding of quadruplex structure in the G-rich strand of the minisatellite repeat by the binding protein UP1. *Proc. Natl. Acad. Sci. U S A.* 99, 12685–12690. doi: 10.1073/pnas.152456899

Gao, G., Dhar, S., and Bedford, M. T. (2017). PRMT5 regulates IRES-dependent translation via methylation of hnRNP A1. *Nucleic Acids Res.* 45, 4359–4369.

Geuens, T., Bouhy, D., and Timmerman, V. (2016). The hnRNP family: insights into their role in health and disease. *Hum. Genet.* 135, 851–867. doi: 10.1007/s00439-016-1683-5

Ghosh, M., and Singh, M. (2018). RGG-box in hnRNPA1 specifically recognizes the telomere G-quadruplex DNA and enhances the G-quadruplex unfolding ability of UP1 domain. *Nucleic Acids Res.* 46, 10246–10261. doi: 10.1093/nar/gky854

Godet, A. C., David, F., Hantelys, F., Tatin, F., Lacazette, E., Garmy-Susini, B., et al. (2019). IRES Trans-Acting Factors, Key Actors of the Stress Response. *Int. J. Mol. Sci.* 20:924. doi: 10.3390/ijms20040924

Gomes, E., and Shorter, J. (2019). The molecular language of membraneless organelles. *J. Biol. Chem.* 294, 7115–7127. doi: 10.1074/jbc.tm118.001192

Gorlach, M., Wittekind, M., Beckman, R. A., Mueller, L., and Dreyfuss, G. (1992). Interaction of the RNA-binding domain of the hnRNP C proteins with RNA. *EMBO J.* 11, 3289–3295. doi: 10.1002/j.1460-2075.1992.tb05407.x

Gran, B., Hemmer, B., Vergelli, M., McFarland, H. F., and Martin, R. (1999). Molecular mimicry and multiple sclerosis: degenerate T-cell recognition and the induction of autoimmunity. *Ann. Neurol.* 45, 559–567. doi: 10.1002/1531-8249(199905)45:5<559::aid-ana3>3.0.co;2-q

Guil, S., and Caceres, J. F. (2007). The multifunctional RNA-binding protein hnRNP A1 is required for processing of miR-18a. *Nat. Struct. Mol. Biol.* 14, 591–596. doi: 10.1038/nsmb1250

Guil, S., Long, J. C., and Caceres, J. F. (2006). hnRNP A1 relocalization to the stress granules reflects a role in the stress response. *Mol. Cell Biol.* 26, 5744–5758. doi: 10.1128/mcb.00224-06

Guo, L., Kim, H. J., Wang, H., Monaghan, J., Freyermuth, F., Sung, J. C., et al. (2018). Nuclear-Import Receptors Reverse Aberrant Phase Transitions of RNA-Binding Proteins with Prion-like Domains. *Cell* 173, 677–92e20.

Guo, X., Disatnik, M. H., Monbureau, M., Shamloo, M., Mochly-Rosen, D., and Qi, X. (2013). Inhibition of mitochondrial fragmentation diminishes Huntington's disease-associated neurodegeneration. *J. Clin. Invest.* 123, 5371–5388. doi: 10.1172/jci70911

Hamilton, B. J., Nagy, E., Malter, J. S., Arrick, B. A., and Rigby, W. F. (1993). Association of heterogeneous nuclear ribonucleoprotein A1 and C proteins with reiterated AUUUA sequences. *J. Biol. Chem.* 268, 8881–8887. doi: 10.1016/s0021-9258(18)52955-0

Han, K., Yeo, G., An, P., Burge, C. B., and Grabowski, P. J. (2005). A combinatorial code for splicing silencing: UAGG and GGGG motifs. *PLoS Biol.* 3:e158. doi: 10.1371/journal.pbio.0030158

Harahap, I. S., Saito, T., San, L. P., Sasaki, N., Gunadi, Nurputra, D. K., et al. (2012). Valproic acid increases SMN2 expression and modulates SF2/ASF and hnRNPA1 expression in SMA fibroblast cell lines. *Brain Dev.* 34, 213–222. doi: 10.1016/j.braindev.2011.04.010

Hart, G. W., Slawson, C., Ramirez-Correa, G., and Lagerlof, O. (2011). Cross talk between O-GlcNAcylation and phosphorylation: roles in signaling, transcription, and chronic disease. *Annu. Rev. Biochem.* 80, 825–858. doi: 10.1146/annurev-biochem-060608-102511

Hartel, N. G., Chew, B., Qin, J., Xu, J., and Graham, N. A. (2019). Deep Protein Methylation Profiling by Combined Chemical and Immunoaffinity Approaches Reveals Novel PRMT1 Targets. *Mol. Cell Proteomics* 18, 2149–2164. doi: 10.1074/mcp.ra119.001625

Hay, D. C., Kemp, G. D., Dargemont, C., and Hay, R. T. (2001). Interaction between hnRNPA1 and IkappaBalpha is required for maximal activation of NF-kappaB-dependent transcription. *Mol. Cell Biol.* 21, 3482–3490. doi: 10.1128/mcb.21.10.3482-3490.2001

He, Y., and Smith, R. (2009). Nuclear functions of heterogeneous nuclear ribonucleoproteins A/B. *Cell Mol. Life Sci.* 66, 1239–1256. doi: 10.1007/s00018-008-8532-1

Herrmann, F., Pably, P., Eckerich, C., Bedford, M. T., and Fackelmayer, F. O. (2009). Human protein arginine methyltransferases in vivo–distinct properties of eight canonical members of the PRMT family. *J. Cell Sci.* 122(Pt 5), 667–677. doi: 10.1242/jcs.039933

Hsu, M. C., Pan, M. R., Chu, P. Y., Tsai, Y. L., Tsai, C. H., Shan, Y. S., et al. (2018). Protein Arginine Methyltransferase 3 Enhances Chemoresistance in Pancreatic Cancer by Methylating hnRNPA1 to Increase ABCG2 Expression. *Cancers* 11:8. doi: 10.3390/cancers11010008

Hua, Y., Vickers, T. A., Baker, B. F., Bennett, C. F., and Krainer, A. R. (2007). Enhancement of SMN2 exon 7 inclusion by antisense oligonucleotides targeting the exon. *PLoS Biol.* 5:e73. doi: 10.1371/journal.pbio.0050073

Hua, Y., Vickers, T. A., Okunola, H. L., Bennett, C. F., and Krainer, A. R. (2008). Antisense masking of an hnRNP A1/A2 intronic splicing silencer corrects SMN2 splicing in transgenic mice. *Am. J. Hum. Genet.* 82, 834–848. doi: 10.1016/j.ajhg.2008.01.014

Hudson, J. S., Ding, L., Le, V., Lewis, E., and Graves, D. (2014). Recognition and binding of human telomeric G-quadruplex DNA by unfolding protein 1. *Biochemistry* 53, 3347–3356. doi: 10.1021/bi500351u

Hyman, A. A., Weber, C. A., and Julicher, F. (2014). Liquid-liquid phase separation in biology. *Annu. Rev. Cell Dev. Biol.* 30, 39–58.

Jernigan, M., Morcos, Y., Lee, S. M., Dohan, F. C. Jr., Raine, C., and Levin, M. C. (2003). IgG in brain correlates with clinicopathological damage in HTLV-1 associated neurologic disease. *Neurology* 60, 1320–1327. doi: 10.1212/01.wnl.0000059866.03880.ba

Jo, O. D., Martin, J., Bernath, A., Masri, J., Lichtenstein, A., and Gera, J. (2008). Heterogeneous nuclear ribonucleoprotein A1 regulates cyclin D1 and c-myc internal ribosome entry site function through Akt signaling. *J. Biol. Chem.* 283, 23274–23287. doi: 10.1074/jbc.m801185200

Jones, S., Daley, D. T., Luscombe, N. M., Berman, H. M., and Thornton, J. M. (2001). Protein-RNA interactions: a structural analysis. *Nucleic Acids Res.* 29, 943–954. doi: 10.1093/nar/29.4.943

Kalume, F., Lee, S. M., Morcos, Y., Callaway, J. C., and Levin, M. C. (2004). Molecular mimicry: cross-reactive antibodies from patients with immune-mediated neurologic disease inhibit neuronal firing. *J. Neurosci. Res.* 77, 82–89. doi: 10.1002/jnr.20137

Kamma, H., Portman, D. S., and Dreyfuss, G. (1995). Cell type-specific expression of hnRNP proteins. *Exp. Cell Res.* 221, 187–196. doi: 10.1006/excr.1995.1366

Kashima, T., and Manley, J. L. (2003). A negative element in SMN2 exon 7 inhibits splicing in spinal muscular atrophy. *Nat. Genet.* 34, 460–463. doi: 10.1038/ng1207

Kashima, T., Rao, N., David, C. J., and Manley, J. L. (2007). hnRNP A1 functions with specificity in repression of SMN2 exon 7 splicing. *Hum. Mol. Genet.* 16, 3149–3159. doi: 10.1093/hmg/ddm276

Kim, H. J., Kim, N. C., Wang, Y. D., Scarborough, E. A., Moore, J., Diaz, Z., et al. (2013). Mutations in prion-like domains in hnRNPA2B1 and hnRNPA1 cause multisystem proteinopathy and ALS. *Nature* 495, 467–473. doi: 10.1038/nature11922

Koo, J. H., Lee, H. J., Kim, W., and Kim, S. G. (2016). Endoplasmic Reticulum Stress in Hepatic Stellate Cells Promotes Liver Fibrosis via PERK-Mediated Degradation of HNRNPA1 and Up-regulation of SMAD2. *Gastroenterology* 150, 181–93e8.

Kritsilis, M., Rizou, S. V., Koutsoudaki, P. N., Evangelou, K., and Gorgoulis, V. G. (2018). Papadopoulos D. Ageing, Cellular Senescence and Neurodegenerative Disease. *Int. J. Mol. Sci.* 19:2937. doi: 10.3390/ijms19102937

Lau, J. S., Baumeister, P., Kim, E., Roy, B., Hsieh, T. Y., Lai, M., et al. (2000). Heterogeneous nuclear ribonucleoproteins as regulators of gene expression through interactions with the human thymidine kinase promoter. *J. Cell Biochem.* 79, 395–406. doi: 10.1002/1097-4644(20001201)79:3<395::aid-jcb50>3.0.co;2-m

Lee, B. J., Cansizoglu, A. E., Suel, K. E., Louis, T. H., Zhang, Z., and Chook, Y. M. (2006). Rules for nuclear localization sequence recognition by karyopherin beta 2. *Cell* 126, 543–558. doi: 10.1016/j.cell.2006.05.049

Lee, J. H., Cook, J. R., Yang, Z. H., Mirochnitchenko, O., Gunderson, S. I., Felix, A. M., et al. (2005). PRMT7, a new protein arginine methyltransferase that synthesizes symmetric dimethylarginine. *J. Biol. Chem.* 280, 3656–3664. doi: 10.1074/jbc.m405295200

Lee, S. M., Dunnavant, F. D., Jang, H., Zunt, J., and Levin, M. C. (2006). Autoantibodies that recognize functional domains of hnRNPA1 implicate molecular mimicry in the pathogenesis of neurological disease. *Neurosci. Lett.* 401, 188–193. doi: 10.1016/j.neulet.2006.03.016

Lee, S., and Levin, M. (2014). Novel somatic single nucleotide variants within the RNA binding protein hnRNP A1 in multiple sclerosis patients. *F1000Res* 3:132. doi: 10.12688/f1000research.4436.1

Lee, S., and Levin, M. C. (2008). Molecular mimicry in neurological disease: what is the evidence? *Cell Mol. Life Sci.* 65, 1161–1175. doi: 10.1007/s00018-007-7312-7

Lee, S., Salapa, H. E., and Levin, M. C. (2019). Localization of near-infrared labeled antibodies to the central nervous system in experimental autoimmune encephalomyelitis. *PLoS One* 14:e0212357. doi: 10.1371/journal.pone.0212357

Lee, S., Shin, Y., Clark, D., Gotuzzo, E., and Levin, M. C. (2012). Cross-reactive antibodies to target proteins are dependent upon oligomannose glycosylated epitopes in HTLV-1 associated neurological disease. *J. Clin. Immunol.* 32, 736–745. doi: 10.1007/s10875-012-9652-9

Lee, S., Shin, Y., Marler, J., and Levin, M. C. (2008). Post-translational glycosylation of target proteins implicate molecular mimicry in the pathogenesis of HTLV-1 associated neurological disease. *J. Neuroimmunol.* 204, 140–148. doi: 10.1016/j.jneuroim.2008.07.020

Lee, S., Xu, L., Shin, Y., Gardner, L., Hartzes, A., Dohan, F. C., et al. (2011). A potential link between autoimmunity and neurodegeneration in immune-mediated neurological disease. *J. Neuroimmunol.* 235, 56–69. doi: 10.1016/j.jneuroim.2011.02.007

Lefebvre, S., Burglen, L., Reboullet, S., Clermont, O., Burlet, P., Viollet, L., et al. (1995). Identification and characterization of a spinal muscular atrophy-determining gene. *Cell* 80, 155–165.

Lefebvre, S., Burlet, P., Liu, Q., Bertrandy, S., Clermont, O., Munnich, A., et al. (1997). Correlation between severity and SMN protein level in spinal muscular atrophy. *Nat. Genet.* 16, 265–269. doi: 10.1038/ng0797-265

Levin, M. C., Krichavsky, M., Berk, J., Foley, S., Rosenfeld, M., Dalmau, J., et al. (1998). Neuronal molecular mimicry in immune-mediated neurologic disease. *Ann. Neurol.* 44, 87–98. doi: 10.1002/ana.410440115

Levin, M. C., Lee, S. M., Kalume, F., Morcos, Y., Dohan, F. C. Jr., Hasty, K. A., et al. (2002a). Autoimmunity due to molecular mimicry as a cause of neurological disease. *Nat. Med.* 8, 509–513. doi: 10.1038/nm0502-509

Levin, M. C., Lee, S. M., Morcos, Y., Brady, J., and Stuart, J. (2002b). Cross-reactivity between immunodominant human T lymphotropic virus type I tax and neurons: implications for molecular mimicry. *J. Infect. Dis.* 186, 1514–1517. doi: 10.1086/344734

Levin, M. C., Lee, S., Gardner, L. A., Shin, Y., Douglas, J. N., and Groover, C. J. (2012). Pathogenic mechanisms of neurodegeneration based on the phenotypic expression of progressive forms of immune-mediated neurologic disease. *Degener. Neurol. Neuromuscul. Dis.* 2, 175–187. doi: 10.2147/dnnd.s38353

Levin, M. C., Lee, S., Gardner, L. A., Shin, Y., Douglas, J. N., and Cooper, C. (2013). Autoantibodies to Non-myelin Antigens as Contributors to the Pathogenesis of Multiple Sclerosis. *J. Clin. Cell Immunol.* 4:148.

Lewis, S. M., Veyrier, A., Hosszu Ungureanu, N., Bonnal, S., Vagner, S., and Holcik, M. (2007). Subcellular relocalization of a trans-acting factor regulates XIAP IRES-dependent translation. *Mol. Biol. Cell.* 18, 1302–1311. doi: 10.1091/mbc.e06-06-0515

Libner, C. D., Salapa, H. E., Hutchinson, C., Lee, S., and Levin, M. C. (2020). Antibodies to the RNA binding protein heterogeneous nuclear ribonucleoprotein A1 contribute to neuronal cell loss in an animal model of multiple sclerosis. *J. Comp. Neurol.* 528, 1704–1724. doi: 10.1002/cne.24845

Lichtenstein, M., Guo, W., and Tartakoff, A. M. (2001). Control of nuclear export of hnRNP A1. *Traffic* 2, 261–267. doi: 10.1034/j.1600-0854.2001.1o002.x

Liu, E. Y., Cali, C. P., and Lee, E. B. (2017). RNA metabolism in neurodegenerative disease. *Dis. Model Mech.* 10, 509–518. doi: 10.1242/dmm.028613

Liu, Q., Shu, S., Wang, R. R., Liu, F., Cui, B., Guo, X. N., et al. (2016). Whole-exome sequencing identifies a missense mutation in hnRNPA1 in a family with flail arm ALS. *Neurology* 87, 1763–1769. doi: 10.1212/wnl.0000000000003256

Liu, X. Y., Li, H. L., Su, J. B., Ding, F. H., Zhao, J. J., Chai, F., et al. (2015). Regulation of RAGE splicing by hnRNP A1 and Tra2beta-1 and its potential role in AD pathogenesis. *J. Neurochem.* 133, 187–198. doi: 10.1111/jnc.13069

Liu, X., and Xu, Y. (2018). HnRNPA1 Specifically Recognizes the Base of Nucleotide at the Loop of RNA G-Quadruplex. *Molecules* 23:237. doi: 10.3390/molecules23010237

Liu, Y., Kim, D., Choi, N., Oh, J., Ha, J., Zhou, J., et al. (2020). hnRNP A1 Regulates Alternative Splicing of Tau Exon 10 by Targeting 3' Splice Sites. *Cells* 9:936. doi: 10.3390/cells9040936

Lue, L. F., Walker, D. G., Brachova, L., Beach, T. G., Rogers, J., Schmidt, A. M., et al. (2001). Involvement of microglial receptor for advanced glycation endproducts (RAGE) in Alzheimer's disease: identification of a cellular activation mechanism. *Exp. Neurol.* 171, 29–45. doi: 10.1006/exnr.2001.7732

Markmiller, S., Soltanieh, S., Server, K. L., Mak, R., Jin, W., Fang, M. Y., et al. (2018). Context-Dependent and Disease-Specific Diversity in Protein Interactions within Stress Granules. *Cell* 172, 590–604e13.

Martin, J., Masri, J., Cloninger, C., Holmes, B., Artinian, N., Funk, A., et al. (2011). Phosphomimetic substitution of heterogeneous nuclear ribonucleoprotein A1 at serine 199 abolishes AKT-dependent internal ribosome entry site-transacting factor (ITAF) function via effects on strand annealing and results in mammalian

target of rapamycin complex 1 (mTORC1) inhibitor sensitivity. *J. Biol. Chem.* 286, 16402–16413. doi: 10.1074/jbc.m110.205096

Martinez-Cue, C., and Rueda, N. (2020). Cellular Senescence in Neurodegenerative Diseases. *Front. Cell Neurosci.* 14:16. doi: 10.3389/fncel.2020.00016

Mayeda, A., Munroe, S. H., Xu, R. M., and Krainer, A. R. (1998). Distinct functions of the closely related tandem RNA-recognition motifs of hnRNP A1. *RNA* 4, 1111–1123. doi: 10.1017/s135583829898089x

Mercuri, E., Darras, B. T., Chiriboga, C. A., Day, J. W., Campbell, C., Connolly, A. M., et al. (2018). Nusinersen versus Sham Control in Later-Onset Spinal Muscular Atrophy. *N. Engl. J. Med.* 378, 625–635.

Merrill, B. M., Stone, K. L., Cobianchi, F., Wilson, S. H., and Williams, K. R. (1988). Phenylalanines that are conserved among several RNA-binding proteins form part of a nucleic acid-binding pocket in the A1 heterogeneous nuclear ribonucleoprotein. *J. Biol. Chem.* 263, 3307–3313. doi: 10.1016/s0021-9258(18)69073-8

Meyer, R., Wolf, S. S., and Obendorf, M. (2007). PRMT2, a member of the protein arginine methyltransferase family, is a coactivator of the androgen receptor. *J. Steroid Biochem. Mol. Biol.* 107, 1–14. doi: 10.1016/j.jsbmb.2007.05.006

Michael, W. M., Choi, M., and Dreyfuss, G. (1995). A nuclear export signal in hnRNP A1: a signal-mediated, temperature-dependent nuclear protein export pathway. *Cell* 83, 415–422. doi: 10.1016/0092-8674(95)90119-1

Michlewski, G., and Caceres, J. F. (2010). Antagonistic role of hnRNP A1 and KSRP in the regulation of let-7a biogenesis. *Nat. Struct. Mol. Biol.* 17, 1011–1018. doi: 10.1038/nsmb.1874

Michlewski, G., Guil, S., and Caceres, J. F. (2010). Stimulation of pri-miR-18a processing by hnRNP A1. *Adv. Exp. Med. Biol.* 700, 28–35. doi: 10.1007/978-1-4419-7823-3_3

Mohamed, H. A., Mosier, D. R., Zou, L. L., Siklos, L., Alexianu, M. E., Engelhardt, J. I., et al. (2002). Immunoglobulin Fc gamma receptor promotes immunoglobulin uptake, immunoglobulin-mediated calcium increase, and neurotransmitter release in motor neurons. *J. Neurosci. Res.* 69, 110–116. doi: 10.1002/jnr.10271

Moller, J. R., Johnson, D., Brady, R. O., Tourtellotte, W. W., and Quarles, R. H. (1989). Antibodies to myelin-associated glycoprotein (MAG) in the cerebrospinal fluid of multiple sclerosis patients. *J. Neuroimmunol.* 22, 55–61. doi: 10.1016/0165-5728(89)90009-x

Molliex, A., Temirov, J., Lee, J., Coughlin, M., Kanagaraj, A. P., Kim, H. J., et al. (2015). Phase separation by low complexity domains promotes stress granule assembly and drives pathological fibrillization. *Cell* 163, 123–133. doi: 10.1016/j.cell.2015.09.015

Moursy, A., Allain, F. H., and Clery, A. (2014). Characterization of the RNA recognition mode of hnRNP G extends its role in SMN2 splicing regulation. *Nucl. Acids Res.* 42, 6659–6672. doi: 10.1093/nar/gku244

Nadler, S. G., Merrill, B. M., Roberts, W. J., Keating, K. M., Lisbin, M. J., Barnett, S. F., et al. (1991). Interactions of the A1 heterogeneous nuclear ribonucleoprotein and its proteolytic derivative, UP1, with RNA and DNA: evidence for multiple RNA binding domains and salt-dependent binding mode transitions. *Biochemistry* 30, 2968–2976. doi: 10.1021/bi00225a034

Naruse, H., Ishiura, H., Mitsui, J., Date, H., Takahashi, Y., Matsukawa, T., et al. (2018). Molecular epidemiological study of familial amyotrophic lateral sclerosis in Japanese population by whole-exome sequencing and identification of novel HNRNPA1 mutation. *Neurobiol. Aging* 61, 9–16e.

Nishikawa, T., Kuwano, Y., Takahara, Y., Nishida, K., and Rokutan, K. (2019). HnRNPA1 interacts with G-quadruplex in the TRA2B promoter and stimulates its transcription in human colon cancer cells. *Sci. Rep.* 9:10276.

Nozaki, I., Watanabe, T., Kawaguchi, M., Akatsu, H., Tsuneyama, K., Yamamoto, Y., et al. (2007). Reduced expression of endogenous secretory receptor for advanced glycation endproducts in hippocampal neurons of Alzheimer's disease brains. *Arch. Histol. Cytol.* 70, 279–290. doi: 10.1679/aohc.70.279

Oldstone, M. B. (1998). Molecular mimicry and immune-mediated diseases. *FASEB J.* 12, 1255–1265. doi: 10.1096/fasebj.12.13.1255

Paramasivam, M., Membrino, A., Cogoi, S., Fukuda, H., Nakagama, H., and Xodo, L. E. (2009). Protein hnRNP A1 and its derivative Up1 unfold quadruplex DNA in the human KRAS promoter: implications for transcription. *Nucleic Acids Res.* 37, 2841–2853. doi: 10.1093/nar/gkp138

Park, S. J., Lee, H., Jo, D. S., Jo, Y. K., Shin, J. H., Kim, H. B., et al. (2015). Heterogeneous nuclear ribonucleoprotein A1 post-transcriptionally regulates Drp1 expression in neuroblastoma cells. *Biochim. Biophys. Acta* 1849, 1423–1431. doi: 10.1016/j.bbagrm.2015.10.017

Peterson, L. K., and Fujinami, R. S. (2007). Inflammation, demyelination, neurodegeneration and neuroprotection in the pathogenesis of multiple sclerosis. *J. Neuroimmunol.* 184, 37–44. doi: 10.1016/j.jneuroim.2006.11.015

Pinol-Roma, S., Choi, Y. D., Matunis, M. J., and Dreyfuss, G. (1988). Immunopurification of heterogeneous nuclear ribonucleoprotein particles reveals an assortment of RNA-binding proteins. *Genes Dev.* 2, 215–227. doi: 10.1101/gad.2.2.215

Protter, D. S. W., and Parker, R. (2016). Principles and Properties of Stress Granules. *Trends Cell Biol.* 26, 668–679. doi: 10.1016/j.tcb.2016.05.004

Quarles, R. H. (2007). Myelin-associated glycoprotein (MAG): past, present and beyond. *J. Neurochem.* 100, 1431–1448.

Rebane, A., Aab, A., and Steitz, J. A. (2004). Transportins 1 and 2 are redundant nuclear import factors for hnRNP A1 and HuR. *RNA* 10, 590–599. doi: 10.1261/rna.5224304

Redon, S., Zemp, I., and Lingner, J. A. (2013). three-state model for the regulation of telomerase by TERRA and hnRNPA1. *Nucleic Acids Res.* 41, 9117–9128. doi: 10.1093/nar/gkt695

Rho, J., Choi, S., Seong, Y. R., Cho, W. K., Kim, S. H., and Im, D. S. (2001). Prmt5, which forms distinct homo-oligomers, is a member of the protein-arginine methyltransferase family. *J. Biol. Chem.* 276, 11393–11401. doi: 10.1074/jbc.m008660200

Roth, S., and Khalaila, I. (2017). The effect of O-GlcNAcylation on hnRNP A1 translocation and interaction with transportin1. *Exp. Cell Res.* 350, 210–217. doi: 10.1016/j.yexcr.2016.11.023

Roy, R., Durie, D., Li, H., Liu, B. Q., Skehel, J. M., Mauri, F., et al. (2014). hnRNPA1 couples nuclear export and translation of specific mRNAs downstream of FGF-2/S6K2 signalling. *Nucleic Acids Res.* 42, 12483–12497. doi: 10.1093/nar/gku953

Ryan, V. H., Watters, S., Amaya, J., Khatiwada, B., Venditti, V., Naik, M. T., et al. (2020). Weak binding to the A2RE RNA rigidifies hnRNPA2 RRMs and reduces liquid-liquid phase separation and aggregation. *Nucleic Acids Res.* 48, 10542–10554. doi: 10.1093/nar/gkaa710

Salapa, H. E., Hutchinson, C., Popescu, B. F., and Levin, M. C. (2020). Neuronal RNA-binding protein dysfunction in multiple sclerosis cortex. *Ann. Clin. Transl. Neurol.* 7, 1214–1224. doi: 10.1002/acn3.51103

Salapa, H. E., Johnson, C., Hutchinson, C., Popescu, B. F., and Levin, M. C. (2018). Dysfunctional RNA binding proteins and stress granules in multiple sclerosis. *J. Neuroimmunol.* 324, 149–156. doi: 10.1016/j.jneuroim.2018.08.015

Shamoo, Y., Krueger, U., Rice, L. M., Williams, K. R., and Steitz, T. A. (1997). Crystal structure of the two RNA binding domains of human hnRNP A1 at 1.75 A resolution. *Nat. Struct. Biol.* 4, 215–222. doi: 10.1038/nsb0397-215

Shimada, N., Rios, I., Moran, H., Sayers, B., and Hubbard, K. (2009). p38 MAP kinase-dependent regulation of the expression level and subcellular distribution of heterogeneous nuclear ribonucleoprotein A1 and its involvement in cellular senescence in normal human fibroblasts. *RNA Biol.* 6, 293–304. doi: 10.4161/rna.6.3.8497

Shin, Y., Berry, J., Pannucci, N., Haataja, M. P., Toettcher, J. E., and Brangwynne, C. P. (2017). Spatiotemporal Control of Intracellular Phase Transitions Using Light-Activated optoDroplets. *Cell* 168, 159–71e14.

Shirendeb, U. P., Calkins, M. J., Manczak, M., Anekonda, V., Dufour, B., McBride, J. L., et al. (2012). Mutant huntingtin's interaction with mitochondrial protein Drp1 impairs mitochondrial biogenesis and causes defective axonal transport and synaptic degeneration in Huntington's disease. *Hum. Mol. Genet.* 21, 406–420. doi: 10.1093/hmg/ddr475

Skundric, D. S., Dai, R., Zakarian, V. L., and Zhou, W. (2008). Autoimmune-induced preferential depletion of myelin-associated glycoprotein (MAG) is genetically regulated in relapsing EAE (B6 x SJL) F1 mice. *Mol. Neurodegener.* 3:7. doi: 10.1186/1750-1326-3-7

Son, S. M., Jung, E. S., Shin, H. J., Byun, J., and Mook-Jung, I. (2012). Abeta-induced formation of autophagosomes is mediated by RAGE-CaMKKbeta-AMPK signaling. *Neurobiol. Aging* 33, 11–23e.

Song, W., Chen, J., Petrilli, A., Liot, G., Klinglmayr, E., Zhou, Y., et al. (2011). Mutant huntingtin binds the mitochondrial fission GTPase dynamin-related protein-1 and increases its enzymatic activity. *Nat. Med.* 17, 377–382. doi: 10.1038/nm.2313

Sui, J., Lin, Y. F., Xu, K., Lee, K. J., Wang, D., and Chen, B. P. (2015). DNA-PKcs phosphorylates hnRNP-A1 to facilitate the RPA-to-POT1 switch and telomere capping after replication. *Nucleic Acids Res.* 43, 5971–5983. doi: 10.1093/nar/gkv539

Sun, Y., Luo, M., Chang, G., Ren, W., Wu, K., Li, X., et al. (2017). Phosphorylation of Ser6 in hnRNPA1 by S6K2 regulates glucose metabolism and cell growth in colorectal cancer. *Oncol. Lett.* 14, 7323–7331.

Takimoto, M., Tomonaga, T., Matunis, M., Avigan, M., Krutzsch, H., Dreyfuss, G., et al. (1993). Specific binding of heterogeneous ribonucleoprotein particle protein K to the human c-myc promoter, in vitro. *J. Biol. Chem.* 268, 18249–18258. doi: 10.1016/s0021-9258(17)46837-2

Tang, J., Gary, J. D., Clarke, S., and Herschman, H. R. (1998). PRMT 3, a type I protein arginine N-methyltransferase that differs from PRMT1 in its oligomerization, subcellular localization, substrate specificity, and regulation. *J. Biol. Chem.* 273, 16935–16945. doi: 10.1074/jbc.273.27.16935

van der Houven van Oordt, W., Diaz-Meco, M. T., Lozano, J., Krainer, A. R., Moscat, J., and Caceres, J. F. (2000). The MKK(3/6)-p38-signaling cascade alters the subcellular distribution of hnRNP A1 and modulates alternative splicing regulation. *J. Cell. Biol.* 149, 307–316. doi: 10.1083/jcb.149.2.307

Vashistha, V., Bhardwaj, S., Yadav, B. K., and Yadav, A. K. (2020). Depleting deubiquitinating enzymes promotes apoptosis in glioma cell line via RNA binding proteins SF2/ASF1. *Biochem. Biophys. Rep.* 24:100846. doi: 10.1016/j.bbrep.2020.100846

Villa, C., Fenoglio, C., De Riz, M., Clerici, F., Marcone, A., Benussi, L., et al. (2011). Role of hnRNP-A1 and miR-590-3p in neuronal death: genetics and expression analysis in patients with Alzheimer disease and frontotemporal lobar degeneration. *Rejuvenat. Res.* 14, 275–281. doi: 10.1089/rej.2010.1123

Wall, M. L., and Lewis, S. M. (2017). Methylarginines within the RGG-Motif Region of hnRNP A1 Affect Its IRES Trans-Acting Factor Activity and Are Required for hnRNP A1 Stress Granule Localization and Formation. *J. Mol. Biol.* 429, 295–307. doi: 10.1016/j.jmb.2016.12.011

Wang, F., Fu, X., Chen, P., Wu, P., Fan, X., Li, N., et al. (2017). SPSB1-mediated HnRNP A1 ubiquitylation regulates alternative splicing and cell migration in EGF signaling. *Cell Res.* 27, 540–558. doi: 10.1038/cr.2017.7

Wang, H., Han, L., Zhao, G., Shen, H., Wang, P., Sun, Z., et al. (2016). hnRNP A1 antagonizes cellular senescence and senescence-associated secretory phenotype via regulation of SIRT1 mRNA stability. *Aging Cell.* 15, 1063–1073. doi: 10.1111/acel.12511

Wang, T. H., Chen, C. C., Hsiao, Y. C., Lin, Y. H., Pi, W. C., Huang, P. R., et al. (2019). Heterogeneous Nuclear Ribonucleoproteins A1 and A2 Function in Telomerase-Dependent Maintenance of Telomeres. *Cancers* 11:334. doi: 10.3390/cancers11030334

Wen, Z., Lian, L., Ding, H., Hu, Y., Xiao, Z., Xiong, K., et al. (2020). LncRNA ANCR promotes hepatocellular carcinoma metastasis through upregulating HNRNPA1 expression. *RNA Biol.* 17, 381–394. doi: 10.1080/15476286.2019.1708547

Wilbertz, J. H., Voigt, F., Horvathova, I., Roth, G., Zhan, Y., and Chao, J. A. (2019). Single-Molecule Imaging of mRNA Localization and Regulation during the Integrated Stress Response. *Mol. Cell* 73, 946–58e7.

Xia, H. (2005). Regulation of gamma-fibrinogen chain expression by heterogeneous nuclear ribonucleoprotein A1. *J. Biol. Chem.* 280, 13171–13178. doi: 10.1074/jbc.m414120200

Xiang, S., Kato, M., Wu, L. C., Lin, Y., Ding, M., Zhang, Y., et al. (2015). The LC Domain of hnRNPA2 Adopts Similar Conformations in Hydrogel Polymers, Liquid-like Droplets, and Nuclei. *Cell* 163, 829–839. doi: 10.1016/j.cell.2015.10.040

Yang, H., Zhu, R., Zhao, X., Liu, L., Zhou, Z., Zhao, L., et al. (2019). Sirtuin-mediated deacetylation of hnRNP A1 suppresses glycolysis and growth in hepatocellular carcinoma. *Oncogene* 38, 4915–4931. doi: 10.1038/s41388-019-0764-z

Yang, Y., and Wang, Z. (2019). IRES-mediated cap-independent translation, a path leading to hidden proteome. *J. Mol. Cell Biol.* 11, 911–919. doi: 10.1093/jmcb/mjz091

Youn, J. Y., Dyakov, B. J. A., Zhang, J., Knight, J. D. R., Vernon, R. M., Forman-Kay, J. D., et al. (2019). Properties of Stress Granule and P-Body Proteomes. *Mol. Cell.* 76, 286–294. doi: 10.1016/j.molcel.2019.09.014

Zaslavsky, B. Y., Ferreira, L. A., Darling, A. L., and Uversky, V. N. (2018). The solvent side of proteinaceous membrane-less organelles in light of aqueous two-phase systems. *Int. J. Biol. Macromol.* 117, 1224–1251. doi: 10.1016/j.ijbiomac.2018.06.030

Zearfoss, N. R., Clingman, C. C., Farley, B. M., McCoig, L. M., and Ryder, S. P. (2011). Quaking regulates Hnrnpa1 expression through its 3' UTR in oligodendrocyte precursor cells. *PLoS Genet.* 7:e1001269. doi: 10.1371/journal.pgen.1001269

Zearfoss, N. R., Johnson, E. S., and Ryder, S. P. (2013). hnRNP A1 and secondary structure coordinate alternative splicing of Mag. *RNA* 19, 948–957. doi: 10.1261/rna.036780.112

Zhang, H., Deng, T., Liu, R., Ning, T., Yang, H., Liu, D., et al. (2020). CAF secreted miR-522 suppresses ferroptosis and promotes acquired chemo-resistance in gastric cancer. *Mol. Cancer* 19:43.

Zhang, S., Schlott, B., Gorlach, M., and Grosse, F. (2004). DNA-dependent protein kinase (DNA-PK) phosphorylates nuclear DNA helicase II/RNA helicase A and hnRNP proteins in an RNA-dependent manner. *Nucleic Acids Res.* 32, 1–10. doi: 10.1093/nar/gkg933

Ziaei, S., Shimada, N., Kucharavy, H., and Hubbard, K. (2012). MNK1 expression increases during cellular senescence and modulates the subcellular localization of hnRNP A1. *Exp. Cell Res.* 318, 500–508. doi: 10.1016/j.yexcr.2011.12.015

Conflict of Interest: The authors declare that the research was conducted in the absence of any commercial or financial relationships that could be construed as a potential conflict of interest.

frontiers in Molecular Biosciences

MINI REVIEW
published: 27 April 2021
doi: 10.3389/fmolb.2021.658852

Post-translational Control of RNA-Binding Proteins and Disease-Related Dysregulation

*Alejandro Velázquez-Cruz, Blanca Baños-Jaime, Antonio Díaz-Quintana, Miguel A. De la Rosa and Irene Díaz-Moreno**

Instituto de Investigaciones Químicas, Centro de Investigaciones Científicas Isla de la Cartuja, Universidad de Sevilla, Consejo Superior de Investigaciones Científicas, Seville, Spain

Cell signaling mechanisms modulate gene expression in response to internal and external stimuli. Cellular adaptation requires a precise and coordinated regulation of the transcription and translation processes. The post-transcriptional control of mRNA metabolism is mediated by the so-called RNA-binding proteins (RBPs), which assemble with specific transcripts forming messenger ribonucleoprotein particles of highly dynamic composition. RBPs constitute a class of *trans*-acting regulatory proteins with affinity for certain consensus elements present in mRNA molecules. However, these regulators are subjected to post-translational modifications (PTMs) that constantly adjust their activity to maintain cell homeostasis. PTMs can dramatically change the subcellular localization, the binding affinity for RNA and protein partners, and the turnover rate of RBPs. Moreover, the ability of many RBPs to undergo phase transition and/or their recruitment to previously formed membrane-less organelles, such as stress granules, is also regulated by specific PTMs. Interestingly, the dysregulation of PTMs in RBPs has been associated with the pathophysiology of many different diseases. Abnormal PTM patterns can lead to the distortion of the physiological role of RBPs due to mislocalization, loss or gain of function, and/or accelerated or disrupted degradation. This Mini Review offers a broad overview of the post-translational regulation of selected RBPs and the involvement of their dysregulation in neurodegenerative disorders, cancer and other pathologies.

Keywords: post-translational modifications, RNA-binding proteins, liquid–liquid phase separation, HuR, TIA-1/TIAR, KSRP, hnRNP K, FUS

OPEN ACCESS

Edited by:
Roberto Giambruno, Italian Institute of Technology (IIT), Italy

Reviewed by:
Fátima Gebauer, Centre for Genomic Regulation (CRG), Spain
Pavel Ivanov, Brigham and Women's Hospital and Harvard Medical School, United States

****Correspondence:***
Irene Díaz-Moreno
idiazmoreno@us.es

Specialty section:
This article was submitted to Protein and RNA Networks, a section of the journal Frontiers in Molecular Biosciences

Received: *26 January 2021*
Accepted: *22 March 2021*
Published: *27 April 2021*

Citation:
Velázquez-Cruz A, Baños-Jaime B, Díaz-Quintana A, De la Rosa MA and Díaz-Moreno I (2021) Post-translational Control of RNA-Binding Proteins and Disease-Related Dysregulation. Front. Mol. Biosci. 8:658852. doi: 10.3389/fmolb.2021.658852

INTRODUCTION

Gene regulatory networks are constantly tuning mRNA and protein levels according to cellular needs, affecting all steps of the expression process, from transcription to protein degradation, and including mRNA maturation, transport and translation (Adeli, 2011). mRNA molecules are permanently associated with a dynamic set of proteins and non-coding RNAs, such as microRNAs (miRNAs), in the so-called messenger ribonucleoprotein particles (mRNPs). RNA-binding proteins (RBPs) serve different purposes within mRNPs and their combined effects determine the fate of the transcript at each stage of its life cycle (Müller-McNicoll and Neugebauer, 2013; Mitchell and Parker, 2014).

The interaction of most known RBPs with their cognate transcripts is mediated by a small group of RNA-binding domains (RBDs), such as the RNA recognition motif (RRM), K homology (KH), zinc-finger and DEAD/DEAH box helicase. These structural motifs have been extensively studied, their modes of interaction are widely known and represent a criterion for the classification of RBPs (Corley et al., 2020). RBPs usually contain several repeats

of the same RBD, which synergistically contribute to improve the specificity and affinity for their target mRNAs (Gerstberger et al., 2014; Corley et al., 2020). However, an increasing number of RBPs lacks a defined or 'classic' RBD, harboring instead at least one intrinsically disordered region (IDR) through which they can bind to RNA with a wide spectrum of affinities (Hentze et al., 2018).

Control of mRNA Life Cycle

RBPs constitute a class of *trans*-acting regulatory proteins with affinity for certain consensus sequences present in RNA molecules. Most of the identified and well-studied RBPs specifically bind mRNA, typically through the recognition of *cis*-acting elements located in the 5′ and 3′ untranslated regions (UTRs), although binding sites can also be found in the coding sequence (Gerstberger et al., 2014; Hentze et al., 2018; Van Nostrand et al., 2020). Since a particular *cis*-acting sequence is typically shared by many different transcripts, a single RBP can control the expression of multiple mRNAs and can thus profoundly alter cellular functions (Keene, 2010; Adeli, 2011; Müller-McNicoll and Neugebauer, 2013). In fact, there are many functionally related mRNAs that display a common element for co-regulation by RBPs, which is essential for a rapid and coordinated response to physiological and stress signals (Keene, 2010; Pope and Medzhitov, 2018). In this regard, one of the most important advantages of RNA networks is their great versatility, characterized by a constantly fluctuating transcriptome, thanks to the ability of the mRNA synthesis and degradation machinery to operate at a relatively high pace (Keene, 2010).

Numerous RBPs can associate with the same mRNA, either cooperating or competing for binding (Rougemaille et al., 2008; Müller-McNicoll and Neugebauer, 2013; Mitchell and Parker, 2014; Van Nostrand et al., 2020). The interaction with RBPs influences the maturation of mRNAs (alternative polyadenylation and splicing) and their cellular distribution, and either increases or decreases their stability, translation and degradation (Witten and Ule, 2011; Erson-Bensan, 2016; García-Mauriño et al., 2017). Many RBPs can also bind to their own transcript and/or that of other RBPs. The cross-talk between RBPs is an essential part of the regulation of this class of proteins and, therefore, of the gene expression itself (García-Mauriño et al., 2017).

The biosynthesis and function of miRNAs are also regulated by RBPs, with relevant consequences for mRNA fate. In the canonical miRNA biogenesis pathway, immature miRNAs are typically transcribed into long primary transcripts (pri-miRNAs) bearing a stem-loop structure. These pri-mRNAs are cleaved in the nucleus by the ribonuclease Drosha, which is part of the so-called microprocessor complex, along with two molecules of the RBP termed DiGeorge syndrome critical region gene 8 (DGCR8). The resulting pre-miRNAs are translocated by the exportin-5 receptor to the cytoplasm, where another RNAse, Dicer, recognizes and cleaves their hairpin motif producing miRNA duplexes. Then, the Argonaute (AGO) proteins bind to double-stranded miRNAs and both assemble into the miRNA-induced silencing complex (miRISC), where one strand of the mRNA duplex becomes functional and the other is removed. Complementary base pairing of the mature single-stranded miRNA with sequences of target mRNAs, mostly located in the 3′ UTRs, guides the translational inhibition and/or RNA degradation activity of miRISC (Zealy et al., 2017; Correia de Sousa et al., 2019; Michlewski and Cáceres, 2019).

RBPs can both up- and downregulate miRNAs at various levels, through direct binding to pri-/pre-miRNAs and/or indirectly via interaction with components of the miRNA processing machinery and their transcripts (e.g., modifying the expression and activity of Drosha and Dicer, or miRNA loading into miRISC) (Iadevaia and Gerber, 2015; Loffreda et al., 2015). Moreover, RBPs can either facilitate or prevent miRNAs binding to mRNAs, thus modulating their translational repression activity (Iadevaia and Gerber, 2015).

Intrinsic Phase Separation Ability

RBPs are major constituents of membrane-less organelles (MLOs) or condensates, which are dynamic macromolecular assemblies that become segregated from the surrounding

Abbreviations: AGO, argonaute protein; ALP, autophagy lysosomal pathway; ALS, amyotrophic lateral sclerosis; AMPK, AMP-activated protein kinase; ARE-RBP, RNA-binding proteins that recognize AU-rich elements; ARE, AU-rich element; ATM, ataxia-telangiectasia mutated; CARM1, coactivator-associated arginine methyltransferase 1; CBP, cAMP-response element binding protein (CREB)-binding protein; CD62E, E-selectin; Chk2, checkpoint kinase 2; Clk1, Cdc-like kinase 1; COX-2, cyclooxygenase 2; CSE, cystathionine γ-lyase; CTSS, cathepsin S; CUREs, CU-rich elements; DDR, DNA damage response; DGCR8, DiGeorge syndrome critical region 8; DICE, differentiation control element; ECRG2, esophageal cancer-related gene 2; eNOS, endothelial nitric oxide synthase; ERK, extracellular signal-regulated kinase; EV71, enterovirus 71; FASTK, Fas-activated serine/threonine kinase; FBXW2, F-box/WD repeat-containing protein 2; FTLD, fronto-temporal lobar degeneration; FUS, fused in sarcoma; FXR2P, fragile X-related protein 2; GM-CSF, granulocyte-macrophage colony-stimulating factor; GSK3β, glycogen synthase kinase 3β; G3BP1, Ras-GAP SH3 domain-binding protein 1; HDM2/MDM2, human/mouse double minute 2; hnRNP A1/A2/K, heterogeneous nuclear ribonucleoprotein A1, A2 and K; HNS, HuR nucleocytoplasmic shuttling sequence; Hsp27, heat shock protein 27; HuR, human antigen R; IDR, intrinsically disordered region; IKKα, IκB kinase α; IRES, internal ribosome entry site; JAK3, Janus kinase 3; KH, K homology; KI, K interactive region; KLF2, Krüppel-like factor 2; KNS, K nuclear shuttling domain; KSRP, KH-type splicing regulatory protein; LCR, low-complexity region; LLPS, liquid–liquid phase separation; MAPK, mitogen-activated protein kinase; MAPKAPK-2/3, MAPK-activated protein kinase 2 and 3; mFas, membrane-bound Fas; miRISC, miRNA-induced silencing complex; miRNA, micro-RNA; MK2/3, MAPK-activated protein kinase 2 and 3; MLO, membrane-less organelle; MMP2/7, matrix metalloproteinase 2 and 7; mRNP, messenger ribonucleoprotein particle; NCL, nucleolin; NEDD8, neural precursor cell expressed, developmentally downregulated 8; NLS, nuclear localization signal; *O*-GlcNAc, *O*-glycosyl-*N*-acetylation; PABP, poly(A)-binding protein; PAD4, peptidyl arginine deiminase 4; PAR, poly(ADP-ribose); PARP-1, PAR polymerase 1; Pc2, polycomb 2 protein; Pin1, protein interacting with NIMA (never in mitosis A)-1; PKA, protein kinase A; PKCα/δ/ζ, protein kinase C α, δ and ζ; PLD, prion-like domain; pre-miRNA, precursor miRNA; pri-miRNA, primary miRNA; PRMT1, protein arginine N-methyltransferase 1; PTH, parathyroid hormone; PTM, post-translational modification; r15-LOX, erythroid-15-lipoxygenase; RBD, RNA-binding domain; RBP, RNA-binding protein; RGG/RG, arginine/glycine-rich; RRM, RNA recognition motif; sFas, soluble Fas; SGs, stress granules; SIRT1, Sirtuin 1; SMN, survival of motor neuron; snRNP U1, small nuclear ribonucleoprotein particle U1; SR, serine/arginine-rich; SRPK1/2, SR protein kinase 1 and 2; SRSF1/3, SR splicing factor 1 and 3; StUbL, SUMO-targeted ubiquitin ligase; SUMO, small ubiquitin-like modifier; TDP-43, TAR DNA-binding protein of 43 kDa; TIA-1, T-cell intracellular antigen 1; TIAR, TIA-1-related; TIAR, TIA-1-related protein; TRAF6, TNF receptor-associated factor 6; TRN, transportin; TTP, tristetraprolin; Ub, ubiquitin; UBXD8, ubiquitin regulatory X domain-containing protein 8; UCP2, uncoupling protein-2; UPS, ubiquitin-proteasome system; UTR, untranslated region; XIAP, X chromosome-linked inhibitor of apoptosis protein; β-TrCP1, β-transducin repeat-containing protein 1.

protoplasm through the process of liquid-liquid phase separation (LLPS) (Owen and Shewmaker, 2019; Ryan and Fawzi, 2019). The nucleoplasm and cytosol are not homogeneous fluids, but instead contain different liquid-droplet phases where proteins and/or RNA are accumulated (Brangwynne, 2013; Ryan and Fawzi, 2019). Once certain concentration threshold is reached, these biomolecules assemble into different MLOs with a specific composition and physiological function (Darling et al., 2018). For example, the cytosolic stress granules (SGs)—which are formed in response to diverse stimuli—typically include the RBPs T-cell intracellular antigen 1 (TIA-1) and poly(A)-binding protein (PABP) and are associated to mRNA metabolism (Darling et al., 2018; Wolozin and Ivanov, 2019). Other MLOs, constantly present under homeostasis, are nucleoli, which are distinctively enriched in the RBP nucleolin (NCL) and specialized in ribosome biogenesis (Lo et al., 2006; Darling et al., 2018).

Due to the relatively weak, non-covalent nature of the interactions stablished by MLO components, diffusion of biomolecules into and out of the condensates is favored, which allows the fast assembly and disassembly of these structures (Brangwynne, 2013; Drino and Schaefer, 2018). The total interaction strength provided by the network of multivalent contacts between proteins and/or RNA is high enough to promote LLPS while ensuring reversible associations and great mobility inside condensates (Strom and Brangwynne, 2019). RBPs can contribute to phase separation by using both well-structured RBDs and IDRs for binding with RNA molecules, which act as scaffolds during condensation and determine the physicochemical and material properties of the resulting MLO (Drino and Schaefer, 2018; Ryan and Fawzi, 2019; Loughlin et al., 2021). IDRs from RBPs are also involved in protein-protein interactions, including self-association, thanks to the high proportion and distribution pattern of particular residues in their sequences, often clustered in repetitive low-complexity regions (LCRs), such as the arginine/glycine-rich (RGG/RG) boxes and the glutamine/asparagine-rich prion-like domains (PLDs) (Darling et al., 2018; Ryan and Fawzi, 2019). The weak cation–π intermolecular interactions between arginines from RGG motifs and aromatic residues (mostly tyrosines) of RBPs—e.g., heterogeneous nuclear ribonucleoprotein A2 (hnRNP A2) and fused in sarcoma (FUS)—are the driving force for their aggregation and liquid demixing (Hofweber et al., 2018; Qamar et al., 2018; Ryan et al., 2018; Hofweber and Dormann, 2019).

MLOs play an essential role in the cell by enabling the controlled and selective concentration of particular RBPs, among other biomolecules, to carry out critical biochemical reactions under optimal conditions, separated from the rest of their environment (Drino and Schaefer, 2018; Strom and Brangwynne, 2019). However, dysregulation of phase-separating RBPs such as FUS and TAR DNA-binding protein of 43 KDa (TDP-43) can lead to irreversible and aberrant condensate formation, a process deleterious to cells and frequently associated with neurodegenerative diseases, as discussed below (Bowden and Dormann, 2016; St George-Hyslop et al., 2018; Fernandopulle et al., 2019; Xue et al., 2020).

PTM-Dependent Activity

As noted previously, RBPs are prominently involved in the post-transcriptional modulation of mRNAs, accompanying them throughout their entire life-cycle. Nonetheless, the activity of RBPs is, in turn, heavily controlled by post-translational modifications (PTMs), which constitute an extra layer of regulation of gene expression. PTMs of proteins refer to generally enzymatic reactions that occur after their synthesis and consist of the covalent addition of small functional groups (e.g., phosphate, methyl and acetyl) or biomolecules (e.g., peptides, glycans and lipids) to one amino acid, its chemical modification (e.g., citrullination) and the cleavage of peptide bonds (e.g., caspase proteolysis) (Lovci et al., 2016; Virág et al., 2020). PTMs can dramatically change the properties of RBPs, including subcellular localization, association with target RNAs and other RNA-associated proteins, and degradation. This Mini Review focuses on the role of important PTMs (listed in **Supplementary Table 1**) in the biology of a subset of well-studied RBPs (listed in **Supplementary Table 2**), and their relevance in the development of various diseases. To this end, multiple examples are provided, which highlight the profound effects that these changes produce in RBPs under different cellular contexts. Note that the comprehensive compilation of the totality of PTMs described for all identified RBPs is beyond the scope of this Mini Review. All selected examples, including proteins, chemical modifications and diseases, are intended to qualitatively represent the intricate mechanisms and medical implications underlying the post-translational regulation and dysregulation of RBPs.

REGULATION OF RBP BIOLOGY BY PTMs

A rigorous, yet dynamic regulation of PTMs on the entire population of RBPs is essential for the maintenance of cellular balance, since these chemical marks have the potential to reconfigure the structure and redefine the function of RBPs. In the following sections, we will delve into the main characteristics of RBPs subject to significant variations due to PTMs.

Subcellular Localization

There are multiple reports on the influence that PTMs exert on the subcellular distribution of RBPs, with important consequences on RNA metabolism, either due to impaired nuclear export or spatial separation from their target RNAs into different compartments. For example, many of the PTMs identified in the RBP human antigen R (HuR) alter its localization. Most are phosphorylations and a great part of the modified residues are present in the so-called hinge region, an unstructured stretch containing the HuR nucleocytoplasmic shuttling (HNS) sequence (Grammatikakis et al., 2017). These phosphorylations are associated with the cytosolic accumulation of HuR, normally triggered by stress, since this RBP is predominantly nuclear in unstimulated cells (Doller et al., 2007, 2008, 2010; Kim et al., 2008; Lafarga et al., 2009; Chu et al., 2012; Filippova et al., 2012; Yoon et al., 2014).

Subcellular localization of the serine/arginine-rich (SR) protein family of splicing factors is also regulated by phosphorylations. Mostly nuclear, some members such as serine/arginine-rich splicing factor 1 (SRSF1) and SRSF3 can shuttle to the to participate in other post-transcriptional processes. However, the nuclear import of these RBPs through the transportin (TRN)-SR2 requires phosphorylation by the SR protein kinases 1 and 2 (SRPK1/2) (Lai et al., 2000, 2001; Long et al., 2019). In contrast, another previously identified importin-β, TRN-SR1, mediates the nuclear translocation of unphosphorylated SR proteins (Kataoka et al., 1999), although it remains unclear whether it can also transport phosphorylated forms (Kataoka et al., 1999; Lai et al., 2000, 2001).

The localization of another well-known RBP, hnRNP K, relies on several phosphorylatable serines and methylatable arginines (Xu et al., 2019). In general, phosphorylations at the K-interactive region (KI) and the K-nuclear shuttling domain (KNS) of hnRNP K control its subcellular distribution. For instance, this primarily nuclear RBP was shown to increase its cytosolic levels after phosphorylation by extracellular signal-regulated kinase (ERK) at Ser284 and Ser353 (Habelhah et al., 2001a,b; Huang et al., 2017). However, a phosphoproteomic study of hnRNP K revealed that phospho-Ser116 could also be involved in the subcellular distribution of this RBP. Furthermore, the same study linked the phosphorylation of Ser284 to the nuclear accumulation of hnRNP K (Kimura et al., 2010), in contrast to other reports (Habelhah et al., 2001a,b; Huang et al., 2017). On the other hand, methylations at the intrinsically disordered RGG-box of hnRNP K by the arginine N-methyltransferase 1 (PRMT1) have been related to the nuclear retention of this RBP (Chang et al., 2011).

An example of interplay between PTMs can be found in the nucleo-cytoplasmic shuttling of the KH-type splicing regulatory protein (KSRP). Phosphorylation of this RBP at Ser193 by Akt1 causes the unfolding of its first KH domain, giving rise to a binding site for the chaperone protein 14-3-3ζ, whose interaction is involved in the nuclear confinement observed for the phospho-isoform of KSRP (Díaz-Moreno et al., 2009). On the contrary, SUMOylation, i.e., the covalent attachment of the small ubiquitin-like modifier (SUMO) peptide, of KSRP at Lys87 by SUMO1 promotes nuclear export and increases its cytosolic levels (**Figure 1A**) (Yuan et al., 2017).

A less known PTM called myristoylation, i.e., the covalent addition of the fatty acid myristate to a N-terminal glycine, controls the axonal distribution of the neuronal fragile X-related protein 2 (FXR2P), restricting the localization of this RBP to proximal axon segments (Stackpole et al., 2014).

There are many documented cases of PTMs regulating the compartmentalization of RBPs into diverse MLOs. For instance, FUS acetylation at Lys510 by CREB-binding protein (CBP)/p300 impedes its nuclear import via TRN1, sequestering this RBP in the cytoplasm where it assembles into stress granule-like inclusions (Arenas et al., 2020). The opposite occurs to HuR when it is phosphorylated at Tyr200 by Janus kinase 3 (JAK3), as this PTM prevents its localization in arsenite-induced SGs (Yoon et al., 2014). Similar to HuR, Ras-GAP SH3 domain-binding protein 1 (G3BP1) phosphorylation at Ser149 might regulate its ability to mediate SG assembly (Tourrière et al., 2003). However, a recent examination of this hypothesis attributes the observed phenotype to an accidental mutation in the G3BP1 S149E phosphomimetic construct (Panas et al., 2019).

As another example, acetylation of NCL at Lys88 can mobilize this nucleolar RBP to the nuclear speckles, one type of MLO enriched in splicing and transcription factors, suggesting the involvement of NCL in mRNA synthesis and processing (Das et al., 2013). Conversely, phosphorylation by Cdc2-like kinase 1 (Clk1) facilitates the release of SRSF1 from nuclear speckles to the nucleoplasm (Ngo et al., 2005).

Interactions With Transcripts and Other RNA-Associated Proteins

PTMs can either facilitate or hinder the interaction of RBPs with their cognate transcripts and other RNA-associated proteins. For example, HuR binds to AU-rich elements (ARE) in the 3′ UTRs of target mRNAs (ARE-RBP), normally stabilizing them and/or enhancing their translation (García-Mauriño et al., 2017; Pabis et al., 2019). Phosphorylation of this ARE-RBP at residues within or near its three RRM domains often modulates the interaction with transcripts (Grammatikakis et al., 2017). For example, the ionizing radiation-triggered phosphorylation at Ser88, Ser100 and Thr118 by the checkpoint kinase 2 (Chk2) disengages HuR from most mRNA complexes throughout the cell, favoring its survival (Masuda et al., 2011). Strikingly, a previous report also associated the aforementioned Chk2-mediated phosphorylations on HuR, especially at Ser100, with impaired binding to Sirtuin 1 (SIRT1) mRNA but higher levels of cell death under oxidative stress conditions (Abdelmohsen et al., 2007). On the contrary, there are other documented cases involving Ser88- (Yu et al., 2011) and Ser100-phosphorylation (Liu et al., 2009) by Chk2, in which an increased binding of HuR to a specific mRNA was observed. Indeed, many phosphorylations by other kinases such as p38 mitogen-activated protein kinase (MAPK) and protein kinase C α and δ (PKCα/δ) lead to higher HuR affinity for certain transcripts (Doller et al., 2007, 2010; Lafarga et al., 2009; Bergalet et al., 2011; Liao et al., 2011; Gummadi et al., 2012; Scheiba et al., 2012).

Alternative PTMs can also modulate the interaction between HuR and mRNA with antagonistic effects. For instance, Arg217-methylation by coactivator-associated arginine methyltransferase 1 (CARM1) promotes HuR association with transcripts (Li et al., 2002; Calvanese et al., 2010; Pang et al., 2013), whereas ubiquitylation by the ubiquitin regulatory X domain-containing protein 8 (UBXD8)-p97 complex dissociates HuR from mRNPs (Zhou et al., 2013).

hnRNP K preferentially interacts with CU-rich elements (CUREs), such as the differentiation control element (DICE), in the 3′ UTRs of mRNAs and undergoes phosphorylations at residues within or near the three KH domains that regulate its association with nucleic acids (Xu et al., 2019). For example, Tyr458-phosphorylation by Src kinase impairs the KH3-mediated binding of hnRNP K to the transcripts of erythroid-15-lipoxygenase (r15-LOX) (Ostareck-Lederer et al., 2002; Messias et al., 2006) and uncoupling protein-2 (UCP2) (Tahir et al., 2014), thus suppressing the inhibitory effect on

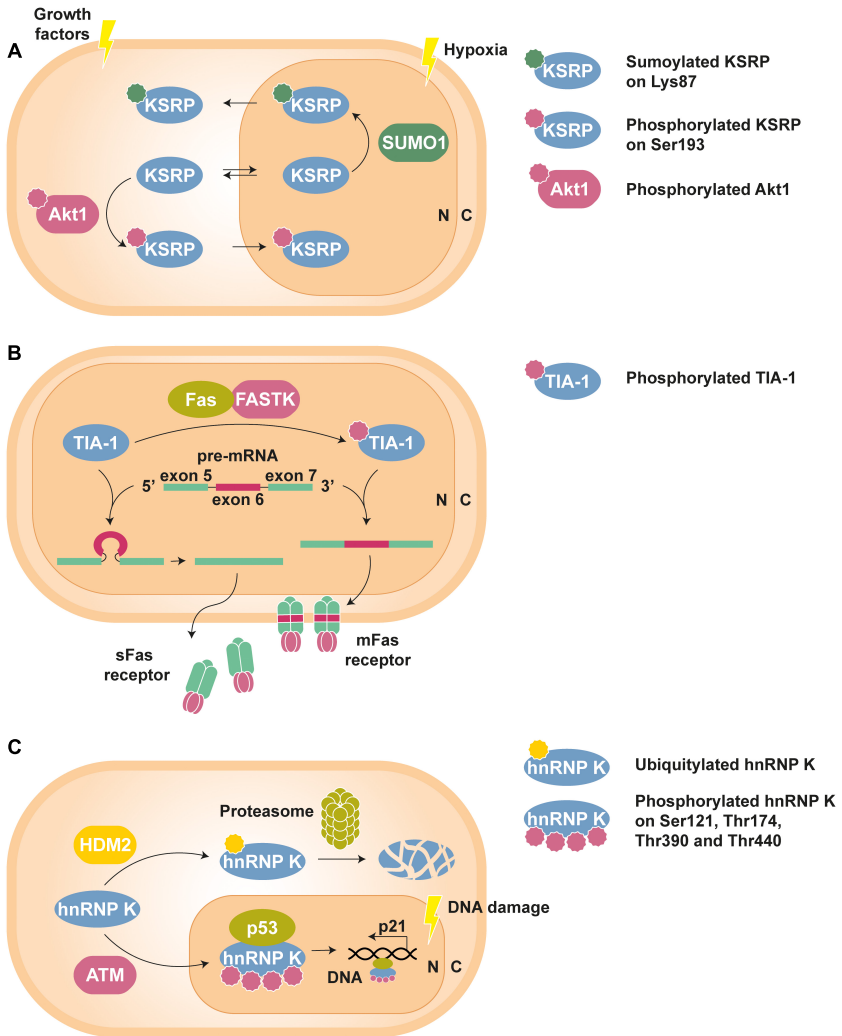

FIGURE 1 | Examples of PTM-mediated regulation of RBPs. **(A)** KSRP can shuttle between nucleus (N) and cytoplasm (C) to perform specific functions in each compartment. However, phosphorylation at Ser193 by Akt1, stimulated by growth factors, promotes the translocation of KSRP to the nucleus, whereas hypoxia-induced SUMOylation at Lys83 leads to its nuclear export (Díaz-Moreno et al., 2009; Yuan et al., 2017). **(B)** Phosphorylation of TIA-1 by FASTK improves its ability to recruit the U1 snRNP spliceosomal complex to the 5′ splice site region of the Fas receptor pre-mRNA exon 6. The resulting mature mRNA will express mFas, which plays an important role in the extrinsic apoptosis signaling pathways. In contrast, splicing of Fas receptor in the presence of unphosphorylated TIA-1 results in exon 6 skipping and the synthesis of sFas, that blocks apoptosis (Förch et al., 2002; Izquierdo and Valcárcel, 2007). **(C)** Under standard conditions, hnRNP K is targeted by the E3 Ub-ligase HDM2 for proteasomal degradation. Nonetheless, DNA damage triggers ATM-dependent phosphorylation of hnRNP K at Ser121, Thr174, Thr390, and Thr440, thus lowering its turnover rate. In addition, phosphorylated hnRNP K stimulates p53-mediated p21 gene expression, which causes cell cycle arrest (Moumen et al., 2005, 2013).

translation by this RBP. Moreover, the KH3 domain of hnRNP K is removed by caspase-3 cleavage at Asp334, 'unlocking' r15-LOX mRNA translation during erythroid differentiation (Naarmann-de Vries et al., 2013). Interestingly, arginine methylation of hnRNP K RGG motif by PRMT1 precludes its phosphorylation by Src (Ostareck-Lederer et al., 2006) and PKCδ (Yang et al., 2014), which have important repercussions for the DNA damage response (DDR). Under genotoxic stress, methylated hnRNP K shows an increased affinity for the apoptosis regulator p53 and enhances its transcriptional activity, thus facilitating cell cycle arrest and DNA repair (Chen et al., 2008).

AU-rich binding factor 1 (AUF-1) generally promotes mRNA decay and possesses four splice isoforms (García-Mauriño et al., 2017). The p40 isoform ($p40^{AUF1}$) is phosphorylated at Ser83 and Ser87 by glycogen synthase kinase 3β (GSK3β) and protein kinase A (PKA), respectively. $p40^{AUF1}$ form dimers that bind sequentially to the ARE sequence from the tumor necrosis factor α (TNFα) mRNA, up to a maximum of two dimers per RNA oligo. *In vitro* binding assays showed that single Ser83-phosphorylation reduces by roughly 40% the binding of $p40^{AUF1}$ dimers to a free TNFα-ARE oligo. Intriguingly, when $p40^{AUF1}$ dimers are singly-phosphorylated at Ser87, the affinity of the second binding event increases

twice, relative to the unphosphorylated $p40^{AUF1}$ dimer. Moreover, simultaneous phosphorylation of both serines has the same impact on $p40^{AUF1}$ interaction with TNFα-ARE oligo than Ser83 single-phosphorylation, i.e., the negative effect of phospho-Ser83 dominates the positive one by phospho-Ser87 (Wilson et al., 2003).

The function of KSRP and AUF-1 as mediators of exosomal mRNA decay is regulated by the protein interacting with NIMA (never in mitosis A)-1 (Pin1) enzyme, which specifically isomerizes phosphorylated Ser/Thr-Pro peptide bonds (Shen and Malter, 2015). Phospho-isoforms of these ARE-RBPs are modified by Pin1, impacting on their affinity for mRNA. For example, prolyl isomerization increases the binding of KSRP to the parathyroid hormone (PTH) mRNA (Nechama et al., 2009) while attenuates the association of all four AUF-1 isoforms with the granulocyte-macrophage colony-stimulating factor (GM-CSF) mRNA (Shen et al., 2005). Of note, Pin1 activity plays a prominent role in the inflammatory and immune response, as several RBP substrates of this enzyme control the expression of many cytokines (Shen and Malter, 2015).

Tristetraprolin (TTP) is another ARE-RBP that facilitates mRNA degradation, including its own transcript (García-Mauriño et al., 2017). Phosphorylation of TTP at Ser52 and Ser178 by MAPK-activated protein kinase 2 and 3 (MAPKAPK-2/3 or MK2/3) improves its stability and expression, but also diminishes its capacity to recruit deadenylases to target mRNAs, among which are the transcripts of many cytokines (Hitti et al., 2006; Ronkina et al., 2007, 2019; Clement et al., 2011). In fact, there is much evidence pointing to an essential role of TTP phosphorylation and dephosphorylation in the regulation of inflammation (Clark and Dean, 2016). Ser52- and Ser178-phosphorylation is necessary and sufficient to suppress the mRNA-destabilizing activity of TTP through complex formation with the 14-3-3 chaperone, allowing the expression and participation of its target cytokines in the inflammatory response, until reactivation of TTP via dephosphorylation. However, MK2/3 phosphorylates several other residues of TTP and it has been proposed, based on recent experimental data, that phospho-Ser316 could contribute to the complete inactivation of TTP (Ronkina et al., 2019).

Structural details on the binding of TIA-1 to RNA have been thoroughly determined (Aroca et al., 2011; Bauer et al., 2012; Cruz-Gallardo et al., 2013, 2014, 2015; Wang et al., 2014; Waris et al., 2017; Loughlin et al., 2021), although very little information is available about the effect of PTMs on this ARE-RBP. Nevertheless, it is well-known that phosphorylation of TIA-1 and its homolog TIA-1-related protein (TIAR) modulates their activity in the alternative splicing of the Fas receptor. Pre-mRNA splicing radically influences the properties and function of the Fas receptor expressed by the mature mRNA: the inclusion of exon 6 gives rise to a pro-apoptotic membrane protein (mFas), whereas the skipping of this exon determines the synthesis of a soluble (sFas) and anti-apoptotic isoform (Ruberti et al., 1996). TIA-1/TIAR phosphorylation by FASTK has been associated to the expression of the mFas isoform (**Figure 1B**). Furthermore, TIA-1 phosphorylation by FASTK has been shown to increase the recruitment of the spliceosomal U1 small nuclear RNP (snRNP U1) to Fas receptor pre-mRNA suboptimal 5′ splice sites (Izquierdo and Valcárcel, 2007), presumably due to enhanced interaction of phospho-TIA-1 with the U1-C protein subunit (Förch et al., 2002). Importantly, the binding affinity of TIA-1 for RNA remained unaltered upon phosphorylation (Izquierdo and Valcárcel, 2007).

PTM-mediated disruption of the complexes between phase-separating RBPs and RNA can alter their condensation capacity. Such is the case for the acetylation of FUS (Lys315 and Lys316) and G3BP1 (Lys376) by CBP/p300, which impairs the binding of these RBPs to target RNAs (Gal et al., 2019; Arenas et al., 2020). Moreover, it has been proposed that lysine acetylation of G3BP1 assists SGs disassembly, a physiological mechanism that could be exploited for therapeutic purposes (Gal et al., 2019).

Turnover and Degradation

Maintenance of cell homeostasis requires tight regulation of protein concentrations (Hanna et al., 2019). Protein turnover, i.e., the dynamic balance between synthesis and degradation, ensures the replacement of old proteins, potentially defective and/or harmful, with new copies, and the adaptation of the proteome composition to different cellular contexts and stimuli (Toyama and Hetzer, 2013; Alber and Suter, 2019).

There are two main pathways for protein degradation: the autophagy lysosomal pathway (ALP) and the ubiquitin (Ub)-proteasome system (UPS). The ALP consists of the unspecific breakdown of cellular material (including non-protein biomolecules and even complete organelles), which is isolated in double-membrane vesicles called autophagosomes and digested after lysosome fusion. In contrast, the UPS is based on the labeling of proteins with the 76-amino acid polypeptide Ub for their targeting and destruction by large protease complexes termed proteasomes (Ohsumi, 2006; Varshavsky, 2017). The covalent binding of Ub to lysine residues requires the concerted action of three enzymes generically known as E1, E2 and E3 (Alber and Suter, 2019). Susceptible proteins carry degradation signals or 'degrons' that allow their recognition and binding by E3 Ub-protein ligases (Geffen et al., 2016). Then, targeted proteins can be mono-ubiquitylated on one or more lysines (multi-mono-ubiquitylation), and poly-ubiquitylated, i.e., attached to a poly-Ub chain of a variable length and structure. Finally, ubiquitylated proteins are processed by the proteasomal machinery and their components are subsequently recycled (Hanna et al., 2019).

The abovementioned three-tier process is also used for the attachment of Ub-like proteins (e.g., SUMO and neural precursor cell expressed developmentally downregulated 8 or NEDD8) to target substrates (Enchev et al., 2015; Pichler et al., 2017). Importantly, ubiquitylation, SUMOylation and NEDDylation are involved in different cellular events other than degradation, as shown by various examples throughout this Mini Review.

The cellular levels of RBPs, as master regulators of gene expression, are continuously adjusted via UPS. For instance, KSRP proteasome-mediated turnover controls the exosome recruitment activity of this ARE-RBP for target mRNA degradation (García-Mayoral et al., 2007; Díaz-Moreno et al., 2010; Gherzi et al., 2010; Briata et al., 2013; Wang et al., 2020). As another example, HuR ubiquitylation specifically at Lys182 has

been related to a decrease in its cellular levels after heat shock (Abdelmohsen et al., 2009).

Crosstalk between PTMs targeting the same RBP has a decisive influence on its turnover rate. HuR phosphorylation at Ser304 and Ser318 by IκB kinase α (IKKα) and PKCα, respectively, precedes its ubiquitylation and subsequent degradation in cancer cells upon glycolysis inhibition. Specifically, Ser318-phosphorylation facilitates HuR nuclear export, whereas phospho-Ser304 is essential for HuR binding to the E3 Ub-ligase β-transducin repeat-containing protein 1 (β-TrCP1). Interestingly, β-TrCP1 recognizes a particular sequence stretch in HuR RRM3, which includes Ser304 at its N-terminal end (Chu et al., 2012).

Similarly, the phosphorylation of the molecular chaperone and RBP heat shock protein 27 (Hsp27) drives AUF-1 proteolysis and indirectly increases the half-life of ARE-containing mRNAs. Hsp27 Ser15-phosphorylation by p38 MAPK and/or MK2 could trigger its proteasomal co-degradation with AUF-1, thus preventing the destabilizing effect of both ARE-RBPs (Knapinska et al., 2011). In contrast, the previously mentioned MK2/3-mediated phosphorylations that inactivate TTP, i.e., phospho-Ser52 and phospho-Ser178, also protect it against proteasomal degradation. However, it has been described that TTP can be processed by the proteasome in a Ub-independent manner through degradation 'by default,' in which the presence of IDRs in the RBP would be essential (Ngoc et al., 2014).

The expression and turnover rate of the splicing factors SRSF2 and hnRNP A1 are significantly affected by the action of α-ketoglutarate-dependent hydroxylases. Prolyl hydroxylation of these RBPs lowers their degradation rate, although it also downregulates hnRNP A1 protein synthesis (Stoehr et al., 2016).

The role of hnRNP K in DDR is also regulated by protein turnover. The E3 Ub-ligase human/mouse double minute 2 (HDM2/MDM2) targets hnRNP K for proteasomal degradation in undamaged cells. Nevertheless, genotoxic stimuli trigger ataxia-telangiectasia mutated (ATM)-mediated phosphorylation of hnRNP K at Ser121, Thr174, Thr390, and Thr440, with the consequent decrease in the turnover of the RBP and increase in its activity as p53 transcriptional co-activator (**Figure 1C**) (Moumen et al., 2005, 2013). DNA damage was also shown to induce hnRNP K SUMOylation at Lys422 by the E3 SUMO-ligase polycomb 2 (Pc2), thereby leading to upregulation of p53 function (Pelisch et al., 2012).

PTMs OF RBPs IN THE PATHOPHYSIOLOGY OF DISEASES

Given the extraordinary relevance of RBPs for the viability and correct functioning of the cell, it is not surprising that their dysregulation is involved in the etiology and/or pathogenesis of a wide variety of diseases (Vidal, 2011; Gerstberger et al., 2014; Conlon and Manley, 2017; Pereira et al., 2017; Moore et al., 2018; Gebauer et al., 2021). Next, the molecular mechanisms that connect some PTMs of RBPs with various pathologies are described, with special attention to neurodegenerative diseases and cancers.

Neurodegenerative Diseases

The presence of intracellular protein aggregates is pathognomonic for neurological disorders such as fronto-temporal lobar degeneration (FTLD) and amyotrophic lateral sclerosis (ALS). Besides the classic β-amyloid deposits, the abnormal accumulation of various RBPs within gel-like or insoluble droplets in neurons and glia has been widely documented and their study has aroused increasing interest during the last decade. The irreversible solidification experienced by condensates is often associated with key mutations in RBP-encoding genes. However, the ability of both wild-type and mutant RBPs to undergo LLPS and gelation can be profoundly altered by PTMs (Bowden and Dormann, 2016; St George-Hyslop et al., 2018; Fernandopulle et al., 2019; Xue et al., 2020). For example, aberrant hyper-phosphorylation, ubiquitylation, acetylation, cysteine oxidation and caspase cleavage of TDP-43 have been related to a pathogenic behavior of this RBP in FTLD and/or ALS, including loss of physiological function, mislocalization and higher aggregation (Buratti, 2018; François-Moutal et al., 2019; Prasad et al., 2019).

PARylation, i.e., the covalent addition of poly(ADP-ribose) or PAR residues, is another important PTM for the phase separation of the RBPs TDP-43 and hnRNP A1. TDP-43 binding to PAR molecules stimulates the recruitment of this RBP to SGs, temporarily blocking its pathological phosphorylation. However, tankyrase-1/2 PARylation activity under chronic stress has been correlated to increased accumulation of phosphorylated TDP-43 in cytosolic foci, which may eventually evolve to a solid-like state (McGurk et al., 2018). On the other hand, Lys298-PARylation of hnRNP A1 by PAR polymerase 1 (PARP-1) is involved in stress-induced cytosolic translocation, while the PAR-binding ability of hnRNP A1 positively controls its association and co-LLPS with TDP-43 (Duan et al., 2019). Interestingly, toxicity of both PAR 'readers' is proportional to the cellular PARylation levels (McGurk et al., 2018; Duan et al., 2019).

Methylation of RGG motifs by PRMT1 hinders hnRNP A2 *in vitro* self-assembly into condensates by impairing cation–π interactions between arginines and aromatic residues (Ryan et al., 2018). The same mechanism seems to drive FUS demixing, since loss of methylation (Hofweber et al., 2018) and reduced asymmetric dimethylation (Qamar et al., 2018) have been linked to a greater propensity of FUS to form stable aggregates (**Figure 2A**). In fact, it has been proposed that arginine methylation in RBPs could be a 'friendly' PTM, with a protective role against pathological phase transition (Hofweber and Dormann, 2019). Nonetheless, this PTM has also been reported to promote aggregation by enhanced interaction of RGG box-containing RBPs with another phase separating partner (Dammer et al., 2012; Tanikawa et al., 2018) and/or facilitating nuclear export and cytosolic accumulation (Tradewell et al., 2012). Indeed, citrullination, i.e., the conversion of arginine to citrulline, by peptidyl arginine deiminase 4 (PAD4) competes with methylation and reduces the aggregation of ALS-associated proteins (including FUS) and hnRNP A1 (Tanikawa et al., 2018). In principle, both PTMs disrupt the same electrostatic forces

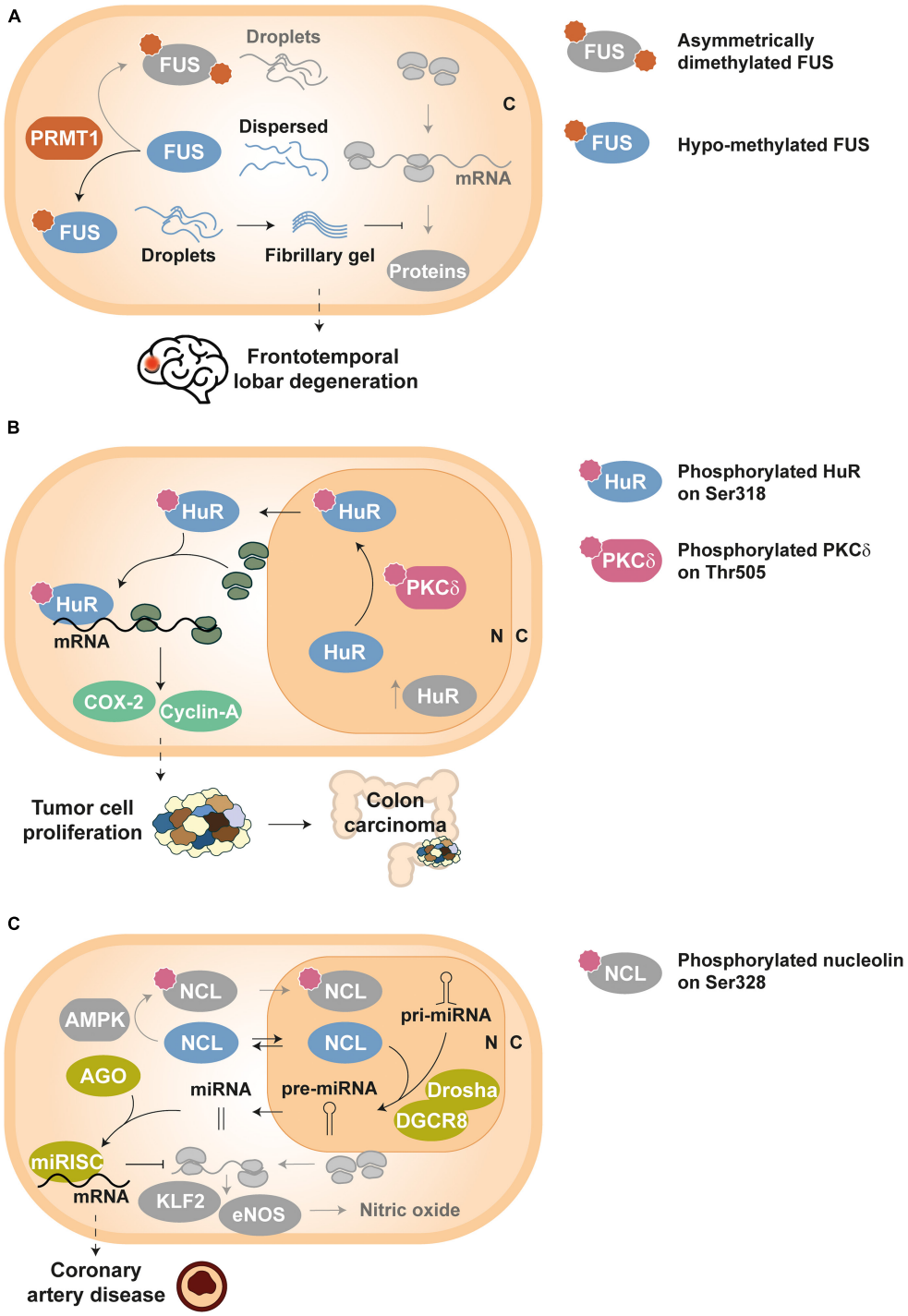

FIGURE 2 | Examples of disease-related dysregulation of PTMs in RBPs. Proteins and components involved in homeostatic pathways are depicted in grayscale, except symbols that stand for PTMs. **(A)** Frontotemporal lobar degeneration (FTLD): FUS molecules can build either droplets or droplets evolving into fibrillary gel state depending on its arginine methylation level, which is controlled by PRMT1 enzymes. Asymmetrically dimethylated FUS yields physiological droplets under homeostatic conditions, whereas hypo-methylated FUS forms highly stable fibrillary gels in FTLD; such fibrillary gels impede normal activity of RNP granules and decrease protein synthesis in neurons (Qamar et al., 2018). **(B)** Tumor cell proliferation: HuR is translocated from the nucleus (N) to the cytoplasm (C) upon PKCδ-dependent phosphorylation at Ser318, thus increasing the stability of tumor related transcripts such as COX-2 and cyclin-A. Elevated levels of Ser318-phosphorylated HuR have been detected in colon carcinoma (Doller et al., 2011). **(C)** Coronary artery disease: unphosphorylated NCL can shuttle between cytoplasm (C) and nucleus (N), and participates in the processing of key pri-miRNAs by the Drosha-DGCR8 complex. Such mature miRNAs associate with AGO proteins to activate the miRISC complex and thus guide the degradation of KLF2 and eNOS mRNAs. As a result, nitric oxide levels in endothelial cells decrease, producing vascular dysfunction (Gongol et al., 2019).

that assist the phase transition of RBPs like FUS (St George-Hyslop et al., 2018; Hofweber and Dormann, 2019), although it has also been hypothesized that citrullination inhibits the selective recognition of methylarginines by survival of motor neuron (SMN) proteins and thus prevents co-aggregation (St George-Hyslop et al., 2018; Tanikawa et al., 2018).

Dysfunction of the proteasomal degradation pathway has also been implicated in neurodegenerative disorders (Lukaesko and Meller, 2011). As mentioned before, ubiquitylated TDP-43 is characteristic of inclusions in FTLD and ALS. Increasing evidence associates ubiquitylation of TDP-43 with enhanced self-assembly and aggregation into insoluble droplets (Seyfried et al., 2010; Dammer et al., 2012; Hans et al., 2014), which could be indicative of a deficient turnover regulation of this RBP. Proteomic studies have detected Ub- and SUMO-enriched inclusions, suggesting a possible interplay between both PTMs (Seyfried et al., 2010). Indeed, prior SUMOylation of the ALS-linked FUS P525L mutant was reported to be essential for its destruction via UPS, suppressing its accumulation in SGs. The SUMO-targeted ubiquitin ligase (StUbL) pathway could establish an interdependence relationship between SUMOylation of RBPs in the cell nucleus and dissolution of SGs in the cytosol. A failure in this system was shown to enhance the pathological aggregation of this FUS mutant (Keiten-Schmitz et al., 2020).

Cancer

Dysregulation of numerous RBPs have been related to cancer and their overexpression can be used as a prognostic marker (Jia et al., 2017; Pereira et al., 2017; Moore et al., 2018; Wolfson et al., 2018; Schuschel et al., 2020). In addition, the aberrant post-translational control of RBPs disrupts their activity and can induce tumor development. For example, HuR phosphorylation at Ser318 by PKCδ promotes its translocation to the cytoplasm, where this RBP stabilizes the mRNAs of cyclooxygenase 2 (COX-2) and cyclin-A (Doller et al., 2007, 2008, 2010, 2011). Since elevated levels of both COX-2 and cyclin-A proteins are associated to abnormal cellular proliferation, Ser318-phosphorylated HuR has been proposed as a tumor marker for colon carcinoma, where cellular concentrations of this phospho-isoform have also been found increased (**Figure 2B**) (Doller et al., 2011).

Inflammation is a hallmark of cancer (Colotta et al., 2009) and HuR has been implicated in the inflammatory response due to its role in the regulation of the transcripts of many cytokines such as TNF-α, and several chemokines and interleukins (Srikantan and Gorospe, 2012). Recently, PARP1-mediated PARylation at Asp226 was shown to be indispensable for HuR cytosolic translocation (Ke et al., 2017), as well as to promote its oligomerization and to prevent miRISC-mediated decay of HuR transcript targets under inflammatory stimulation (Ke et al., 2021). Moreover, HuR Trp261 was demonstrated as a key residue for mRNA stabilization upon PARylation, indicating that the oligomerization of this RBP is essential for its protective effect (Scheiba et al., 2014; Díaz-Quintana et al., 2015; Pabis et al., 2019; Ke et al., 2021). Intriguingly, it has also been reported that lethal stress induces caspase-7/-3 cleavage of HuR at Asp226, whose proteolytic products promote apoptosis (Mazroui et al., 2008; von Roretz and Gallouzi, 2010). The overexpression of PARP1 observed in several cancers (Sun et al., 2014; Mazzotta et al., 2016; Wang et al., 2017) can produce an uncontrolled PARylation of HuR that may preclude its caspase processing and thus contribute to tumor development (Ke et al., 2021).

Alteration of HuR turnover can elicit the malignant transformation of the cell. For example, the tumor suppressor esophageal cancer-related gene 2 (ECRG2) is upregulated upon DNA damage and promotes HuR ubiquitylation, possibly involving Lys182. As a result, HuR concentration decreases, as does the expression of the X chromosome-linked inhibitor of apoptosis protein (XIAP), whose mRNA is stabilized by this RBP. However, the ECRG2 V30E mutant, found in human lung cancer, cannot reduce HuR levels through the UPS, and enhance cell survival and resistance to chemotherapeutic drugs (Lucchesi et al., 2016). On the other hand, HuR can be NEDDylated at Lys283, Lys313 and Lys326 by the E3 NEDD8-ligase MDM2. These PTMs mobilize HuR to the nucleus and have a protective effect against proteasomal degradation (Embade et al., 2012). Interestingly, increased NEDDylated HuR levels have been detected in liver and colon cancer cells (Embade et al., 2012; Fernández-Ramos and Martínez-Chantar, 2015).

hnRNP K *O*-glycosyl-N-acetylation (*O*-GlcNAc) has been associated to the metastasis of cholangiocarcinoma. This PTM promotes the nuclear translocation of hnRNP K, which acts as a transcription factor of proteins implicated in cellular proliferation, migration and apoptosis inhibition, such as cyclin D1, matrix metalloproteinase 2 and 7 (MMP2/7), and vimentin (Phoomak et al., 2019).

The role of KSRP in miRNA biosynthesis is regulated by the crosstalk between phosphorylation and SUMOylation, and its imbalance could lead to tumorigenesis (Yuan et al., 2017). ATM-mediated phosphorylation of nuclear KSRP at Ser132, Ser274, and Ser670 facilitates its binding to pri-miRNA and boosts generation of mature miRNAs (Zhang et al., 2011), e.g., the let-7 family of tumor suppressors (Trabucchi et al., 2009; Nicastro et al., 2012; Repetto et al., 2012). On the contrary, KSRP SUMOylation at Lys87 by SUMO-1 hinders its interaction with pri-miRNAs and halts processing of let-7 miRNAs by the Drosha-DGCR8 complex, thus preventing their oncogene silencing activity (Yuan et al., 2017).

hnRNP A1 is ubiquitylated by the E3 Ub-ligase TNF receptor-associated factor 6 (TRAF6) (Fang et al., 2017) and then assembles with FUS and the transcription factor c-Jun for the proteasomal degradation of both RBPs (Perrotti et al., 2000). However, the expression of the BCR/ABL oncogene prevents the UPS-mediated destruction of hnRNP A1 and enhances its ability to export mRNAs from the nucleus, possibly via PKCζ-dependent phosphorylation of this RBP. Increased cellular concentrations of hnRNP A1 and altered nucleocytoplasmic traffiking of its target transcripts have been related to BCR/ABL-mediated leukemogenesis (Iervolino et al., 2002; Carrà et al., 2019).

Other Diseases

The role of RBPs in a broad spectrum of pathologies has been the focus of much research. For example, the correct

regulation of HuR sulfhydration has been recently shown to be critical for the physiological function of endothelial cells. Cystathionine γ-lyase (CSE) generates H_2S, whose ionic form (HS^-) induces electrophile sulfhydration of HuR at Cys13, blocking its homodimerization. As a consequence, HuR-mediated upregulation of pro-atherogenic E-selectin (CD62E) and cathepsin S (CTSS) mRNAs is impaired. Interestingly, vascular dysfunction and atherosclerosis have been correlated with abnormally high L-cystathionine plasma levels, indicative of CSE inactivation and deficient HuR sulfhydration (Bibli et al., 2019).

The phosphorylation status of NCL has also been proven crucial for vascular endothelial cell homeostasis. NCL Ser328-phosphorylation by AMP-activated protein kinase (AMPK) causes nuclear retention of the RBP and blocks pre-miRNA-93 and pre-miRNA-484 processing. This mechanism allows higher expression of Krüppel-like factor 2 (KLF2) and endothelial nitric oxide synthase (eNOS), key regulators of the vascular function and targets of miRNA-93 and miRNA-484. In contrast, unphosphorylated NCL assists the maturation of the aforementioned miRNAs and the downregulation of KLF2 and eNOS. Interestingly, augmented serum levels of miRNA-93 and miRNA-484 have been correlated to coronary artery disease (**Figure 2C**) (Gongol et al., 2019).

Ubiquitylation of KSRP has also been associated to metabolic disorders such as atherosclerosis and obesity. The pathological upregulation of the E3 Ub-ligase F-box/WD repeat-containing protein 2 (FBXW2) in macrophages increases KSRP degradation, undermining the normal translational repression of pro-inflammatory factors by this RBP (Wang et al., 2020). On the other hand, ubiquitylated KSRP has also exhibited high activity against picornavirus infection. The C-terminal domain of this RBP is essential for its ubiquitylation, presumably at Lys109, Lys121 and Lys122. Such PTMs give KSRP a competitive advantage for binding to the internal ribosome entry site (IRES) of enterovirus 71 (EV71), inhibiting its cap-independent translation (Kung et al., 2017). However, EV71 eventually induces caspase cleavage of the KSRP C-terminal domain, not only disrupting its anti-infective role, but also transforming this RBP into a positive regulator of viral translation (Chen et al., 2013; Kung et al., 2017).

CONCLUDING REMARKS

The heterogeneous collection of examples presented in this Mini Review illustrates the abundance of factors modulating the impact of PTMs on RBPs. Among them, the crosstalk between PTMs stands out as a key element governing RBPs (Venne et al., 2014; Vu et al., 2018; Huang K. Y. et al., 2019). Different PTMs can exert similar or opposite effects on a given RBP, acting in synergy or interfering with each other, so that certain PTMs assist or exclude the occurrence of additional ones. Furthermore, PTM-specific outputs on RBP biology varies significantly depending on the position and reactivity of the residue affected, the presence or absence of bound partners, and the cellular conditions. Indeed, some relationships can be established between the PTM effect and the role of the modified region. For example, phosphorylation events at or around the RBDs of HuR and hnRNP K usually alter their binding to nucleic acids, while phosphorylation events at nucleocytoplasmic shuttling sequences generally control their subcellular distribution (Grammatikakis et al., 2017; Xu et al., 2019). Similarly, lysine acetylation of FUS in its nuclear localization signal (NLS) restricts its cellular distribution to the cytoplasm, whereas the same PTM in its RRM disrupts its association with RNA (Arenas et al., 2020). Moreover, PTMs at low-complexity IDRs (e.g., arginine methylation of RGG regions) of some phase-separating RBPs such as FUS strongly influence the formation and characteristics of condensates (Hofweber et al., 2018; Qamar et al., 2018; Hofweber and Dormann, 2019), including the irreversible transition into hardened aggregates (Bowden and Dormann, 2016; St George-Hyslop et al., 2018; Fernandopulle et al., 2019; Xue et al., 2020).

Given the well documented connection between many RBPs and their PTMs with a wide variety of diseases, the study of the post-translational regulation of this class of proteins could provide a better understanding of pathophysiological processes. A detailed knowledge of the molecular bases of disease-related dysregulation of PTMs on RBPs hold promise for helping to diagnosis, prognosis and treatment of many severe illnesses by revealing new biomarkers and therapeutic targets. Such a research task will indeed benefit from a multidisciplinary approach that allows investigators to keep pushing the boundaries in this field, through the combination of genomic and proteomic tools, cell-based assays, biophysical techniques and bioinformatic methods (Foshag et al., 2018; Huang R. et al., 2019; Liu and Liu, 2020; Pérez-Mejías et al., 2020; Van Nostrand et al., 2020). Nonetheless, further technological and methodological advances will also be necessary to fully unravel the mechanisms behind the PTM control of RBPs.

AUTHOR CONTRIBUTIONS

All authors have made a substantial, direct and intellectual contribution to the work, and approved it for publication.

FUNDING

Financial support was provided by the Andalusian Government (BIO-198, US-1254317 US/JUNTA/FEDER, UE, US-1257019 US/JUNTA/FEDER, UE, P18-FR-3487, and P18-HO-4091), the Spanish Ministry of Science, Innovation and Universities (PGC2018-096049-B), the Spanish Ministry of Education, Culture and Sports (FPU016/01513), and the Ramón Areces Foundation.

SUPPLEMENTARY MATERIAL

The Supplementary Material for this article can be found online at: https://www.frontiersin.org/articles/10.3389/fmolb.2021.658852/full#supplementary-material

REFERENCES

Abdelmohsen, K., Pullmann, R. Jr., Lal, A., Kim, H. H., Galban, S., Yang, X., et al. (2007). Phosphorylation of HuR by Chk2 regulates SIRT1 expression. *Mol. Cell* 25, 543–557. doi: 10.1016/j.molcel.2007.01.011

Abdelmohsen, K., Srikantan, S., Yang, X., Lal, A., Kim, H. H., Kuwano, Y., et al. (2009). Ubiquitin-mediated proteolysis of HuR by heat shock. *EMBO J.* 28, 1271–1282. doi: 10.1038/emboj.2009.67

Adeli, K. (2011). Translational control mechanisms in metabolic regulation: critical role of RNA binding proteins, microRNAs, and cytoplasmic RNA granules. *Am. J. Physiol. Endocrinol. Metab.* 301, E1051–E1064. doi: 10.1152/ajpendo.00399.2011

Alber, A. B., and Suter, D. M. (2019). Dynamics of protein synthesis and degradation through the cell cycle. *Cell Cycle* 18, 784–794. doi: 10.1080/15384101.2019.1598725

Arenas, A., Chen, J., Kuang, L., Barnett, K. R., Kasarskis, E. J., Gal, J., et al. (2020). Lysine acetylation regulates the RNA binding, subcellular localization and inclusion formation of FUS. *Hum. Mol. Genet.* 29, 2684–2697. doi: 10.1093/hmg/ddaa159

Aroca, A., Díaz-Quintana, A., and Díaz-Moreno, I. (2011). A structural insight into the C-terminal RNA recognition motifs of T-cell intracellular antigen-1 protein. *FEBS Lett.* 585, 2958–2964. doi: 10.1016/j.febslet.2011.07.037

Bauer, W. J., Heath, J., Jenkins, J. L., and Kielkopf, C. L. (2012). Three RNA recognition motifs participate in RNA recognition and structural organization by the pro-apoptotic factor TIA-1. *J. Mol. Biol.* 415, 727–740. doi: 10.1016/j.jmb.2011.11.040

Bergalet, J., Fawal, M., Lopez, C., Desjobert, C., Lamant, L., Delsol, G., et al. (2011). HuR-mediated control of C/EBPβ mRNA stability and translation in ALK-positive anaplastic large cell lymphomas. *Mol. Cancer Res.* 9, 485–496. doi: 10.1158/1541-7786.MCR-10-0351

Bibli, S. I., Hu, J., Sigala, F., Wittig, I., Heidler, J., Zukunft, S., et al. (2019). Cystathionine γ lyase sulfhydrates the RNA binding protein Human antigen R to preserve endothelial cell function and delay atherogenesis. *Circulation* 139, 101–114. doi: 10.1161/CIRCULATIONAHA.118.034757

Bowden, H. A., and Dormann, D. (2016). Altered mRNP granule dynamics in FTLD pathogenesis. *J. Neurochem.* 138, 112–133. doi: 10.1111/jnc.13601

Brangwynne, C. P. (2013). Phase transitions and size scaling of membrane-less organelles. *J. Cell Biol.* 203, 875–881. doi: 10.1083/jcb.201308087

Briata, P., Chen, C. Y., Ramos, A., and Gherzi, R. (2013). Functional and molecular insights into KSRP function in mRNA decay. *Biochim. Biophys. Acta* 1829, 689–694. doi: 10.1016/j.bbagrm.2012.11.003

Buratti, E. (2018). TDP-43 post-translational modifications in health and disease. *Expert Opin. Ther. Targets* 22, 279–293. doi: 10.1080/14728222.2018.1439923

Calvanese, V., Lara, E., Suárez-Alvarez, B., Abu Dawud, R., Vázquez-Chantada, M., Martínez-Chantar, M. L., et al. (2010). Sirtuin 1 regulation of developmental genes during differentiation of stem cells. *Proc. Natl. Acad. Sci. U.S.A.* 107, 13736–13741. doi: 10.1073/pnas.1001399107

Carrà, G., Russo, I., Guerrasio, A., and Morotti, A. (2019). Nuclear-cytoplasmic shuttling in chronic myeloid leukemia: implications in leukemia maintenance and therapy. *Cells* 8:1248. doi: 10.3390/cells8101248

Chang, Y. I., Hsu, S. C., Chau, G. Y., Huang, C. Y., Sung, J. S., Hua, W. K., et al. (2011). Identification of the methylation preference region in heterogeneous nuclear ribonucleoprotein K by protein arginine methyltransferase 1 and its implication in regulating nuclear/cytoplasmic distribution. *Biochem. Biophys. Res. Commun.* 404, 865–869. doi: 10.1016/j.bbrc.2010.12.076

Chen, L. L., Kung, Y. A., Weng, K. F., Lin, J. Y., Horng, J. T., and Shih, S. R. (2013). Enterovirus 71 infection cleaves a negative regulator for viral internal ribosomal entry site-driven translation. *J. Virol.* 87, 3828–3838. doi: 10.1128/JVI.02278-12

Chen, Y., Zhou, X., Liu, N., Wang, C., Zhang, L., Mo, W., et al. (2008). Arginine methylation of hnRNP K enhances p53 transcriptional activity. *FEBS Lett.* 582, 1761–1765. doi: 10.1016/j.febslet.2008.04.051

Chu, P. C., Chuang, H. C., Kulp, S. K., and Chen, C. S. (2012). The mRNA-stabilizing factor HuR protein is targeted by β-TrCP protein for degradation in response to glycolysis inhibition. *J. Biol. Chem.* 287, 43639–43650.

Clark, A. R., and Dean, J. L. (2016). The control of inflammation via the phosphorylation and dephosphorylation of tristetraprolin: a tale of two phosphatases. *Biochem. Soc. Trans.* 44, 1321–1337. doi: 10.1042/BST20160166

Clement, S. L., Scheckel, C., Stoecklin, G., and Lykke-Andersen, J. (2011). Phosphorylation of tristetraprolin by MK2 impairs AU-rich element mRNA decay by preventing deadenylase recruitment. *Mol. Cell. Biol.* 31, 256–266. doi: 10.1128/MCB.00717-10

Colotta, F., Allavena, P., Sica, A., Garlanda, C., and Mantovani, A. (2009). Cancer-related inflammation, the seventh hallmark of cancer: links to genetic instability. *Carcinogenesis* 30, 1073–1081. doi: 10.1093/carcin/bgp127

Conlon, E. G., and Manley, J. L. (2017). RNA-binding proteins in neurodegeneration: mechanisms in aggregate. *Genes Dev.* 31, 1509–1528. doi: 10.1101/gad.304055.117

Corley, M., Burns, M. C., and Yeo, G. W. (2020). How RNA-binding proteins interact with RNA: molecules and mechanisms. *Mol. Cell* 78, 9–29. doi: 10.1016/j.molcel.2020.03.011

Correia de Sousa, M., Gjorgjieva, M., Dolicka, D., Sobolewski, C., and Foti, M. (2019). Deciphering miRNAs' action through miRNA editing. *Int. J. Mol. Sci.* 20:6249. doi: 10.3390/ijms20246249

Cruz-Gallardo, I., Aroca, Á, Persson, C., Karlsson, B. G., and Díaz-Moreno, I. (2013). RNA binding of T-cell intracellular antigen-1 (TIA-1) C-terminal RNA recognition motif is modified by pH conditions. *J. Biol. Chem.* 288, 25986–25994. doi: 10.1074/jbc.M113.489070

Cruz-Gallardo, I., Aroca, Á, Gunzburg, M. J., Sivakumaran, A., Yoon, J. H., et al. (2014). The binding of TIA-1 to RNA C-rich sequences is driven by its C-terminal RRM domain. *RNA Biol.* 11, 766–776. doi: 10.4161/rna.28801

Cruz-Gallardo, I., Del Conte, R., Velázquez-Campoy, A., García-Mauriño, S. M., and Díaz-Moreno, I. (2015). A non-invasive NMR method based on histidine imidazoles to analyze the pH-modulation of protein-nucleic acid interfaces. *Chemistry* 21, 7588–7595. doi: 10.1002/chem.201405538

Dammer, E. B., Fallini, C., Gozal, Y. M., Duong, D. M., Rossoll, W., Xu, P., et al. (2012). Coaggregation of RNA-binding proteins in a model of TDP-43 proteinopathy with selective RGG motif methylation and a role for RRM1 ubiquitination. *PLoS One* 7:e38658. doi: 10.1371/journal.pone.0038658

Darling, A. L., Liu, Y., Oldfield, C. J., and Uversky, V. N. (2018). Intrinsically disordered proteome of human membrane-less organelles. *Proteomics*. 18:e1700193. doi: 10.1002/pmic.201700193

Das, S., Cong, R., Shandilya, J., Senapati, P., Moindrot, B., Monier, K., et al. (2013). Characterization of nucleolin K88 acetylation defines a new pool of nucleolin colocalizing with pre-mRNA splicing factors. *FEBS Lett.* 587, 417–424. doi: 10.1016/j.febslet.2013.01.035

Díaz-Quintana, A., García-Mauriño, S. M., and Díaz-Moreno, I. (2015). Dimerization model of the C-terminal RNA recognition motif of HuR. *FEBS Lett.* 2015, 1059–1066. doi: 10.1016/j.febslet.2015.03.013

Díaz-Moreno, I., Hollingworth, D., Frenkiel, T. A., Kelly, G., Martin, S., Howell, S., et al. (2009). Phosphorylation-mediated unfolding of a KH domain regulates KSRP localization via 14-3-3 binding. *Nat. Struct. Mol. Biol.* 16, 238–246. doi: 10.1038/nsmb.1558

Díaz-Moreno, I., Hollingworth, D., Kelly, G., Martin, S., García-Mayoral, M., Briata, P., et al. (2010). Orientation of the central domains of KSRP and its implications for the interaction with the RNA targets. *Nucleic Acids Res.* 38, 5193–5205. doi: 10.1093/nar/gkq216

Doller, A., Huwiler, A., Müller, R., Radeke, H. H., Pfeilschifter, J., and Eberhardt, W. (2007). Protein kinase Cα-dependent phosphorylation of the mRNA-stabilizing factor HuR: implications for posttranscriptional regulation of cyclooxygenase-2. *Mol. Biol. Cell* 18, 2137–2148. doi: 10.1091/mbc.e06-09-0850

Doller, A., Akool, L.-S., Huwiler, A., Müller, R., Radeke, H. H., Pfeilschifter, J., et al. (2008). Posttranslational modification of the AU-rich element binding protein HuR by protein kinase Cδ elicits angiotensin II-induced stabilization and nuclear export of cyclooxygenase 2 mRNA. *Mol. Cell Biol.* 28, 2608–2625. doi: 10.1128/MCB.01530-07

Doller, A., Schlepckow, K., Schwalbe, H., Pfeilschifter, J., and Eberhardt, W. (2010). Tandem phosphorylation of serines 221 and 318 by protein kinase Cδ coordinates mRNA binding and nucleocytoplasmic shuttling of HuR. *Mol. Cell Biol.* 30, 1397–1410. doi: 10.1128/MCB.01373-09

Doller, A., Winkler, C., Azrilian, I., Schulz, S., Hartmann, S., Pfeilschifter, J., et al. (2011). High-constitutive HuR phosphorylation at Ser 318 by PKCδ propagates tumor relevant functions in colon carcinoma cells. *Carcinogenesis* 32, 676–685. doi: 10.1093/carcin/bgr024

Drino, A., and Schaefer, M. R. (2018). RNAs, phase separation, and membraneless organelles: are post-transcriptional modifications modulating organelle dynamics? *Bioessays* 40:e1800085. doi: 10.1002/bies.201800085

Duan, Y., Du, A., Gu, J., Duan, G., Wang, C., Gui, X., et al. (2019). PARylation regulates stress granule dynamics, phase separation, and neurotoxicity of disease-related RNA-binding proteins. *Cell Res.* 29, 233–247. doi: 10.1038/s41422-019-0141-z

Embade, N., Fernández-Ramos, D., Varela-Rey, M., Beraza, N., Sini, M., Gutiérrez de Juan, V., et al. (2012). Murine double minute 2 regulates Hu antigen R stability in human liver and colon cancer through NEDDylation. *Hepatology* 55, 1237–1248. doi: 10.1002/hep.24795

Enchev, R. I., Schulman, B. A., and Peter, M. (2015). Protein neddylation: beyond cullin-RING ligases. *Nat. Rev. Mol. Cell Biol.* 16, 30–44. doi: 10.1038/nrm3919

Erson-Bensan, A. E. (2016). Alternative polyadenylation and RNA-binding proteins. *J. Mol. Endocrinol.* 57, F29–F34. doi: 10.1530/JME-16-0070

Fang, J., Bolanos, L. C., Choi, K., Liu, X., Christie, S., Akunuru, S., et al. (2017). Ubiquitination of hnRNPA1 by TRAF6 links chronic innate immune signaling with myelodysplasia. *Nat. Immunol.* 18, 236–245. doi: 10.1038/ni.3654

Fernández-Ramos, D., and Martínez-Chantar, M. L. (2015). NEDDylation in liver cancer: the regulation of the RNA binding protein Hu antigen R. *Pancreatology* 15, S49–S54. doi: 10.1016/j.pan.2015.03.006

Fernandopulle, M., Wang, G., Nixon-Abell, J., Qamar, S., Balaji, V., Morihara, R., et al. (2019). Inherited and sporadic amyotrophic lateral sclerosis and fronto-temporal lobar degenerations arising from pathological condensates of phase separating proteins. *Hum. Mol. Genet.* 28, R187–R196. doi: 10.1093/hmg/ddz162

Filippova, N., Yang, X., King, P., and Nabors, L. B. (2012). Phosphoregulation of the RNA-binding protein Hu antigen R (HuR) by Cdk5 affects centrosome function. *J. Biol. Chem.* 287, 32277–32287.

Förch, P., Puig, O., Martínez, C., Séraphin, B., and Valcárcel, J. (2002). The splicing regulator TIA-1 interacts with U1-C to promote U1 snRNP recruitment to 5' splice sites. *EMBO J.* 21, 6882–6892. doi: 10.1093/emboj/cdf668

Foshag, D., Henrich, E., Hiller, E., Schäfer, M., Kerger, C., Burger-Kentischer, A., et al. (2018). The *E. coli* S30 lysate proteome: A prototype for cell-free protein production. *N. Biotechnol.* 40, 245–260. doi: 10.1016/j.nbt.2017.09.005

François-Moutal, L., Pérez-Miller, S., Scott, D. D., MiRNAanda, V. G., Mollasalehi, N., and Khanna, M. (2019). Structural insights into TDP-43 and effects of post-translational modifications. *Front. Mol. Neurosci.* 12:301. doi: 10.3389/fnmol.2019.00301

Gal, J., Chen, J., Na, D. Y., Tichacek, L., Barnett, K. R., and Zhu, H. (2019). The acetylation of lysine-376 of G3BP1 regulates RNA binding and stress granule dynamics. *Mol. Cell Biol.* 39, e52–e19. doi: 10.1128/MCB.00052-19

García-Mauriño, S. M., Rivero-Rodríguez, F., Velázquez-Cruz, A., Hernández-Vellisca, M., Díaz-Quintana, A., De la Rosa, M. A., et al. (2017). RNA binding protein regulation and cross-talk in the control of AU-rich mRNA fate. *Front. Mol. Biosci.* 4:71. doi: 10.3389/fmolb.2017.00071

García-Mayoral, M. F., Hollingworth, D., Masino, L., Díaz-Moreno, I., Kelly, G., Gherzi, R., et al. (2007). The structure of the C-terminal KH domains of KSRP reveals a noncanonical motif important for mRNA degradation. *Structure* 15, 485–498. doi: 10.1016/j.str.2007.03.006

Gebauer, F., Schwarzl, T., Valcárcel, J., and Hentze, M. W. (2021). RNA-binding proteins in human genetic disease. *Nat. Rev. Genet.* 22, 185–198. doi: 10.1038/s41576-020-00302-y

Geffen, Y., Appleboim, A., Gardner, R. G., Friedman, N., Sadeh, R., and Ravid, T. (2016). Mapping the landscape of a eukaryotic degronome. *Mol. Cell.* 63, 1055–1065. doi: 10.1016/j.molcel.2016.08.005

Gerstberger, S., Hafner, M., and Tuschl, T. (2014). A census of human RNA-binding proteins. *Nat. Rev. Genet*. 15, 829–845. doi: 10.1038/nrg3813

Gherzi, R., Chen, C. Y., Trabucchi, M., Ramos, A., and Briata, P. (2010). The role of KSRP in mRNA decay and microRNA precursor maturation. *Wiley Interdiscip. Rev. RNA* 1, 230–239. doi: 10.1002/wrna.2

Gongol, B., Marin, T., Zhang, J., Wang, S. C., Sun, W., He, M., et al. (2019). Shear stress regulation of miRNA-93 and miRNA-484 maturation through nucleolin. *Proc. Natl. Acad. Sci. U.S.A.* 116, 12974–12979. doi: 10.1073/pnas.1902844116

Grammatikakis, I., Abdelmohsen, K., and Gorospe, M. (2017). Posttranslational control of HuR function. *Wiley Interdiscip. Rev. RNA* 8:1372. doi: 10.1002/wrna.1372

Gummadi, L., Taylor, L., and Curthoys, N. P. (2012). Concurrent binding and modifications of AUF1 and HuR mediate the pH-responsive stabilization of phosphoenolpyruvate carboxykinase mRNA in kidney cells. *Am. J. Physiol. Renal Physiol.* 303, F1545–F1554. doi: 10.1152/ajprenal.00400.2012

Habelhah, H., Shah, K., Huang, L., Ostareck-Lederer, A., Burlingame, A. L., Shokat, K. M., et al. (2001a). ERK phosphorylation drives cytoplasmic accumulation of hnRNP-K and inhibition of mRNA translation. *Nat. Cell Biol.* 2001, 325–330. doi: 10.1038/35060131

Habelhah, H., Shah, K., Huang, L., Burlingame, A. L., Shokat, K. M., and Ronai, Z. (2001b). Identification of new JNK substrate using ATP pocket mutant JNK and a corresponding ATP analogue. *J. Biol. Chem.* 276, 18090–18095. doi: 10.1074/jbc.M011396200

Hanna, J., Guerra-Moreno, A., Ang, J., and Micoogullari, Y. (2019). Protein degradation and the pathologic basis of disease. *Am. J. Pathol.* 189, 94–103. doi: 10.1016/j.ajpath.2018.09.004

Hans, F., Fiesel, F. C., Strong, J. C., Jäckel, S., Rasse, T. M., Geisler, S., et al. (2014). UBE2E ubiquitin-conjugating enzymes and ubiquitin isopeptidase Y regulate TDP-43 protein ubiquitination. *J. Biol. Chem.* 289, 19164–19179. doi: 10.1074/jbc.M114.561704

Hentze, M. W., Castello, A., Schwarzl, T., and Preiss, T. (2018). A brave new world of RNA-binding proteins. *Nat. Rev. Mol. Cell Biol.* 19, 327–341. doi: 10.1038/nrm.2017.130

Hitti, E., Iakovleva, T., Brook, M., Deppenmeier, S., Gruber, A. D., Radzioch, D., et al. (2006). Mitogen-activated protein kinase-activated protein kinase 2 regulates tumor necrosis factor mRNA stability and translation mainly by altering tristetraprolin expression, stability, and binding to adenine/uridine-rich element. *Mol. Cell. Biol.* 26, 2399–2407. doi: 10.1128/MCB.26.6.2399-2407.2006

Hofweber, M., and Dormann, D. (2019). Friend or foe–Post-translational modifications as regulators of phase separation and RNP granule dynamics. *J. Biol. Chem.* 294, 7137–7150. doi: 10.1074/jbc.TM118.001189

Hofweber, M., Hutten, S., Bourgeois, B., Spreitzer, E., Niedner-Boblenz, A., Schifferer, M., et al. (2018). Phase separation of FUS is suppressed by its nuclear import receptor and arginine methylation. *Cell* 173, 706.e–719.e. doi: 10.1016/j.cell.2018.03.004

Huang, W. S., Xu, F. M., Zeng, Q. Z., Liu, X. H., Gao, X. J., and Liu, L. X. (2017). ERK1/2-mediated cytoplasmic accumulation of hnRNPK antagonizes TRAIL-induced apoptosis through upregulation of XIAP in H1299 cells. *Biomed. Environ. Sci.* 30, 473–481. doi: 10.3967/bes2017.063

Huang, K. Y., Lee, T. Y., Kao, H. J., Ma, C. T., Lee, C. C., Lin, T. H., et al. (2019a). dbPTM in 2019: exploring disease association and cross-talk of post-translational modifications. *Nucleic Acids Res.* 47, D298–D308. doi: 10.1093/nar/gky1074

Huang, R., Huang, Y., Guo, Y., Ji, S., Lu, M., and Li, T. (2019b). Systematic characterization and prediction of post-translational modification cross-talk between proteins. *Bioinformatics* 35, 2626–2633. doi: 10.1093/bioinformatics/bty1033

Iadevaia, V., and Gerber, A. P. (2015). Combinatorial control of mRNA fates by RNA-binding proteins and non-coding RNAs. *Biomolecules* 5, 2207–2222. doi: 10.3390/biom5042207

Iervolino, A., Santilli, G., Trotta, R., Guerzoni, C., Cesi, V., Bergamaschi, A., et al. (2002). hnRNP A1 nucleocytoplasmic shuttling activity is required for normal myelopoiesis and BCR/ABL leukemogenesis. *Mol. Cell. Biol.* 22, 2255–2266. doi: 10.1128/mcb.22.7.2255-2266.2002

Izquierdo, J. M., and Valcárcel, J. (2007). Fas-activated serine/threonine kinase (FAST K) synergizes with TIA-1/TIAR proteins to regulate Fas alternative splicing. *J. Biol. Chem.* 282, 1539–1543. doi: 10.1074/jbc.C600198200

Jia, W., Yao, Z., Zhao, J., Guan, Q., and Gao, L. (2017). New perspectives of physiological and pathological functions of nucleolin (NCL). *Life Sci.* 186, 1–10. doi: 10.1016/j.lfs.2017.07.025

Kataoka, N., Bachorik, J. L., and Dreyfuss, G. (1999). Transportin-SR, a nuclear import receptor for SR proteins. *J. Cell Biol.* 1999, 1145–1152. doi: 10.1083/jcb.145.6.1145

Ke, Y., Han, Y., Guo, X., Wen, J., Wang, K., Jiang, X., et al. (2017). PARP1 promotes gene expression at the post-transcriptional level by modulating the RNA-binding protein HuR. *Nat. Commun.* 8:14632. doi: 10.1038/ncomms14632

Ke, Y., Lv, X., Fu, X., Zhang, J., Bohio, A. A., Zeng, X., et al. (2021). Poly(ADP-ribosyl)ation enhances HuR oligomerization and contributes to pro-inflammatory gene mRNA stabilization. *Cell Mol. Life Sci.* 78, 1817–1835. doi: 10.1007/s00018-020-03618-4

Keene, J. D. (2010). Minireview: global regulation and dynamics of ribonucleic acid. *Endocrinology* 151, 1391–1397. doi: 10.1210/en.2009-1250

Keiten-Schmitz, J., Wagner, K., Piller, T., Kaulich, M., Alberti, S., and Müller, S. (2020). The nuclear SUMO-targeted ubiquitin quality control network regulates the dynamics of cytoplasmic stress granules. *Mol. Cell* 79, 54.e–67.e. doi: 10.1016/j.molcel.2020.05.017

Kim, H. H., Abdelmohsen, K., Lal, A., Pullmann, R. Jr., Yang, X., Galban, S., et al. (2008). Nuclear HuR accumulation through phosphorylation by Cdk1. *Genes Dev.* 22, 1804–1815. doi: 10.1101/gad.1645808

Kimura, Y., Nagata, K., Suzuki, N., Yokoyama, R., Yamanaka, Y., Kitamura, H., et al. (2010). Characterization of multiple alternative forms of heterogeneous nuclear ribonucleoprotein K by phosphate-affinity electrophoresis. *Proteomics* 10, 3884–3895. doi: 10.1002/pmic.201000349

Knapinska, A. M., Gratacós, F. M., Krause, C. D., Hernandez, K., Jensen, A. G., and Bradley, J. J. (2011). Chaperone Hsp27 modulates AUF1 proteolysis and AU-rich element-mediated mRNA degradation. *Mol. Cell. Biol.* 31, 1419–1431. doi: 10.1128/MCB.00907-10

Kung, Y. A., Hung, C. T., Chien, K. Y., and Shih, S. R. (2017). Control of the negative IRES trans-acting factor KHSRP by ubiquitination. *Nucleic Acids Res.* 45, 271–287. doi: 10.1093/nar/gkw1042

Lafarga, V., Cuadrado, A., López, de Silanes, I., Bengoechea, R., Fernández-Capetillo, O., et al. (2009). p38 Mitogen-activated protein kinase- and HuR-dependent stabilization of p21(Cip1) mRNA mediates the G1/S checkpoint. *Mol. Cell Biol.* 29, 4341–4351. doi: 10.1128/MCB.00210-09

Lai, M. C., Lin, R. I., Huang, S. Y., Tsai, C. W., and Tarn, W. Y. (2000). A human importin-beta family protein, transportin-SR2, interacts with the phosphorylated RS domain of SR proteins. *J. Biol. Chem.* 275, 7950–7957. doi: 10.1074/jbc.275.11.7950

Lai, M. C., Lin, R. I., and Tarn, W. Y. (2001). Transportin-SR2 mediates nuclear import of phosphorylated SR proteins. *Proc. Natl. Acad. Sci. U.S.A.* 98, 10154–10159. doi: 10.1073/pnas.181354098

Li, H., Park, S., Kilburn, B., Jelinek, M. A., Henschen-Edman, A., Aswad, D. W., et al. (2002). Lipopolysaccharide-induced methylation of HuR, an mRNA-stabilizing protein, by CARM1. *J. Biol. Chem.* 277, 44623–44630. doi: 10.1074/jbc.M206187200

Liao, W. L., Wang, W. C., Chang, W. C., and Tseng, J. T. (2011). The RNA-binding protein HuR stabilizes cytosolic phospholipase A2α mRNA under interleukin-1β treatment in non-small cell lung cancer A549 Cells. *J. Biol. Chem.* 286, 35499–35508. doi: 10.1074/jbc.M111.263582

Liu, H. F., and Liu, R. (2020). Structure-based prediction of post-translational modification cross-talk within proteins using complementary residue- and residue pair-based features. *Brief Bioinform.* 21, 609–620. doi: 10.1093/bib/bby123

Liu, L., Rao, J. N., Zou, T., Xiao, L., Wang, P. Y., Turner, D. J., et al. (2009). Polyamines regulate c-Myc translation through Chk2-dependent HuR phosphorylation. *Mol. Biol. Cell* 20, 4885–4898. doi: 10.1091/mbc.e09-07-0550

Lo, S. J., Lee, C. C., and Lai, H. J. (2006). The nucleolus: reviewing oldies to have new understandings. *Cell Res.* 16, 530–538. doi: 10.1038/sj.cr.7310070

Loffreda, A., Rigamonti, A., Barabino, S. M., and Lenzken, S. C. (2015). RNA-binding proteins in the regulation of miRNA activity: a focus on neuronal functions. *Biomolecules* 5, 2363–2387. doi: 10.3390/biom5042363

Long, Y., Sou, W. H., Yung, K. W. Y., Liu, H., Wan, S. W. C., Li, Q., et al. (2019). Distinct mechanisms govern the phosphorylation of different SR protein splicing factors. *J. Biol. Chem.* 294, 1312–1327. doi: 10.1074/jbc.RA118.003392

Loughlin, F. E., West, D. L., Gunzburg, M. J., Waris, S., Crawford, S. A., Wilce, M. C. J., et al. (2021). Tandem RNA binding sites induce self-association of the stress granule marker protein TIA-1. *Nucleic Acids Res.* 49, 2403–2417. doi: 10.1093/nar/gkab080

Lovci, M. T., Bengtson, M. H., and Massirer, K. B. (2016). Post-translational modifications and RNA-binding proteins. *Adv. Exp. Med. Biol.* 907, 297–317. doi: 10.1007/978-3-319-29073-7_12

Lucchesi, C., Sheikh, M. S., and Huang, Y. (2016). Negative regulation of RNA-binding protein HuR by tumor-suppressor ECRG2. *Oncogene* 35, 2565–2573. doi: 10.1038/onc.2015.339

Lukaesko, L., and Meller, R. (2011). "Regulation of gene expression by the ubiquitin–proteasome system and implications for neurological disease," in *Post-translational modifications in health and disease*, ed. C. Vidal (New York, NY: Springer), 281–315. doi: 10.1007/978-1-4419-6382-6_12

Masuda, K., Abdelmohsen, K., Kim, M. M., Srikantan, S., Lee, E. K., Tominaga, K., et al. (2011). Global dissociation of HuR-mRNA complexes promotes cell survival after ionizing radiation. *EMBO J.* 30, 1040–1053. doi: 10.1038/emboj.2011.24

Mazroui, R., Di Marco, S., Clair, E., von Roretz, C., Tenenbaum, S. A., Keene, J. D., et al. (2008). Caspase-mediated cleavage of HuR in the cytoplasm contributes to pp32/PHAP-I regulation of apoptosis. *J. Cell. Biol.* 180, 113–127. doi: 10.1083/jcb.200709030

Mazzotta, A., Partipilo, G., De Summa, S., Giotta, F., Simone, G., and Mangia, A. (2016). Nuclear PARP1 expression and its prognostic significance in breast cancer patients. *Tumour Biol.* 37, 6143–6153. doi: 10.1007/s13277-015-4465-0

McGurk, L., Gomes, E., Guo, L., Mojsilovic-Petrovic, J., Tran, V., Kalb, R. G., et al. (2018). Poly(ADP-Ribose) prevents pathological phase separation of TDP-43 by promoting liquid demixing and stress granule localization. *Mol. Cell* 71, 703.e–717.e. doi: 10.1016/j.molcel.2018.07.002

Messias, A. C., Harnisch, C., Ostareck-Lederer, A., Sattler, M., and Ostareck, D. H. (2006). The DICE-binding activity of KH domain 3 of hnRNP K is affected by c-Src-mediated tyrosine phosphorylation. *J. Mol. Biol.* 361, 470–481. doi: 10.1016/j.jmb.2006.06.025

Michlewski, G., and Cáceres, J. F. (2019). Post-transcriptional control of miRNA biogenesis. *RNA* 25, 1–16. doi: 10.1261/rna.068692.118

Mitchell, S. F., and Parker, R. (2014). Principles and properties of eukaryotic mRNPs. *Mol. Cell* 54, 547–558. doi: 10.1016/j.molcel.2014.04.033

Moore, S., Järvelin, A. I., Davis, I., Bond, G. L., and Castello, A. (2018). Expanding horizons: new roles for non-canonical RNA-binding proteins in cancer. *Curr. Opin. Genet. Dev.* 48, 112–120. doi: 10.1016/j.gde.2017.11.006

Moumen, A., Masterson, P., O'Connor, M. J., and Jackson, S. P. (2005). hnRNP K: an HDM2 target and transcriptional coactivator of p53 in response to DNA damage. *Cell* 123, 1065–1078. doi: 10.1016/j.cell.2005.09.032

Moumen, A., Magill, C., Dry, K. L., and Jackson, S. P. (2013). ATM-dependent phosphorylation of heterogeneous nuclear ribonucleoprotein K promotes p53 transcriptional activation in response to DNA damage. *Cell Cycle* 12, 698–704. doi: 10.4161/cc.23592

Müller-McNicoll, M., and Neugebauer, K. M. (2013). How cells get the message: dynamic assembly and function of mRNA-protein complexes. *Nat. Rev. Genet.* 14, 275–287. doi: 10.1038/nrg3434

Naarmann-de Vries, I. S., Urlaub, H., Ostareck, D. H., and Ostareck-Lederer, A. (2013). Caspase-3 cleaves hnRNP K in erythroid differentiation. *Cell Death Dis.* 4:e548. doi: 10.1038/cddis.2013.75

Nechama, M., Uchida, T., Mor Yosef-Levi, I., Silver, J., and Naveh-Many, T. (2009). The peptidyl-prolyl isomerase Pin1 determines parathyroid hormone mRNA levels and stability in rat models of secondary hyperparathyroidism. *J. Clin. Invest.* 119, 3102–3114. doi: 10.1172/JCI39522

Ngo, J. C., Chakrabarti, S., Ding, J. H., Velázquez-Dones, A., Nolen, B., and Aubol, B. E. (2005). Interplay between SRPK and Clk/Sty kinases in phosphorylation of the splicing factor ASF/SF2 is regulated by a docking motif in ASF/SF2. *Mol. Cell.* 20, 77–89. doi: 10.1016/j.molcel.2005.08.025

Ngoc, L. V., Wauquier, C., Soin, R., Bousbata, S., Twyffels, L., Kruys, V., et al. (2014). Rapid proteasomal degradation of posttranscriptional regulators of the TIS11/tristetraprolin family is induced by an intrinsically unstructured region independently of ubiquitination. *Mol. Cell. Biol.* 34, 4315–4328. doi: 10.1128/MCB.00643-14

Nicastro, G., García-Mayoral, M. F., Hollingworth, D., Kelly, G., Martin, S. R., Briata, P., et al. (2012). Noncanonical G recognition mediates KSRP regulation of let-7 biogenesis. *Nat. Struct. Mol. Biol.* 19, 1282–1286. doi: 10.1038/nsmb.2427

Ohsumi, Y. (2006). Protein turnover. *IUBMB Life* 58, 363–369. doi: 10.1080/15216540600758539

Ostareck-Lederer, A., Ostareck, D. H., Cans, C., Neubauer, G., Bomsztyk, K., Superti-Furga, G., et al. (2002). c-Src-mediated phosphorylation of hnRNP K drives translational activation of specifically silenced mRNAs. *Mol. Cell Biol.* 22, 4535–4543. doi: 10.1128/mcb.22.13.4535-4543.2002

Ostareck-Lederer, A., Ostareck, D. H., Rucknagel, K. P., Schierhorn, A., Moritz, B., Huttelmaier, S., et al. (2006). Asymmetric arginine dimethylation of heterogeneous nuclear ribonucleoprotein K by protein-arginine methyltransferase 1 inhibits its interaction with c-Src. *J. Biol. Chem.* 281, 11115–11125. doi: 10.1074/jbc.M513053200

Owen, I., and Shewmaker, F. (2019). The role of post-translational modifications in the phase transitions of intrinsically disordered proteins. *Int. J. Mol. Sci.* 20:5501. doi: 10.3390/ijms20215501

Pabis, M., Popowicz, G. M., Stehle, R., Fernández-Ramos, D., Asami, S., Warner, L., et al. (2019). HuR biological function involves RRM3-mediated dimerization and RNA binding by all three RRMs. *Nucleic Acids Res.* 47, 1011–1029. doi: 10.1093/nar/gky1138

Panas, M. D., Kedersha, N., Schulte, T., Branca, R. M., Ivanov, P., and Anderson, P. (2019). Phosphorylation of G3BP1-S149 does not influence stress granule assembly. *J. Cell Biol.* 218, 2425–2432. doi: 10.1083/jcb.201801214

Pang, L., Tian, H., Chang, N., Yi, J., Xue, L., Jiang, B., et al. (2013). Loss of CARM1 is linked to reduced HuR function in replicative senescence. *BMC Mol. Biol.* 14:15. doi: 10.1186/1471-2199-14-15

Pelisch, F., Pozzi, B., Risso, G., Muñoz, M. J., and Srebrow, A. (2012). DNA damage-induced heterogeneous nuclear ribonucleoprotein K sumoylation regulates p53 transcriptional activation. *J. Biol. Chem.* 287, 30789–30799. doi: 10.1074/jbc.M112.390120

Pereira, B., Billaud, M., and Almeida, R. (2017). RNA-binding proteins in cancer: old players and new actors. *Trends Cancer* 3, 506–528. doi: 10.1016/j.trecan.2017.05.003

Pérez-Mejías, G., Velázquez-Cruz, A., Guerra-Castellano, A., Baños-Jaime, B., Díaz-Quintana, A., González-Arzola, K., et al. (2020). Exploring protein phosphorylation by combining computational approaches and biochemical methods. *Comput. Struct. Biotechnol. J.* 18, 1852–1863. doi: 10.1016/j.csbj.2020.06.043

Perrotti, D., Iervolino, A., Cesi, V., Cirinná, M., Lombardini, S., Grassilli, E., et al. (2000). BCR-ABL prevents c-jun-mediated and proteasome-dependent FUS (TLS) proteolysis through a protein kinase CbetaII-dependent pathway. *Mol. Cell. Biol.* 20, 6159–6169. doi: 10.1128/mcb.20.16.6159-6169.2000

Phoomak, C., Park, D., Silsirivanit, A., Sawanyawisuth, K., Vaeteewoottacharn, K., Detarya, M., et al. (2019). O-GlcNAc-induced nuclear translocation of hnRNP-K is associated with progression and metastasis of cholangiocarcinoma. *Mol. Oncol.* 13, 338–357. doi: 10.1002/1878-0261.12406

Pichler, A., Fatouros, C., Lee, H., and Eisenhardt, N. (2017). SUMO conjugation – a mechanistic view. *Biomol. Concepts*. 8, 13–36. doi: 10.1515/bmc-2016-0030

Pope, S. D., and Medzhitov, R. (2018). Emerging principles of gene expression programs and their regulation. *Mol. Cell* 71, 389–397. doi: 10.1016/j.molcel.2018.07.017

Prasad, A., Bharathi, V., Sivalingam, V., Girdhar, A., and Patel, B. K. (2019). Molecular mechanisms of TDP-43 misfolding and pathology in amyotrophic lateral sclerosis. *Front. Mol. Neurosci.* 12:25. doi: 10.3389/fnmol.2019.00025

Qamar, S., Wang, G., Randle, S. J., Ruggeri, F. S., Varela, J. A., Lin, J. Q., et al. (2018). FUS phase separation is modulated by a molecular chaperone and methylation of arginine cation-π interactions. *Cell* 173, 720.e–734.e. doi: 10.1016/j.cell.2018.03.056

Repetto, E., Briata, P., Kuziner, N., Harfe, B. D., McManus, M. T., Gherzi, R., et al. (2012). Let-7b/c enhance the stability of a tissue-specific mRNA during mammalian organogenesis as part of a feedback loop involving KSRP. *PLoS Genet.* 8:e1002823. doi: 10.1371/journal.pgen.1002823

Ronkina, N., Kotlyarov, A., Dittrich-Breiholz, O., Kracht, M., Hitti, E., Milarski, K., et al. (2007). The mitogen-activated protein kinase (MAPK)-activated protein kinases MK2 and MK3 cooperate in stimulation of tumor necrosis factor biosynthesis and stabilization of p38 MAPK. *Mol. Cell. Biol.* 27, 170–181. doi: 10.1128/MCB.01456-06

Ronkina, N., Shushakova, N., Tiedje, C., Yakovleva, T., Tollenaere, M. A. X., Scott, A., et al. (2019). The role of TTP phosphorylation in the regulation of inflammatory cytokine production by MK2/3. *J. Immunol.* 203, 2291–2300. doi: 10.4049/jimmunol.1801221

Rougemaille, M., Villa, T., Gudipati, R. K., and Libri, D. (2008). mRNA journey to the cytoplasm: attire required. *Biol. Cell* 100, 327–342. doi: 10.1042/BC20070143

Ruberti, G., Cascino, I., Papoff, G., and Eramo, A. (1996). Fas splicing variants and their effect on apoptosis. *Adv. Exp. Med. Biol.* 406, 125–134. doi: 10.1007/978-1-4899-0274-0_13

Ryan, V. H., Dignon, G. L., Zerze, G. H., Chabata, C. V., Silva, R., Conicella, A. E., et al. (2018). Mechanistic view of hnRNPA2 low-complexity domain structure, interactions, and phase separation altered by mutation and arginine methylation. *Mol. Cell* 69, 465.e–479.e. doi: 10.1016/j.molcel.2017.12.022

Ryan, V. H., and Fawzi, N. L. (2019). Physiological, pathological, and targetable membraneless organelles in neurons. *Trends Neurosci.* 42, 693–708. doi: 10.1016/j.tins.2019.08.005

Scheiba, R. M., Aroca, A., and Díaz-Moreno, I. (2012). HuR thermal stability is dependent on domain binding and upon phosphorylation. *Eur. Biophys. J.* 41, 597–605. doi: 10.1007/s00249-012-0827-3

Scheiba, R. M., de Opakua, A. I., Díaz-Quintana, A., Cruz-Gallardo, I., Martínez-Cruz, L. A., Martínez-Chantar, M. L., et al. (2014). The C-terminal RNA binding motif of HuR is a multi-functional domain leading to HuR oligomerization and binding to U-rich RNA targets. *RNA Biol.* 11, 1250–1261. doi: 10.1080/15476286.2014.996069

Schuschel, K., Helwig, M., Hüttelmaier, S., Heckl, D., Klusmann, J. H., and Hoell, J. I. (2020). RNA-binding proteins in acute leukemias. *Int. J. Mol. Sci.* 21:3409. doi: 10.3390/ijms21103409

Seyfried, N. T., Gozal, Y. M., Dammer, E. B., Xia, Q., Duong, D. M., Cheng, D., et al. (2010). Multiplex SILAC analysis of a cellular TDP-43 proteinopathy model reveals protein inclusions associated with SUMOylation and diverse polyubiquitin chains. *Mol. Cell. Proteomics* 2010, 705–718. doi: 10.1074/mcp.M800390-MCP200

Shen, Z. J., Esnault, S., and Malter, J. S. (2005). The peptidyl-prolyl isomerase Pin1 regulates the stability of granulocyte-macrophage colony-stimulating factor mRNA in activated eosinophils. *Nat. Immunol.* 6, 1280–1287. doi: 10.1038/ni1266

Shen, Z. J., and Malter, J. S. (2015). Regulation of AU-rich element RNA binding proteins by phosphorylation and the prolyl isomerase Pin1. *Biomolecules* 5, 412–434. doi: 10.3390/biom5020412

Srikantan, S., and Gorospe, M. (2012). HuR function in disease. *Front. Biosci.* 17, 189–205. doi: 10.2741/3921

Stackpole, E. E., Akins, M. R., and Fallon, J. R. (2014). N-myristoylation regulates the axonal distribution of the Fragile X-related protein FXR2P. *Mol. Cell. Neurosci.* 62, 42–50. doi: 10.1016/j.mcn.2014.08.003

St George-Hyslop, P., Lin, J. Q., Miyashita, A., Phillips, E. C., Qamar, S., Randle, S. J., et al. (2018). The physiological and pathological biophysics of phase separation and gelation of RNA binding proteins in amyotrophic lateral sclerosis and fronto-temporal lobar degeneration. *Brain Res.* 1693, 11–23. doi: 10.1016/j.brainres.2018.04.036

Stoehr, A., Yang, Y., Patel, S., Evangelista, A. M., Aponte, A., Wang, G., et al. (2016). Prolyl hydroxylation regulates protein degradation, synthesis, and splicing in human induced pluripotent stem cell-derived cardiomyocytes. *Cardiovasc. Res.* 110, 346–358. doi: 10.1093/cvr/cvw081

Strom, A. R., and Brangwynne, C. P. (2019). The liquid nucleome - phase transitions in the nucleus at a glance. *J. Cell Sci.* 132, jcs235093. doi: 10.1242/jcs.235093

Sun, Y., Gallacchi, D., Zhang, E. Y., Reynolds, S. B., Robinson, L., Malinowska, I. A., et al. (2014). Rapamycin-resistant poly (ADP-ribose) polymerase-1 overexpression is a potential therapeutic target in lymphangioleiomyomatosis. *Am. J. Respir. Cell Mol. Biol.* 51, 738–749. doi: 10.1165/rcmb.2014-0033OC

Tahir, T. A., Singh, H., and Brindle, N. P. (2014). The RNA binding protein hnRNP-K mediates post-transcriptional regulation of uncoupling protein-2 by angiopoietin-1. *Cell. Signal.* 26, 1379–1384. doi: 10.1016/j.cellsig.2014.03.005

Tanikawa, C., Ueda, K., Suzuki, A., Iida, A., Nakamura, R., Atsuta, N., et al. (2018). Citrullination of RGG motifs in FET proteins by PAD4 regulates protein aggregation and ALS susceptibility. *Cell Rep.* 22, 1473–1483. doi: 10.1016/j.celrep.2018.01.031

Tourrière, H., Chebli, K., Zekri, L., Courselaud, B., Blanchard, J. M., Bertrand, E., et al. (2003). The RasGAP-associated endoribonuclease G3BP assembles stress granules. *J. Cell. Biol.* 160, 823–831. doi: 10.1083/jcb.200212128

Toyama, B. H., and Hetzer, M. W. (2013). Protein homeostasis: live long, won't prosper. *Nat. Rev. Mol. Cell Biol.* 14, 55–61. doi: 10.1038/nrm3496

Trabucchi, M., Briata, P., Garcia-Mayoral, M., Haase, A. D., Filipowicz, W., Ramos, A., et al. (2009). The RNA-binding protein KSRP promotes the biogenesis of a subset of microRNAs. *Nature* 459, 1010–1014. doi: 10.1038/nature08025

Tradewell, M. L., Yu, Z., Tibshirani, M., Boulanger, M. C., Durham, H. D., and Richard, S. (2012). Arginine methylation by PRMT1 regulates nuclear-cytoplasmic localization and toxicity of FUS/TLS harbouring ALS-linked mutations. *Hum. Mol. Genet.* 21, 136–149. doi: 10.1093/hmg/ddr448

Van Nostrand, E. L., Freese, P., Pratt, G. A., Wang, X., Wei, X., Xiao, R., et al. (2020). A large-scale binding and functional map of human RNA-binding proteins. *Nature* 583, 711–719. doi: 10.1038/s41586-020-2077-3

Varshavsky, A. (2017). The ubiquitin system, autophagy, and regulated protein degradation. *Annu. Rev. Biochem.* 86, 123–128. doi: 10.1146/annurev-biochem-061516-044859

Venne, A. S., Kollipara, L., and Zahedi, R. P. (2014). The next level of complexity: crosstalk of posttranslational modifications. *Proteomics* 14, 513–524. doi: 10.1002/pmic.201300344

Vidal, C. (2011). *Post-translational modifications in health and disease*. New York, NY: Springer, doi: 10.1007/978-1-4419-6382-6

Virág, D., Dalmadi-Kiss, B., Vékey, K., Drahos, L., Klebovich, I., Antal, I., et al. (2020). Current trends in the analysis of post-translational modifcations. *Chromatographia* 83, 1–10. doi: 10.1007/s10337-019-03796-9

von Roretz, C., and Gallouzi, I. E. (2010). Protein kinase RNA/FADD/caspase-8 pathway mediates the proapoptotic activity of the RNA-binding protein human antigen R (HuR). *J. Biol. Chem.* 285, 16806–16813. doi: 10.1074/jbc.M109.087320

Vu, L. D., Gevaert, K., and De Smet, I. (2018). Protein language: post-translational modifications talking to each other. *Trends Plant Sci.* 23, 1068–1080. doi: 10.1016/j.tplants.2018.09.004

Wang, I., Hennig, J., Jagtap, P. K., Sonntag, M., Valcárcel, J., and Sattler, M. (2014). Structure, dynamics and RNA binding of the multi-domain splicing factor TIA-1. *Nucleic Acids Res.* 42, 5949–5966. doi: 10.1093/nar/gku193

Wang, L., Liang, C., Li, F., Guan, D., Wu, X., Fu, X., et al. (2017). PARP1 in carcinomas and PARP1 inhibitors as antineoplastic drugs. *Int. J. Mol. Sci.* 18:2111. doi: 10.3390/ijms18102111

Wang, C., Xu, W., Chao, Y., Liang, M., Zhang, F., and Huang, K. (2020). E3 ligase FBXW2 is a new therapeutic target in obesity and atherosclerosis. *Adv. Sci.* 7:2001800. doi: 10.1002/advs.202001800

Waris, S., García-Mauriño, S. M., Sivakumaran, A., Beckham, S. A., Loughlin, F. E., Gorospe, M., et al. (2017). TIA-1 RRM23 binding and recognition of target oligonucleotides. *Nucleic Acids Res.* 45, 4944–4957. doi: 10.1093/nar/gkx102

Wilson, G. M., Lu, J., Sutphen, K., Suarez, Y., Sinha, S., Brewer, B., et al. (2003). Phosphorylation of p40AUF1 regulates binding to A + U-rich mRNA-destabilizing elements and protein-induced changes in ribonucleoprotein structure. *J. Biol. Chem.* 278, 33039–33048. doi: 10.1074/jbc.M305775200

Witten, J. T., and Ule, J. (2011). Understanding splicing regulation through RNA splicing maps. *Trends Genet.* 27, 89–97. doi: 10.1016/j.tig.2010.12.001

Wolfson, E., Solomon, S., Schmukler, E., Goldshmit, Y., and Pinkas-Kramarski, R. (2018). Nucleolin and ErbB2 inhibition reduces tumorigenicity of ErbB2-positive breast cancer. *Cell Death Dis.* 9:47. doi: 10.1038/s41419-017-0067-7

Wolozin, B., and Ivanov, P. (2019). Stress granules and neurodegeneration. *Nat Rev Neurosci.* 20, 649–666. doi: 10.1038/s41583-019-0222-5

Xu, Y., Wu, W., Han, Q., Wang, Y., Li, C., Zhang, P., et al. (2019). Post-translational modification control of RNA-binding protein hnRNPK function. *Open Biol.* 9:180239. doi: 10.1098/rsob.180239

Xue, Y. C., Ng, C. S., Xiang, P., Liu, H., Zhang, K., Mohamud, Y., et al. (2020). Dysregulation of RNA-binding proteins in amyotrophic lateral sclerosis. *Front. Mol. Neurosci.* 13:78. doi: 10.3389/fnmol.2020.00078

Yang, J. H., Chiou, Y. Y., Fu, S. L., Shih, I. Y., Weng, T. H., Lin, W. J., et al. (2014). Arginine methylation of hnRNPK negatively modulates apoptosis upon DNA damage through local regulation of phosphorylation. *Nucleic Acids Res.* 42, 9908–9924. doi: 10.1093/nar/gku705

Yoon, J. H., Abdelmohsen, K., Srikantan, S., Guo, R., Yang, X., Martindale, J. L., et al. (2014). Tyrosine phosphorylation of HuR by JAK3 triggers dissociation and degradation of HuR target mRNAs. *Nucleic Acids Res.* 42, 1196–1208. doi: 10.1093/nar/gkt903

Yu, T. X., Wang, P. Y., Rao, J. N., Zou, T., Liu, L., Xiao, L., et al. (2011). Chk2-dependent HuR phosphorylation regulates occludin mRNA translation and epithelial barrier function. *Nucleic Acids Res.* 39, 8472–8487. doi: 10.1093/nar/gkr567

Yuan, H., Deng, R., Zhao, X., Chen, R., Hou, G., Zhang, H., et al. (2017). SUMO1 modification of KHSRP regulates tumorigenesis by preventing the TL-G-Rich miRNANA biogenesis. *Mol. Cancer*. 16:157. doi: 10.1186/s12943-017-0724-6

Zealy, R. W., Wrenn, S. P., Davila, S., Min, K. W., and Yoon, J. H. (2017). microRNA-binding proteins: specificity and function. *Wiley Interdiscip. Rev. RNA* 8:e1414. doi: 10.1002/wrna.1414

Zhang, X., Wan, G., Berger, F. G., He, X., and Lu, X. (2011). The ATM kinase induces microRNA biogenesis in the DNA damage response. *Mol. Cell.* 2011, 371–383. doi: 10.1016/j.molcel.2011.01.020

Zhou, H. L., Geng, C., Luo, G., and Lou, H. (2013). The p97-UBXD8 complex destabilizes mRNA by promoting release of ubiquitinated HuR from mRNP. *Genes Dev.* 27, 1046–1058. doi: 10.1101/gad.215681.113

Conflict of Interest: The authors declare that the research was conducted in the absence of any commercial or financial relationships that could be construed as a potential conflict of interest.

frontiers in Molecular Biosciences

MINI REVIEW
published: 07 May 2021
doi: 10.3389/fmolb.2021.673038

SUMO: Glue or Solvent for Phase-Separated Ribonucleoprotein Complexes and Molecular Condensates?

Jan Keiten-Schmitz[1†], Linda Röder[1†], Eran Hornstein[2,3], Michaela Müller-McNicoll[4] and Stefan Müller[1*]*

[1] Faculty of Medicine, Institute of Biochemistry II, Goethe University, Frankfurt, Germany, [2] Department of Molecular Genetics, Weizmann Institute of Science, Rehovot, Israel, [3] Department of Molecular Neuroscience, Weizmann Institute of Science, Rehovot, Israel, [4] Faculty of Biosciences, Institute for Molecular Biosciences, Goethe University, Frankfurt am Main, Germany

OPEN ACCESS

Edited by:
Dorothee Dormann,
University of Munich, Germany

Reviewed by:
Serena Carra,
University of Modena and Reggio Emilia, Italy
Umut Sahin,
Boğaziçi University, Turkey

***Correspondence:**
Michaela Müller-McNicoll
Mueller-McNicoll@bio.uni-frankfurt.de
Stefan Müller
ste.mueller@em.uni-frankfurt.de

[†] These authors have contributed equally to this work

Specialty section:
This article was submitted to Protein and RNA Networks, a section of the journal Frontiers in Molecular Biosciences

Received: 26 February 2021
Accepted: 08 April 2021
Published: 07 May 2021

Citation:
Keiten-Schmitz J, Röder L, Hornstein E, Müller-McNicoll M and Müller S (2021) SUMO: Glue or Solvent for Phase-Separated Ribonucleoprotein Complexes and Molecular Condensates? Front. Mol. Biosci. 8:673038. doi: 10.3389/fmolb.2021.673038

Spatial organization of cellular processes in membranous or membrane-less organelles (MLOs, alias molecular condensates) is a key concept for compartmentalizing biochemical pathways. Prime examples of MLOs are the nucleolus, PML nuclear bodies, nuclear splicing speckles or cytosolic stress granules. They all represent distinct sub-cellular structures typically enriched in intrinsically disordered proteins and/or RNA and are formed in a process driven by liquid-liquid phase separation. Several MLOs are critically involved in proteostasis and their formation, disassembly and composition are highly sensitive to proteotoxic insults. Changes in the dynamics of MLOs are a major driver of cell dysfunction and disease. There is growing evidence that post-translational modifications are critically involved in controlling the dynamics and composition of MLOs and recent evidence supports an important role of the ubiquitin-like SUMO system in regulating both the assembly and disassembly of these structures. Here we will review our current understanding of SUMO function in MLO dynamics under both normal and pathological conditions.

Keywords: SUMO, RNF4, PML, membrane-less organelles, nucleolus, stress granules, splicing

INTRODUCTION

Most cellular processes are compartmentalized in membranous or membrane-less organelles (MLOs, also termed molecular condensates). Prototypical MLOs in the nucleus are the nucleolus, paraspeckles, nuclear speckles (NS), Cajal bodies, PML nuclear bodies (PML NBs) or nuclear stress bodies (nSBs), and in the cytoplasm P-bodies and stress granules (SGs) (Banani et al., 2017; Alberti and Hyman, 2021). All these structures typically contain disordered proteins and/or RNA and form in a process that is driven by liquid-liquid phase separation (LLPS). LLPS describes the condensation of biological macromolecules in a dense phase that resembles liquid droplets and is stabilized by multivalent interactions. Intrinsically disordered regions (IDRs) of RNA binding proteins (RBPs) often play important roles in these condensates, in which specific RNAs or proteins act as scaffolds that recruit other client proteins. Several MLOs function as RNA or protein quality control centers and, accordingly, their formation, disassembly

and composition are highly sensitive to cellular stress, including proteotoxic stress (Gartner and Muller, 2014; Advani and Ivanov, 2019). Post-translational modifications (PTMs) have emerged as regulators of phase separation in the dynamics of MLOs and accumulating evidence points to the involvement of the SUMO system in these processes (Banani et al., 2016; Hofweber and Dormann, 2019). The SUMO pathway constitutes an evolutionary conserved ubiquitin-like post-translational modification system. SUMO (Small ubiquitin-related modifier) proteins (SUMO1,2,3 in humans) are covalently attached to a multitude of cellular proteins via lysine-linked isopeptide bonds (Flotho and Melchior, 2013; Cappadocia and Lima, 2018). At the amino acid level human SUMO2 and SUMO3 are 98% identical to each other and share about 50% identity to SUMO1. Conjugation of all three modifiers involves the heterodimeric E1 enzyme (AOS1/UBA2), the E2 enzyme UBC9 and a relatively small set of E3 SUMO ligases serving as specificity factors. SUMOylation is reversed by SUMO-specific isopeptidases. Notably, compared to the ubiquitin (Ub) system, the SUMO conjugation-deconjugation machinery is far less complex and SUMO E3 ligases or isopeptidases mostly target groups of related proteins that are physically and functionally connected (Jentsch and Psakhye, 2013). SUMO can be conjugated as a monomer, but also forms different types of polymeric chains via internal lysine residues (Keiten-Schmitz et al., 2019; Perez Berrocal et al., 2019). Compared to SUMO2/3, SUMO1 is less prone to chain formation and at least in some instances terminates SUMO2/3 chains (Jansen and Vertegaal, 2021). SUMOylation generally coordinates the plasticity of protein networks by modulating protein-protein interactions. This is mediated by specific SUMO interaction motifs (SIMs) that bind to SUMO conjugates thereby reading and interpreting the SUMO signal. There are multiple examples, where SUMO-SIM interactions can function in a "glue-like" manner to control the assembly of protein complexes (Matunis et al., 2006). SUMO chains, however, can trigger a particular signaling cascade, known as the SUMO-targeted ubiquitin ligase (StUbL) pathway (Kumar and Sabapathy, 2019). In this pathway, polySUMOylated proteins are bound by distinct ubiquitin ligases that harbor tandemly repeated SIMs. In mammals the RING-type E3 ligases RNF4 and RNF111 function as StUbLs triggering proteolytic or non-proteolytic ubiquitylation of polySUMOylated proteins, thereby directly bridging SUMO signaling to the Ub machinery. SUMO chain formation and the StUbL pathway are induced in response to proteotoxic or genotoxic stress (Jansen and Vertegaal, 2021). Under proteotoxic stress SUMO-primed ubiquitylation by RNF4 contributes to protein quality control by degrading misfolded nuclear proteins (Gartner and Muller, 2014; Guo et al., 2014). In the genotoxic stress response StUbLs are critical for remodeling of protein complexes (Keiten-Schmitz et al., 2019). The importance of the StUbL pathway for resolving protein complexes is best exemplified in the DNA damage response, where the disassembly of DNA repair complexes at sites of DNA damage is often mediated by polySUMO-primed RNF4-mediated ubiquitylation either triggering their degradation or their extraction from chromatin (Keiten-Schmitz et al., 2019). The latter process typically involves the AAA-ATPase p97/VCP and its co-factors (Bergink et al., 2013). In the following sections we will exemplify the role of the SUMO system in controlling the dynamics of membrane-less organelles.

SUMO AND THE DYNAMICS OF PML NUCLEAR BODIES

A paradigm for SUMO-SIM-dependent complex assembly and phase separation are PML (promyelocytic leukemia protein) nuclear bodies. The biomedical interest in PML NBs stems from the initial observation that the structural integrity of these macromolecular assemblies is lost in acute promyelocytic leukemia (APL). Disruption of NBs in APL is caused by expression of the oncogenic fusion protein PML-RARα (PML-retinoic acid receptor alpha) resulting from the aberrant t(15, 17) chromosomal translocation (Lallemand-Breitenbach and de The, 2018). PML NB biology is still not fully understood, but one well-established role is their function as hubs for post-translational modifications and centers of nuclear protein quality control (Gartner and Muller, 2014; Guo et al., 2014; Sha et al., 2019). Newly synthesized aberrant polypeptide chains, such as defective ribosomal products (DRiPs), or misfolded proteins, e.g., polyQ proteins, are sequestered into PML NBs, where they are cleared by the chaperone machinery or the ubiquitin proteasome system (Guo et al., 2014; Mediani et al., 2019a,b; Sha et al., 2019). It has been proposed that PML itself can recognize aberrant or misfolded proteins subsequently triggering their SUMOylation and StUbL-mediated ubiquitylation (Gartner and Muller, 2014; Guo et al., 2014). A role of PML NBs as centers of proteostasis is further supported by their enhanced formation in response to reactive oxygen species suggesting that they act as sensors for oxidative stress (Jeanne et al., 2010; Sahin et al., 2014). PML, which functions as the scaffold and organizer of this multiprotein complex, is expressed in seven different isoforms in humans and belongs to the tripartite motif (TRIM) family of proteins, characterized by a RING finger domain, two B-box zinc finger domains and a coiled-coil region (Jensen et al., 2001). PML represents a major cellular target for covalent modification by SUMO and also harbors a SIM for non-covalent SUMO binding (Muller et al., 1998; Zhong et al., 2000; Shen et al., 2006). Similarly, most proteins associated with PML NBs are modified by SUMO and/or contain SIMs. A plethora of cell-biological studies over more than 20 years led to a model, in which SUMO-SIM interactions provide the glue for the assembly of mature PML NBs. The biogenesis of PML NBs occurs in at least two steps (**Figure 1**). The initial nucleation phase, which generates an outer shell primarily comprised of PML, requires oligomerization of PML. It has been proposed that disulfide bridges between oxidized PML monomers as well as intermolecular non-covalent interactions between its RBCC domains are the major drivers of this event (Jeanne et al., 2010; Sahin et al., 2014). At least for some PML isoforms SUMO-SIM-dependent oligomerization also contributes to this process (Zhong et al., 2000; Shen et al., 2006; Li et al., 2017). The subsequent maturation phase of PML NBs is triggered by the recruitment of multiple proteins to the inner core of

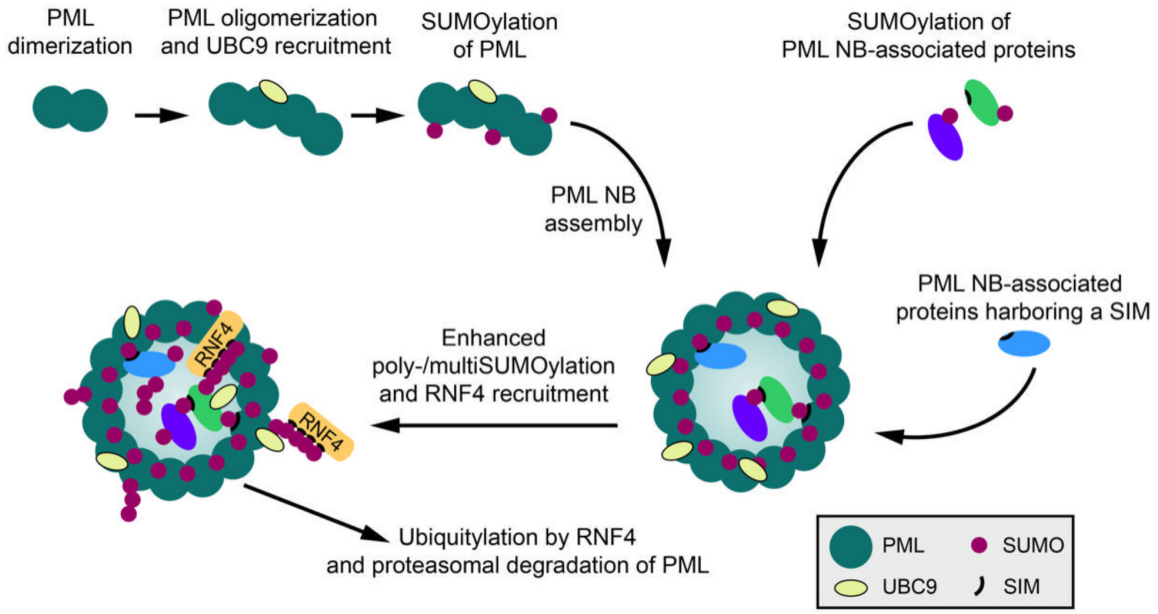

FIGURE 1 | SUMO and the dynamics of PML nuclear bodies. PML NB formation begins with PML oligomerization via its N-terminal domain. UBC9 is recruited to PML oligomers and PML is SUMOylated. PML SUMOylation and consequential SUMO-SIM interactions further promote PML NB assembly and the recruitment of PML NB-associated proteins into PML NBs. Stimuli such as arsenic trioxide treatment can lead to multi- and polySUMOylation of PML and NB-associated proteins. The StUbL RNF4 can subsequently ubiquitylate PML, thereby targeting it for proteolytic degradation and causing the clearance of PML NBs.

the scaffold. Importantly, this process is primarily dictated by SUMO-SIM-dependent protein-protein interactions. It is indeed well established that SUMOylation of PML induces recruitment of other SIM-containing factors to these bodies, such as DAXX, HIPK2 or SP100 (**Figure 1**; Weidtkamp-Peters et al., 2008; Sung et al., 2011). Upon recruitment to NBs these factors typically also undergo covalent modification by SUMO, amplifying the assembly process. More recent *in vitro* biochemical and biophysical studies strengthened this conceptual framework and provided evidence that phase separation in PML NBs is driven by SUMO polymers that recruit SIM-containing proteins (Banani et al., 2017). In line with the current model, partitioning of these clients into PML NBs requires SUMO-SIM binding and depends on the levels of PML SUMOylation. By controlling SUMO conjugation-deconjugation, cells can regulate PML NB composition. This is exemplified by an increase in their number and size upon inactivation of the SUMO deconjugase SENP6 (Mukhopadhyay et al., 2006; Hattersley et al., 2011), which limits chain formation on PML. Another way to control PML dynamics is the regulation of SUMO-SIM interactions through additional PTMs in either SUMO or the SIM region (Stehmeier and Muller, 2009; Ullmann et al., 2012; Cappadocia et al., 2015; Cappadocia and Lima, 2018). Notably, SUMO-SIM-dependent LLPS also contributes to the formation of ALT (alternative lengthening of telomeres)-associated PML NBs that mediate telomerase-independent telomere maintenance in a subset of cancer cells (Min et al., 2019; Zhang et al., 2020). However, one important aspect of the SUMO-SIM glue model in PML NB condensation is that polymeric SUMO chains on PML can also recruit and activate the StUbL RNF4, ultimately leading to the proteolytic degradation of PML and the disassembly of the NBs (Lallemand-Breitenbach et al., 2008; Tatham et al., 2008; **Figure 1**). This scenario can be experimentally induced by treating cells with arsenic trioxide, which triggers polySUMOylation of PML. Initially this causes an increase in size and number of PML NBs via recruitment of SIM-containing clients, but at a later stage leads to the complete disappearance of NBs. SUMO-dependent degradation of PML, followed by disassembly of NBs, is also observed upon infection with Herpes simplex virus, which encodes the viral StUbL ICP0 (Muller and Dejean, 1999; Jan Fada et al., 2020). Altogether these data demonstrate that, dependent on the nature of the SUMO signal, SUMOylation can exert dual functions on MLOs by either fostering their assembly or disassembly. PolySUMO chains on PML or other NB component that exceed a certain length are preferentially targeted by RNF4-mediated ubiquitylation and proteasomal degradation. In this context, SUMO loses its glue-like functions and contributes to the dissolution of MLOs by mediating scaffold degradation. Notably, recent work suggests that at least in certain cases stress-induced SUMO conjugation can keep unfolded proteins soluble and prevent their accumulation into insoluble aggregates independent from ubiquitylation (Liebelt and Vertegaal, 2016; Liebelt et al., 2019).

SUMO CONJUGATION-DECONJUGATION IN THE NUCLEOLUS

The nucleolus is another prototypic membrane-less organelle forming by liquid-liquid phase separation

(Lafontaine et al., 2020). Nucleoli are complex structures, where ribosomal and non-ribosomal proteins form a macromolecular network through interactions with RNA, such as rRNAs or snoRNAs. Nucleoli are organized in three morphologically distinct sub-regions, where successive steps of ribosome biogenesis take place. The inner core, termed fibrillar center (FC), is the site of rRNA transcription. Early and late nucleolar maturation of ribosomal subunits occur in the dense fibrillar component (DFC) and in the more peripheral granular components (GC), respectively. FC, DFC, and GC likely represent coexisting, immiscible, liquid phases determined by differences in the biophysical properties of their constituents. A key organizer of the liquid-like structure of the GC is nucleophosmin (NPM1 or B23). It has been proposed that multiple NPM1-regulated LLPS mechanisms influence the ordered assembly of pre-ribosomal particles and their exit from the nucleolus (Mitrea et al., 2018). Importantly, there is evidence that the function of NPM1 is interconnected with the SUMO system by stabilization of the SUMO deconjugases SENP3 and SENP5 and by recruiting them to the GC region (Yun et al., 2008; Raman et al., 2014). SENP3/5 control the SUMOylation status of many nucleolar, ribosomal and non-ribosomal proteins and the lack of nucleolar SENP3 induces unscheduled SUMOylation at 60S pre-ribosomes leading to nucleolar exit of immature pre-60S particles (Finkbeiner et al., 2011; Castle et al., 2012; Raman et al., 2016). Noteworthy, NPM1 itself is a major nucleolar target of SUMOylation, which inhibits 28S maturation (Haindl et al., 2008). Although it remains to be determined whether the balance of SUMO conjugation-deconjugation on NPM1 or other nucleolar proteins affects the different LLPS processes in the nucleolus, it is attractive to speculate that SUMO may modulate protein-protein or RNA-protein interactions that drive phase separation. In support of this idea, SUMOylation of the snoRNP component NOP58 was shown to facilitate its interaction with Box C/D snoRNA, thereby targeting snoRNPs to the nucleolus (Westman et al., 2010). Similarly, miscibility of Dyskerin (DKC1) within the nucleolar DFC was proposed to rely on SUMO-dependent binding of DKC1 to a SIM in GAR1, a component of the H/ACA snoRNP complex (MacNeil et al., 2021). Altogether, these data suggest that SUMO may contribute to phase separation in the nucleolar compartment. Notably, under specific conditions the StUbL pathway also plays a role in resolving nucleolar condensates as exemplified by the SUMO/RNF4-dependent nucleolar release of repair complexes that act on damaged rDNA in the nucleolus (Capella et al., 2021).

Importantly, new data indicate that in addition to their crucial role in ribosome biogenesis nucleoli exert critical functions in protein quality control and proteostasis (Alberti and Carra, 2019; Amer-Sarsour and Ashkenazi, 2019; Mende and Muller, 2021). Similar to what was observed in PML NBs, aberrant translation products or misfolded proteins accumulate transiently in nucleoli for further clearance by the chaperone machinery (Frottin et al., 2019; Mediani et al., 2019b). Intriguingly, under stress conditions, misfolded proteins enter the GC region, where association with NPM1 or other GC components prevent their irreversible aggregation. Considering that NPM1 SUMOylation is strongly induced upon proteotoxic stress and that at least *in vitro* SUMOylation functions as a general solubility "tag" it is tempting to speculate that SUMO may contribute to this process.

SUMO CONTROL OF THE SPLICING MACHINERY AND NUCLEAR SPECKLES

Nuclear speckles are phase-separated MLOs with key functions in mRNA processing and quality control (Galganski et al., 2017). Acting as a physical barrier, they temporarily retain incompletely processed and export-incompetent mRNA-protein complexes (mRNPs) after their release from chromatin (Girard et al., 2012). Nuclear speckles also retain and release mRNPs as part of a regulated, nuclear stress response (Hochberg-Laufer et al., 2019). Furthermore, it was recently proposed that the interface of phase-separated and non-phase-separated areas of nuclear speckles spatially organize the biochemical reaction of alternative splicing (Liao and Regev, 2021). Pre-mRNA splicing is catalyzed by the spliceosome that assembles at each intron from five small nuclear ribonucleoprotein particles, termed U1, U2, U4, U5, and U6 snRNP. Each snRNP consists of a small nuclear RNA (snRNAs) and a large set of associated proteins (Wahl et al., 2009). Assembly of spliceosomes starts with the formation of the A complex comprising U1 and U2 snRNP bound to the intron. Binding of the U4/U6U5 tri-snRNP generates the B complex, which is converted to its active form releasing U1 and U4 snRNP. The C complex then catalyzes intron excision and ligation of the exons followed by spliceosome disassembly (Kastner et al., 2019).

Nuclear speckles are built from two RBPs, SRRM2, and SON, that contain long low complexity regions rich in arginine and serine dipeptides (RS domain) and form a dense meshwork via multivalent interactions (Ilik et al., 2020). RS domains are also a feature of many components of the splicing machinery and other RNA processing factors, including SR proteins (SRSF1-SRSF12) (Wegener and Muller-McNicoll, 2019). Through multivalent RS-RS interactions SR proteins are retained in nuclear speckles and stored in an inactive state, but during stress or changes in transcription they are activated and released to the nucleoplasm. RS-RS interactions and hence nuclear speckle residency is modulated through PTMs that control the RNA-binding and phase separation propensities of nuclear speckle RBPs and retained mRNPs (Snead and Gladfelter, 2019). Recent high-throughput proteomic screens revealed that splicing components, including SR proteins, are also prime targets of SUMOylation, and some members of the SUMOylation machinery, e.g. UBC9, also localize to nuclear speckles (Richard et al., 2017). Moreover, it was shown that SRSF1, which is involved in assembly of the A complex, promotes SUMOylation of RNA processing factors, in particular in response to heat stress through interaction with UBC9 (Pelisch et al., 2010). This led to the proposition that SUMOylation might be required for spliceosome assembly and splicing efficiency (Pozzi et al., 2018). In line with this idea, addition of a recombinant SUMO-isopeptidase decreases the efficiency of splicing in *in vitro* assays pre-mRNA splicing assays (Pozzi et al., 2017). Moreover, a SUMO-deficient variant of PRP3, a component of the U4/U6 di-snRNP, fails to co-precipitate U2 and U5 snRNAs and the

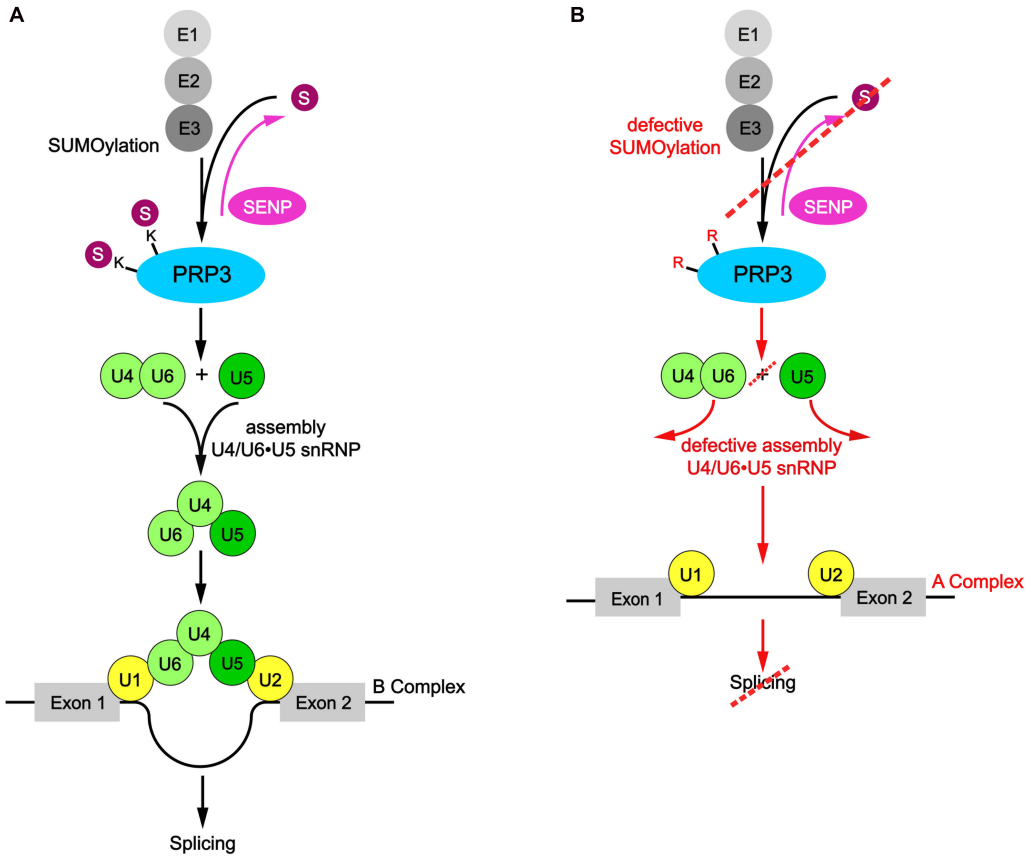

FIGURE 2 | SUMOylation of PRP3 promotes U4/U6U5 tri-snRNP formation. **(A)** The human PRP3 protein, as a component of the U4/U6 di-snRNP, is a SUMOylation target and promotes U4/U6U5 tri-snRNP formation to convert the A complex into the active B complex by interacting with U2 and U5 thereby promoting the splicing process. **(B)** After mutation of the relevant lysine residues into arginine, the SUMO-deficient PRP3 fails to co-precipitate U2 and U5 snRNAs resulting in hampered U4/U6U5 tri-snRNP assembly and shows diminished recruitment to splice sites indicating that SUMOylation of PRP3 promotes U4/U6U5 tri-snRNP formation.

splicing factors SF3 and Snu114, suggesting that SUMOylation of PRP3 promotes U4/U6U5 tri-snRNP formation (Pozzi et al., 2017; **Figure 2**). This PRP3 mutant also exhibited diminished recruitment to active spliceosomes and did not rescue splicing defects observed in PRP3-depleted cells. Interestingly, however, we have recently shown that the PRP19 splicing complex is tightly associated with the SUMO peptidase SENP6, suggesting that SUMO deconjugation of the spliceosome is also needed for proper splicing (Wagner et al., 2019). This idea is also supported by recent findings from the Lamond lab, which linked impaired SUMO deconjugation to the inhibition of splicing (Pawellek et al., 2017). The authors proposed that treatment of cells with the splicing inhibitor hinokiflavone, a plant-derived biflavonoid, inhibits SUMO deconjugases. They also demonstrated that hinokiflavone prevents transition of the spliceosome from the A complex to the catalytic activated B complex and proteomic studies revealed that this was accompanied by dramatically enhanced SUMOylation of U2 snRNP proteins. Their data suggest that deSUMOylation of U2 components is needed for formation of the activated B complex. Although these data provide strong circumstantial evidence for a role of conjugation-deconjugation in controlling spliceosome dynamics, it remains to be demonstrated that the lack of deSUMOylation in response to hinokiflavone is directly responsible for the observed splicing defects. SUMOylation might also affect the dynamics of nuclear speckles. Indeed, splicing inhibition by hinokiflavone changed the morphology and composition of nuclear speckles. They now formed "mega-speckles" that accumulated SUMO1/2/3, splicing factors, snRNPs and unspliced, polyadenylated mRNAs (Pawellek et al., 2017). Enlarged nuclear speckles have also been observed with other splicing inhibitors (Araki et al., 2015; Carvalho et al., 2017), but it is currently unknown whether they impair the deSUMOylation pathway.

SUMO AND THE DYNAMICS OF STRESS GRANULES

The best-studied example of cytosolic MLOs are stress granules (SGs), which form through LLPS in response to various stress conditions, including heat or oxidative stress (Protter and Parker, 2016). SGs are ribonucleoprotein particles comprised of untranslated mRNAs and RBPs. Their assembly is tightly linked to the inhibition of translation initiation, which helps in relieving

cellular protein quality control systems from additional protein influx during stress exposure. Together with mRNA, stalled translation pre-initiation complexes comprising 40S ribosomal subunits and translation initiation factors provide the seed for further recruitment of cytosolic and nuclear RBPs, such as G3BP, FMR1, FUS, or TDP-43. The mRNAs stored in SGs can be either directed toward mRNA decay or their translation can be reinitiated when stress is released and SGs disassemble. The mechanism of SG formation and dissolution are still not fully understood, but there is accumulating evidence that post-translational modifications contribute to these processes (Turakhiya et al., 2018; Hofweber and Dormann, 2019; Hofmann et al., 2021; Tolay and Buchberger, 2021). Recent independent findings by the Hornstein and Müller groups suggest that the SUMO system and the StUbL pathway are critically involved in both assembly and dissolution of SGs (Keiten-Schmitz et al., 2020; Marmor-Kollet et al., 2020). A role of SUMOylation in modulating the formation and composition of SGs was initially inferred from work on eIF4A2, a subunit of the cap-binding eIF4 complex (Jongjitwimol et al., 2016). Watts and co-workers reported that recruitment of eIF4A2 to SGs upon arsenite-induced oxidative stress goes along with its enhanced SUMOylation, whereas expression of a SUMOylation deficient mutant of eIF4A2 results in impaired SG formation. Work by the Hornstein laboratory now supports the idea that SG assembly or targeting may involve SUMOylation (Marmor-Kollet et al., 2020). It was observed that mutation of two reported SUMOylation sites in FMR1 leads to its reduced recruitment to SGs in response to arsenite. Furthermore, delayed SG formation in response to arsenite was detected upon inhibition of the SUMO E2 enzyme UBC9 prior to stress exposure, by genetic means or by small molecule inhibitors, suggesting that SUMOylation of SG-associated proteins is involved in their recruitment to these structures. These findings are consistent with mass-spectrometry-based SUMO proteomics that identified many SG-associated RBPs as stress-induced SUMOylation targets and APEX-based proximity-proteomics that detected SUMO at SGs (Matic et al., 2009; Hendriks and Vertegaal, 2016; Marmor-Kollet et al., 2020). However, endogenous SUMO has so far never been stably detected within SGs by immunofluorescence, thus it remains unclear whether SUMO functions as an essential glue-like scaffold in SGs. In an alternative model transient SUMO conjugation may prime SG components for recruitment and assembly in SGs. Once incorporated into the complex SUMO could be removed potentially explaining why only a small fraction of a substrate is modified at a given time (Hay, 2005). For validation of this model, it remains to be determined where SUMO conjugation and deconjugation of SG components occurs. Since SUMO ligases (e.g., RanBP2) and isopeptidases (SENP1 and SENP2) are associated with nuclear pore complexes, transient SUMOylation of nuclear RBPs may occur upon nucleo-cytoplasmic shuttling (Flotho and Melchior, 2013; Cappadocia and Lima, 2018; Kunz et al., 2018).

While the above-mentioned data involve SUMO in SG targeting and assembly, the SUMO pathway is also critical for SG disassembly upon stress release. In a search for stress-induced targets of RNF4 we identified and validated a large number of SG-associated RBPs, including the nuclear RBPs FUS and TDP-43, as targets of SUMO-primed ubiquitylation (Keiten-Schmitz et al., 2020). We further found that impairment of the StUbL pathway by chemical or genetic inhibition of SUMO2/3 or depletion of RNF4 significantly delays SG clearance in cells recovering from heat or arsenite-induced proteotoxic stress. By contrast, overexpression of the chain-selective SUMO isopeptidases SENP6 or SENP7 triggers SG assembly. Altogether, these data show that SUMOylation and polySUMO-primed ubiquitylation by RNF4 fosters the disassembly of SGs. This concept was strengthened by work from Hornstein and co-workers (Marmor-Kollet et al., 2020). Marmor-Kollet et al. used APEX-based proximity-proteomics to characterize the SG-associated proteome in response to stress induction and release. Among a set of "disassembly engaged proteins," which are specifically associated with SG proteins when they disassemble, they identified and validated the SUMO E1 subunit AOS1 (alias SAE1), the E2 UBC9, and the SUMO E3 ligases TOPORS and RANBP2. It was further demonstrated that inhibition of SUMOylation by siRNA-mediated depletion of AOS1 or UBC9, or small molecule inhibitor of UBC9 (2D08), impaired SG disassembly. The ensemble of these data provides compelling evidence that SUMOylation is functionally connected to SG disassembly. However, important mechanistic questions are still open. For example, it remains to be determined whether SUMOylation and RNF4-mediated ubiquitylation occur directly on disassembling SGs or at a later stage, for example when nuclear SG-associated proteins re-enter the nucleus. Since we were unable to detect RNF4 at SGs and found stress-induced SUMO conjugates predominantly compartmentalized in the nucleus, we favor a model of RNF4-mediated ubiquitylation taking place in the nuclear compartment at PML NBs. In support of this, we observed that lack of PML also impairs SG disassembly. Based on these data we propose that in response to proteotoxic stress the StUbL pathway primarily targets the nuclear fraction of SG-associated RBPs thereby bridging nuclear to cytosolic protein quality control. To reconcile this concept with data from Marmor-Kollet et al. one possible scenario might be that SUMO-priming occurs at SGs upon their disassembly, whereas subsequent polySUMOylation and ubiquitylation primarily involves the nuclear StUbL machinery. Regardless of these molecular details, a compelling hypothesis is that—similar to what is described for PML NBs—the SUMO system controls both the assembly and dissolution of SGs. Whether this dual function is also controlled by a switch from mono- to polySUMOylation needs to be addressed in future experiments.

Importantly, these data also open up new perspectives in the understanding of neurodegenerative disease, such as amyotrophic lateral sclerosis (ALS) or frontotemporal lobar degeneration (FTLD) which have been linked to aberrant and persistent SGs (Wolozin and Ivanov, 2019). In a subset of ALS or FTLD patients, mutations in FUS or TDP-43 induce a transition of SGs from a liquid-like dynamic to a solid state and FUS/TDP-43 aggregates are found in affected brain regions of patients

suffering from ALS or FTLD. Interestingly, we could demonstrate that the StUbL pathway limits the formation of aberrant SGs caused by expression of the ALS-associated FUS^{P525L} mutant, pointing to a possible role of SUMO in protecting from ALS pathology (Keiten-Schmitz et al., 2020; Marmor-Kollet et al., 2020). In support of this idea, Marmor-Kollet and colleagues provided evidence that impairment of the SUMO pathway may affect formation of aberrant SGs and ALS pathology in the context of *C9orf72* mutations. Genetic alterations of the *C9orf72* gene, due to expansion of a GGGGCC hexanucleotide repeat in the first intron, represent the most frequently observed inherited form of ALS and generate different dipeptide repeat proteins. Intriguingly, expression of one of these dipeptides, the poly-PR(50) repeat protein, impaired SUMO ligase recruitment to SGs and SG SUMOylation. Further, enhanced SUMOylation activity ameliorated photoreceptor neurodegeneration in a *drosophila* model of *C9orf72*-related ALS (Marmor-Kollet et al., 2020). How expression of poly-PR(50) dipeptide repeat proteins inhibits SUMOylation activity at SGs is currently unknown. Notably, poly-PR(50) is found in nuclear aggregates indicating that it might sequester the SUMO machinery in these aggregates.

CONCLUSION AND PERSPECTIVES

Investigation of MLOs and characterization of their assembly-disassembly mechanisms are an emerging field of biophysics and cell biology. The role of SUMO in controlling MLO dynamics likely goes beyond the above-mentioned examples, since formation of Cajal bodies (alias coiled bodies), processing bodies (P-bodies, PBs) and the recently described NELF bodies are also controlled by SUMOylation. Thus, SUMOylation and a SIM-like-domain in SMN are critical for the assembly of Cajal bodies thereby likely controlling in snRNP and snoRNP biogenesis (Tapia et al., 2014). P-bodies are cytoplasmic RNPs with functions in translational repression and/or mRNA decay. PBs and SGs share a close relationship and exchange RNAs as well as proteins. One example is the RNA helicase DDX6, which was shown to be associated with SUMO E3 ligase TIF1β and a number of SUMOylation substrates (Bish et al., 2015). A very recent example in SUMO-dependent phase separation is the formation of heat-induced NELF (negative elongation factor)-containing condensates (Rawat et al., 2021). The NELF complex is a hetero-tetramer composed of the subunits NELFA, B, C/D, and E. In response to heat stress NELF forms nuclear condensates that drive transcriptional downregulation and cellular survival under stressful conditions. It has been proposed that these structures represent nuclear counterparts of cytosolic stress granules functioning as critical nodes of cellular stress survival by adapting gene expression programs. NELF condensates cause transcriptional pausing by negatively regulating transcriptional elongation by RNA polymerase II. Intriguingly, stress-induced SUMOylation and the E3 SUMO ligase ZNF451 are required for NELF condensation providing another intriguing example how the SUMO system integrates the cellular stress response with phase separation. Another important aspect for future research concerns the role of SUMO conjugation-deconjugation in regulating the interdependency and interplay of distinct MLO, such as PML NBs with nucleoli and SGs, under stress (Condemine et al., 2007; Keiten-Schmitz et al., 2020).

AUTHOR CONTRIBUTIONS

JK-S, LR, EH, MM-M, and SM wrote the article. JK-S and LR designed the figures. All authors contributed to the article and approved the submitted version.

FUNDING

Work in the Müller lab was funded by DFG collaborative research cebters SFB815 and SFB1177. MM-M and SM are part of the Cluster project ENABLE funded by the State of Hesse. Work in the Hornstein lab is supported by Mondry Family Professorial Chair, RADALA Foundation, Weizmann – Brazil Center for Research on Neurodegeneration and Minerva Foundation with funding from the Federal German Ministry for Education and Research.

ACKNOWLEDGMENTS

We thank all members of our group and members of IBC2 for constructive feedback and discussions.

REFERENCES

Advani, V. M., and Ivanov, P. (2019). Translational control under stress: reshaping the translatome. *Bioessays* 41: e1900009.

Alberti, S., and Carra, S. (2019). Nucleolus: a liquid droplet compartment for misbehaving proteins. *Curr. Biol.* 29, R930–R932.

Alberti, S., and Hyman, A. A. (2021). Biomolecular condensates at the nexus of cellular stress, protein aggregation disease and ageing. *Nat. Rev. Mol. Cell Biol.* 22, 196-213

Amer-Sarsour, F., and Ashkenazi, A. (2019). The nucleolus as a proteostasis regulator. *Trends Cell Biol.* 29, 849–851. doi: 10.1016/j.tcb.2019.08.002

Araki, S., Dairiki, R., Nakayama, Y., Murai, A., Miyashita, R., Iwatani, M., et al. (2015). Inhibitors of CLK protein kinases suppress cell growth and induce apoptosis by modulating pre-mRNA splicing. *PLoS One* 10:e0116929. doi: 10.1371/journal.pone.0116929

Banani, S. F., Lee, H. O., Hyman, A. A., and Rosen, M. K. (2017). Biomolecular condensates: organizers of cellular biochemistry. *Nat. Rev. Mol. Cell Biol.* 18, 285–298. doi: 10.1038/nrm.2017.7

Banani, S. F., Rice, A. M., Peeples, W. B., Lin, Y., Jain, S., Parker, R., et al. (2016). Compositional control of phase-separated cellular bodies. *Cell* 166, 651–663. doi: 10.1016/j.cell.2016.06.010

Bergink, S., Ammon, T., Kern, M., Schermelleh, L., Leonhardt, H., and Jentsch, S. (2013). Role of Cdc48/p97 as a SUMO-targeted segregase curbing Rad51-Rad52 interaction. *Nat. Cell Biol.* 15, 526–532. doi: 10.1038/ncb2729

Bish, R., Cuevas-Polo, N., Cheng, Z., Hambardzumyan, D., Munschauer, M., Landthaler, M., et al. (2015). Comprehensive protein interactome analysis of a key RNA helicase: detection of novel stress granule proteins. *Biomolecules* 5, 1441–1466. doi: 10.3390/biom5031441

Capella, M., Mandemaker, I. K., den Brave, F., Caballero, L. M., Pfander, B., Ladurner, A. G., et al. (2021). Relocation of rDNA repeats for repair is

dependent on SUMO-mediated nucleolar release by the Cdc48/p97 segregase. *bioRxiv* [Preprint]. 2021.01.05.425376.

Cappadocia, L., and Lima, C. D. (2018). Ubiquitin-like protein conjugation: structures. *Chem. Mech. Chem. Rev.* 118, 889–918. doi: 10.1021/acs.chemrev.6b00737

Cappadocia, L., Mascle, X. H., Bourdeau, V., Tremblay-Belzile, S., Chaker-Margot, M., Lussier-Price, M., et al. (2015). Structural and functional characterization of the phosphorylation-dependent interaction between PML and SUMO1. *Structure* 23, 126–138. doi: 10.1016/j.str.2014.10.015

Carvalho, T., Martins, S., Rino, J., Marinho, S., and Carmo-Fonseca, M. (2017). Pharmacological inhibition of the spliceosome subunit SF3b triggers exon junction complex-independent nonsense-mediated decay. *J. Cell Sci.* 130, 1519–1531. doi: 10.1242/jcs.202200

Castle, C. D., Cassimere, E. K., and Denicourt, C. (2012). LAS1L interacts with the mammalian Rix1 complex to regulate ribosome biogenesis. *Mol. Biol. Cell* 23, 716–728. doi: 10.1091/mbc.e11-06-0530

Condemine, W., Takahashi, Y., Le Bras, M., and de The, H. (2007). A nucleolar targeting signal in PML-I addresses PML to nucleolar caps in stressed or senescent cells. *J. Cell Sci.* 120, 3219–3227. doi: 10.1242/jcs.007492

Finkbeiner, E., Haindl, M., and Muller, S. (2011). The SUMO system controls nucleolar partitioning of a novel mammalian ribosome biogenesis complex. *EMBO J.* 30, 1067–1078. doi: 10.1038/emboj.2011.33

Flotho, A., and Melchior, F. (2013). Sumoylation: a regulatory protein modification in health and disease. *Annu. Rev. Biochem.* 82, 357–385. doi: 10.1146/annurev-biochem-061909-093311

Frottin, F., Schueder, F., Tiwary, S., Gupta, R., Korner, R., Schlichthaerle, T., et al. (2019). The nucleolus functions as a phase-separated protein quality control compartment. *Science* 365, 342–347. doi: 10.1126/science.aaw9157

Galganski, L., Urbanek, M. O., and Krzyzosiak, W. J. (2017). Nuclear speckles: molecular organization, biological function and role in disease. *Nucleic Acids Res.* 45, 10350–10368. doi: 10.1093/nar/gkx759

Gartner, A., and Muller, S. (2014). PML, SUMO, and RNF4: guardians of nuclear protein quality. *Mol. Cell* 55, 1–3. doi: 10.1016/j.molcel.2014.06.022

Girard, C., Will, C. L., Peng, J., Makarov, E. M., Kastner, B., Lemm, I., et al. (2012). Post-transcriptional spliceosomes are retained in nuclear speckles until splicing completion. *Nat. Commun.* 3:994.

Guo, L., Giasson, B. I., Glavis-Bloom, A., Brewer, M. D., Shorter, J., Gitler, A. D., et al. (2014). A cellular system that degrades misfolded proteins and protects against neurodegeneration. *Mol. Cell* 55, 15–30. doi: 10.1016/j.molcel.2014.04.030

Haindl, M., Harasim, T., Eick, D., and Muller, S. (2008). The nucleolar SUMO-specific protease SENP3 reverses SUMO modification of nucleophosmin and is required for rRNA processing. *EMBO Rep.* 9, 273–279. doi: 10.1038/embor.2008.3

Hattersley, N., Shen, L., Jaffray, E. G., and Hay, R. T. (2011). The SUMO protease SENP6 is a direct regulator of PML nuclear bodies. *Mol. Biol. Cell* 22, 78–90. doi: 10.1091/mbc.e10-06-0504

Hay, R. T. (2005). SUMO: a history of modification. *Mol. Cell* 18, 1–12.

Hendriks, I. A., and Vertegaal, A. C. (2016). A comprehensive compilation of SUMO proteomics. *Nat. Rev. Mol. Cell Biol.* 17, 581–595. doi: 10.1038/nrm.2016.81

Hochberg-Laufer, H., Schwed-Gross, A., Neugebauer, K. M., and Shav-Tal, Y. (2019). Uncoupling of nucleo-cytoplasmic RNA export and localization during stress. *Nucleic Acids Res.* 47, 4778–4797. doi: 10.1093/nar/gkz168

Hofmann, S., Kedersha, N., Anderson, P., and Ivanov, P. (2021). Molecular mechanisms of stress granule assembly and disassembly. *Biochim. Biophys. Acta Mol. Cell Res.* 1868:118876. doi: 10.1016/j.bbamcr.2020.118876

Hofweber, M., and Dormann, D. (2019). Friend or foe-post-translational modifications as regulators of phase separation and RNP granule dynamics. *J. Biol. Chem.* 294, 7137–7150. doi: 10.1074/jbc.tm118.001189

Ilik, I. A., Malszycki, M., Lubke, A. K., Schade, C., Meierhofer, D., and Aktas, T. (2020). SON and SRRM2 are essential for nuclear speckle formation. *eLife* 9:e60579.

Jan Fada, B., Kaadi, E., Samrat, S. K., Zheng, Y., and Gu, H. (2020). Effect of SUMO-SIM interaction on the ICP0-mediated degradation of PML isoform II and its associated proteins in herpes simplex virus 1 infection. *J. Virol.* 94:e00470-20.

Jansen, N. S., and Vertegaal, A. C. O. (2021). A Chain of events: regulating target proteins by SUMO polymers. *Trends Biochem. Sci.* 46, 113–123. doi: 10.1016/j.tibs.2020.09.002

Jeanne, M., Lallemand-Breitenbach, V., Ferhi, O., Koken, M., Le Bras, M., Duffort, S., et al. (2010). PML/RARA oxidation and arsenic binding initiate the antileukemia response of As2O3. *Cancer Cell* 18, 88–98. doi: 10.1016/j.ccr.2010.06.003

Jensen, K., Shiels, C., and Freemont, P. S. (2001). PML protein isoforms and the RBCC/TRIM motif. *Oncogene* 20, 7223–7233. doi: 10.1038/sj.onc.1204765

Jentsch, S., and Psakhye, I. (2013). Control of nuclear activities by substrate-selective and protein-group SUMOylation. *Annu. Rev. Genet.* 47, 167–186. doi: 10.1146/annurev-genet-111212-133453

Jongjitwimol, J., Baldock, R. A., Morley, S. J., and Watts, F. Z. (2016). Sumoylation of eIF4A2 affects stress granule formation. *J. Cell Sci.* 129, 2407–2415. doi: 10.1242/jcs.184614

Kastner, B., Will, C. L., Stark, H., and Luhrmann, R. (2019). Structural insights into nuclear pre-mRNA splicing in higher eukaryotes. *Cold Spring Harb. Perspect. Biol.* 11:a032417. doi: 10.1101/cshperspect.a032417

Keiten-Schmitz, J., Schunck, K., and Muller, S. (2019). SUMO chains rule on chromatin occupancy. *Front. Cell Dev. Biol.* 7:343. doi: 10.3389/fcell.2019.00343

Keiten-Schmitz, J., Wagner, K., Piller, T., Kaulich, M., Alberti, S., and Muller, S. (2020). The nuclear sumo-targeted ubiquitin quality control network regulates the dynamics of cytoplasmic stress granules. *Mol. Cell* 79, 54–67.e7.

Kumar, R., and Sabapathy, K. (2019). RNF4-A paradigm for SUMOylation-mediated ubiquitination. *Proteomics* 19:e1900185.

Kunz, K., Piller, T., and Muller, S. (2018). SUMO-specific proteases and isopeptidases of the SENP family at a glance. *J. Cell Sci.* 131:jcs211904. doi: 10.1242/jcs.211904

Lafontaine, D. L. J., Riback, J. A., Bascetin, R., and Brangwynne, C. P. (2020). The nucleolus as a multiphase liquid condensate. *Nat. Rev. Mol. Cell Biol.* 22, 165–182 doi: 10.1038/s41580-020-0272-6

Lallemand-Breitenbach, V., and de The, H. (2018). PML nuclear bodies: from architecture to function. *Curr. Opin. Cell Biol.* 52, 154–161. doi: 10.1016/j.ceb.2018.03.011

Lallemand-Breitenbach, V., Jeanne, M., Benhenda, S., Nasr, R., Lei, M., Peres, L., et al. (2008). Arsenic degrades PML or PML-RARalpha through a SUMO-triggered RNF4/ubiquitin-mediated pathway. *Nat. Cell Biol.* 10, 547–555. doi: 10.1038/ncb1717

Li, C., Peng, Q., Wan, X., Sun, H., and Tang, J. (2017). C-terminal motifs in promyelocytic leukemia protein isoforms critically regulate PML nuclear body formation. *J. Cell Sci.* 130, 3496–3506. doi: 10.1242/jcs.202879

Liao, S. E., and Regev, O. (2021). Splicing at the phase-separated nuclear speckle interface: a model. *Nucleic Acids Res.* 49, 636–645. doi: 10.1093/nar/gkaa1209

Liebelt, F., Sebastian, R. M., Moore, C. L., Mulder, M. P. C., Ovaa, H., and Shoulders, M. D. (2019). SUMOylation and the HSF1-regulated chaperone network converge to promote proteostasis in response to heat shock. *Cell Rep.* 26, 236–249.e4.

Liebelt, F., and Vertegaal, A. C. (2016). Ubiquitin-dependent and independent roles of SUMO in proteostasis. *Am. J. Physiol. Cell Physiol.* 311, C284–C296.

MacNeil, D. E., Lambert-Lanteigne, P., Qin, J., McManus, F., Bonneil, E., Thibault, P., et al. (2021). SUMOylation- and GAR1-dependent regulation of dyskerin nuclear and subnuclear localization. *Mol. Cell Biol.* 41:e00464-20.

Marmor-Kollet, H., Siany, A., Kedersha, N., Knafo, N., Rivkin, N., Danino, Y. M., et al. (2020). Spatiotemporal proteomic analysis of stress granule disassembly using APEX reveals regulation by sumoylation and links to ALS pathogenesis. *Mol. Cell* 80, 876–891.e6.

Matic, I., Tatham, M. H., Cole, C., Yin, Y., Nakamura, A., Cox, J., et al. (2009). System-wide changes to SUMO modifications in response to heat shock. *Sci. Signal.* 2:ra24. doi: 10.1126/scisignal.2000282

Matunis, M. J., Zhang, X. D., and Ellis, N. A. (2006). SUMO: the glue that binds. *Dev. Cell* 11, 596–597. doi: 10.1016/j.devcel.2006.10.011

Mediani, L., Guillen-Boixet, J., Alberti, S., and Carra, S. (2019a). Nucleoli and Pomyelocytic Leukemia Protein (PML) bodies are phase separated nuclear protein quality control compartments for misfolded proteins. *Mol. Cell. Oncol.* 6:e1415624. doi: 10.1080/23723556.2019.1652519

Mediani, L., Guillen-Boixet, J., Vinet, J., Franzmann, T. M., Bigi, I., Mateju, D., et al. (2019b). Defective ribosomal products challenge nuclear function by

impairing nuclear condensate dynamics and immobilizing ubiquitin. *EMBO J.* 38:e101341.

Mende, H., and Muller, S. (2021). Surveillance of nucleolar homeostasis and ribosome maturation by autophagy and the ubiquitin-proteasome system. *Matrix Biol.* doi: 10.1016/j.matbio.2021.02.001 [Epub ahead of print].

Min, J., Wright, W. E., and Shay, J. W. (2019). Clustered telomeres in phase-separated nuclear condensates engage mitotic DNA synthesis through BLM and RAD52. *Genes Dev.* 33, 814–827. doi: 10.1101/gad.324905.119

Mitrea, D. M., Cika, J. A., Stanley, C. B., Nourse, A., Onuchic, P. L., Banerjee, P. R., et al. (2018). Self-interaction of NPM1 modulates multiple mechanisms of liquid-liquid phase separation. *Nat. Commun.* 9: 842.

Mukhopadhyay, D., Ayaydin, F., Kolli, N., Tan, S. H., Anan, T., Kametaka, A., et al. (2006). SUSP1 antagonizes formation of highly SUMO2/3-conjugated species. *J. Cell Biol.* 174, 939–949. doi: 10.1083/jcb.200510103

Muller, S., and Dejean, A. (1999). Viral immediate-early proteins abrogate the modification by SUMO-1 of PML and Sp100 proteins, correlating with nuclear body disruption. *J. Virol.* 73, 5137–5143. doi: 10.1128/jvi.73.6.5137-5143.1999

Muller, S., Matunis, M. J., and Dejean, A. (1998). Conjugation with the ubiquitin-related modifier SUMO-1 regulates the partitioning of PML within the nucleus. *EMBO J.* 17, 61–70. doi: 10.1093/emboj/17.1.61

Pawellek, A., Ryder, U., Tammsalu, T., King, L. J., Kreinin, H., Ly, T., et al. (2017). Characterisation of the biflavonoid hinokiflavone as a pre-mRNA splicing modulator that inhibits SENP. *eLife* 6:e27402

Pelisch, F., Gerez, J., Druker, J., Schor, I. E., Munoz, M. J., Risso, G., et al. (2010). The serine/arginine-rich protein SF2/ASF regulates protein sumoylation. *Proc. Natl. Acad. Sci. U.S.A.* 107, 16119–16124. doi: 10.1073/pnas.1004653107

Perez Berrocal, D. A., Witting, K. F., Ovaa, H., and Mulder, M. P. C. (2019). Hybrid chains: a collaboration of ubiquitin and ubiquitin-like modifiers introducing cross-functionality to the ubiquitin code. *Front. Chem.* 7:931. doi: 10.3389/fchem.2019.00931

Pozzi, B., Bragado, L., Will, C. L., Mammi, P., Risso, G., Urlaub, H., et al. (2017). SUMO conjugation to spliceosomal proteins is required for efficient pre-mRNA splicing. *Nucleic Acids Res.* 45, 6729–6745. doi: 10.1093/nar/gkx213

Pozzi, B., Mammi, P., Bragado, L., Giono, L. E., and Srebrow, A. (2018). When SUMO met splicing. *RNA Biol.* 15, 689–695.

Protter, D. S. W., and Parker, R. (2016). Principles and Properties of stress granules. *Trends Cell Biol.* 26, 668–679. doi: 10.1016/j.tcb.2016.05.004

Raman, N., Nayak, A., and Muller, S. (2014). mTOR signaling regulates nucleolar targeting of the SUMO-specific isopeptidase SENP3. *Mol. Cell Biol.* 34, 4474–4484. doi: 10.1128/mcb.00801-14

Raman, N., Weir, E., and Muller, S. (2016). The AAA ATPase MDN1 acts as a SUMO-targeted regulator in mammalian pre-ribosome remodeling. *Mol. Cell* 64, 607–615. doi: 10.1016/j.molcel.2016.09.039

Rawat, P., Boehning, M., Hummel, B., Aprile-Garcia, F., Pandit, A. S., Eisenhardt, N., et al. (2021). Stress-induced nuclear condensation of NELF drives transcriptional downregulation. *Mol. Cell* 81, 1013-1026.e11

Richard, P., Vethantham, V., and Manley, J. L. (2017). Roles of sumoylation in mRNA processing and metabolism. *Adv. Exp. Med. Biol.* 963, 15–33. doi: 10.1007/978-3-319-50044-7_2

Sahin, U., Ferhi, O., Jeanne, M., Benhenda, S., Berthier, C., Jollivet, F., et al. (2014). Oxidative stress-induced assembly of PML nuclear bodies controls sumoylation of partner proteins. *J. Cell Biol.* 204, 931–945. doi: 10.1083/jcb.201305148

Sha, Z., Blyszcz, T., Gonzalez-Prieto, R., Vertegaal, A. C. O., and Goldberg, A. L. (2019). Inhibiting ubiquitination causes an accumulation of SUMOylated newly synthesized nuclear proteins at PML bodies. *J. Biol. Chem.* 294, 15218–15234. doi: 10.1074/jbc.ra119.009147

Shen, T. H., Lin, H. K., Scaglioni, P. P., Yung, T. M., and Pandolfi, P. P. (2006). The mechanisms of PML-nuclear body formation. *Mol. Cell* 24, 331–339.

Snead, W. T., and Gladfelter, A. S. (2019). the control centers of biomolecular phase separation: how membrane surfaces, PTMs, and active processes regulate condensation. *Mol. Cell* 76, 295–305. doi: 10.1016/j.molcel.2019.09.016

Stehmeier, P., and Muller, S. (2009). Phospho-regulated SUMO interaction modules connect the SUMO system to CK2 signaling. *Mol. Cell* 33, 400–409. doi: 10.1016/j.molcel.2009.01.013

Sung, K. S., Lee, Y. A., Kim, E. T., Lee, S. R., Ahn, J. H., and Choi, C. Y. (2011). Role of the SUMO-interacting motif in HIPK2 targeting to the PML nuclear bodies and regulation of p53. *Exp. Cell Res.* 317, 1060–1070. doi: 10.1016/j.yexcr.2010.12.016

Tapia, O., Lafarga, V., Bengoechea, R., Palanca, A., Lafarga, M., and Berciano, M. T. (2014). The SMN Tudor SIM-like domain is key to SmD1 and coilin interactions and to Cajal body biogenesis. *J. Cell Sci.* 127, 939–946. doi: 10.1242/jcs.138537

Tatham, M. H., Geoffroy, M. C., Shen, L., Plechanovova, A., Hattersley, N., Jaffray, E. G., et al. (2008). RNF4 is a poly-SUMO-specific E3 ubiquitin ligase required for arsenic-induced PML degradation. *Nat. Cell Biol.* 10, 538–546. doi: 10.1038/ncb1716

Tolay, N., and Buchberger, A. (2021). Comparative profiling of stress granule clearance reveals differential contributions of the ubiquitin system. *Life Sci. Alliance* 4:e202000927. doi: 10.26508/lsa.202000927

Turakhiya, A., Meyer, S. R., Marincola, G., Bohm, S., Vanselow, J. T., Schlosser, A., et al. (2018). ZFAND1 Recruits p97 and the 26S proteasome to promote the clearance of arsenite-induced stress granules. *Mol. Cell* 70, 906–919.e7.

Ullmann, R., Chien, C. D., Avantaggiati, M. L., and Muller, S. (2012). An acetylation switch regulates SUMO-dependent protein interaction networks. *Mol. Cell* 46, 759–770. doi: 10.1016/j.molcel.2012.04.006

Wagner, K., Kunz, K., Piller, T., Tascher, G., Holper, S., Stehmeier, P., et al. (2019). The SUMO isopeptidase SENP6 functions as a rheostat of chromatin residency in genome maintenance and chromosome dynamics. *Cell Rep.* 29 480–494.e5.

Wahl, M. C., Will, C. L., and Luhrmann, R. (2009). The spliceosome: design principles of a dynamic RNP machine. *Cell* 136, 701–718. doi: 10.1016/j.cell.2009.02.009

Wegener, M., and Muller-McNicoll, M. (2019). View from an mRNP: the roles of sr proteins in assembly, maturation and turnover. *Adv. Exp. Med. Biol.* 1203, 83–112. doi: 10.1007/978-3-030-31434-7_3

Weidtkamp-Peters, S., Lenser, T., Negorev, D., Gerstner, N., Hofmann, T. G., Schwanitz, G., et al. (2008). Dynamics of component exchange at PML nuclear bodies. *J. Cell Sci.* 121, 2731–2743. doi: 10.1242/jcs.031922

Westman, B. J., Verheggen, C., Hutten, S., Lam, Y. W., Bertrand, E., and Lamond, A. I. (2010). A proteomic screen for nucleolar SUMO targets shows SUMOylation modulates the function of Nop5/Nop58. *Mol. Cell* 39, 618–631. doi: 10.1016/j.molcel.2010.07.025

Wolozin, B., and Ivanov, P. (2019). Stress granules and neurodegeneration. *Nat. Rev. Neurosci.* 20, 649–666. doi: 10.1038/s41583-019-0222-5

Yun, C., Wang, Y., Mukhopadhyay, D., Backlund, P., Kolli, N., Yergey, A., et al. (2008). Nucleolar protein B23/nucleophosmin regulates the vertebrate SUMO pathway through SENP3 and SENP5 proteases. *J. Cell Biol.* 183, 589–595. doi: 10.1083/jcb.200807185

Zhang, H., Zhao, R., Tones, J., Liu, M., Dilley, R. L., Chenoweth, D. M., et al. (2020). Nuclear body phase separation drives telomere clustering in ALT cancer cells. *Mol. Biol. Cell* 31, 2048–2056. doi: 10.1091/mbc.e19-10-0589

Zhong, S., Muller, S., Ronchetti, S., Freemont, P. S., Dejean, A., and Pandolfi, P. P. (2000). Role of SUMO-1-modified PML in nuclear body formation. *Blood* 95, 2748–2752. doi: 10.1182/blood.v95.9.2748.009k31a_2748_2752

Conflict of Interest: The authors declare that the research was conducted in the absence of any commercial or financial relationships that could be construed as a potential conflict of interest.

frontiers in Molecular Biosciences

PERSPECTIVE
published: 13 May 2021
doi: 10.3389/fmolb.2021.669939

Opportunities and Challenges in Global Quantification of RNA-Protein Interaction *via* UV Cross-Linking

*Carlos H. Vieira-Vieira[1,2] and Matthias Selbach[1]**

[1] Proteome Dynamics, Max Delbrück Center for Molecular Medicine in the Helmholtz Association, Berlin, Germany, [2] Faculty of Life Sciences, Humboldt Universität zu Berlin, Berlin, Germany

RNA-binding proteins (RBPs) are key mediators of posttranscriptional gene expression control. However, the links between cell signaling on the one hand and RBP function on the other are understudied. While thousands of posttranslational modification (PTM) sites on RBPs have been identified, their functional roles are only poorly characterized. RNA-interactome capture (RIC) and cross-linking and immunoprecipitation (CLIP) are attractive methods that provide information about RBP-RNA interactions on a genome-wide scale. Both approaches rely on the *in situ* UV cross-linking of RBPs and RNAs, biochemical enrichment and analysis by RNA-sequencing (CLIP) or mass spectrometry (RIC). In principle, RIC- and CLIP-like methods could be used to globally quantify RBP-RNA interactions in response to perturbations. However, several biases have to be taken into account to avoid misinterpretation of the results obtained. Here, we focus on RIC-like methods and discuss four key aspects relevant for quantitative interpretation: (1) the RNA isolation efficiency, (2) the inefficient and highly variable UV cross-linking, (3) the baseline RNA occupancy of RBPs, and (4) indirect factors affecting RBP-RNA interaction. We highlight these points by presenting selected examples of PTMs that might induce differential quantification in RIC-like experiments without necessarily affecting RNA-binding. We conclude that quantifying RBP-RNA interactions via RIC or CLIP-like methods should not be regarded as an end in itself but rather as starting points for deeper analysis.

Keywords: cell signaling, posttranscriptional regulation, post-translational modifications, RBPs, RNA binding proteins, RNA interactome capture, Clip, RNA-binding quantification

OPEN ACCESS

Edited by:
Dorothee Dormann, University of Munich, Germany

Reviewed by:
Dorothee Staiger, Bielefeld University, Germany
Mathias Munschauer, Helmholtz Institute for RNA-based Infection Research (HIRI), Germany

****Correspondence:***
Matthias Selbach
matthias.selbach@mdc-berlin.de

Specialty section:
This article was submitted to Protein and RNA Networks, a section of the journal Frontiers in Molecular Biosciences

Received: *19 February 2021*
Accepted: *12 April 2021*
Published: *13 May 2021*

Citation:
Vieira-Vieira CH and Selbach M (2021) Opportunities and Challenges in Global Quantification of RNA-Protein Interaction via UV Cross-Linking. Front. Mol. Biosci. 8:669939. doi: 10.3389/fmolb.2021.669939

INTRODUCTION

Posttranscriptional regulation is an essential part of gene expression control (Buccitelli and Selbach, 2020), and RNA-binding proteins (RBPs) are particularly important players (Gehring et al., 2017; Gebauer et al., 2020). However, in contrast to transcription factors, the links between cell signaling events and RBP function are not well characterized. Posttranslational modifications (PTMs) of RBPs are expected to play a key role in this process. On the one hand, PTMs are key mediators of cell signaling. On the other hand, PTMs can affect the activity of RBPs (Yu, 2011; Thapar, 2015; Lovci et al., 2016). For example, PTMs have been shown to regulate RBPs in diverse cellular contexts, including protein translation (Imami et al., 2018; Jia et al., 2021), RNA

stability and processing (Durand et al., 2016; Zhang et al., 2018), splicing (Stamm, 2008), and phase separation (Hofweber and Dormann, 2019).

Tens of thousands of PTM sites have been identified in the proteome, but the functional significance of the vast majority of them is currently unknown (Sharma et al., 2014; Larsen et al., 2016; Ochoa et al., 2020). A key challenge is that experimental techniques to assess the function of individual PTM sites are typically not scalable. Hence, systematic approaches to identify functionally relevant PTM sites in proteins is a topic of intense research (Imami et al., 2018; Huang et al., 2019; Masuda et al., 2020; Ochoa et al., 2020).

Since the defining feature of RBPs is their ability to bind RNA, an attractive approach to assess the function of PTM sites in RBPs would be to quantify how they affect RNA binding. Methods that employ UV cross-linking of RBPs and RNA *in situ* followed by "omic" analyses enable identification and quantification of hundreds of RBPs or thousands of RNA-binding sites in a single experiment (Wheeler et al., 2018; Lin and Miles, 2019; Gebauer et al., 2020). These experiments come in two flavors: In protein-centric methods like cross-linking and immunoprecipitation (CLIP), RBPs are purified and RNA targets identified by sequencing (Wheeler et al., 2018; Lin and Miles, 2019). CLIP-like methods provide a detailed picture of the RBP-RNA interactome with single nucleotide resolution for a specific RBP of interest (Hafner et al., 2010; König et al., 2010). Conversely, RNA-centric methods like RNA-interactome capture (RIC) use mass spectrometry-based proteomics to identify the RNA-bound proteome following biochemical isolation of RNAs (Gebauer et al., 2020; Gräwe et al., 2020). In analogy to CLIP, amino acid resolution of RBP-RNA interactions can be obtained (Kramer et al., 2014; Bae et al., 2020). Finally, related methods take advantage of specific biochemical properties of ribonucleoprotein complexes to purify both RBPs and RNAs at the same time (Smith et al., 2020). All of these methods can be categorized as CLIP- or RIC-like depending on the readout (transcriptomics or proteomics, respectively). For a detailed methodological discussion, we refer the interested reader to excellent reviews on the available methods and their limitations (Ramanathan et al., 2019; Gebauer et al., 2020; Gräwe et al., 2020; Smith et al., 2020).

Studying the impact of PTMs on RBP-RNA interactions is conceptually simple: the biological system under study is perturbed, and changes in RBP-RNA binding are studied via CLIP- or RIC-like assays. RIC-like methods are particularly attractive because the readout via mass spectrometry can be used to directly assess PTMs. However, despite this conceptual simplicity, interpreting results from such experiments can be challenging. Here, we discuss the biases involved, with the goal to highlight both the challenges and also the opportunities for systematically identifying functional PTMs in RBPs. First, we will emphasize the differences between the read-outs of CLIP- and RIC-like assays. We will then discuss specific biases that are particularly relevant for RIC-like experiments. Finally, we outline how PTMs can affect specific aspects of RBP function via known examples.

CLIP- and RIC-Like Methods Provide Different Types of RBP-RNA Interaction Data

Before discussing specific biases, it is important to remember that CLIP- and RIC-like methods provide fundamentally different types of RBP-RNA measures: CLIP maps RBP binding sites globally, while RIC captures the proteins that bind to RNA. Quantitative interpretation of CLIP-like experiments is difficult (Ramanathan et al., 2019), and only performed in exceptional cases (Schueler et al., 2014) or indirectly (Gregersen et al., 2014; Milek et al., 2017; Smith et al., 2021). In contrast, RIC-like experiments are often used to assess changes in RNA-binding for RBPs across conditions (Hentze et al., 2018), and several groups have identified context-specific regulatory RBPs in mammalian tissue culture cells (Boucas et al., 2015; Liepelt et al., 2016; Milek et al., 2017; Perez-Perri et al., 2018; Garcia-Moreno et al., 2019; Ignarski et al., 2019; Queiroz et al., 2019; Trendel et al., 2019; Hiller et al., 2020; Smith et al., 2021), zebrafish and fly embryos (Sysoev et al., 2016; Despic et al., 2017), yeast (Shchepachev et al., 2019; Bresson et al., 2020), and plant cells (Marondedze et al., 2019). While it is tempting to interpret differences in RIC-like experiments as changes in RBP-RNA interaction (RNA-bound protein fraction), this is not to be taken for granted. In this perspective, we focus on UV-crosslinking-based RIC-like experiments (**Figure 1**), although some points raised are also relevant for CLIP-like assays and other cross-linking approaches.

Isolation Efficiency of Bound RNAs Biases Quantification of RBP Binding

In CLIP-like assays, the pull-down efficiency of RBPs (usually with antibodies) is generally assumed to be independent of the bound RNA sequences. In RIC-like assays on the other hand, the pull-down efficiency of RBPs strongly depends on the isolation efficiency of their RNA targets (Gräwe et al., 2020). Features such as RNA length, subcellular localization, base composition, modifications and secondary structures can all influence RNA isolation. For example, RIC-like experiments using oligo(dT)-beads first isolate poly-A mRNAs through the A-T hybridization with beads (Baltz et al., 2012; Castello et al., 2012; Perez-Perri et al., 2018). In this case, the RNA isolation is affected by the A-T hybridization strength, such that there is a bias against mRNAs with shorter poly-A tails. Since the oligo(dT)-beads used for isolation are typically as short as 18–20 bases, this bias is probably mostly relevant for mRNAs with very short poly-A tails (shorter than 20 nts) (Park et al., 2016). Importantly, poly-A tail length is itself regulated during specific biological processes like the cell cycle (Park et al., 2016) and maternal to zygotic transition (Despic et al., 2017). Hence, isolation efficiency deserves special attention when analyzing such biological processes.

Oligo(dT)-enrichment is not the only RNA isolation method prone to biases (Perez-Perri et al., 2018, 2021; Scholes and Lewis, 2020). For instance, enrichment of the RBP-RNA complex using organic phase separation isolates complexes bound to RNAs as small as 30 nucleotides, but isolation efficiency drops dramatically for smaller RNAs (Urdaneta et al., 2019). Also, methods that enrich specific RNAs via hybridization to complementary

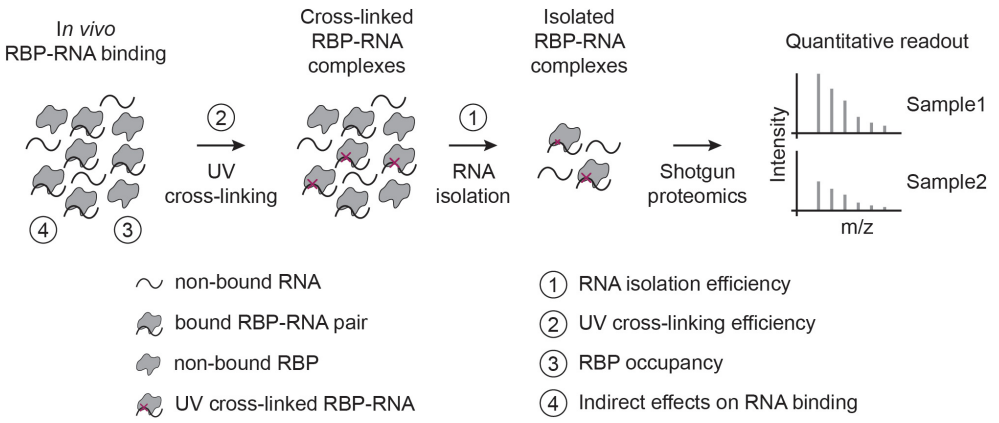

FIGURE 1 | RIC-like assays and biases involved in quantifying RBP-RNA interactions. In RIC-like experiments, *in vivo* RBP-RNA interactions are stabilized by UV cross-linking. RNAs are isolated and the bound proteome is quantified with shotgun proteomics. We identify here four biases in the interpretation of RBP-RNA quantification results: RNA isolation (1), UV cross-linking (2), RBP occupancy (3), and indirect effects on RNA binding (4).

oligonucleotide probes are sensitive to modifications of the RNA sequence that might impair hybridization (Gräwe et al., 2020).

UV Cross-Linking Efficiency Is a Major Factor for RBP-RNA Quantification

RIC-like experiments rely on the ability of the bound RBP to cross-link to the RNA it is interacting with. UV cross-linking is an attractive method to study RBP-RNA interactions, mainly due to its ability to stabilize interactions *in situ* in otherwise unmodified cells or tissues (Meisenheimer and Koch, 1997; Ramanathan et al., 2019). However, multiple factors influence cross-linking efficiencies, and not all RBP-RNA pairs are cross-linked equally well.

Upon single-photon excitation with UV light (∼254 nm), atoms of the nucleotide are excited to a higher energy state for a short time period. Only during this short time period (microseconds) nucleotides can form covalent cross-links with amino acid residues in close proximity ("zero-distance") (Budowsky et al., 1986; Meisenheimer and Koch, 1997). This is crucial for achieving high specificity but also makes the cross-linking reaction very inefficient. RBP-RNA cross-linking efficiency with continuous wave UV irradiation has been estimated to range from <0.1 to 5% (Budowsky et al., 1986; Fecko et al., 2007; Darnell, 2010). In addition to the overall low efficiency, differences exist between different RBP-RNA pairs. For example, uridines are favored *in vitro* (Meisenheimer and Koch, 1997) and are possibly the only detectable cross-linking nucleotide *in vivo* (Kramer et al., 2014; Bae et al., 2020). Also, double stranded RNAs poorly cross-link to bound proteins, and the direction with which the nucleotide makes contact (base, sugar, and phosphate backbone) also affects cross-linking efficiency (Meisenheimer and Koch, 1997). Finally, cross-linking efficiency also varies depending on the amino acid side chains in the RBP (Meisenheimer and Koch, 1997). While all amino acids have been shown to cross-link to some extent, amino acid-specific differences in cross-linking efficiency appear to exist *in vivo* (Kramer et al., 2014; Bae et al., 2020).

In summary, cross-linking efficiencies are generally low and affected by site-specific factors. The extremely low efficiency implies that minor differences in UV cross-linking can have a large impact on quantification. This point is mostly relevant when different sites are compared with each other in CLIP-like experiments. When comparing the same sites across different samples a low crosslinking efficiency *per se* is unlikely to lead to biases since it is expected to affect all samples equally.

Baseline RBP Occupancy by RNAs Limits the Outcome in Relative Quantification

To form novel interactions with RNA in response to perturbations, RBPs must be free (that is, not RNA-bound). Therefore, the baseline occupancy of an RBP (that is, the fraction of all RBP molecules that are already bound to RNA) restricts the changes that can be observed in relative quantitative analysis: Low RBP occupancy at baseline allows larger increases, while RBPs with high baseline occupancy are already close to maximal binding, and the opposite is true for decreases in RNA-binding. It is important to consider the baseline global RBP occupancy when studying changes across conditions, as this will affect the biological interpretation of results obtained in RIC-like experiments.

Consistent with the considerations above, we observed that several classical core RBPs (splicing factors, ribosomal proteins, and hnRNPs) show decreased binding in four comparative RIC studies employing different perturbations in distinct mammalian cell lines (**Figure 2**; Milek et al., 2017; Perez-Perri et al., 2018; Garcia-Moreno et al., 2019; Hiller et al., 2020). Conversely, proteins with moonlighting RNA-binding activity such as metabolic enzymes tend to show increased binding. It is tempting to refer to the first (core RBPs) and second (moonlighting RBPs) group of proteins as high and low baseline occupancy RBPs, respectively. These data thus support our considerations on the relationship between baseline occupancy and quantitative outcome. However, we do not know if this observation can be extended to other comparative RIC studies. It is also important

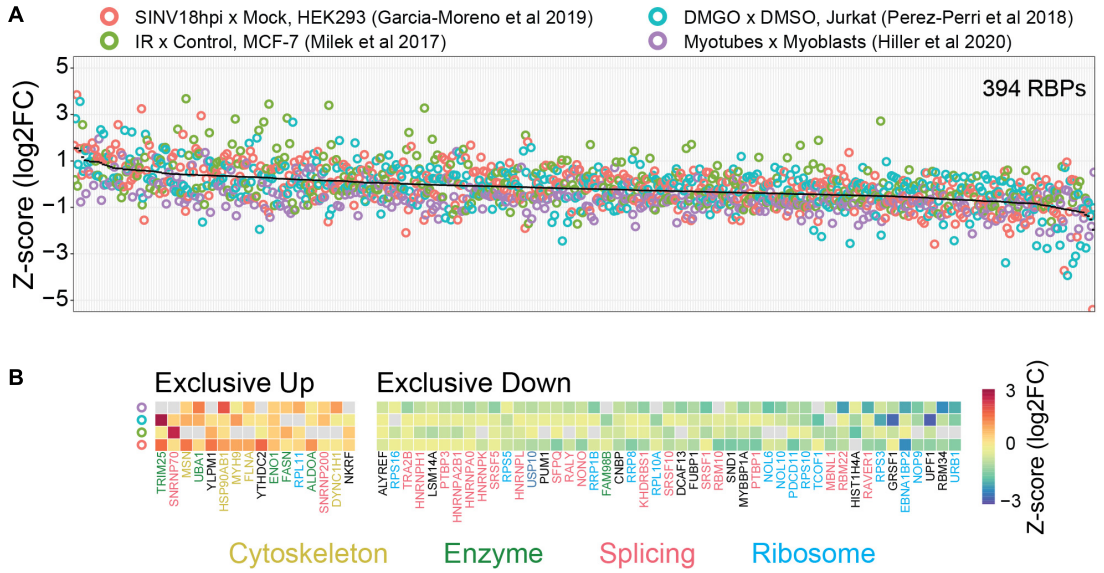

FIGURE 2 | Possible link between baseline RBP occupancy and observed changes in comparative RIC experiments. We used published data from four different cellular systems and perturbations [HEK293 cells infected with Sindbis virus (SINV), Infrared (IR) radiated MCF-7 cells, DMGO treated Jurkat cells, and differentiated myoblasts (myotubes)]. **(A)** Intra-experimentally *z*-scored log2 fold changes for 394 RBPs quantified in at least three experiments. Proteins were ranked by their mean fold change (black line). **(B)** RBPs exclusively up- or down-regulated in all experiments. Protein function was annotated manually. "Cytoskeleton" includes cytoskeleton dynamics-related proteins (yellow), "Enzymes" includes metabolic enzymes and protein modifiers (green), "Splicing" includes spliceosome components and splicing-related RBPs (red), "Ribosome" includes both core ribosome components and ribosome biogenesis-related factors (light-blue). We note that "moonlighting" RBPs (Cytoskeleton and Enzymes) and "core" RBPs (Splicing and Ribosome) tend to be up- and down-regulated, respectively. See text for more details.

to keep in mind that the situation *in vivo* is probably more complex. Most importantly, the actual baseline occupancy of RBPs is not known and also depends on the cellular context. In general, the occupancy depends on the binding affinity, the (local) concentration of the RBP and the number of available binding sites. For example, low concentration RBPs with a high number of RNA-binding sites are likely to be highly occupied. While the RNA-binding sites of a given RBP can be identified using CLIP-like methods, competition over binding sites between components in the cellular RNA network (other RBPs, RNA-RNA interactions, etc.) complicates estimating actual number of available sites for RBP interactions (Jens and Rajewsky, 2015). Measuring protein concentrations is also difficult, particularly because RBPs tend to localize in specific subcellular compartments where they exert their functions (Sundararaman et al., 2016). Finally, it is not yet possible to measure the *in vivo* RBP-RNA binding affinities. In combination, these factors complicate estimation of baseline occupancies and how this might impact the outcome of RIC-like experiments.

Indirect Effects on RNA Binding Independent of RBP Regulation

While binding to RNA is the defining feature of all RBPs, important aspects of their cellular function (like protein–protein interaction) do not depend on changes in their interaction with RNA. Conversely, changes in RNA-binding might occur as a secondary effect of other cellular events. For example, cells typically shut down translation in response to stress, which releases mRNAs that would otherwise be bound by ribosomes (Liu and Qian, 2014; Advani and Ivanov, 2019). Cellular stress also leads to formation of stress granules, where multiple RNAs are sequestered away (Ivanov et al., 2019). In both cases, corresponding RBPs can experience drastic changes in the amount of available RNA-binding sites. The fact that RBP-RNA binding depends on the availability of RNA-binding sites also hinders comparison across conditions where transcriptomes vary greatly. This might be the case when comparing stages during embryonic development (Sysoev et al., 2016; Despic et al., 2017), viral infection (Garcia-Moreno et al., 2019), or strong cellular perturbations like arsenite-induced stress (Trendel et al., 2019). Hence, some regulatory events affecting RBP function will not be captured by quantifying changes in their RNA-binding.

RBP Functional Regulation by PTMs

Despite the challenges outlined above, both RIC and CLIP are powerful methods that can provide information about RBP-RNA interactions on a genome-wide scale. A particularly attractive application of RIC-like methods (specially comparative RIC) is to study how RBP function is modulated by PTMs. Since most PTMs have not yet been studied via RIC-like experiments, we instead focus on exemplary cases of RBPs whose regulation by PTMs is sufficiently well characterized to allow us to speculate on their impact, taking the aforementioned biases into account.

RNA Affinity

The most direct way by which PTMs could affect RBP-RNA interaction is to change binding affinities. Amino acids in RBPs that directly contact RNAs are enriched in serine, threonine and tyrosine phosphorylation, lysine acetylation and arginine methylation sites (Bae et al., 2020). Several PTM sites have been shown to change the RBP affinity toward RNA targets, although that is not always the case (Thapar, 2015).

Intuitively, higher binding affinities result in increased RNA-binding (and vice-versa). However, due to the biases described above, an increased abundance in RIC-like experiments might not necessarily follow. For example, if the occupancy of the RBP is already close to maximum at baseline, major changes are not expected. Also, changes in the group of transcripts targeted by the RBP might lead to unexpected results in case this group of transcripts shows different isolation and/or UV cross-linking efficiencies. LARP1 might be a good example for the latter case: Upon inhibition of the upstream kinase mTORC1, the abundance of LARP1 in RIC-like experiments increases (Smith et al., 2020), suggesting stronger RNA-binding. While LARP1 interacts in cells with multiple transcripts (Hong et al., 2017), mTORC1-dependent phosphorylation modulates affinity toward the specific group containing the 5′ TOP motif (Jia et al., 2021). Whether 5′ TOP motif RNAs have different isolation/cross-linking efficiency is not known. Interestingly, both phosphorylation sites that increase or decrease affinity toward TOP mRNAs are regulated by mTORC1. Instead of increasing the mRNA-bound protein fraction as suggested by the higher abundance in RIC-like experimental results, mTORC1-induced phosphorylation might instead shift LARP1 binding preference to mRNA targets with different isolation and/or cross-linking efficiency.

Subcellular Localization

RNA-binding proteins are often localized to specific subcellular compartments where they interact with their targets (Sundararaman et al., 2016). This is important since the local concentrations of RBPs and target RNAs affect their interaction. PTMs in several RBPs have been shown to influence subcellular localization (Thapar, 2015; Lorton and Shechter, 2019). ELAVL1 (a.k.a. HuR) is a well-studied example for this: Phosphorylation of several sites near a nuclear localization signal induces protein accumulation in the cytosol, where it binds to and regulates mRNA targets stability (Abdelmohsen et al., 2007; Doller et al., 2007; Kim et al., 2008a,b; Lafarga et al., 2009). As is the case for ELAVL1, shuttling between subcellular compartments affects RBP interaction with RNA targets individually, increasing the interaction with some and decreasing with other RNAs. UV cross-linking and RNA isolation are also specific to each RBP-RNA pair. Altogether, it is very difficult to predict fold changes in RIC-like experiments following subcellular localization regulation of RBPs by PTMs.

Protein–Protein Interaction and Complex Formation

An important function of many RBPs is to bring target RNAs in contact with core ribonucleoprotein machineries, like the exosome, the ribosome and the spliceosome (Gehring et al., 2017). Several PTMs have been shown to regulate formation and stability of protein–protein interactions in RBPs with consequences for target RNAs (Zarnack et al., 2020). The consequence of such regulation for quantification in RIC-like experiments will depend on the protein partners. For instance, phosphorylation of NCL activates the deadenylase activity of its binding partner PARN, leading to shortening of poly-A tails in NCL-targeted RNAs (Zhang et al., 2018). Another example is phosphorylation of UPF1, which triggers formation of the RNA-decay complex and degradation of UPF1-bound RNAs (Durand et al., 2016). In both cases, phosphorylation is expected to affect pulldown efficiencies in RIC-like experiments without necessarily changing RNA-binding.

Phase Separation

Posttranslational modification of RBPs recently emerged as important regulators of liquid-liquid phase separation and ribonucleoprotein granule dynamics (Hofweber and Dormann, 2019). Particularly, methylation of arginine- and glycine-rich regions in RBPs plays an important role (Hofweber et al., 2018; Qamar et al., 2018). During phase separation, proteins interact with other proteins and RNAs to form membraneless condensates. RBP arginine methylation affects this condensation and thereby likely changes the set of RNAs bound by an RBP. On the one hand, it is not known if RNAs in condensates are efficiently isolated in RIC-like experiments. On the other hand, as discussed above, selection of RNA targets might lead to differential quantification in RIC-like experiments due to altered RNA isolation and UV cross-linking efficiency. Therefore, even though RBPs might interact more with RNAs in condensates, it is not clear if this results in corresponding changes in RIC-like experiments.

DISCUSSION

The last decade has seen great advances in the systematic identification of RBPs (Gebauer et al., 2020). In particular, CLIP- and RIC-like approaches provide global pictures of RBPs and their target RNAs. While the number of known RBPs now exceeds the number of known transcription factors, we are just beginning to understand how cell signaling and PTMs affect their function. In contrast to transcription factors that interact with an essentially constant genome, the fact that the transcriptome is highly dynamic complicates interpretation of RBP function. Here, we discussed challenges involved in interpreting CLIP and especially RIC-like results quantitatively and presented selected examples of how PTMs in RBPs could affect quantification. Particular qualities of the RBP (cellular functions, bound RNAs, protein interactors, etc.) and aspects of the conditions investigated (cell cycle state, global cellular adaptations to perturbation, discrepant transcriptomes, etc.) all affect the experimental results obtained. Therefore, an observed change (or lack thereof) in RIC-like experiments should not be

interpreted to indicate altered (or constant) RNA-association of an RBP. Having said this, it is also important to point out that CLIP- and RIC-like methods are very powerful approaches for the analysis of posttranscriptional regulation. However, apparent changes in RNA-binding observed with these methods should not be regarded as an end in themselves but rather as starting points for deeper analyses. It is instructive to more generously interpret such changes as possible RBP perturbation events rather than increased or decreased binding. It is then important to take a closer look at the biology of the protein under study and consider also other factors that might affect pull-down efficiency, besides RNA-binding. These factors include (but are not limited to) the examples given above, like changes in subcellular localization, altered protein-protein interactions, global proteome and/or transcriptome changes, phase separation, and switching between the classes of RNAs bound by an RBP.

DATA AVAILABILITY STATEMENT

Data presented in this study was directly obtained from the respective references. No new data was generated for this work.

AUTHOR CONTRIBUTIONS

CHV-V analyzed data and prepared figures with input from MS. CHV-V and MS wrote the manuscript. Both authors contributed to the article and approved the submitted version.

ACKNOWLEDGMENTS

We would like to thank Marvin Jens (MDC, Berlin, Germany) for the careful reading, comments, and suggestions during preparation of the manuscript.

REFERENCES

Abdelmohsen, K., Pullmann, R., Lal, A., Kim, H. H., Galban, S., Yang, X., et al. (2007). Phosphorylation of HuR by Chk2 regulates SIRT1 expression. *Mol. Cell* 25, 543–557. doi: 10.1016/j.molcel.2007.01.011

Advani, V. M., and Ivanov, P. (2019). Translational control under stress: reshaping the translatome. *Bioessays* 41:e1900009.

Bae, J. W., Kwon, S. C., Na, Y., Kim, V. N., and Kim, J.-S. (2020). Chemical RNA digestion enables robust RNA-binding site mapping at single amino acid resolution. *Nat. Struct. Mol. Biol.* 27, 678–682. doi: 10.1038/s41594-020-0436-2

Baltz, A. G., Munschauer, M., Schwanhäusser, B., Vasile, A., Murakawa, Y., Schueler, M., et al. (2012). The mRNA-bound proteome and its global occupancy profile on protein-coding transcripts. *Mol. Cell* 46, 674–690. doi: 10.1016/j.molcel.2012.05.021

Boucas, J., Fritz, C., Schmitt, A., Riabinska, A., Thelen, L., Peifer, M., et al. (2015). Label-free protein-RNA interactome analysis identifies khsrp signaling downstream of the p38/Mk2 kinase complex as a critical modulator of cell cycle progression. *PLoS One* 10:e0125745. doi: 10.1371/journal.pone.0125745

Bresson, S., Shchepachev, V., Spanos, C., Turowski, T. W., Rappsilber, J., and Tollervey, D. (2020). Stress-induced translation inhibition through rapid displacement of scanning initiation factors. *Mol. Cell* 80, 470–484.e8.

Buccitelli, C., and Selbach, M. (2020). mRNAs, proteins and the emerging principles of gene expression control. *Nat. Rev. Genet.* 21, 630–644.

Budowsky, E. I., Axentyeva, M. S., Abdurashidova, G. G., Simukova, N. A., and Rubin, L. B. (1986). Induction of polynucleotide-protein cross-linkages by ultraviolet irradiation. Peculiarities of the high-intensity laser pulse irradiation. *Eur. J. Biochem.* 159, 95–101. doi: 10.1111/j.1432-1033.1986.tb09837.x

Castello, A., Fischer, B., Eichelbaum, K., Horos, R., Beckmann, B. M., Strein, C., et al. (2012). Insights into RNA biology from an atlas of mammalian mRNA-binding proteins. *Cell* 149, 1393–1406. doi: 10.1016/j.cell.2012.04.031

Darnell, R. B. (2010). HITS-CLIP: panoramic views of protein-RNA regulation in living cells. *Wiley Interdiscip. Rev. RNA* 1, 266–286. doi: 10.1002/wrna.31

Despic, V., Dejung, M., Gu, M., Krishnan, J., Zhang, J., Herzel, L., et al. (2017). Dynamic RNA-protein interactions underlie the zebrafish maternal-to-zygotic transition. *Genome Res.* 27, 1184–1194. doi: 10.1101/gr.215954.116

Doller, A., Huwiler, A., Müller, R., Radeke, H. H., Pfeilschifter, J., and Eberhardt, W. (2007). Protein Kinase Cα-dependent Phosphorylation of the mRNA-stabilizing Factor HuR: implications for posttranscriptional regulation of cyclooxygenase-2. *Mol. Biol. Cell* 18, 2137–2148. doi: 10.1091/mbc.e06-09-0850

Durand, S., Franks, T. M., and Lykke-Andersen, J. (2016). Hyperphosphorylation amplifies UPF1 activity to resolve stalls in nonsense-mediated mRNA decay. *Nat. Commun.* 7:12434.

Fecko, C. J., Munson, K. M., Saunders, A., Sun, G., Begley, T. P., Lis, J. T., et al. (2007). Comparison of femtosecond laser and continuous wave UV sources for protein–nucleic acid crosslinking. *Photochem. Photobiol.* 83, 1394–1404. doi: 10.1111/j.1751-1097.2007.00179.x

Garcia-Moreno, M., Noerenberg, M., Ni, S., Järvelin, A. I., González-Almela, E., Lenz, C. E., et al. (2019). System-wide Profiling of RNA-binding proteins uncovers key regulators of virus infection. *Mol. Cell* 74, 196–211.e11.

Gebauer, F., Schwarzl, T., Valcárcel, J., and Hentze, M. W. (2020). RNA-binding proteins in human genetic disease. *Nat. Rev. Genet* 22, 185–198.

Gehring, N. H., Wahle, E., and Fischer, U. (2017). Deciphering the mRNP Code: RNA-bound determinants of post-transcriptional gene regulation. *Trends Biochem. Sci.* 42, 369–382. doi: 10.1016/j.tibs.2017.02.004

Gräwe, C., Stelloo, S., van Hout, F. A. H., and Vermeulen, M. (2020). RNA-centric methods: toward the interactome of specific RNA transcripts. *Trends Biotechnol.* doi: 10.1016/j.tibtech.2020.11.011 [Epup ahead of print],

Gregersen, L. H., Schueler, M., Munschauer, M., Mastrobuoni, G., Chen, W., Kempa, S., et al. (2014). MOV10 Is a 5′ to 3′ RNA helicase contributing to UPF1 mRNA target degradation by translocation along 3′ UTRs. *Mol. Cell* 54, 573–585. doi: 10.1016/j.molcel.2014.03.017

Hafner, M., Landthaler, M., Burger, L., Khorshid, M., Hausser, J., Berninger, P., et al. (2010). Transcriptome-wide identification of RNA-binding protein and microRNA target sites by PAR-CLIP. *Cell* 141, 129–141.

Hentze, M. W., Castello, A., Schwarzl, T., and Preiss, T. (2018). A brave new world of RNA-binding proteins. *Nat. Rev. Mol. Cell Biol.* 19, 327–341. doi: 10.1038/nrm.2017.130

Hiller, M., Geissler, M., Janssen, G., van Veelen, P., Aartsma-Rus, A., and Spitali, P. (2020). The mRNA binding proteome of proliferating and differentiated muscle cells. *Genomics Proteomics Bioinformatics* doi: 10.1016/j.gpb.2020.06.004 [Epup ahead of print],

Hofweber, M., and Dormann, D. (2019). Friend or foe—Post-translational modifications as regulators of phase separation and RNP granule dynamics. *J. Biol. Chem.* 294, 7137–7150. doi: 10.1074/jbc.tm118.001189

Hofweber, M., Hutten, S., Bourgeois, B., Spreitzer, E., Niedner-Boblenz, A., Schifferer, M., et al. (2018). Phase separation of FUS is suppressed by its nuclear import receptor and arginine methylation. *Cell* 173, 706–719.e13.

Hong, S., Freeberg, M. A., Han, T., Kamath, A., Yao, Y., Fukuda, T., et al. (2017). LARP1 functions as a molecular switch for mTORC1-mediated translation of an essential class of mRNAs. *Elife* 6:e25237. doi: 10.7554/eLife.25237

Huang, J. X., Lee, G., Cavanaugh, K. E., Chang, J. W., Gardel, M. L., and Moellering, R. E. (2019). High throughput discovery of functional protein modifications by Hotspot Thermal Profiling. *Nat. Methods* 16, 894–901.

Ignarski, M., Rill, C., Kaiser, R. W. J., Kaldirim, M., Neuhaus, R., Esmaillie, R., et al. (2019). The RNA-protein interactome of differentiated kidney tubular

epithelial cells. *J. Am. Soc. Nephrol.* 30, 564–576. doi: 10.1681/asn.2018090914

Imami, K., Milek, M., Bogdanow, B., Yasuda, T., Kastelic, N., Zauber, H., et al. (2018). Phosphorylation of the ribosomal protein RPL12/uL11 affects translation during mitosis. *Mol. Cell* 72, 84–98.e9.

Ivanov, P., Kedersha, N., and Anderson, P. (2019). Stress granules and processing bodies in translational control. *Cold Spring Harb. Perspect. Biol.* 11:a032813. doi: 10.1101/cshperspect.a032813

Jens, M., and Rajewsky, N. (2015). Competition between target sites of regulators shapes post-transcriptional gene regulation. *Nat. Rev. Genet.* 16, 113–126.

Jia, J.-J., Lahr, R. M., Solgaard, M. T., Moraes, B. J., Pointet, R., Yang, A.-D., et al. (2021). mTORC1 promotes TOP mRNA translation through site-specific phosphorylation of LARP1. *Nucleic Acids Res.* 49, 3461–3489.

Kim, H. H., Abdelmohsen, K., Lal, A., Pullmann, R. Jr., Yang, X., Galban, S., et al. (2008a). Nuclear HuR accumulation through phosphorylation by Cdk1. *Genes Dev.* 22, 1804–1815. doi: 10.1101/gad.1645808

Kim, H. H., Yang, X., Kuwano, Y., and Gorospe, M. (2008b). Modification at HuR(S242) alters HuR localization and proliferative influence. *Cell Cycle* 7, 3371–3377. doi: 10.4161/cc.7.21.6895

König, J., Zarnack, K., Rot, G., Curk, T., Kayikci, M., Zupan, B., et al. (2010). iCLIP reveals the function of hnRNP particles in splicing at individual nucleotide resolution. *Nat. Struct. Mol. Biol.* 17, 909–915. doi: 10.1038/nsmb.1838

Kramer, K., Sachsenberg, T., Beckmann, B. M., Qamar, S., Boon, K.-L., Hentze, M. W., et al. (2014). Photo-cross-linking and high-resolution mass spectrometry for assignment of RNA-binding sites in RNA-binding proteins. *Nat. Methods* 11, 1064–1070. doi: 10.1038/nmeth.3092

Lafarga, V., Cuadrado, A., Lopez de Silanes, I., Bengoechea, R., Fernandez-Capetillo, O., and Nebreda, A. R. (2009). p38 Mitogen-activated protein kinase- and HuR-dependent stabilization of p21(Cip1) mRNA mediates the G(1)/S checkpoint. *Mol. Cell. Biol.* 29, 4341–4351. doi: 10.1128/mcb.00210-09

Larsen, S. C., Sylvestersen, K. B., Mund, A., Lyon, D., Mullari, M., Madsen, M. V., et al. (2016). Proteome-wide analysis of arginine monomethylation reveals widespread occurrence in human cells. *Sci. Signal.* 9:rs9.

Liepelt, A., Naarmann-de Vries, I. S., Simons, N., Eichelbaum, K., Föhr, S., Archer, S. K., et al. (2016). Identification of RNA-binding proteins in macrophages by interactome capture. *Mol. Cell. Proteomics* 15, 2699–2714. doi: 10.1074/mcp.m115.056564

Lin, C., and Miles, W. O. (2019). Beyond CLIP: advances and opportunities to measure RBP–RNA and RNA–RNA interactions. *Nucleic Acids Res.* 47, 5490–5501. doi: 10.1093/nar/gkz295

Liu, B., and Qian, S.-B. (2014). Translational reprogramming in cellular stress response. *Wiley Interdisciplinary Rev. RNA* 5, 301–305. doi: 10.1002/wrna.1212

Lorton, B. M., and Shechter, D. (2019). Cellular consequences of arginine methylation. *Cell. Mol. Life Sci.* 76, 2933–2956.

Lovci, M. T., Bengtson, M. H., and Massirer, K. B. (2016). Post-Translational Modifications and RNA-Binding Proteins. *Adv. Exp. Med. Biol.* 907, 297–317. doi: 10.1007/978-3-319-29073-7_12

Marondedze, C., Thomas, L., Gehring, C., and Lilley, K. S. (2019). Changes in the *Arabidopsis* RNA-binding proteome reveal novel stress response mechanisms. *BMC Plant Biol.* 19:139.

Masuda, T., Sugiyama, N., Tomita, M., Ohtsuki, S., and Ishihama, Y. (2020). Mass spectrometry-compatible subcellular fractionation for proteomics. *J. Proteome Res.* 19, 75–84. doi: 10.1021/acs.jproteome.9b00347

Meisenheimer, K. M., and Koch, T. H. (1997). Photocross-linking of nucleic acids to associated proteins. *Crit. Rev. Biochem. Mol. Biol.* 32, 101–140. doi: 10.3109/10409239709108550

Milek, M., Imami, K., Mukherjee, N., Bortoli, F. D., Zinnall, U., Hazapis, O., et al. (2017). DDX54 regulates transcriptome dynamics during DNA damage response. *Genome Res.* 27, 1344–1359. doi: 10.1101/gr.218438.116

Ochoa, D., Jarnuczak, A. F., Viéitez, C., Gehre, M., Soucheray, M., Mateus, A., et al. (2020). The functional landscape of the human phosphoproteome. *Nat. Biotechnol.* 38, 365–373. doi: 10.1038/s41587-019-0344-3

Park, J.-E., Yi, H., Kim, Y., Chang, H., and Kim, V. N. (2016). Regulation of Poly(A) tail and translation during the somatic cell cycle. *Mol. Cell* 62, 462–471. doi: 10.1016/j.molcel.2016.04.007

Perez-Perri, J. I., Noerenberg, M., Kamel, W., Lenz, C. E., Mohammed, S., Hentze, M. W., et al. (2021). Global analysis of RNA-binding protein dynamics by comparative and enhanced RNA interactome capture. *Nat. Protoc.* 16, 27–60. doi: 10.1038/s41596-020-00404-1

Perez-Perri, J. I., Rogell, B., Schwarzl, T., Stein, F., Zhou, Y., Rettel, M., et al. (2018). Discovery of RNA-binding proteins and characterization of their dynamic responses by enhanced RNA interactome capture. *Nat. Commun.* 9, 4408.

Qamar, S., Wang, G., Randle, S. J., Ruggeri, F. S., Varela, J. A., Lin, J. Q., et al. (2018). FUS phase separation is modulated by a molecular chaperone and methylation of arginine cation-π interactions. *Cell* 173, 720–734.e15.

Queiroz, R. M. L., Smith, T., Villanueva, E., Marti-Solano, M., Monti, M., Pizzinga, M., et al. (2019). Comprehensive identification of RNA-protein interactions in any organism using orthogonal organic phase separation (OOPS). *Nat. Biotechnol.* 37, 169–178. doi: 10.1038/s41587-018-0001-2

Ramanathan, M., Porter, D. F., and Khavari, P. A. (2019). Methods to study RNA–protein interactions. *Nat. Methods* 16, 225–234.

Scholes, A. N., and Lewis, J. A. (2020). Comparison of RNA isolation methods on RNA-Seq: implications for differential expression and meta-analyses. *BMC Genomics* 21:249.

Schueler, M., Munschauer, M., Gregersen, L. H., Finzel, A., Loewer, A., Chen, W., et al. (2014). Differential protein occupancy profiling of the mRNA transcriptome. *Genome Biol.* 15:R15.

Sharma, K., D'Souza, R. C. J., Tyanova, S., Schaab, C., Wiśniewski, J. R., Cox, J., et al. (2014). Ultradeep human phosphoproteome reveals a distinct regulatory nature of Tyr and Ser/Thr-based signaling. *Cell Rep.* 8, 1583–1594. doi: 10.1016/j.celrep.2014.07.036

Shchepachev, V., Bresson, S., Spanos, C., Petfalski, E., Fischer, L., Rappsilber, J., et al. (2019). Defining the RNA interactome by total RNA-associated protein purification. *Mol. Syst. Biol.* 15:e8689.

Smith, E. M., Benbahouche, N. E. H., Morris, K., Wilczynska, A., Gillen, S., Schmidt, T., et al. (2021). The mTOR regulated RNA-binding protein LARP1 requires PABPC1 for guided mRNA interaction. *Nucleic Acids Res.* 49, 458–478.

Smith, T., Villanueva, E., Queiroz, R. M. L., Dawson, C. S., Elzek, M., Urdaneta, E. C., et al. (2020). Organic phase separation opens up new opportunities to interrogate the RNA-binding proteome. *Curr. Opin. Chem. Biol.* 54, 70–75.

Stamm, S. (2008). Regulation of alternative splicing by reversible protein phosphorylation. *J. Biol. Chem.* 283, 1223–1227. doi: 10.1074/jbc.r700034200

Sundararaman, B., Zhan, L., Blue, S. M., Stanton, R., Elkins, K., Olson, S., et al. (2016). Resources for the comprehensive discovery of functional RNA elements. *Mol. Cell* 61, 903–913. doi: 10.1016/j.molcel.2016.02.012

Sysoev, V. O., Fischer, B., Frese, C. K., Gupta, I., Krijgsveld, J., Hentze, M. W., et al. (2016). Global changes of the RNA-bound proteome during the maternal-to-zygotic transition in *Drosophila*. *Nat. Commun.* 7:12128.

Thapar, R. (2015). Structural basis for regulation of RNA-binding proteins by phosphorylation. *ACS Chem. Biol.* 10, 652–666. doi: 10.1021/cb500860x

Trendel, J., Schwarzl, T., Horos, R., Prakash, A., Bateman, A., Hentze, M. W., et al. (2019). The human RNA-binding proteome and its dynamics during translational arrest. *Cell* 176, 391–403.e19.

Urdaneta, E. C., Vieira-Vieira, C. H., Hick, T., Wessels, H.-H., Figini, D., Moschall, R., et al. (2019). Purification of cross-linked RNA-protein complexes by phenol-toluol extraction. *Nat. Commun.* 10:990.

Wheeler, E. C., Van Nostrand, E. L., and Yeo, G. W. (2018). Advances and challenges in the detection of transcriptome-wide protein-RNA interactions. *Wiley Interdisciplinary Rev. RNA* 9:e1436. doi: 10.1002/wrna.1436

Yu, M. C. (2011). The role of protein arginine methylation in mRNP dynamics. *Mol. Biol. Int.* 2011, 1–10. doi: 10.4061/2011/163827

Zarnack, K., Balasubramanian, S., Gantier, M. P., Kunetsky, V., Kracht, M., Schmitz, M. L., et al. (2020). Dynamic mRNP remodeling in response to internal and external stimuli. *Biomolecules* 10:1310. doi: 10.3390/biom10091310

Zhang, X., Xiao, S., Rameau, R. D., Devany, E., Nadeem, Z., Caglar, E., et al. (2018). Nucleolin phosphorylation regulates PARN deadenylase activity during cellular stress response. *RNA Biol.* 15, 251–260. doi: 10.1080/15476286.2017.1408764

Conflict of Interest: The authors declare that the research was conducted in the absence of any commercial or financial relationships that could be construed as a potential conflict of interest.

frontiers in Molecular Biosciences

MINI REVIEW
published: 11 June 2021
doi: 10.3389/fmolb.2021.692668

Arginine Methyltransferases as Regulators of RNA-Binding Protein Activities in Pathogenic Kinetoplastids

*Gustavo D. Campagnaro[1], Edward Nay[2], Michael J. Plevin[2], Angela K. Cruz[1] and Pegine B. Walrad[2]**

[1]Department of Cell and Molecular Biology, Ribeirão Preto Medical School, University of São Paulo, Ribeirão Preto, Brazil, [2]York Biomedical Research Institute, Department of Biology, University of York, York, United Kingdom

A large number of eukaryotic proteins are processed by single or combinatorial post-translational covalent modifications that may alter their activity, interactions and fate. The set of modifications of each protein may be considered a "regulatory code". Among the PTMs, arginine methylation, catalyzed by protein arginine methyltransferases (PRMTs), can affect how a protein interacts with other macromolecules such as nucleic acids or other proteins. In fact, many RNA-binding (RBPs) proteins are targets of PRMTs. The methylation status of RBPs may affect the expression of their bound RNAs and impact a diverse range of physiological and pathological cellular processes. Unlike most eukaryotes, Kinetoplastids have overwhelmingly intronless genes that are arranged within polycistronic units from which mature mRNAs are generated by *trans*-splicing. Gene expression in these organisms is thus highly dependent on post-transcriptional control, and therefore on the action of RBPs. These genetic features make trypanosomatids excellent models for the study of post-transcriptional regulation of gene expression. The roles of PRMTs in controlling the activity of RBPs in pathogenic kinetoplastids have now been studied for close to 2 decades with important advances achieved in recent years. These include the finding that about 10% of the *Trypanosoma brucei* proteome carries arginine methylation and that arginine methylation controls *Leishmania*:host interaction. Herein, we review how trypanosomatid PRMTs regulate the activity of RBPs, including by modulating interactions with RNA and/or protein complex formation, and discuss how this impacts cellular and biological processes. We further highlight unique structural features of trypanosomatid PRMTs and how it contributes to their singular functionality.

Keywords: arginine methylation, PRMT, RNA-binding protein, *Trypanosoma*, *Leishmania*, gene expression, Kinetoplastid, post-translational modification

OPEN ACCESS

Edited by:
Nicolas Lux Fawzi, Brown University, United States

Reviewed by:
Luca Parca, Casa Sollievo Della Sofferenza (IRCCS), Italy
Christopher De Graffenried, Brown University, United States
David Shechte, Albert Einstein College of Medicine, United States

****Correspondence:***
Pegine B. Walrad
pegine.walrad@york.ac.uk

Specialty section:
This article was submitted to Protein and RNA Networks, a section of the journal Frontiers in Molecular Biosciences

Received: *08 April 2021*
Accepted: *28 May 2021*
Published: *11 June 2021*

Citation:
Campagnaro GD, Nay E, Plevin MJ, Cruz AK and Walrad PB (2021) Arginine Methyltransferases as Regulators of RNA-Binding Protein Activities in Pathogenic Kinetoplastids. Front. Mol. Biosci. 8:692668. doi: 10.3389/fmolb.2021.692668

INTRODUCTION

A large number of eukaryotic proteins are processed by single or combinatorial post-translational modifications (PTMs) that may alter protein function, conformation, localization, and/or their interaction with other macromolecules (Tak et al., 2019). The methylation of arginine residues is mediated by Protein Arginine Methyltransferases (PRMTs), of which three types exist: I, II and III. All three types generate ω-monomethylarginine (MMA) by transferring the methyl group from S-adenosylmethionine (SAM) to a ω-nitrogen atom. Type I PRMTs can add a further methyl to the same nitrogen to form asymmetric ω-dimethylarginine (aDMA) while type II PRMTs modify the

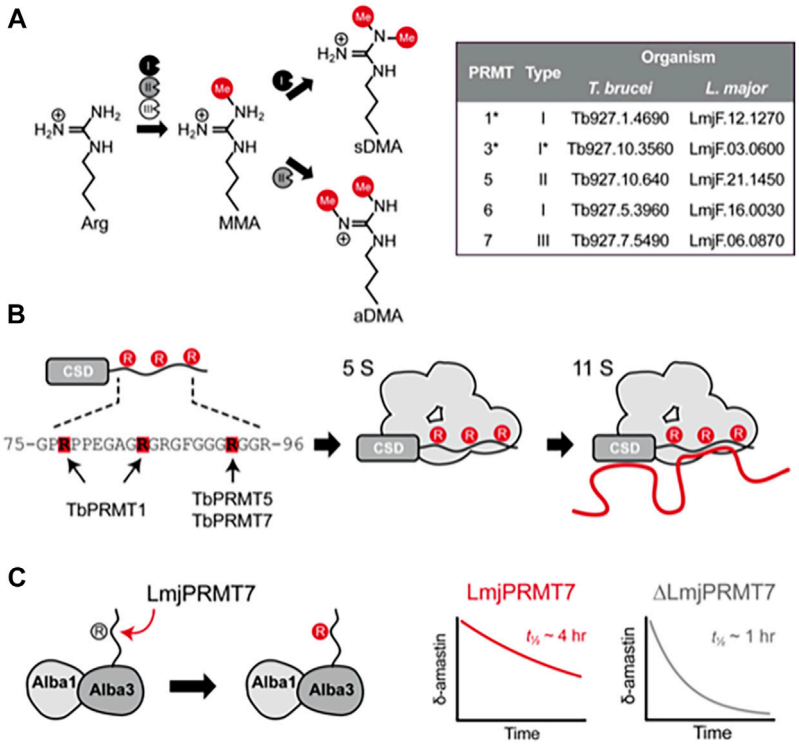

PRMT	Type	Organism	
		T. brucei	*L. major*
1*	I	Tb927.1.4690	LmjF.12.1270
3*	I*	Tb927.10.3560	LmjF.03.0600
5	II	Tb927.10.640	LmjF.21.1450
6	I	Tb927.5.3960	LmjF.16.0030
7	III	Tb927.7.5490	LmjF.06.0870

FIGURE 1 | Molecular effects of arginine methylation in *T. brucei* and *L. major*. **(A)**, Protein arginine methyltranferases (PRMTs) from types I, II and III are able to generate monomethylarginine (MMA) by transfering the methyl group from S-adenosylmethionine to the terminal nitrogen atom of arginine residues. While type III PRMTs only produce monomethylated products, type I PRMTs catalyze a second round of methylation at the same atom, generating asymmetrically dimethylated arginine (aDMA), whereas type II PRMTs add another methyl group to the adjacent terminal nitrogen, forming symmetric dimethylarginine (sDMA). The inset table contains the gene IDs of PRMT genes found in the genome of *T. brucei* and *L. major*. **(B)**, Schematic representation of how methylation affects the capability of RBP16 to form macromolecular complexes containing proteins (gray) and RNA (red line) in *T. brucei*. The RBP16 intrinsically disordered RGG domain is methylated by *Tb*PRMT1 on Arg78 and Arg85, whereas Arg93 is (potentially) methylated by either or both *Tb*PRMT5 and *Tb*PRMT7 **(left)**. In its methylated state, RBP16 can associate with other proteins (5S complex) or with proteins and RNA (11S complex). A non-methylatable version of RBP16 is still able to associate with RNA but loses the capability to form multiprotein complexes. Non-methylated arginines are represented by gray circles and methylated arginines by red circles. **(C)**, Representation of the methylation mediated by *L. major* PRMT7 on Alba3. Alba3 interacts with Alba1 and δ-amastin transcripts. Methylated Alba3 has a stronger association with δ-amastin transcripts and protects the RNA from degradation. The ability of Alba3 to bind δ-*amastin* is reduced upon *Lmj*PRMT7-knockout, which reduces the half-life of the transcripts from approximately 4 h to around 1 h. *PRMT3 is currently known as $PRMT1^{PRO}$ in *T. brucei*; despite its similarity to mammalian PRMT3, *Tb*PRMT3 misses key residues for PRMT activity, and is rather a prozyme for the catalytic *Tb*PRMT1, which was thus renamed to $TbPRMT1^{ENZ}$.

other ω-nitrogen to generate symmetric ω-dimethylarginine (sDMA) (Bedford, 2007) (**Figure 1A**). PRMTs show a preference for arginine-glycine (RGG) rich motifs, which are commonly enriched in intrinsically unstructured regions of proteins and implicated in RNA binding and biomolecular liquid-liquid phase separation (Chong et al., 2018).

Kinetoplastida are the only parasitic protozoa to harbor genes encoding for PRMTs of types I, II and III (Fisk and Read, 2011) (**Figure 1A**). This group of early branching eukaryotes includes the causative agents of important human diseases: Sleeping Sickness (*Trypanosoma brucei*), Chagas disease (*Trypanosoma cruzi*) and the leishmaniases (*Leishmania* spp.). During their life cycles, trypanosomatids alternate between several morphologically and metabolically different stages, which requires fine-tuned regulation of gene expression.

As part of the class Kinetoplastea, trypanosomatids display some particular features, such as the arrangement of genes in long polycistronic transcription units (PTUs) and *trans*-splicing of all mRNAs (Adl et al., 2019). Given the lack of individual promoters and terminators, virtually all genes in Kinetoplastids are constitutively transcribed as part of PTUs (Clayton, 2016; Damasceno et al., 2020), which makes these parasites good models for the study of mechanisms involved in post-transcriptional gene regulation.

A multitude of studies have shown that the levels of RNA-binding proteins (RBPs) fluctuate throughout the life cycle of trypanosomatids, some being stage-specific, even dictating the transition from one biological form to another (Kolev et al., 2014; de Pablos et al., 2019). Less, however, is understood about the mechanisms regulating the activity of RBPs. In this sense, arginine methylation has been gaining attention as a regulatory mechanism of nucleic acid-binding protein activities in trypanosomatids (Lott et al., 2013; Ferreira et al., 2020). In fact, knowledge of trypanosomatid PRMTs has grown substantially in the recent years, with the disclosure of protein structures, and the

determination of the molecular effects of arginine methylation, particularly on RBPs. The differences observed in the biochemical, biophysical and structural properties of trypanosomatid PRMTs in comparison to their mammalian counterparts suggest that PRMTs may be good targets for drug development.

Here, we provide an up-to-date review of the activities of PRMTs in pathogenic trypanosomatids, as well as discuss the effect of arginine methylation in cellular and molecular processes, particularly on the function of RBPs. Moreover, we discuss the structural features of trypanosomatid PRMTs and how these might enable revised design and repurposing of current drugs to combat these parasites.

PROTEIN ARGININE METHYLTRANSFERASES IN *TRYPANOSOMA*

The first evidence for arginine methylation in *T. brucei* dates from 1991 (Yarlett et al., 1991), that was directly confirmed a decade later (Pelletier et al., 2001). Recently, the use of high-throughput techniques revealed that close to 10% of the *T. brucei* proteome harbors methylated arginines (Lott et al., 2013), the product of the cooperative action of five PRMTs found in its genome (Lott et al., 2014). Nomenclature of *Trypanosoma* proteins corresponds to the human PRMTs.

Trypanosoma brucei Protein Arginine Methyltransferase 1, the First Discovered in Kinetoplastids

The first *T. brucei* protein identified to harbor methylated arginine residues was RBP16, a protein involved in mitochondrial RNA processing (Hayman and Read, 1999; Pelletier and Read, 2003). Three arginine residues, Arg-78, Arg-85 and Arg-93, are part of the RGG domain of RBP16 and methylation influences RBP16-RNA interactions (Pelletier et al., 2000; Miller and Read, 2003). Of these, only Arg-93 is constitutively methylated, while methylation of Arg-78 or Arg-85 appears to be mutually exclusive.

In vitro methylation assays using recombinant RBP16 and *T. brucei* procyclic whole cell protein extracts in the presence of classic substrates of type I and type II PRMTs indicated RBP16 is methylated by a trypanosome type I PRMT (Pelletier et al., 2001). The search for the type I PRMT that methylates RBP16 led to the identification of a protein 51% identical to the human PRMT1, thus named *Tb*PRMT1, whose knockdown (KD) abolished $RBP16^{Arg78}$ and $RBP16^{Arg85}$ methylation (Pelletier et al., 2005; Goulah et al., 2006). Arg-93 remains methylated, likely due to the action of another PRMT. Curiously, *Tb*PRMT1 is mostly present in the cytoplasm, suggesting RBP16 might be methylated before import into the mitochondrion (Fisk et al., 2010).

In *T. brucei*, RBP16 forms complexes of various sizes, but most notably 5S and 11S complexes; the latter likely represents the proteinaceous 5S complex bound to RNAs. Curiously, cells depleted for *Tb*PRMT1 or expressing the R78K, R85K and R93K triple mutant RBP16 formed a 5S complex composed of RBP16 bound only to mitochondrial guide RNAs (gRNAs), implicit in RNA editing, but not mRNAs (**Figure 1B**). Accordingly, non-methylatable RBP16 has an increased affinity for gRNAs, yet displays lower affinity for mitochondrial mRNAs (Goulah and Read, 2007). It is, however, unknown which proteins interact with RBP16 and whether mitochondrial mRNAs bind directly to RBP16 in the complex. Nonetheless, expression of non-methylatable RBP16 has been associated with destabilization of *NADH dehydrogenase subunit 4* mRNA, whose quantity is also lower in *Tb*PRMT1-KD cells, though *Tb*PRMT1-knockdown also impacts levels of other mRNAs (Goulah et al., 2006). The effects of arginine methylation by *Tb*PRMT1 are not limited to the mitochondrion. DRBD18 is a cytoplasmic RBP whose methylation state leads to different protein complex formation and alters mRNA expression. RNAs stabilized by methylated DRBD18 are less stable in the absence of *Tb*PRMT1 or when non-methylatable DRBD18 is expressed; the opposite is true for RNAs destabilized by DRBD18 (Lott et al., 2015). In fact, *Tb*PRMT1 knockout has a broad, complex effect on mRNP associations, which impacts cell metabolism, particularly energy production pathways, as well as stress granule formation, and results in reduced *in vitro T. brucei* growth and virulence in mice (Kafková et al., 2018).

Trypanosoma brucei Protein Arginine Methyltransferase 1 Activity Is Dependent on *Tb*PRMT3

Like *Tb*PRMT1, *Tb*PRMT3 was also identified as a potential type I PRMT and knockdown of either *Tb*PRMT1 or *Tb*PRMT3 reduced aDMA levels in the cells. Interestingly, the reduction in the protein level of either was accompanied by a reduction of the other, suggesting an interdependent stability between *Tb*PRMT1 and *Tb*PRMT3 (Pelletier et al., 2005; Lott et al., 2014).

However, *Tb*PRMT3 is inactive *in vitro* (Kafková et al., 2017), and its primary sequence lacks conserved residues in THW and double E loops, which are typically well conserved and responsible for substrate binding and positioning, respectively (Tewary et al., 2019). Structural data showed that although *Tb*PRMT3 retains the four canonical PRMT domains (N-terminus, SAM-binding Rossman fold domain, dimerization arm and β-barrel domain; **Figure 2A**), it lacks a crucial 3_{10} α-helix in the Rossman fold, which alters the dimerization interface and precludes SAM binding (Kafková et al., 2017; Hashimoto et al., 2020). Importantly, *T. cruzi* PRMT3 also lacks conserved THW and double E loops.

Functional studies have shown that *Tb*PRMT3 is essential for *Tb*PRMT1 stability and activity, establishing it as a "prozyme" or "pseudoenzyme" that supports the catalytically active *Tb*PRMT1. *Tb*PRMT1 and *Tb*PRMT3 have, thus, been renamed as $TbPRMT1^{ENZ}$ and $TbPRMT1^{PRO}$, respectively (Kafková et al., 2017; Hashimoto et al., 2020) (**Figure 1A**). Interestingly, when amino acids 41–52 were removed from $TbPRMT1^{PRO}$, methyltransferase activity was lost as the complex could no longer bind substrates. Although enzymatically inactive,

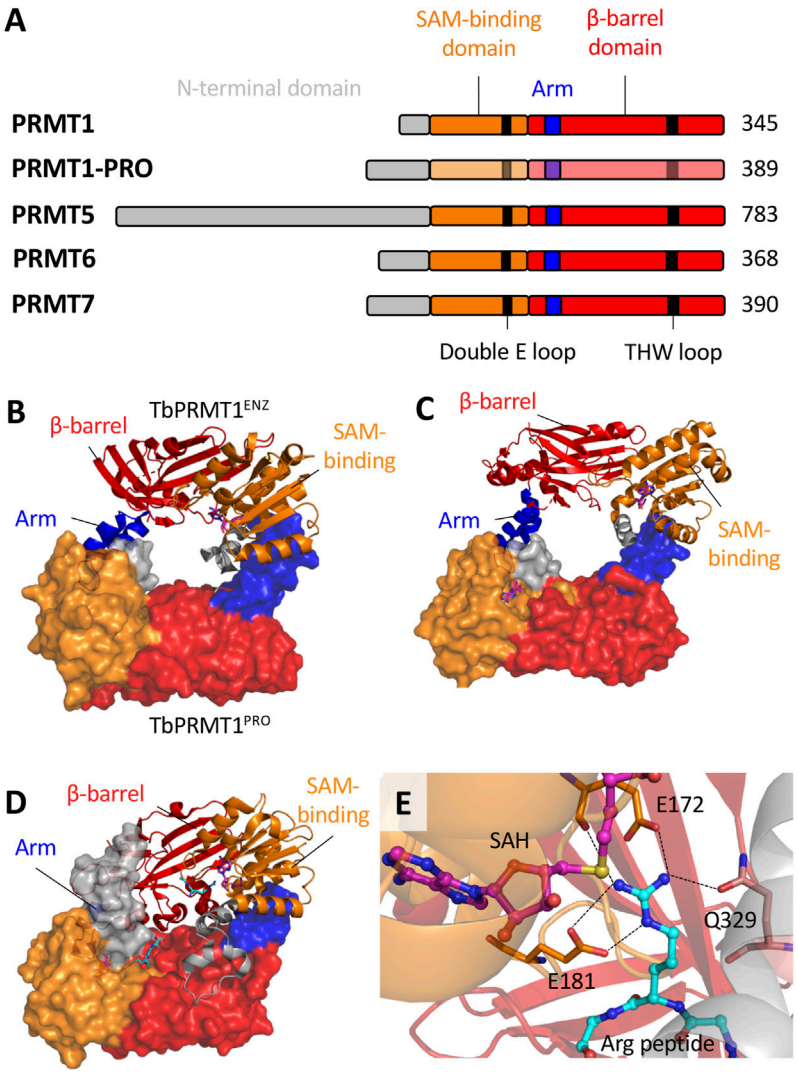

FIGURE 2 | The structural biology of *T. brucei* PRMTs. **(A)**, Each of the five PRMT homologs in *T. brucei* contain the four canonical domains indicated. The SAM-binding domain contains the residues that interact with a SAM molecule and the target arginine substrate. The β-barrel domain contains residues that interact with the arginine substrate. The arm (dimerization arm) within the β-barrel domain interacts with another subunit via contacts to the SAM-binding domain. *Tb*PRMT N-termini have significant variability with elusive functional roles. Key conserved double E loop and THW loop are also indicated. B-D, The core dimeric interfaces of **(B)** *Tb*PRMT1^{ENZ}-*Tb*PRMT1^{PRO} (PDB: 6DNZ) **(C)** *Tb*PRMT6 (PDB: 4LWP) and **(D)** *Tb*PRMT7 (PDB: 4M38). The surface structure represents the second subunit (or *Tb*PRMT1^{PRO} indicated in B. The SAH and Arg peptides are indicated by pink-blue-red and cyan-blue-red sticks respectively. **(E)** The active site of *Tb*PRMT7 (PDB: 4M38) as a representative. The SAH molecule and arginine substrate are indicated. The double E loop (E172 and E181) and THW loop (Q329) residues interact with the arginine substrate side chain. Dashed lines indicate hydrogen bonds. The combination of hydrogen bonds and electrostatic interactions from E172 and E181 with the arginine guanidino group result in strong salt bridges. Q329 forms a hydrogen bond to the guanidino group via its side chain amide oxygen.

*Tb*PRMT1^{PRO} contributes to substrate recognition (Hashimoto et al., 2020).

Unlike mammalian counterparts, *Tb*PRMT1^{ENZ} and *Tb*PRMT1^{PRO} interact via a hydrophobic interface to form a ring-like heterodimeric structure (**Figure 2B**), similar to homodimeric PRMTs. Two *Tb*PRMT1^{ENZ}–*Tb*PRMT1^{PRO} heterodimers together form the functional heterotetramer (Hashimoto et al., 2020). Curiously, *Tb*PRMT1^{PRO} can homodimerize in solution, albeit minimally (Kafková et al., 2017), whereas *Tb*PRMT1^{ENZ} is challenged to form homodimers (Hashimoto et al., 2020), supporting structural dependence on *Tb*PRMT1^{PRO}.

It is possible that *Tb*PRMT1^{PRO} (alone or as a homodimer) performs moonlighting functions in the cell, as *Tb*PRMT1^{PRO} transcripts were slightly increased upon DNA damage induction, while *Tb*PRMT1^{ENZ} transcripts were reduced. *Tb*PRMT1^{PRO} has also been shown to bind mRNA both *in vitro* and *in vivo* independent of tetramer formation (Lueong et al., 2016; Stortz et al., 2017; Kafková et al., 2018). The biological relevance of proposed moonlighting properties remains unclear.

Trypanosoma brucei Protein Arginine Methyltransferase 5

*Tb*PRMT5 is the only type II PRMT expressed by the parasite, yet the least studied *T. brucei* PRMT and the only one whose structure remains unsolved. *Tb*PRMT5 is by far the largest *T. brucei* PRMT due to a very long N-terminal region, the biological relevance of which is unknown (**Figure 2A**). *In vitro*, recombinant *Tb*PRMT5 displays a broad substrate specificity that includes RBP16 (Pasternack et al., 2007). Whether *Tb*PRMT5 methylates RBP16 *in vivo* is unknown, but if so, *Tb*PRMT5 may be responsible for constitutive methylation of RBP16^{Arg93}. Moreover, the fact that recombinant *Tb*PRMT5 is active suggests that, unlike mammalian PRMT5, it does not require a co-factor to function. Further to this, no homologues of mammalian PRMT5 methylosome components were identified in *Tb*PRMT5 immunoprecipitation experiments (Pasternack et al., 2007).

Under native conditions, *Tb*PRMT5 is found in different protein complexes, with sizes ranging between 150 and 700 kDa (Pasternack et al., 2007). Strikingly, *Tb*PRMT5 interacts with Kinetoplastid-specific proteins, suggesting importance in Kinetoplastid-specific pathways (Pasternack et al., 2007). Further studies are necessary to verify *Tb*PRMT5 substrates and determine consequences of PRMT5-dependent methylation. In addition, sequence data indicates that the currently uncharacterized *Leishmania* PRMT5 is much larger (>1,000 amino acids) than its orthologues in humans and *T. brucei* (637 and 784 amino acids, respectively) due to a much longer N-terminus that contains no known conserved functional domains. Elucidating the 3D structure of at least one trypanosomatid PRMT5 will lend insight into potential functional roles of this N-terminus.

Trypanosoma brucei Protein Arginine Methyltransferase 6

*Tb*PRMT6 is a type I PRMT that displays a narrow substrate specificity. Accordingly, *Tb*PRMT6 knockdown does not visibly alter the cellular arginine methylation profile (Lott et al., 2014). Results suggest that protein targets of *Tb*PRMT6 methylation are important for *T. brucei* cellular replication, given *Tb*PRMT6-KD caused a mild growth defect *in vitro* and led to the appearance of aberrant cells (Fisk et al., 2010).

*Tb*PRMT6 is expressed by both *T. brucei* procyclic and bloodstream forms at equal levels and, despite being primarily cytoplasmic, it interacts with several histones. *Tb*PRMT6 also co-purifies with proteins involved in nucleocytoplasmic transport and RNA processing, indicating it might be important in controlling nucleic acid metabolism and transport (Fisk et al., 2010). Disruption of these processes is known to cause growth defects *in vitro* and *Tb*PRMT6 transcription is reduced in cells exposed to DNA damage (Stortz et al., 2017).

*Tb*PRMT6 contains the four canonical PRMT domains (**Figures 2A,C**), and holds unique sequence and structural features that appear conserved across the Kinetoplastids. Secondary structure analysis of type I PRMTs indicates that *Tb*PRMT6 contains four insert regions and a truncated C-terminus. The insertions seem to extend or introduce additional α-helices (Wang et al., 2014b), indicating potential relevance to methyltransferase activity and/or regulation, as well as substrate selection. The exact role of these peculiarities is still to be determined.

Importantly, the 3D structure of apo-*Tb*PRMT6 complexed with S-adenosylhomocysteine (SAH) revealed that substrate binding remodels the active site to allow correct positioning of the target arginine residue. These conformational changes involve residues that are conserved in type I PRMTs, including His318 in the THW loop and Glu142 in the Double E loop, suggesting this feature may be conserved among type I enzymes (Wang et al., 2014b).

Trypanosoma brucei Protein Arginine Methyltransferase 7

Kinetoplastids are the only unicellular eukaryotes known to express a PRMT7 homolog. Whereas the mammalian PRMT7 polypeptide contains two copies of the core PRMT fold, which interact with each other to form an intramolecular- or pseudo-dimer (Cura et al., 2014), *Tb*PRMT7 contains only a single active site and is almost half the size of human PRMT7, although much more active (Fisk et al., 2009). *Tb*PRMT7 is a cytoplasmic enzyme expressed by both long-slender bloodstream and procyclic form *Trypanosoma brucei*, and at least in the latter, it forms different macromolecule complexes (Fisk et al., 2009, Fisk et al., 2010). The composition of these complexes is still unknown, but it likely contains RNA, as *Tb*PRMT7 can bind RNA *in vitro* and *in vivo* (Lueong et al., 2016; Kafková et al., 2018).

Curiously, knockdown of *Tb*PRMT7 only minimally affects the MMA profile, which might be due to an increase in the monomethylation activity of other PRMTs (Lott et al., 2014). Simultaneous knockdown of *Tb*PRMT7 and *Tb*PRMT1 reduced both MMA and aDMA levels in the cells, whereas the knockdown of *Tb*PRMT1 alone caused an accumulation of MMA. All evidence suggests that *Tb*PRMT7 generates monomethylated substrates for other PRMTs and that *Tb*PRMT1 activity can compensate for reduction of *Tb*PRMT7 activity (Lott et al., 2014). Accordingly, recombinant *Tb*PRMT7 displays broad substrate specificity *in vitro*, which includes proteins known to be methylated by *Tb*PRMT1 and *Tb*PRMT5, such as RBP16 and *Tb*RGG1 (Fisk et al., 2009). It is therefore possible that *Tb*PRMT7 is also involved in RBP16^{Arg93} constitutive methylation.

The *Tb*PRMT7 3D structure showed the expected four canonical domains of PRMTs (**Figures 2A,D**). Similar to the other Kinetoplastid PRMTs, homodimerization is facilitated by hydrophobic interactions between a dimerization arm and the SAM-binding domain of the other subunit (Wang et al., 2014a). Extensive mutations on the dimerization arm abolished dimerization, leaving only residual methyltransferase activity (Debler et al., 2016).

Each *Tb*PRMT7 monomer can bind SAM and arginine substrate molecules (Wang et al., 2014a; Debler et al., 2016), though the arginine substrate binding pocket appears to be significantly narrower than those of type I and II PRMTs,

consistent with its 'monomethylation only' profile. In fact, conserved residues present in the double E and THW loops restrict *Tb*PRMT7 to monomethylation. An E181D mutant was able to catalyze aDMA (Debler et al., 2016), while an E181D/Q329A double mutant generated sDMA (Jain et al., 2016). Simulation studies also indicate that E172 and Q329 are crucial for proper substrate orientation and facilitating the reaction mechanism (Thakur et al., 2019). Furthermore, a F71I mutant was able to form dimethylated products (Jain et al., 2016; Cáceres et al., 2018). These data showed the importance of the double E loop with each of E172 and E181 forming two hydrogen bonds to the guanidino group of the substrate arginine (Wang et al., 2014a) (**Figure 2E**).

PROTEIN ARGININE METHYLTRANSFERASE 7 IN *LEISHMANIA*

Although arginine methylation in *Leishmania* was observed prior to identification in *T. brucei* (Paolantonacci et al., 1986), the PRMT studies in *Leishmania* are much more limited, primarily focused on *Leishmania major* PRMT7. Notably, different from *Trypanosoma* PRMT3, *Leishmania* PRMT3 displays an intact double E loop (although with mutated THW loop), and might be enzymatically active, a matter for further investigation.

In contrast to *T. brucei* findings, *Lmj*PRMT7-knockout clearly changed the MMA profile in cells, although arginine monomethylation was not abolished (Ferreira et al., 2014). Interestingly, MMA seems less pronounced in the stationary culture phase (containing metacyclic promastigotes), which correlates with the absence of PRMT7 expression. Furthermore, unlike mammalian PRMT7, *Lmj*PRMT7 is a cytoplasmic-specific enzyme. The observation that mitochondrial *Lmj*RBP16 became hypomethylated upon *Lmj*PRMT7-knockout suggests that some substrates are modified before sorting to organelles (Ferreira et al., 2014; Ferreira et al., 2020). Importantly, cytoplasmic *Lmj*RBP16 displays a shorter half-life in the absence of *Lmj*PRMT7, indicating the importance of methylation for its stability (Ferreira et al., 2020).

247 *L. major* proteins were found bearing MMA, of which 40 became hypomethylated and 17 became hypermethylated upon *Lmj*PRMT7 deletion (Ferreira et al., 2020). This suggests that at least 40 proteins are *Lmj*PRMT7 substrates and at least 17 display alternative methylation upon *Lmj*PRMT7 depletion. *Lmj*PRMT7-mediated MMA was enriched in RG/RGG motifs and "Nucleic acid binding" and "RNA binding" were the most enriched functions annotated for the hypomethylated proteins. Fifteen out of the 40 hypomethylated proteins in *Lmj*PRMT7-knockout cells and 75 out of the 247 MMA-carrying proteins were orthologues of *L. mexicana* candidate RBPs (de Pablos et al., 2019; Ferreira et al., 2020).

Although MMA often occur at variable proximity to the RNA-binding domains, it can influence both RBP activity and RNA fate. Absence of *Lmj*PRMT7 reduces *Lmj*Alba3:*δ-amastin* mRNA binding, which caused a ~4-fold decrease in the half-life of *δ-amastin* transcripts (Ferreira et al., 2020) (**Figure 1C**). Despite only minor changes in the global transcriptome of *Lmj*PRMT7-KO parasites, this mutation had a clear biological impact as *Lmj*PRMT7-KO cells are more virulent *in vitro* and *in vivo* than wildtype *L. major* (Ferreira et al., 2014; Diniz et al., 2021). Concordantly, the virulent *L. major* LV39 strain expressed lower levels of *Lmj*PRMT7 than the avirulent CC1 strain (Ferreira et al., 2014) and knockout of *Lmj*PRMT7 in the CC1 strain recovered its virulence (Diniz et al., 2021). Curiously, gain of virulence upon *Lmj*PRMT7 deletion was not linked to an increase in parasite burden, but to increased recruitment of neutrophils to the site of infection (Diniz et al., 2021). Further studies will investigate the biological process underlying this altered immune response.

CONCLUDING REMARKS

Our knowledge on trypanosomatid RBPs is still very limited (Clayton, 2013). Although recent high-throughput analyses have expanded the list of actual and potential RBPs in these organisms (Erben et al., 2014; Lueong et al., 2016; de Pablos et al., 2019), many questions remain, particularly concerning how the protein: RNA binding processes are coordinated throughout their lifecycles (de Pablos et al., 2016). In this scenario, the function of PRMTs in regulating post-transcriptional gene expression is of great importance. It has been shown that Kinetoplastid PRMTs interact with proteins from distinct cellular compartments and that their function can impact different biological events, from *in vitro* growth to animal infection. Interference with these processes has been demonstrated to impact parasite fitness. In addition, RBPs enriched in RG/RGG motifs are associated with biomolecular phase separation (Chong et al., 2018). The modification of RG motifs by PRMTs is a mechanism that cells use to regulate formation and dissolution of biomolecular condensates, a phenomenon that has not been widely explored in Kinetoplastids and deserves more attention. Moreover, investigating which other PTMs exist in close proximity to methylated arginine residues and how these functionally interact is of great interest.

The complex functions of Kinetoplastid PRMTs promote their potential as candidate targets for drug or chemical probe development. Although much structural, biochemical, biophysical and inhibition data are still missing for the Kinetoplastid proteins, the structural features known to be specific to Trypanosomatid PRMTs combined with the large inhibitor arsenal targeting human PRMTs may enable the repurposing of drugs and the development of novel anti-parasite strategies. Thus, improving our understanding of the molecular and biological processes that coordinate and are coordinated by PRMT activities in Kinetoplastids is of great relevance for the treatment of diseases caused by these parasites.

AUTHOR CONTRIBUTIONS

GC, EN, MP, AC, and PW wrote, reviewed and edited the manuscript. All authors agreed with the submitted version.

FUNDING

GDC receives a post-doctoral fellowship from the São Paulo Research Foundation (FAPESP 2020/02372-6). EN receives a PhD studentship from the White Rose BBSRC DTP (BB/M011151/1). Collaborative work in AKC, MJP and PBW laboratories is supported by the Newton Fund and Medical Research Council (MR/M02640X/1, MR/N017633/1), São Paulo Research Foundation (MRC/FAPESP 2015/13618-8, 2018/14398-0) and MRC Global Challenges Research Fund (GCRF) through the NTD Network (MR/P027989/1).

ACKNOWLEDGMENTS

We would like to thank all colleagues whose work was discussed here and apologize to those whose work could not be cited.

REFERENCES

Adl, S. M., Bass, D., Lane, C. E., Lukeš, J., Schoch, C. L., Smirnov, A., et al. (2019). Revisions to the Classification, Nomenclature, and Diversity of Eukaryotes. *J. Eukaryot. Microbiol.* 66, 4–119.doi:10.1111/jeu.12691

Bedford, M. T. (2007). Arginine Methylation at a Glance. *J. Cel Sci.* 120, 4243–4246. doi:10.1242/jcs.019885

Cáceres, T. B., Thakur, A., Price, O. M., Ippolito, N., Li, J., Qu, J., et al. (2018). Phe71 in Type III Trypanosomal Protein Arginine Methyltransferase 7 (TbPRMT7) Restricts the Enzyme to Monomethylation. *Biochemistry* 57, 1349–1359. doi:10.1021/acs.biochem.7b01265

Chong, P. A., Vernon, R. M., and Forman-Kay, J. D. (2018). RGG/RG Motif Regions in RNA Binding and Phase Separation. *J. Mol. Biol.* 430, 4650–4665. doi:10.1016/j.jmb.2018.06.014

Clayton, C. (2016). Gene Expression in Kinetoplastids. *Curr. Opin. Microbiol.* 32, 46–51. doi:10.1016/j.mib.2016.04.018

Clayton, C. (2013). The Regulation of Trypanosome Gene Expression by RNA-Binding Proteins. *PLOS Pathog.* 9, e1003680. Available at doi:10.1371/journal.ppat.1003680

Cura, V., Troffer-Charlier, N., Wurtz, J.-M., Bonnefond, L., and Cavarelli, J. (2014). Structural Insight into Arginine Methylation by the Mouse Protein Arginine Methyltransferase 7: a Zinc finger Freezes the Mimic of the Dimeric State into a Single Active Site. *Acta Cryst. D Biol. Crystallogr.* 70, 2401–2412. doi:10.1107/S1399004714014278

Damasceno, J. D., Marques, C. A., Black, J., Briggs, E., and McCulloch, R. (2021). Read, Write, Adapt: Challenges and Opportunities during Kinetoplastid Genome Replication. *Trends Genet.* 37, 21–34. doi:10.1016/j.tig.2020.09.002

de Pablos, L., Ferreira, T., and Walrad, P. (2016). Developmental Differentiation in Leishmania Lifecycle Progression: post-transcriptional Control Conducts the Orchestra. *Curr. Opin. Microbiol.* 34, 82–89. doi:10.1016/j.mib.2016.08.004

de Pablos, L. M., Ferreira, T. R., Dowle, A. A., Forrester, S., Parry, E., Newling, K., et al. (2019). The mRNA-Bound Proteome of Leishmania Mexicana: Novel Genetic Insight into an Ancient Parasite. *Mol. Cell Proteomics* 18, 1271–1284. doi:10.1074/mcp.RA118.001307

Debler, E. W., Jain, K., Warmack, R. A., Feng, Y., Clarke, S. G., Blobel, G., et al. (2016). A Glutamate/aspartate Switch Controls Product Specificity in a Protein Arginine Methyltransferase. *Proc. Natl. Acad. Sci. USA* 113, 2068–2073. doi:10.1073/pnas.1525783113

Diniz, J. A., Chaves, M. M., Vaselek, S., Miserani Magalhães, R. D., Ricci-Azevedo, R., de Carvalho, R. V. H., et al. (2021). Protein Methyltransferase 7 Deficiency in Leishmania Major Increases Neutrophil Associated Pathology in Murine Model. *Plos Negl. Trop. Dis.* 15, e0009230. Available at: doi:10.1371/journal.pntd.0009230

Erben, E. D., Fadda, A., Lueong, S., Hoheisel, J. D., and Clayton, C. (2014). A Genome-wide Tethering Screen Reveals Novel Potential Post-Transcriptional Regulators in Trypanosoma Brucei. *PLOS Pathog.* 10, e1004178. Available at: doi:10.1371/journal.ppat.100417810.1371/journal.ppat.1004178

Ferreira, T. R., Alves-Ferreira, E. V. C., Defina, T. P. A., Walrad, P., Papadopoulou, B., and Cruz, A. K. (2014). Altered Expression of an RBP -associated Arginine Methyltransferase 7 in L Eishmania Major Affects Parasite Infection. *Mol. Microbiol.* 94, 1085–1102. doi:10.1111/mmi.12819

Ferreira, T. R., Dowle, A. A., Parry, E., Alves-Ferreira, E. V. C., Hogg, K., Kolokousi, F., et al. (2020). PRMT7 Regulates RNA-Binding Capacity and Protein Stability in Leishmania Parasites. *Nucleic Acids Res.* 48, 5511–5526. doi:10.1093/nar/gkaa211

Fisk, J. C., and Read, L. K. (2011). Protein Arginine Methylation in Parasitic Protozoa. *Eukaryot. Cel* 10, 1013–1022. doi:10.1128/EC.05103-11

Fisk, J. C., Sayegh, J., Zurita-Lopez, C., Menon, S., Presnyak, V., Clarke, S. G., et al. (2009). A Type III Protein Arginine Methyltransferase from the Protozoan Parasite Trypanosoma Brucei. *J. Biol. Chem.* 284, 11590–11600. doi:10.1074/jbc.M807279200

Fisk, J. C., Zurita-Lopez, C., Sayegh, J., Tomasello, D. L., Clarke, S. G., and Read, L. K. (2010). TbPRMT6 Is a Type I Protein Arginine Methyltransferase that Contributes to Cytokinesis in Trypanosoma Brucei. *Eukaryot. Cel* 9, 866–877. doi:10.1128/EC.00018-10

Goulah, C. C., Pelletier, M., and Read, L. K. (2006). Arginine Methylation Regulates Mitochondrial Gene Expression in Trypanosoma Brucei through Multiple Effector Proteins. *RNA* 12, 1545–1555. doi:10.1261/rna.90106

Goulah, C. C., and Read, L. K. (2007). Differential Effects of Arginine Methylation on RBP16 mRNA Binding, Guide RNA (gRNA) Binding, and gRNA-Containing Ribonucleoprotein Complex (gRNP) Formation. *J. Biol. Chem.* 282, 7181–7190. doi:10.1074/jbc.M609485200

Hashimoto, H., Kafková, L., Raczkowski, A., Jordan, K. D., Read, L. K., and Debler, E. W. (2020). Structural Basis of Protein Arginine Methyltransferase Activation by a Catalytically Dead Homolog (Prozyme). *J. Mol. Biol.* 432, 410–426. doi:10.1016/j.jmb.2019.11.002

Hayman, M. L., and Read, L. K. (1999). Trypanosoma Brucei RBP16 Is a Mitochondrial Y-Box Family Protein with Guide RNA Binding Activity. *J. Biol. Chem.* 274, 12067–12074. doi:10.1074/jbc.274.17.12067

Jain, K., Warmack, R. A., Debler, E. W., Hadjikyriacou, A., Stavropoulos, P., and Clarke, S. G. (2016). Protein Arginine Methyltransferase Product Specificity Is Mediated by Distinct Active-Site Architectures. *J. Biol. Chem.* 291, 18299–18308. doi:10.1074/jbc.M116.740399

Kafková, L., Debler, E. W., Fisk, J. C., Jain, K., Clarke, S. G., and Read, L. K. (2017). The Major Protein Arginine Methyltransferase in Trypanosoma Brucei Functions as an Enzyme-Prozyme Complex. *J. Biol. Chem.* 292, 2089–2100. doi:10.1074/jbc.M116.757112

Kafková, L., Tu, C., Pazzo, K. L., Smith, K. P., Debler, E. W., Paul, K. S., et al. (2018). Trypanosoma Brucei PRMT1 Is a Nucleic Acid Binding Protein with a Role in Energy Metabolism and the Starvation Stress Response. *MBio* 9, e02430–18. doi:10.1128/mBio.02430-18

Kolev, N. G., Ullu, E., and Tschudi, C. (2014). The Emerging Role of RNA-Binding Proteins in the Life Cycle ofTrypanosoma Brucei. *Cell. Microbiol.* 16, 482–489. doi:10.1111/cmi.12268

Lott, K., Li, J., Fisk, J. C., Wang, H., Aletta, J. M., Qu, J., et al. (2013). Global Proteomic Analysis in Trypanosomes Reveals Unique Proteins and Conserved Cellular Processes Impacted by Arginine Methylation. *J. Proteomics* 91, 210–225. doi:10.1016/j.jprot.2013.07.010

Lott, K., Mukhopadhyay, S., Li, J., Wang, J., Yao, J., Sun, Y., et al. (2015). Arginine Methylation of DRBD18 Differentially Impacts its Opposing Effects on the Trypanosome Transcriptome. *Nucleic Acids Res.* 43, 5501–5523. doi:10.1093/nar/gkv428

Lott, K., Zhu, L., Fisk, J. C., Tomasello, D. L., and Read, L. K. (2014). Functional Interplay between Protein Arginine Methyltransferases in Trypanosoma Brucei. *Microbiologyopen* 3, 595–609. doi:10.1002/mbo3.191

Lueong, S., Merce, C., Fischer, B., Hoheisel, J. D., and Erben, E. D. (2016). Gene Expression Regulatory Networks inTrypanosoma Brucei: Insights into the Role of the mRNA-Binding Proteome. *Mol. Microbiol.* 100, 457–471. doi:10.1111/mmi.13328

Miller, M. M., and Read, L. K. (2003). Trypanosoma Brucei: Functions of RBP16 Cold Shock and RGG Domains in Macromolecular Interactions. *Exp. Parasitol.* 105, 140–148. doi:10.1016/j.exppara.2003.12.002

Paolantonacci, P., Lawrence, F., Lederer, F., and Robert-Gero, M. (1986). Protein Methylation and Protein Methylases in Leishmania Donovani and Leishmania Tropica Promastigotes. *Mol. Biochem. Parasitol.* 21, 47–54. doi:10.1016/0166-6851(86)90078-2

Pasternack, D. A., Sayegh, J., Clarke, S., and Read, L. K. (2007). Evolutionarily Divergent Type II Protein Arginine Methyltransferase in Trypanosoma Brucei. *Eukaryot. Cel* 6, 1665–1681. doi:10.1128/EC.00133-07

Pelletier, M., Miller, M. M., and Read, L. K. (2000). RNA-binding Properties of the Mitochondrial Y-Box Protein RBP16. *Nucleic Acids Res.* 28, 1266–1275. doi:10.1093/nar/28.5.1266

Pelletier, M., Pasternack, D. A., and Read, L. K. (2005). *In Vitro* and *In Vivo* Analysis of the Major Type I Protein Arginine Methyltransferase from Trypanosoma Brucei. *Mol. Biochem. Parasitol.* 144, 206–217. doi:10.1016/j.molbiopara.2005.08.015

Pelletier, M., and Read, L. K. (2003). RBP16 Is a Multifunctional Gene Regulatory Protein Involved in Editing and Stabilization of Specific Mitochondrial mRNAS in Trypanosoma Brucei. *RNA* 9, 457–468. doi:10.1261/rna.2160803

Pelletier, M., Xu, Y., Wang, X., Zahariev, S., Pongor, S., Aletta, J. M., et al. (2001). Arginine Methylation of a Mitochondrial Guide RNA Binding Protein from Trypanosoma Brucei. *Mol. Biochem. Parasitol.* 118, 49–59. doi:10.1016/S0166-6851(01)00367-X

Stortz, J. A., Serafim, T. D., Alsford, S., Wilkes, J., Fernandez-Cortes, F., Hamilton, G., et al. (2017). Genome-wide and Protein Kinase-Focused RNAi Screens Reveal Conserved and Novel Damage Response Pathways in Trypanosoma Brucei. *Plos Pathog.* 13, e1006477. doi:10.1371/journal.ppat.1006477

Tak, I.-u. -R., Ali, F., Dar, J. S., Magray, A. R., Ganai, B. A., and Chishti, M. Z. (2019). "Posttranslational Modifications of Proteins and Their Role in Biological Processes and Associated Diseases," in *Protein Modificomics - from Modicications To Clinic Perspectives*. Editors T. A. Dar, and L. R. B. T.-P. M. Singh (London: Academic Press), 1–35. doi:10.1016/B978-0-12-811913-6.00001-1

Tewary, S. K., Zheng, Y. G., and Ho, M.-C. (2019). Protein Arginine Methyltransferases: Insights into the Enzyme Structure and Mechanism at the Atomic Level. *Cell. Mol. Life Sci.* 76, 2917–2932. doi:10.1007/s00018-019-03145-x

Thakur, A., Hevel, J. M., and Acevedo, O. (2019). Examining Product Specificity in Protein Arginine Methyltransferase 7 (PRMT7) Using Quantum and Molecular Mechanical Simulations. *J. Chem. Inf. Model.* 59, 2913–2923. doi:10.1021/acs.jcim.9b00137

Wang, C., Zhu, Y., Caceres, T. B., Liu, L., Peng, J., Wang, J., et al. (2014a). Structural Determinants for the Strict Monomethylation Activity by Trypanosoma Brucei Protein Arginine Methyltransferase 7. *Structure* 22, 756–768. doi:10.1016/j.str.2014.03.003

Wang, C., Zhu, Y., Chen, J., Li, X., Peng, J., Chen, J., et al. (2014b). Crystal Structure of Arginine Methyltransferase 6 from Trypanosoma Brucei. *PLoS One* 9, e87267. Available at:. doi:10.1371/journal.pone.0087267

Yarlett, N., Quamina, A., and Bacchi, C. J. (1991). Protein Methylases in Trypanosoma Brucei Brucei: Activities and Response to Dl--difluoromethylornithine. *J. Gen. Microbiol.* 137, 717–724. doi:10.1099/00221287-137-3-717

Conflict of Interest: The authors declare that the research was conducted in the absence of any commercial or financial relationships that could be construed as a potential conflict of interest.

frontiers in Molecular Biosciences

REVIEW
published: 05 July 2021
doi: 10.3389/fmolb.2021.693325

Post-Translational Modifications Modulate Proteinopathies of TDP-43, FUS and hnRNP-A/B in Amyotrophic Lateral Sclerosis

Stefania Farina[1,2†], *Francesca Esposito*[1,3], *Martina Battistoni*[3], *Giuseppe Biamonti*[1*] and *Sofia Francia*[1*]

[1]Istituto di Genetica Molecolare "Luigi Luca Cavalli-Sforza" - Consiglio Nazionale delle Ricerce (CNR), Pavia, Italy, [2]University School for Advanced Studies IUSS, Pavia, Italy, [3]Università Degli Studi di Pavia, Pavia, Italy

OPEN ACCESS

Edited by:
Roberto Giambruno,
Italian Institute of Technology (IIT), Italy

Reviewed by:
Wayne Carter,
University of Nottingham,
United Kingdom
Jozsef Gal,
University of Kentucky, United States

***Correspondence:**
Giuseppe Biamonti
giuseppe.biamonti@igm.cnr.it
Sofia Francia
sofia.francia@igm.cnr.it

†Present address:
Stefania Farina, Department of Molecular Genetics, Erasmus University Medical Center, Rotterdam, Netherlands

Specialty section:
This article was submitted to Protein and RNA Networks, a section of the journal Frontiers in Molecular Biosciences

Received: 10 April 2021
Accepted: 07 June 2021
Published: 05 July 2021

Citation:
Farina S, Esposito F, Battistoni M, Biamonti G and Francia S (2021) Post-Translational Modifications Modulate Proteinopathies of TDP-43, FUS and hnRNP-A/B in Amyotrophic Lateral Sclerosis. Front. Mol. Biosci. 8:693325. doi: 10.3389/fmolb.2021.693325

It has been shown that protein low-sequence complexity domains (LCDs) induce liquid-liquid phase separation (LLPS), which is responsible for the formation of membrane-less organelles including P-granules, stress granules and Cajal bodies. Proteins harbouring LCDs are widely represented among RNA binding proteins often mutated in ALS. Indeed, LCDs predispose proteins to a prion-like behaviour due to their tendency to form amyloid-like structures typical of proteinopathies. Protein post-translational modifications (PTMs) can influence phase transition through two main events: i) destabilizing or augmenting multivalent interactions between phase-separating macromolecules; ii) recruiting or excluding other proteins and/or nucleic acids into/from the condensate. In this manuscript we summarize the existing evidence describing how PTM can modulate LLPS thus favouring or counteracting proteinopathies at the base of neurodegeneration in ALS.

Keywords: post-translational modifications, RNA binding proteins, low-complexity domain, protein aggregations, amyotrophic lateral sclerosis

INTRODUCTION

In healthy organisms, proteins are properly folded into secondary and tertiary structures suited to their biological functions. However, mutations, cellular stress and aging can perturb protein structure leading to the formation of insoluble protein aggregates. Although it is now well established that protein aggregation is a common hallmark of several neurodegenerative diseases including Amyotrophic Lateral Sclerosis (ALS), Frontotemporal Dementia (FTD) and Alzheimer's disease (AD), the pathological mechanisms that drive their formation are still uncertain (Aguzzi and O'Connor, 2010). Indeed, neurodegenerative disorders are widely defined as proteinopathies, which refers to the fact that these diseases are characterized by the accumulation of protein aggregates in the brain and/or spinal cord of patients (Forman et al., 2004; Ross and Poirier, 2004; Chiti and Dobson, 2006).

Protein aggregation is believed to originate from the alteration of the physiological propensity of some proteins to undergo liquid-liquid phase separation (LLPS), i.e., a transient and normally reversible phase transition that separates two liquid compartments with different viscosity and composition (Posey et al., 2018). LLPS generates cellular condensates, organelles with a biological function but not delimited by a lipid membrane. In the last decade a number of physiological cellular condensates have been characterized, some of which have been purified and their components and

modifications identified by mass spectrometry. Examples are nucleoli, speckles and paraspeckles, nuclear stress bodies, P-granules, stress granules (SGs) and Cajal bodies (Toretsky and Wright, 2014).

A common feature of proteins with the propensity to undergo LLPS is the presence of low complexity domains (LCDs), which exhibit a high level of conformational heterogeneity. The structural plasticity of LCDs makes them ideal for responding to chemical and physical changes, thus providing the potential of rapid tuning of localized molecular functions (van der Lee et al., 2014). Human proteins holding LCDs have features in common with prion proteins, such as the ability to induce mis-folding in interacting peptides, thus propagating proteinopathies within the cells (Alberti et al., 2009) and in the surrounding tissues, eventually affecting big areas of the nervous system (Jucker and Walker, 2013). Typically, LCDs are enriched in charged amino acids, including serine (Ser), glutamine (Gln), glutamic acid (Glu), lysine (Lys) and arginine (Arg) (Romero et al., 2001), which form Arg-Gly-Gly/Arg-Gly (RGG/RG) motifs in a large number of proteins, mostly RNA binding proteins (RBPs) (Thandapani et al., 2013). Moreover, the sequences that drive the formation of condensates often contain regularly interspersed aromatic residues, specifically tyrosine (Tyr) and phenylalanine (Phe) that mediate π-interactions. Depending on the amino acid composition of the LCDs, charge-charge, charge-π hydrogen bonding and π-π stacking interactions can be established between two residues. In the first case, the interaction is between two residues with opposite charges. In the second situation, one positive charge interacts with a negative charge distributed above an aromatic group. In the third case, two aromatic groups are positioned above each other in a stacked conformation (Brangwynne et al., 2015).

RBPs represent a large group of proteins undergoing LLPS, and phase transition is modulated by their secondary structure and by the concentration of RNA (Langdon and Gladfelter, 2018; Roden and Gladfelter, 2021). Indeed, several cellular condensates include an RNA moiety with a structural role. The RNA (which can also coalesce into droplets) provides a multivalent binding site for the interaction with different RBPs, thus promoting further contacts between their LCDs. Different regulatory circuits take advantage of the inherent property of LCDs to induce separate cellular sub-compartments and to tightly modulate phase transition upon specific stimuli and activation of signaling cascades. LCDs, in fact, are preferred targets of post-translational modifications (PTMs) (Dosztányi et al., 2006; Xie et al., 2007; Wright and Dyson, 2009) that can promote or inhibit protein-protein and protein-RNA interactions, thus modulating possible changes in protein compartmentalization and sequestrations.

Here we review different PTMs that finely regulate the biophysical properties of RiboNucleoProtein A and B type (hnRNP-A/B type meaning hnRNP-A1 and hnRNP-A2), Trans-activating response (TAR) element DNA-binding protein of 43 kDa (TDP-43) and Fused in Sarcoma (FUS) in the attempt to in an attempt to shed light on common paradigms that can modulate the pathological phase transition in the context of neurodegeneration. Similarly to other protein functions, PTMs can alter phase transition and protein aggregation in different ways by both stimulating and counteracting it, depending on their charge, the amino acid residue that is modified and its position in the target proteins (Owen and Shewmaker, 2019). A lot still needs to be understood regarding how PTMs can cause or prevent pathological aggregation and proteinopathies. This review aims at summarizing recent studies that describe the impact that specific PTMs have on biophysical properties of three RBPs relevant to ALS: hnRNP-A1 and hnRNP-A2 TDP-43 and FUS.

HNRNP-A1, TDP-43 AND FUS PROTEIN STRUCTURE AND FUNCTION

The hnRNP-A1 protein is the founding member of the A/B group of hnRNPs. These proteins share a common organization consisting of two RNA recognition motifs (RRMs) at the N-terminus followed by a C-terminal LCD that contains RGG/RG repeats (**Figure 1**). The second half of the LCD harbors the nuclear localization signal (NLS) sequence (**Figure 1**) that displays a high affinity for Karyopherin-β2 and controls the distribution of these nucleo-cytoplasmic shuttling proteins. Missense mutations in the LCD are causatively linked to ALS and multisystem proteinopathy (MSP) (Bosco et al., 2010; Hackman et al., 2013; Kim et al., 2013). The LCD is sufficient to drive LLPS of hnRNP-A1. However, the two RRMs contribute to phase separation by binding RNA molecules, whose polymeric structure increases the local protein crowding and lowers the protein concentration required to form LLPS (Molliex et al., 2015).

Biophysical analyses indicate that Arg and aromatic residues (Phe and Tyr), evenly distributed throughout the LCD, play a major role in LLPS by producing a repeated motif that enables multivalent interactions (Molliex et al., 2015). The hnRNP-A1 protein exists in three assembly states: liquid-like droplets, reversible fibrils, and irreversible fibrils. While the first two forms are physiological, the latter assembly is ALS-related and corresponds to a highly ordered stacking of proteins that is very difficult to disassemble. Three segments, each containing Asn-Asp-Asn and (Gly)Phe/Tyr(Gly) motifs separated by Arg/Gly rich stretches, have been mapped within the LCD. Each segment is able to assist the formation of reversible fibrils and hydrogels. Asp residues have a key role in the reversibility of amyloid formation, which explains why the disease-linked mutations of these residues enhance irreversible amyloid aggregation and pathogenesis of ALS (Gui et al., 2019).

TDP-43 and FUS are two RBPs that contain LCDs and undergo phase separation (Conicella et al., 2016; Molliex et al., 2015; Patel et al., 2015; Schmidt and Rohatgi, 2016). TDP-43 has been found in cytosolic aggregates in many neurodegenerative diseases, including ALS, FTD and limbic-predominant age-related TDP-43 encephalopathy (LATE) (de Boer et al., 2020). Similarly to hnRNP-A1, TDP-43 contains two RRMs followed by a C-terminal domain (CTD) that is mostly disordered and enriched in Arg and Gly residues with a regular spacing of

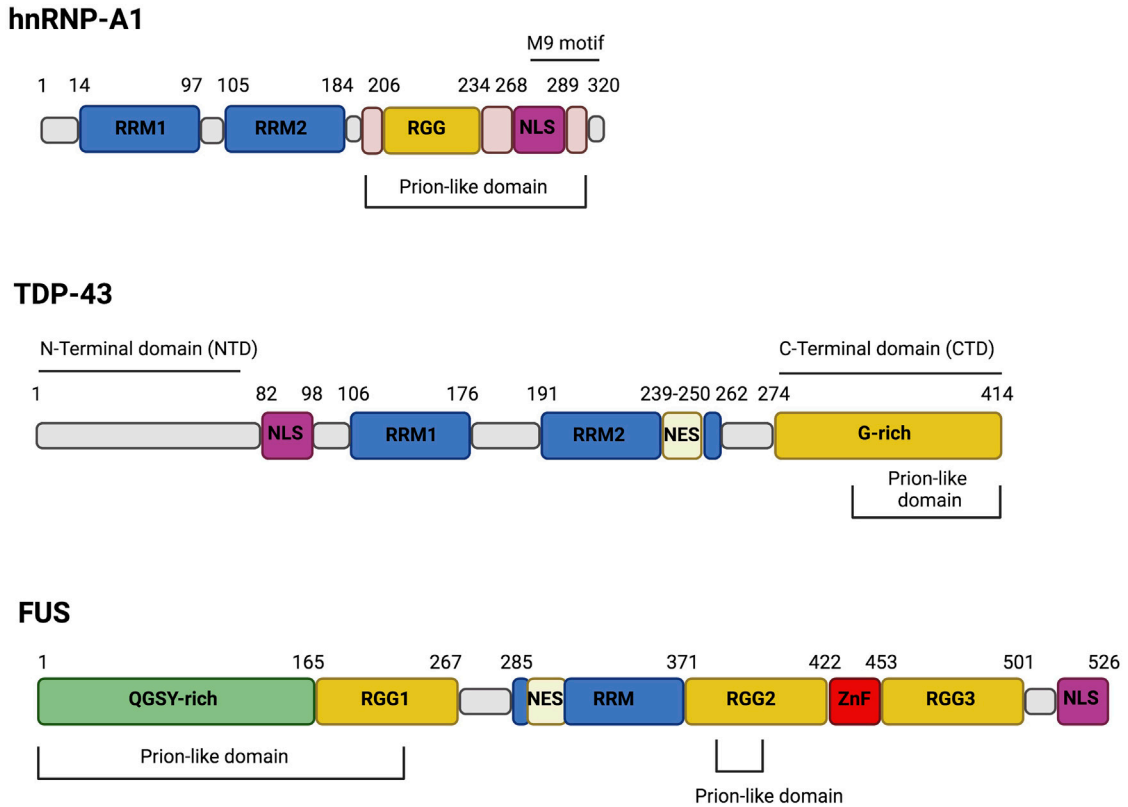

FIGURE 1 | The domain structure of hnRNP-A1, TDP-43 and FUS. The RNA-binding proteins hnRNP-A1, TDP-43 and FUS share structure similarities. Particularly, they harbor Prion-like domain, RNA-recognition motif (RRM) and nuclear localization signal (NLS). hnRNP-A1 and FUS are both characterized by the presence of Arg-Gly-Gly-rich (RGG) domains while TDP-43 has a Gly-rich (G-rich) domain and hnRNP-A1 display a M9 motif. Moreover, both FUS and TDP-43 present nuclear export signal (NES) but only FUS has a zinc-finger (ZnF) domain and a Gln-Gly-Ser-Tyr-rich (QGSY-rich) domain.

hydrophobic residues (Val, Leu, Ile, Met, Phe, Tyr, Trp). However, unlike hnRNP-A1, TDP-43 contains another folded N-terminal domain (NTD) as well (**Figure 1**). The CTD has a central role in determining the functional properties of the protein, since it controls most of its interactions and sub-cellular distribution by regulating the nucleo-cytoplasmic shuttling. Moreover, the CTD has been widely described as the main contributor to LLPS (Conicella et al., 2016; Lim et al., 2016; Schmidt and Rohatgi, 2016). It is, therefore, not surprising that most of ALS-associated mutations in TDP-43 map to this domain. The CTD seems particularly involved in TDP-43 aggregation, especially the glycine-rich region (G-Rich **Figure 1**) that contains three different amyloidogenic cores: residues 286–331, 318–343 and 342–366. The amyloidogenic core 318–343 includes a hydrophobic patch (HP) and a Gln/Asn (QN)-rich motif (Jiang et al., 2013). Deletion of the HP or the QN region reduces the ability of TDP-43 to form aggregates (Jiang et al., 2013). The 318–343 peptide is composed of two α-helices connected by a turn of 4 amino acids (Jiang et al., 2013), forming a helix-turn-helix structure. This structure can generate an antiparallel hairpin-like β-sheet, which can interact with other TDP-43 molecules leading to aggregation. According to Saini and Chauhan, the initial deca-peptide (311–320) of this helix-turn-helix is necessary for TDP-43 aggregation and loss of this region abrogates the formation of inclusions. Furthermore, another deca-peptide (246–255) within RRM2 has been identified as an important region for TDP-43 aggregation, even though its deletion does not completely abolish the formation of TDP-43 filaments (Saini and Chauhan, 2011). Both $Ala^{324}Glu$ and $Met^{337}Glu$ mutants, located in the hydrophobic region, introduce negative charges reducing the ability of TDP-43 to form aggregates (Jiang et al., 2016). The $Gln^{343}Arg$ mutation present in familial ALS (fALS) cases also reduces TDP-43 aggregation by generating a single α-helix that is not stackable into a β-sheet. On the contrary, the $Gly^{335}Asp$ mutation, that has high frequency in Italian ALS patient, causes an increase of amyloidogenic aggregation, due to an extension of the loop in the helix-loop-helix (Jiang et al., 2016). Finally, the mutation $Ala^{315}Thr$ in the CTD has been proposed to increase the ability of TDP-43 to form β-sheet (Guo et al., 2011). The pronounced sensitivity of TDP-43 LLPS to single amino acid substitutions with different properties is consistent with the fact that single PTMs on specific residues can strongly impact on phase transition.

FUS, also known as hnRNP P2, is a member of the FET family together with the EWS protein, the TATA-binding protein

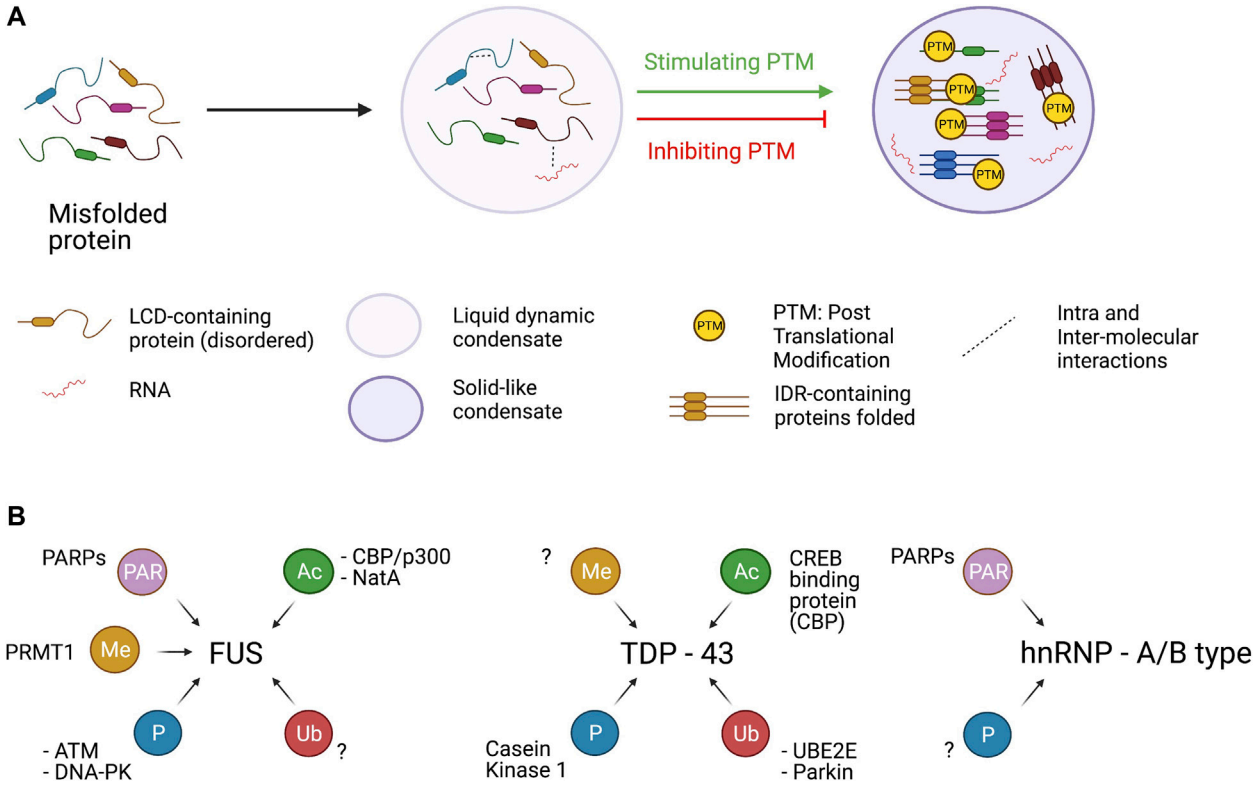

FIGURE 2 | Assembly of condensates and PTMs. **Panel A**. LCD-containing proteins (including TDP-43, FUS and hnRNPA1) under certain conditions assume a misfolded state in which several intra and inter-molecular interaction can be established. Different PTMs tend to stimulate or dampen the formation of insoluble condensate in which LCD-containing proteins are sequestered in a toxic β-sheet structure. However, PTM has protein- and residue-specific impact on protein aggregate formation. **Panel B**. hnRNPA1, FUS and TDP-43 can be target of several PTMs catalyzed by specific enzymes. hnRNP-A1 and FUS can be PARylated by PARPs and PARP1, respectively. FUS protein can be methylated by PRMT1 acetylated by CBP/p300 and NatA. Moreover, the Prion like domain of FUS is phosphorylated at multiple sites by the two kinases ATM and DNA-PK. TDP-43 is actively acetylated by CBP and phosphorylated by Casein Kinase. Finally, UBE2E and Parkin catalyze the ubiquitination of TDP-43.

(TBP)-associated factor (TAFII68/TAF15) and the *Drosophila* cabeza/SARF protein. FUS is a nucleo-cytoplasmic shuttling RBP formed by an N-terminal LCD rich in Gln-Gly-Ser-Tyr (QGSY), an RRM, three RGG repeats, a zinc-finger (ZnF) motif, and C-terminal NLS (Guerrero et al., 2016). Both TDP-43 and FUS are mainly nuclear; nevertheless their insoluble aggregates are cytosolic. The nuclear localization of FUS relies on a non-canonical NLS in the C-terminus of the protein (residues 514–526) that mediates the interaction with the nuclear import receptor transportin (TRN) (Chook and Süel, 2011). FUS mutations in familial ALS/FTD patients are mostly located in the NLS, leading to its cytoplasmic mislocalization and inclusion formation. Cytoplasmic localization, however, although required is not sufficient to promote aggregation. The ability of FUS to undergo LLPS relies on the N-terminal LCDs and PTMs that occurs in the QGSY-rich patch (**Figure 1**) also affects it (Burke et al., 2015; Murakami et al., 2015; Patel et al., 2015; Shorter, 2017). As for other prion-like proteins, the LCD of FUS appears predominantly disordered in reversible condensates (Burke et al., 2015) whereas it is well organized in packed β-sheets when forming irreversible aggregates (Hughes et al., 2018). Specific mutations in the LCD or the NLS of FUS increase the total protein levels, a condition that may enhance the conversion of FUS condensates from liquid to a solid state (Guerrero et al., 2016). The altered subcellular distribution also changes the interactions of FUS with specific RNA subsets, with the cytoplasmic mutants binding more frequently to the 3′ UTRs of target mRNAs instead of nuclear intronic sequences (Hoell et al., 2011).

All these observations support the idea that FUS condensates are in equilibrium between liquid or gel-like states which are both physiological and can alternate each other or even co-exist. When an event perturbs this equilibrium (e.g., familial ALS mutations or reduction in R-methylation state) FUS condensate can shift to a more pathological solid-like state (**Figure 2A**).

Recently, TDP-43 and FUS have been shown to contribute to DNA repair (Rulten et al., 2014; Naumann et al., 2018; Wang H. et al., 2018; Mitra et al., 2019; Singatulina et al., 2019; Levone et al., 2020). FUS is recruited to DNA damage sites in a PARP-1 dependent manner (Rulten et al., 2014) via the interaction with HDAC1 (Wang et al., 2013) and is phosphorylated by ATM and DNA-PK (Monahan et al., 2017; Rhoads et al., 2018a). The recruitment of FUS at sites of DNA lesions correlates with PARP-1 dependent FUS PARylation required

for DNA repair (Singatulina et al., 2019). Moreover, *in vitro* studies have shown that the addition of purified PAR strongly stimulates the formation of FUS-containing droplets essential for the proper activity of FUS in DNA repair mechanism (Patel et al., 2015). TDP-43 can interact with the sensor protein KU70 at sites of DNA damage, suggesting that it plays a role in the non-homologous end joining (NHEJ) mechanism (Freibaum et al., 2010). Furthermore, TDP-43 can interact with other factors of the DNA damage response (DDR), such as DNA-PK and 53BP1 that are being recruited at DNA damage sites during NHEJ (Mitra et al., 2019).

POST-TRANSLATIONAL MODIFICATIONS OF TDP-43, FUS AND HNRNP-A1 CONTROLLING LIQUID-LIQUID PHASE SEPARATION AND PROTEIN AGGREGATION

The role of PTMs in regulating the propensity of LCD-containing proteins to undergo LLPS is an emerging area of study due to its possible therapeutic impact. To date, several PTMs have been described for hnRNP-A1, TDP-43 and FUS but we will discuss mostly the ones that modulate LLPS. These are: protein methylation, phosphorylation, acetylation, ubiquitination and PARylation (Rhoads et al., 2018b; Buratti, 2018).

Arginine Methylation

Several proteins involved in DNA and RNA metabolism, including histones and a large number of RBPs, undergo Arg-methylation, which may occur in different flavors (mono, symmetric and asymmetric di-methylation) (Blanc and Richard, 2017). In mammalian cells, Arg (R)-methylation is catalyzed by at least nine Protein-Arginine-Methyl-Transferases (PRMTs), from 1 to 9 (Bedford and Clarke, 2009; Blanc and Richard, 2017). Of these, at least three (PRMT1, 6 and 8) catalyze asymmetrically di-methylation on arginine (ADMA). PRMT1 catalyses the addition of one or two methyl groups to the R residues from the S-adenosylmethionine donor (Yang and Bedford, 2013). Methylation plays a major role in controlling the biophysical properties of RGG/RG motifs and modulates both protein-protein and RNA-protein interactions. Notably, arginine methylation is very relevant for FET proteins (**Figure 2B**) (Lorton and Shechter, 2019) while not many studies have characterized the impact of arginine methylation in TDP-43 so far, even though some arginine methylated residues had been identified and reported in databases. Indeed, in the phosphosite.org website it is reported that mass spectrometry analyses identified three TDP-43 methylated residues: Arg 42, 275 and 293. The last two modifications are located at the C-terminal domain of TDP-43, thus could in principle influence LLPS, however the functions of these modifications and their regulation have not been investigated yet (**Figure 2B**). Methylation does not alter the net charge of the protein, but changing its distribution can regulate the capacity of Arg to enter cation-π interactions with aromatic residues (Lorton and Shechter, 2019) and hence the ability of FUS to rapidly and reversibly form liquid droplets and hydrogels (**Figure 2A**). In fact, LLPS transition of FUS involves hydrogen bonding between an antiparallel β-sheet in the LCD (residues 39–95) and Arg residues in the three RGG-rich regions (Han et al., 2012; Murakami et al., 2015; Patel et al., 2015; Murray et al., 2017). Under normal conditions these Arg residues are heavily mono- or di-methylated (Rappsilber et al., 2003). In contrast, in FTLD they are hypomethylated and FUS is found in neuronal nuclear and cytoplasmic aggregates that frequently contain other members of the FET family. Several lines of evidence indicate that methylation of specific Arg residues (position 216, 259, 407, 472, 473 and 476) has an inhibitory effect on condensate formation (Qamar et al., 2018). Indeed, inhibition of arginine methyltransferase activities with Adenosine dialdehyde (AdOx) produces a significant reduction in asymmetrical di-methylation of FUS at most of these Arg (216, 259, 407, 473, and 476) and promotes LLPS. In contrast, Arg 394 and 481 remain predominantly di-methylated, indicating that a higher methylation turnover occurs only in the case of Arg residues involved in LLPS, allowing dynamically tuning phase separation. Altogether these data suggest that the number of methylated Arg residues can modulate the type of phase separation (liquid-liquid vs liquid-solid), which is driven by multivalent cation-π interactions. FUS is normally soluble and dimethylated in healthy brains while reduced levels of FUS methylation have been detected in insoluble protein inclusions in brains of FTD patients (Suárez-Calvet et al., 2016).

Paradoxically R-methylation can also promote the formation of aggregates (**Table 1**). Indeed, recent studies demonstrate that R-methylation in the non-canonical NLS domain of FUS influences the subcellular distribution of the protein. This is due to the fact that methylation of Arg residues in the second RGG-rich region of FUS (**Figure 1**) abrogates the interaction of TRN with the third RGG-rich region thus reducing FUS nuclear import and increasing its cytoplasmic concentration, thus favoring LLPS (Dormann et al., 2012). Indeed, cell treatment with methylation inhibitors or PRMT1 knock down can restore the nuclear localization of the ALS-linked FUS mutant protein $Pro^{525}Lys$ (Dormann et al., 2012). Interestingly, immunohistochemical analysis of FUS-$Pro^{525}Lys$ ALS patients revealed the presence of inclusions with methylated FUS that are undetectable in FTD patients (Dormann et al., 2012). Thus, detection and quantification of methylated forms of FUS can be a valuable biomarker of ALS and not of FTD.

Interestingly, methylation events have been shown to affect the nucleo-cytoplasmic trafficking of other RBPs such as hnRNP-A2 (Nichols et al., 2000) and binding of hnRNP-A1 to single-stranded nucleic acid is significantly reduced after arginine methylation (Rajpurohit et al., 1994).

Very little is still known about the mechanisms by which R-methylation can be erased. Recent data suggest the involvement of R-demethylating enzymes such as KDM3A, KDM4E, KDM5C (Walport et al., 2016) and JMJD6 (Chang et al., 2007), all belonging to the large family of 2-oxoglutarate-dependent dioxygenases. Numerous studies indicate that some RGG motifs are protected from methylation, while other motifs are preferentially recognized by the methylating enzymes. The

TABLE 1 | PTMs and their effects on RBP's aggregation.

PTM	RBP	Residue	Effects on Aggregation	References
R-methylation	FUS	Arg 216, Arg 259 Arg 407, Arg 472 Arg 473, Arg 476	↓	Qamar et al. (2018)
Phosphorylation	FUS	Ser 26/Ser 30 Ser 30/Ser42 Thr 109/Ser 115 Ser 115/Ser 117	↓	Deng et al. (2014), Monahan et al. (2017) Rhoads et al. (2018a)
	hnRNP - A2	Tyr (n.d.)	↓	Ryan et al. (2021)
	TDP - 43	Ser 48	↓	Hornbeck et al. (2012), Hornbeck et al. (2015) Rigbolt et al. (2011), Wang A. et al. (2018)
	TDP - 43	Ser 403/404 Ser 409/410	↑	Neumann et al. (2020)
Acetylation	FUS	Lys 510	↑	Arenas et al. (2020)
	FUS	Lys 315/316	↓	Arenas et al. (2020)
	FUS	Ala 2	↓	Bock et al. (2021)
	TDP - 43	Lys 145–149	↓	Cohen et al. (2015)
Ubiquitination	TDP - 43	Lys 48, Lys 63	↑	Hebron et al. (2013)
	TDP - 43	Lys 263	↑	Hans et al. (2014)
PARylation	hnRNP - A1	Lys 298	↑	Duan et al. (2019)
	FUS	n.d	↑	Patel et al. (2015)

PTMs are able to both suppress (red arrow down) and enhance (green arrow up) protein aggregation of FUS, TDP43 and hnRNP-A1/A2. R-methylation mainly suppresses FUS aggregation while ubiquitination and PARylation stimulates aggregation of TDP-43, hnRNP-A1 and FUS. Other PTMs such as phosphorlation and acetylation, have been shown to suppress or enhance aggregation propensity depending on the specific residue and protein modified.

molecular basis of this difference, however, is still a matter of speculation.

Interestingly, Arg residues in the RGG motifs of FET proteins and hnRNP-A1 can also undergo citrullination, catalyzed by peptidyl arginine deiminase 4 (PAD4), which significantly inhibits protein aggregation and the recruitment of FUS in arsenite-induced stress granules. In agreement with this, a lower PAD4 expression is associated with a higher risk of developing ALS (Tanikawa et al., 2018).

Contrary to methylation, phosphorylation and acetylation change the protein charge with consequent impact on proteins conformation (Hofweber and Dormann, 2019) and pattern of interaction, aspects that we will discuss in the following paragraphs.

Phosphorylation

A complex interplay between protein phosphorylation and methylation has been recently found to control the dynamics of some RBPs including hnRNP-A1 and TDP-43. For instance, cisplatin treatment (CDDP) induces phosphorylation of protein methyl-transferase PRMT1 by DNA-PK, which redirects PRMT1 activity toward chromatin-associated proteins at the cost of RBP methylation (Musiani et al., 2020). Interestingly, 82% of the down-regulated Arg-methyl sites following PRMT1 phosphorylation by DNA-PK are inside the RGG-containing LCDs of proteins undergoing LLPS. As described above Arg-methylation by PRMT1 on these proteins weakens cation–π interactions between Arg and aromatic (Phe and Tyr) residues, thus reducing LLPS. The effect of DNA-PK on this phenomenon is double. In fact, in addition to phosphorylating and redirecting PRTM1 toward chromatin, DNA-PK phosphorylates the RBPs that are a target of R-methylation in a way that inhibits their interaction with PRTM1. The net effect is that these RBPs accumulate in SG condensates (Giambruno and Bonaldi, 2020). In the case of hnRNP-A2, Tyr-phosphorylation alters the propensity of the protein to undergo LLPS *in vitro*, prevents partitioning of granule components and hinders aggregation of mutants associated with neurodegenerative disorders. Moreover, different phosphorylation events in the same domain may elicit different effects offering the possibility of tuning protein assemblies (Ryan et al., 2021). *C. elegans* experiments have identified FYN kinase as a candidate for hnRNP-A2 phosphorylation (Ryan et al., 2021). Indeed, Tyr phosphomimetic mutations, i.e., substitutions with aspartic or glutamic acid that mimic the phosphate negative charge, prevent partitioning in droplets of hnRNP-F and ch-TOG, two molecular partners of hnRNP-A2, while Ser phosphomimetic ones do not (Ryan et al., 2021).

Similarly to R-methylation, phosphorylation can either enhance or suppress LLPS of RBPs *in vitro* (**Table 1**), as clearly demonstrated for both FUS and TDP-43. In response to DNA damage the two apical DDR kinases DNA-PK and ATM catalyze the phosphorylation of different sites (Ser-26/Ser-30, Ser-30/Ser-42, Thr-109/Ser-115, and Ser-115/Ser-117 within the ATM and DNA-PK consensus Ser/Thr-Gln) localized in the LCD of FUS, a modification that has been shown to prevent liquid to-solid-state transition and the formation of fibril-like structures (Deng et al., 2014; Monahan et al., 2017; Rhoads et al., 2018a). Although the details of FUS phosphorylation *in vivo* are still under investigation, the involvement of two apical DDR kinases seems to suggest that protein aggregation and DDR activation might be mechanistically linked in causing neurodegeneration for a subset of ALS and FTD cases. Nevertheless, the consequence of

phosphorylation on LLPS is protein- and residue specific. Indeed, Ser/Thr phosphorylation within FUS LCD reduces its aggregation *in vitro* and *in vivo* (Monahan et al., 2017), while it has the opposite effect on other proteins such as fragile-X linked protein FMRP (Tsang et al., 2019). Regarding TDP-43, phosphomimetic substitution with glutamic acid of serine 48 ($Ser^{48}Glu$), a highly phosphorylated residue in the N-terminal domain (Rigbolt et al., 2011; Hornbeck et al., 2012; Hornbeck et al., 2015; Wang A. et al., 2018), also reduces LLPS, suggesting that phosphorylation of this residue interferes with the transient and weak intermolecular interactions necessary for phase transition, possibly promoting a more rigid and structured protein conformation (Wang A. et al., 2018). In line with this, different un-phosphorylatable mutations of Ser to Ala weakly induce phase transition. On the other hand, it is also known that phosphorylated TDP-43 represents one of the predominant components of protein aggregates in ALS and FTD (Hasegawa et al., 2008; Guedes et al., 2017), in which TDP-43 is found phosphorylated in its LCD, mainly on Ser 403/404 and 409/410 (Neumann et al., 2020). Nevertheless, whether this phosphorylation occurs before or after aggregation and its possible causative role in stabilizing protein aggregation need to be yet clarified. A possible explanation for these conflicting observations could be that phosphorylation can occur after TDP-43 aggregation, as an attempt to counteract detrimental interactions throughout electrostatic repulsions (Brady et al., 2011). Conversely, another theory that has been put forward proposes that phosphorylation prevents the clearance of the aggregates, thus causing their accumulation. In support of this, Zhang et al. have shown that phosphorylated fragments are more difficult to degrade than the non-phosphorylated ones (Zhang et al., 2010). Moreover, *in vitro* experiment casein kinases 1 (CK) increases TDP-43 phosphorylation and aggregation (Hasegawa et al., 2008).

Among all the factors that can influence both protein phosphorylation and aggregation, ATP concentration is strictly regulated within cells. On the one hand ATP plays an indirect role in controlling the assembly of condensates via protein phosphorylation; on the other hand, high ATP concentrations (>6 mM) alone can dissolve *in vitro*-generated liquid condensates of several RBPs, including FUS. The effect of ATP on LLPS directly stems from its hydrotropic nature, achieved due to the presence of the aromatic ring, capable of binding the hydrophobic patches in FUS (RGG and RRM domains), and the triphosphate chain that interacts with water molecules, thus leading to dissolution of protein aggregates (Patel et al., 2017; Rice and Rosen, 2017; Kang et al., 2019). It is worth noting that the cellular ATP concentration is usually in the millimolar range (up to 10 mM), while ADP and AMP are 50 and 10 μM respectively. The high ATP consumption of neurons may reduce its cellular concentration and might contribute to why these cell types are more prone than others to fibrillar degeneration of FUS condensates.

Acetylation

While in other contexts of neurodegeneration protein acetylation has been widely associated with reduced protein aggregation (Saito et al., 2019), FUS and TDP-43 Lys acetylation leads to the formation of cytoplasmic protein aggregates (**Table 1**; **Figures 2A,B**).

Recently, three new acetylated Lys residues localized in different domains of FUS have been identified by mass spectrometric approaches (Arenas et al., 2020). In particular, acetylation at Lys315/Lys316 within the RRM domain strongly affects the ability of FUS of binding RNA, while acetylation of Lys510 in the NLS stimulates the formation of FUS-containing cytoplasmic aggregates (Arenas et al., 2020). Moreover, the application of a specific antibody directed against acetylated Lys510 (K510Ac) reveals a significant increase of acetylated FUS in ALS patients-derived dermic fibroblasts, suggesting the involvement of this PTM in FUS pathogenicity (Arenas et al., 2020). In this study, treatments with specific inhibitors proved that Lys510 acetylation is catalyzed by the CREB binding protein (CBP)/p300 (**Figure 2B**), while de-acetylation is carried out by both histone deacetylases (HDACs) and sirtuins (SIRTs) (Arenas et al., 2020). Although acetylation of FUS and TDP-43 seems to act preferably as a driving force for protein aggregates (**Table 1**), when occurring in specific positions it can work in the opposite direction.

Proteomics approaches have always identified the N-terminus of FUS as a preferential target of acetylation (Catherman et al., 2013; Rhoads et al., 2018b). Indeed, a recent study revealed a new FUS acetylation by the N-terminal acetyltransferases (NatA-NatF), confirmed by co-expression of recombinant FUS with the Nat A complex, which stimulates LCD LLPS without increasing the formation of aggregates (Bock et al., 2021). N-terminal acetylation is the addition of an acetyl group to the N-terminal amine group through an amide bond thus impeding protonation of the terminal amine reducing the propensity of the nearly uncharged FUS LCD domain to form aggregates.

Analogously, TDP-43 aggregation state is modulated by acetylation. It has been shown that upon sodium arsenite treatment, the CREB binding protein (CBP) acetylates TDP-43 on Lys145-Lys149. This modification impairs TDP-43 RNA binding ability and produces the accumulation of amyloid-like inclusions containing hyper-phosphorylated TDP-43 (Cohen et al., 2015). Interestingly, TDP-43 mutants bearing acetylation-mimic Lys to Gln substitution form cytosolic aggregates and exhibit other hallmarks of TDP-43 pathology (Wang et al., 2017).

As for arginine methylation in FUS, also TDP-43 tendency to acetylation appears different in ALS and FTD contexts, since the acetylated form of TDP-43 is detectable only in ALS spinal specimens and not in brain specimens from FTD-TDP-43 patients (Cohen et al., 2015), suggesting that this PTM might be a valuable specific biomarker to distinguish between these two pathologies.

Ubiquitination

One of the cellular mechanisms involved in the clearance of misfolded protein is the ubiquitin-proteasomal system that functions as a "quality control" mechanism. In ALS, a remarkable fraction of ubiquitin (Ub) is sequestered into different types of inclusions (Leigh et al., 1991), thus reducing the pool of Ub available for physiological ubiquitination of

different substrates during the execution of many cellular functions including transcription, DNA repair and signal transduction (Hershko and Ciechanover, 1998; Chen and Sun, 2009).

Some evidence suggests that FUS is recruited into ubiquitin-positive cytoplasmic inclusions. However, the ubiquitin-ligase responsible for FUS ubiquitination has not yet been described (Neumann et al., 2009; Deng et al., 2010; Seelaar et al., 2010; Farrawell et al., 2015). It has been proposed that, in a neuronal context, autophagy represents the preferred mechanism for the clearance of misfolded proteins (Nijholt et al., 2011). Recent studies have directly linked autophagy and protein aggregates and the new term "aggrephagy" has been coined to define the mechanism of aggregate clearance by autophagy (Øverbye et al., 2007). Nowadays the contribution of aggrephagy is widely investigated in the context of proteinopathies. Intriguingly, aggrephagy and autophagy compete for limited amounts of intermediate structures (e.g., phagophores) and this could cause reduced autophagy efficiency in resolving the aberrant aggregation of cytoskeleton proteins upon toxic induction (Larsen et al., 2002). On the other hand, it is plausible that the presence of ubiquitin in FUS-containing inclusions indicates an initial attempt to resolve protein aggregates via the proteasome degradation pathway (Farrawell et al., 2015).

Ubiquitination also has an important role in controlling the formation of TDP-43 condensates (**Figure 2**). Indeed, Lys48 and Lys63 ubiquitination by E3 ubiquitin ligase Parkin leads to cytosolic accumulation of TDP-43 and the formation of cytosolic condensates (Hebron et al., 2013). Interestingly, this re-localization reduces the Parkin mRNA level, which is in turn controlled by TDP-43. Overexpression experiments have proven the formation of a multi-protein complex comprising Parkin, ubiquitinated TDP-43 and HDAC6 that facilitates cytosolic accumulation of TDP-43. Although this cytosolic complex is likely to have a physiological function, a failure of the proteasome function in neurodegenerative diseases leads to the appearance of cytosolic TDP-43 condensates (Hebron et al., 2013). Notably, it has been suggested that the Parkin-mediated ubiquitination may contribute to TDP-43 aggregation (Hebron et al., 2013). It is worth noting that TDP-43 can be ubiquitinated by several other enzymes. An example is the UBE2E class of ubiquitin-conjugating enzymes that ubiquitylate TDP-43 at Lys263 (Hans et al., 2014). More recently, it has been reported that cytoplasmic inclusions resulted from the expression of two fALS mutants: TDP-43-Met^{337}Val and FUS-Arg^{495}x. These mutants co-localized with polymeric Ub^{K63}, which is associated with the autophagy-related clearance mechanism. Intriguingly, the expression of FUS-Arg^{495}x causes the reduction of monomeric ubiquitin levels that can disrupt ubiquitin homeostasis (Farrawell et al., 2020).

The level of ubiquitinated proteins within the cell is tightly regulated by deubiquitinating enzymes (DUBs), which counterbalance ubiquitin ligase activity and comprise a large family of enzymes with different specificities and catalytic activities. Due to their role in removing ubiquitin signaling, DUBs are implicated in a wide range of cellular processes and differentially accumulate in distinct functional compartments, based on their primary role (Clague et al., 2019). For instance, some cytosolic DUBs are coupled with the proteasome activity, and therefore may potentially be of major relevance in the modulation of protein aggregation state in the context of neurodegenerative disorders. Among these, Ubiquitin-specific protease 14 (USP14) is catalytically active only when bound to the 26S proteasome and contributes to the cleavage of ubiquitin from substrates before their degradation (Borodovsky et al., 2001; Hu et al., 2005). It has been shown that proteasome-associated USP14 deubiquitinates TDP-43 and that USP14 inhibition accelerates TDP-43 turnover. In particular, overexpression of WT USP14 in mouse embryonic fibroblasts leads to increased TDP-43 levels. This effect is abolished by both the expression of USP14 catalytically inactive form and USP14 small molecule inhibition (Lee et al., 2010), prompting the idea that ubiquitin chain trimming by USP14 might act as an antagonist of proteasome function.

It is worth noting, that DUBs have also been implicated in autophagy mechanisms. A genetic screen in *Drosophila* larval fat body identified Ubiquitin Iso-peptidase Y (UBPY), also called USP8, as a key player in the autophagy flux, whose RNAi-mediated silencing led to lysosomal defects and accumulation of malfunctioning autophagosomes (Jacomin et al., 2015). Notably, TDP-43 Lys^{263}Glu mutant undergoes pathological hyper-ubiquitination and aggregation and if the ubiquitin-conjugating enzyme UBE2E3 actively ubiquitinates it, UBPY is able to counteract this PTM. The silencing of UBPY in fact enhances neurodegeneration in the retina of TDP-43 *Drosophila* ALS model system with accumulation of ubiquitinated and insoluble TDP-43. In this way, UBPY participates in the regulation of TDP-43 Lys^{263}Glu solubility and exerts a neuroprotective function in *Drosophila melanogaster* (Hans et al., 2014). Moreover, recent results demonstrated that the Ubiquitin Specific protease 10 (USP10) positively regulates the stability of the autophagic protein LC3B, counterbalancing LC3B degradation and thus enhancing clearance of protein aggregates under stress conditions (Jia and Bonifacino, 2021).

Intriguingly, not only can DUBs modulate the protein aggregation state but they are also are recruited to membrane-less organelles or even have the ability to phase separate themselves. One example is the human USP42, which drives nuclear speckle phase separation dependent on its de-ubiquitinating activity, thus governing mRNA splicing events (Liu et al., 2021). In addition, it has been proven that other two human DUBs, namely USP5 and USP13, are recruited to stress granules shell and dictate their stabilization or disassembly through their activity of removing ubiquitin chains (Xie et al., 2018). Human USP5 also seems to target and regulate the expression of hnRNP-A1 (Vashistha et al., 2020), whereas the fly DUB Otu possess an LC domain that drives the formation of amyloid-like granules, which resemble FUS and hnRNP-A1 structures and are indispensable for Otu enzymatic activity (Ji et al., 2019).

Overall, while ubiquitinated RBPs seem to be generally associated with aggregates formation, the clearance of this

form by means of DUBs could be useful in reversing or preventing these toxic events. Nevertheless, intricate networks, which are far from being fully understood, controls the cellular balance of protein ubiquitination and ubiquitin mediated signaling, which could contribute to fostering proteinopathies in neurodegenerative disorders.

PARylation

Poly ADP-ribosylation (PARylation) is a reversible PTM in which ADP-ribose (ADPr) units are added to the Glu, Asp, Lys, Arg or Ser residues by poly (ADP-ribose) (PAR) polymerases (PARPs). This process is reversed by PAR glycohydrolase (PARG) (Slade et al., 2011). It has been shown that PARylation regulates the dynamics of the SGs and that PARP1 activation upon cell treatment with H_2O_2 markedly increases the level of PARylated hnRNP-A1 (Duan et al., 2019). Indeed, Lys298 (K298), immediately C-terminal of the M9 motif at the CTD of the protein (**Figure 1**) is a PARylation site. Interestingly, hnRNP-A1 also contains a PAR-binding motif, located between the two RRM domains (position 92–113, **Figure 1**). It mediates the interaction with PARylated proteins and its mutation abrogates the recruitment of hnRNP-A1 to stress granules. Decreased PARylation levels suppress the formation of SGs and the recruitment of hnRNP-A1 and TDP-43 to SGs, while higher PARylation levels delay the disassembly of SGs. Considering the close proximity between the PAR-binding motif and the RRMs in hnRNP-A1, their PARylation has an impact on the interaction with RNA. In addition, K298 PARylation regulates the nucleocytoplasmic transport of hnRNP-A1 and stress induced-K298 PARylation may serve as a nuclear export signal (Duan et al., 2019).

CONCLUSIVE REMARKS

Among different factors that can influence LLPS and its conversion to pathological aggregates, PTMs are now attracting a lot of interest for three main reasons: 1) they can accumulate and be modulated differently in aged and young individuals thus explaining why proteinopathies arise late in patients' lives; 2) they could be used as biomarkers to define the pathology and detect its preclinical stage thus enabling early treatments; 3) they are ideal drug targets, and many compounds are already available which affect on protein PTMs and which could be repurposed for the treatments of specific proteinopathies. Thus, pharmacological approaches targeting PTMs could help dissolve pathological aggregates or prevent their formation, thus enhancing survival of neurons in affected individuals. In addition, the optimization of highly sensitive assays for the precise detection of PTM patterns associated with the disease might be a very useful for early diagnosis in personalized medicine. For example, mass spectrometry (MS) could be used to identify specific peptide patterns, associated with proteins PTMs that could delineate characteristic pathological profiles. Alternatively, antibodies could be generated against pathological PTM patterns and used in diagnosis. The main drawback of these approaches is the availability of useful specimens from patients, which could be very difficult to obtain as it would involve highly invasive techniques. Thus there is a need to identify diagnostic signatures in easily accessible tissues like blood or other body fluids. Another important point to consider is that the generation of antibodies that recognize PTMs in single protein positions may be challenging, since in some cases different proteins may present highly similar motifs and PTMs. Finally, costs and accessibility of MS methodologies might hinder their usage in routine diagnostic processes. In conclusion, we believe that deciphering the impact of PTMs on the formation of protein aggregates in different pathological contexts is the basis for setting up diagnostic and therapeutic tools in order to ameliorate the derived phenotypes.

AUTHOR CONTRIBUTIONS

SF decided the content of text and figures. SteF, MB, FE and GB wrote the first draft of different parts of the text. SteF generated the figures. SF organized the contribution of all the authors and edited the text with the help of GB.

FUNDING

SF is supported by AriSLA (projects "DDRNA&ALS" and its follow up "DDR&ALS") and by Progetti di Ricerca di Interesse Nazionale (PRIN) 2015 and 2017. SF and GB are supported by a grant POR FESR 2014-2020 Regione Lombardia (InterSLA project). SteF was supported by IUSS Pavia and FE was supported by University of Pavia.

REFERENCES

Aguzzi, A., and O'Connor, T. (2010). Protein Aggregation Diseases: Pathogenicity and Therapeutic Perspectives. *Nat. Rev. Drug Discov.* 9, 237–248. doi:10.1038/nrd3050

Alberti, S., Halfmann, R., King, O., Kapila, A., and Lindquist, S. (2009). A Systematic Survey Identifies Prions and Illuminates Sequence Features of Prionogenic Proteins. *Cell* 137, 146–158. doi:10.1016/j.cell.2009.02.044

Arenas, A., Chen, J., Kuang, L., Barnett, K. R., Kasarskis, E. J., Gal, J., et al. (2020). Lysine Acetylation Regulates the RNA Binding, Subcellular Localization and Inclusion Formation of FUS. *Hum. Mol. Genet.* 29, 2684–2697. doi:10.1093/hmg/ddaa159

Bedford, M. T., and Clarke, S. G. (2009). Protein Arginine Methylation in Mammals: Who, what, and Why. *Mol. Cell* 33, 1–13. doi:10.1016/j.molcel.2008.12.013

Blanc, R. S., and Richard, S. (2017). Arginine Methylation: The Coming of Age. *Mol. Cell* 65, 8–24. doi:10.1016/j.molcel.2016.11.003

Bock, A. S., Murthy, A. C., Tang, W. S., Jovic, N., Shewmaker, F., Mittal, J., et al. (2021). N-terminal Acetylation Modestly Enhances Phase Separation and Reduces Aggregation of the Low-Complexity Domain of RNA-Binding Protein Fused in Sarcoma. *Protein Sci.* 30, 1337–1349. doi:10.1002/pro.4029

Borodovsky, A., Kessler, B. M., Casagrande, R., Overkleeft, H. S., Wilkinson, K. D., and Ploegh, H. L. (2001). A Novel Active Site-Directed Probe Specific for

Deubiquitylating Enzymes Reveals Proteasome Association of USP14. *EMBO J.* 20, 5187–5196. doi:10.1093/emboj/20.18.5187

Bosco, D. A., Lemay, N., Ko, H. K., Zhou, H., Burke, C., Kwiatkowski, T. J., JR., et al. (2010). Mutant FUS Proteins that Cause Amyotrophic Lateral Sclerosis Incorporate into Stress Granules. *Hum. Mol. Genet.* 19, 4160–4175. doi:10.1093/hmg/ddq335

Brady, O. A., Meng, P., Zheng, Y., Mao, Y., and Hu, F. (2011). Regulation of TDP-43 Aggregation by Phosphorylation andp62/SQSTM1. *J. Neurochem.* 116, 248–259. doi:10.1111/j.1471-4159.2010.07098.x

Brangwynne, C. P., Tompa, P., and Pappu, R. V. (2015). Polymer Physics of Intracellular Phase Transitions. *Nat. Phys* 11, 899–904. doi:10.1038/nphys3532

Buratti, E. (2018). TDP-43 post-translational Modifications in Health and Disease. *Expert Opin. Ther. Targets* 22, 279–293. doi:10.1080/14728222.2018.1439923

Burke, K. A., Janke, A. M., Rhine, C. L., and Fawzi, N. L. (2015). Residue-by-Residue View of *In Vitro* FUS Granules that Bind the C-Terminal Domain of RNA Polymerase II. *Mol. Cell* 60, 231–241. doi:10.1016/j.molcel.2015.09.006

Catherman, A. D., Durbin, K. R., Ahlf, D. R., Early, B. P., Fellers, R. T., Tran, J. C., et al. (2013). Large-scale Top-Down Proteomics of the Human Proteome: Membrane Proteins, Mitochondria, and Senescence. *Mol. Cell Proteomics* 12, 3465–3473. doi:10.1074/mcp.m113.030114

Chang, B., Chen, Y., Zhao, Y., and Bruick, R. K. (2007). JMJD6 Is a Histone Arginine Demethylase. *Science* 318, 444–447. doi:10.1126/science.1145801

Chen, Z. J., and Sun, L. J. (2009). Nonproteolytic Functions of Ubiquitin in Cell Signaling. *Mol. Cell* 33, 275–286. doi:10.1016/j.molcel.2009.01.014

Chiti, F., and Dobson, C. M. (2006). Protein Misfolding, Functional Amyloid, and Human Disease. *Annu. Rev. Biochem.* 75, 333–366. doi:10.1146/annurev.biochem.75.101304.123901

Chook, Y. M., and Süel, K. E. (2011). Nuclear Import by Karyopherin-Bs: Recognition and Inhibition. *Biochim. Biophys. Acta (Bba) - Mol. Cell Res.* 1813, 1593–1606. doi:10.1016/j.bbamcr.2010.10.014

Clague, M. J., Urbé, S., and Komander, D. (2019). Breaking the Chains: Deubiquitylating Enzyme Specificity Begets Function. *Nat. Rev. Mol. Cell Biol* 20, 338–352. doi:10.1038/s41580-019-0099-1

Cohen, T. J., Hwang, A. W., Restrepo, C. R., Yuan, C. X., Trojanowski, J. Q., and Lee, V. M. (2015). An Acetylation Switch Controls TDP-43 Function and Aggregation Propensity. *Nat. Commun.* 6, 5845. doi:10.1038/ncomms6845

Conicella, A. E., Zerze, G. H., Mittal, J., and Fawzi, N. L. (2016). ALS Mutations Disrupt Phase Separation Mediated by α-Helical Structure in the TDP-43 Low-Complexity C-Terminal Domain. *Structure* 24, 1537–1549. doi:10.1016/j.str.2016.07.007

de Boer, E. M. J., Orie, V. K., Williams, T., Baker, M. R., de Oliveira, H. M., Polvikoski, T., et al. (2020). TDP-43 Proteinopathies: a New Wave of Neurodegenerative Diseases. *J. Neurol. Neurosurg. Psychiatry*.

Deng, H. X., Zhai, H., Bigio, E. H., Yan, J., Fecto, F., Ajroud, K., et al. (2010). FUS-immunoreactive Inclusions Are a Common Feature in Sporadic and Non-SOD1 Familial Amyotrophic Lateral Sclerosis. *Ann. Neurol.* 67, 739–748. doi:10.1002/ana.22051

Deng, Q., Holler, C. J., Taylor, G., Hudson, K. F., Watkins, W., Gearing, M., et al. (2014). FUS Is Phosphorylated by DNA-PK and Accumulates in the Cytoplasm after DNA Damage. *J. Neurosci.* 34, 7802–7813. doi:10.1523/jneurosci.0172-14.2014

Dormann, D., Madl, T., Valori, C. F., Bentmann, E., Tahirovic, S., Abou-Ajram, C., et al. (2012). Arginine Methylation Next to the PY-NLS Modulates Transportin Binding and Nuclear Import of FUS. *EMBO J.* 31, 4258–4275. doi:10.1038/emboj.2012.261

Dosztányi, Z., Chen, J., Dunker, A. K., Simon, I., and Tompa, P. (2006). Disorder and Sequence Repeats in Hub Proteins and Their Implications for Network Evolution. *J. Proteome Res.* 5, 2985–2995. doi:10.1021/pr060171o

Duan, Y., Du, A., Gu, J., Duan, G., Wang, C., Gui, X., et al. (2019). PARylation Regulates Stress Granule Dynamics, Phase Separation, and Neurotoxicity of Disease-Related RNA-Binding Proteins. *Cell Res.* 29, 233–247. doi:10.1038/s41422-019-0141-z

Farrawell, N. E., Lambert-Smith, I. A., Warraich, S. T., Blair, I. P., Saunders, D. N., Hatters, D. M., et al. (2015). Distinct Partitioning of ALS Associated TDP-43, FUS and SOD1 Mutants into Cellular Inclusions. *Sci. Rep.* 5, 13416. doi:10.1038/srep13416

Farrawell, N. E., Mcalary, L., Lum, J. S., Chisholm, C. G., Warraich, S. T., Blair, I. P., et al. (2020). Ubiquitin Homeostasis Is Disrupted in TDP-43 and FUS Cell Models of ALS. *iScience* 23, 101700. doi:10.1016/j.isci.2020.101700

Forman, M. S., Trojanowski, J. Q., and Lee, V. M.-Y. (2004). Neurodegenerative Diseases: a Decade of Discoveries Paves the Way for Therapeutic Breakthroughs. *Nat. Med.* 10, 1055–1063. doi:10.1038/nm1113

Freibaum, B. D., Chitta, R. K., High, A. A., and Taylor, J. P. (2010). Global Analysis of TDP-43 Interacting Proteins Reveals strong Association with RNA Splicing and Translation Machinery. *J. Proteome Res.* 9, 1104–1120. doi:10.1021/pr901076y

Giambruno, R., and Bonaldi, T. (2020). Dual Role of PRMT1-dependent Arginine Methylation in Cellular Responses to Genotoxic Stress. *Mol. Cell Oncol.* 7, 1743808. doi:10.1080/23723556.2020.1743808

Guedes, Á. C. B., Santin, R., Costa, A. S. R., Reiter, K. C., Hilbig, A., and Fernandez, L. L. (2017). Distinct Phospho-TDP-43 Brain Distribution in Two Cases of FTD, One Associated with ALS. *Dement. Neuropsychol.* 11, 249–254. doi:10.1590/1980-57642016dn11-030006

Guerrero, E. N., Wang, H., Mitra, J., Hegde, P. M., Stowell, S. E., Liachko, N. F., et al. (2016). TDP-43/FUS in Motor Neuron Disease: Complexity and Challenges. *Prog. Neurobiol.* 145-146, 78–97. doi:10.1016/j.pneurobio.2016.09.004

Gui, X., Luo, F., Li, Y., Zhou, H., Qin, Z., Liu, Z., et al. (2019). Structural Basis for Reversible Amyloids of hnRNPA1 Elucidates Their Role in Stress Granule Assembly. *Nat. Commun.* 10, 2006. doi:10.1038/s41467-019-09902-7

Guo, W., Chen, Y., Zhou, X., Kar, A., Ray, P., Chen, X., et al. (2011). An ALS-Associated Mutation Affecting TDP-43 Enhances Protein Aggregation, Fibril Formation and Neurotoxicity. *Nat. Struct. Mol. Biol.* 18, 822–830. doi:10.1038/nsmb.2053

Hackman, P., Sarparanta, J., Lehtinen, S., Vihola, A., Evilä, A., Jonson, P. H., et al. (2013). Welander Distal Myopathy Is Caused by a Mutation in the RNA-Binding Protein TIA1. *Ann. Neurol.* 73, 500–509. doi:10.1002/ana.23831

Han, T. W., Kato, M., Xie, S., Wu, L. C., Mirzaei, H., Pei, J., et al. (2012). Cell-free Formation of RNA Granules: Bound RNAs Identify Features and Components of Cellular Assemblies. *Cell* 149, 768–779. doi:10.1016/j.cell.2012.04.016

Hans, F., Fiesel, F. C., Strong, J. C., Jäckel, S., Rasse, T. M., Geisler, S., et al. (2014). UBE2E Ubiquitin-Conjugating Enzymes and Ubiquitin Isopeptidase Y Regulate TDP-43 Protein Ubiquitination. *J. Biol. Chem.* 289, 19164–19179. doi:10.1074/jbc.m114.561704

Hasegawa, M., Arai, T., Nonaka, T., Kametani, F., Yoshida, M., Hashizume, Y., et al. (2008). Phosphorylated TDP-43 in Frontotemporal Lobar Degeneration and Amyotrophic Lateral Sclerosis. *Ann. Neurol.* 64, 60–70. doi:10.1002/ana.21425

Hebron, M. L., Lonskaya, I., Sharpe, K., Weerasinghe, P. P. K., Algarzae, N. K., Shekoyan, A. R., et al. (2013). Parkin Ubiquitinates Tar-DNA Binding Protein-43 (TDP-43) and Promotes its Cytosolic Accumulation via Interaction with Histone Deacetylase 6 (HDAC6). *J. Biol. Chem.* 288, 4103–4115. doi:10.1074/jbc.m112.419945

Hershko, A., and Ciechanover, A. (1998). The Ubiquitin System. *Annu. Rev. Biochem.* 67, 425–479. doi:10.1146/annurev.biochem.67.1.425

Hoell, J. I., Larsson, E., Runge, S., Nusbaum, J. D., Duggimpudi, S., Farazi, T. A., et al. (2011). RNA Targets of Wild-type and Mutant FET Family Proteins. *Nat. Struct. Mol. Biol.* 18, 1428–1431. doi:10.1038/nsmb.2163

Hofweber, M., and Dormann, D. (2019). Friend or foe-Post-translational Modifications as Regulators of Phase Separation and RNP Granule Dynamics. *J. Biol. Chem.* 294, 7137–7150. doi:10.1074/jbc.tm118.001189

Hornbeck, P. V., Kornhauser, J. M., Tkachev, S., Zhang, B., Skrzypek, E., Murray, B., et al. (2012). PhosphoSitePlus: a Comprehensive Resource for Investigating the Structure and Function of Experimentally Determined post-translational Modifications in Man and Mouse. *Nucleic Acids Res.* 40, D261–D270. doi:10.1093/nar/gkr1122

Hornbeck, P. V., Zhang, B., Murray, B., Kornhauser, J. M., Latham, V., and Skrzypek, E. (2015). PhosphoSitePlus, 2014: Mutations, PTMs and Recalibrations. *Nucleic Acids Res.* 43, D512–D520. doi:10.1093/nar/gku1267

Hu, M., Li, P., Song, L., Jeffrey, P. D., Chenova, T. A., Wilkinson, K. D., et al. (2005). Structure and Mechanisms of the Proteasome-Associated Deubiquitinating Enzyme USP14. *EMBO J.* 24, 3747–3756. doi:10.1038/sj.emboj.7600832

Hughes, M. P., Sawaya, M. R., Boyer, D. R., Goldschmidt, L., Rodriguez, J. A., Cascio, D., et al. (2018). Atomic Structures of Low-Complexity Protein

Segments Reveal Kinked β Sheets that Assemble Networks. *Science* 359, 698–701. doi:10.1126/science.aan6398

Jacomin, A. C., Bescond, A., Soleilhac, E., Gallet, B., Schoehn, G., Fauvarque, M. O., et al. (2015). The Deubiquitinating Enzyme UBPY Is Required for Lysosomal Biogenesis and Productive Autophagy in Drosophila. *PLoS One* 10, e0143078. doi:10.1371/journal.pone.0143078

Ji, S., Luo, Y., Cai, Q., Cao, Z., Zhao, Y., Mei, J., et al. (2019). LC Domain-Mediated Coalescence Is Essential for Otu Enzymatic Activity to Extend Drosophila Lifespan. *Mol. Cell* 74, 363–377. doi:10.1016/j.molcel.2019.02.004

Jia, R., and Bonifacino, J. S. (2021). The Ubiquitin Isopeptidase USP10 Deubiquitinates LC3B to Increase LC3B Levels and Autophagic Activity. *J. Biol. Chem.* 296, 100405. doi:10.1016/j.jbc.2021.100405

Jiang, L.-L., Che, M.-X., Zhao, J., Zhou, C.-J., Xie, M.-Y., Li, H.-Y., et al. (2013). Structural Transformation of the Amyloidogenic Core Region of TDP-43 Protein Initiates its Aggregation and Cytoplasmic Inclusion. *J. Biol. Chem.* 288, 19614–19624. doi:10.1074/jbc.m113.463828

Jiang, L. L., Zhao, J., Yin, X. F., He, W. T., Yang, H., Che, M. X., et al. (2016). Two Mutations G335D and Q343R within the Amyloidogenic Core Region of TDP-43 Influence its Aggregation and Inclusion Formation. *Sci. Rep.* 6, 23928. doi:10.1038/srep23928

Jucker, M., and Walker, L. C. (2013). Self-propagation of Pathogenic Protein Aggregates in Neurodegenerative Diseases. *Nature* 501, 45–51. doi:10.1038/nature12481

Kang, J., Lim, L., and Song, J. (2019). ATP Binds and Inhibits the Neurodegeneration-Associated Fibrillization of the FUS RRM Domain. *Commun. Biol.* 2, 223. doi:10.1038/s42003-019-0463-x

Kim, H. J., Kim, N. C., Wang, Y.-D., Scarborough, E. A., Moore, J., Diaz, Z., et al. (2013). Mutations in Prion-like Domains in hnRNPA2B1 and hnRNPA1 Cause Multisystem Proteinopathy and ALS. *Nature* 495, 467–473. doi:10.1038/nature11922

Langdon, E. M., and Gladfelter, A. S. (2018). Probing RNA Structure in Liquid-Liquid Phase Separation Using SHAPE-MaP. *Methods Enzymol.* 611, 67–79. doi:10.1016/bs.mie.2018.09.039

Larsen, A.-K. R., Møller, M. T. N., Blankson, H., Samari, H. R., Holden, L., and Seglen, P. O. (2002). Naringin-sensitive Phosphorylation of Plectin, a Cytoskeletal Cross-Linking Protein, in Isolated Rat Hepatocytes. *J. Biol. Chem.* 277, 34826–34835. doi:10.1074/jbc.m205028200

Lee, B.-H., Lee, M. J., Park, S., Oh, D.-C., Elsasser, S., Chen, P.-C., et al. (2010). Enhancement of Proteasome Activity by a Small-Molecule Inhibitor of USP14. *Nature* 467, 179–184. doi:10.1038/nature09299

Leigh, P. N., Whitwell, H., Garofalo, O., Buller, J., Swash, M., Martin, J. E., et al. (1991). Ubiquitin-immunoreactive Intraneuronal Inclusions in Amyotrophic Lateral Sclerosis. Morphology, Distribution, and Specificity. *Brain* 114 (Pt 2), 775–788. doi:10.1093/brain/114.2.775

Levone, B. R., Lenzken, S. C., Antonaci, M., Maiser, A., Rapp, A., Conte, F., et al. (2020). FUS-dependent Liquid-Liquid Phase Separation Is an Early Event in Double-Strand Break Repair. bioRxiv, 798884. doi:10.1101/798884

Lim, L., Wei, Y., Lu, Y., and Song, J. (2016). ALS-Causing Mutations Significantly Perturb the Self-Assembly and Interaction with Nucleic Acid of the Intrinsically Disordered Prion-like Domain of TDP-43. *Plos Biol.* 14, e1002338. doi:10.1371/journal.pbio.1002338

Liu, S., Wang, T., Shi, Y., Bai, L., Wang, S., Guo, D., et al. (2021). USP42 Drives Nuclear Speckle mRNA Splicing via Directing Dynamic Phase Separation to Promote Tumorigenesis. *Cell Death Differ*. doi:10.1038/s41418-021-00763-6

Lorton, B. M., and Shechter, D. (2019). Cellular Consequences of Arginine Methylation. *Cell. Mol. Life Sci.* 76, 2933–2956. doi:10.1007/s00018-019-03140-2

Mitra, J., Guerrero, E. N., Hegde, P. M., Liachko, N. F., Wang, H., Vasquez, V., et al. (2019). Motor Neuron Disease-Associated Loss of Nuclear TDP-43 Is Linked to DNA Double-Strand Break Repair Defects. *Proc. Natl. Acad. Sci. USA* 116, 4696–4705. doi:10.1073/pnas.1818415116

Molliex, A., Temirov, J., Lee, J., Coughlin, M., Kanagaraj, A. P., Kim, H. J., et al. (2015). Phase Separation by Low Complexity Domains Promotes Stress Granule Assembly and Drives Pathological Fibrillization. *Cell* 163, 123–133. doi:10.1016/j.cell.2015.09.015

Monahan, Z., Ryan, V. H., Janke, A. M., Burke, K. A., Rhoads, S. N., Zerze, G. H., et al. (2017). Phosphorylation of the FUS Low-complexity Domain Disrupts Phase Separation, Aggregation, and Toxicity. *Embo j* 36, 2951–2967. doi:10.15252/embj.201696394

Murakami, T., Qamar, S., Lin, J. Q., Schierle, G. S. K., Rees, E., Miyashita, A., et al. (2015). ALS/FTD Mutation-Induced Phase Transition of FUS Liquid Droplets and Reversible Hydrogels into Irreversible Hydrogels Impairs RNP Granule Function. *Neuron* 88, 678–690. doi:10.1016/j.neuron.2015.10.030

Murray, D. T., Kato, M., Lin, Y., Thurber, K. R., Hung, I., Mcknight, S. L., et al. (2017). Structure of FUS Protein Fibrils and its Relevance to Self-Assembly and Phase Separation of Low-Complexity Domains. *Cell* 171, 615–627 e16. doi:10.1016/j.cell.2017.08.048

Musiani, D., Giambruno, R., Massignani, E., Ippolito, M. R., Maniaci, M., Jammula, S., et al. (2020). PRMT1 Is Recruited via DNA-PK to Chromatin where it Sustains the Senescence-Associated Secretory Phenotype in Response to Cisplatin. *Cell Rep.* 30, 1208–1222. doi:10.1016/j.celrep.2019.12.061

Naumann, M., Pal, A., Goswami, A., Lojewski, X., Japtok, J., Vehlow, A., et al. (2018). Impaired DNA Damage Response Signaling by FUS-NLS Mutations Leads to Neurodegeneration and FUS Aggregate Formation. *Nat. Commun.* 9, 335. doi:10.1038/s41467-017-02299-1

Neumann, M., Frick, P., Paron, F., Kosten, J., Buratti, E., and Mackenzie, I. R. (2020). Antibody against TDP-43 Phosphorylated at Serine 375 Suggests Conformational Differences of TDP-43 Aggregates Among FTLD-TDP Subtypes. *Acta Neuropathol.* 140, 645–658. doi:10.1007/s00401-020-02207-w

Neumann, M., Rademakers, R., Roeber, S., Baker, M., Kretzschmar, H. A., and Mackenzie, I. R. A. (2009). A New Subtype of Frontotemporal Lobar Degeneration with FUS Pathology. *Brain* 132, 2922–2931. doi:10.1093/brain/awp214

Nichols, R. C., Wang, X. W., Tang, J., Hamilton, B. J., High, F. A., Herschman, H. R., et al. (2000). The RGG Domain in hnRNP A2 Affects Subcellular Localization. *Exp. Cell Res.* 256, 522–532. doi:10.1006/excr.2000.4827

Nijholt, D. A., de Kimpe, L., Elfrink, H. L., Hoozemans, J. J., and Scheper, W. (2011). Removing Protein Aggregates: the Role of Proteolysis in Neurodegeneration. *Curr. Med. Chem.* 18, 2459–2476. doi:10.1038/cdd.2010.176

Øverbye, A., Brinchmann, M. F., and Seglen, P. O. (2007). Proteomic Analysis of Membrane-Associated Proteins from Rat Liver Autophagosomes. *Autophagy* 3, 300–322. doi:10.4161/auto.3910

Owen, I., and Shewmaker, F. (2019). The Role of Post-Translational Modifications in the Phase Transitions of Intrinsically Disordered Proteins. *Int. J. Mol. Sci.* 20. doi:10.3390/ijms20215501

Patel, A., Lee, H. O., Jawerth, L., Maharana, S., Jahnel, M., Hein, M. Y., et al. (2015). A Liquid-To-Solid Phase Transition of the ALS Protein FUS Accelerated by Disease Mutation. *Cell* 162, 1066–1077. doi:10.1016/j.cell.2015.07.047

Patel, A., Malinovska, L., Saha, S., Wang, J., Alberti, S., Krishnan, Y., et al. (2017). ATP as a Biological Hydrotrope. *Science* 356, 753–756. doi:10.1126/science.aaf6846

Posey, A. E., Holehouse, A. S., and Pappu, R. V. (2018). Phase Separation of Intrinsically Disordered Proteins. *Methods Enzymol.* 611, 1–30. doi:10.1016/bs.mie.2018.09.035

Qamar, S., Wang, G., Randle, S. J., Ruggeri, F. S., Varela, J. A., Lin, J. Q., et al. (2018). FUS Phase Separation Is Modulated by a Molecular Chaperone and Methylation of Arginine Cation-π Interactions. *Cell* 173, 720–734.e15. doi:10.1016/j.cell.2018.03.056

Rajpurohit, R., Paik, W. K., and Kim, S. (1994). Effect of Enzymic Methylation of Heterogeneous Ribonucleoprotein Particle A1 on its Nucleic-Acid Binding and Controlled Proteolysis. *Biochem. J.* 304 (Pt 3), 903–909. doi:10.1042/bj3040903

Rappsilber, J., Friesen, W. J., Paushkin, S., Dreyfuss, G., and Mann, M. (2003). Detection of Arginine Dimethylated Peptides by Parallel Precursor Ion Scanning Mass Spectrometry in Positive Ion Mode. *Anal. Chem.* 75, 3107–3114. doi:10.1021/ac026283q

Rhoads, S. N., Monahan, Z. T., Yee, D. S., Leung, A. Y., Newcombe, C. G., O'Meally, R. N., et al. (2018a). The Prionlike Domain of FUS Is Multiphosphorylated Following DNA Damage without Altering Nuclear Localization. *MBoC* 29, 1786–1797. doi:10.1091/mbc.e17-12-0735

Rhoads, S. N., Monahan, Z. T., Yee, D. S., and Shewmaker, F. P. (2018b). The Role of Post-Translational Modifications on Prion-like Aggregation and Liquid-Phase Separation of FUS. *Int. J. Mol. Sci.* 19, 886. doi:10.3390/ijms19030886

Rice, A. M., and Rosen, M. K. (2017). ATP Controls the Crowd. *Science* 356, 701–702. doi:10.1126/science.aan4223

Rigbolt, K. T. G., Prokhorova, T. A., Akimov, V., Henningsen, J., Johansen, P. T., Kratchmarova, I., et al. (2011). System-wide Temporal Characterization of the Proteome and Phosphoproteome of Human Embryonic Stem Cell Differentiation. *Sci. Signaling* 4, rs3. doi:10.1126/scisignal.2001570

Roden, C., and Gladfelter, A. S. (2021). RNA Contributions to the Form and Function of Biomolecular Condensates. *Nat. Rev. Mol. Cell Biol* 22, 183–195. doi:10.1038/s41580-020-0264-6

Romero, P., Obradovic, Z., Li, X., Garner, E. C., Brown, C. J., and Dunker, A. K. (2001). Sequence Complexity of Disordered Protein. *Proteins* 42, 38–48. doi:10.1002/1097-0134(20010101)42:1<38::aid-prot50>3.0.co;2-3

Ross, C. A., and Poirier, M. A. (2004). Protein Aggregation and Neurodegenerative Disease. *Nat. Med.* 10 (Suppl. l), S10–S17. doi:10.1038/nm1066

Rulten, S. L., Rotheray, A., Green, R. L., Grundy, G. J., Moore, D. A. Q., Gómez-Herreros, F., et al. (2014). PARP-1 Dependent Recruitment of the Amyotrophic Lateral Sclerosis-Associated Protein FUS/TLS to Sites of Oxidative DNA Damage. *Nucleic Acids Res.* 42, 307–314. doi:10.1093/nar/gkt835

Ryan, V. H., Perdikari, T. M., Naik, M. T., Saueressig, C. F., Lins, J., Dignon, G. L., et al. (2021). Tyrosine Phosphorylation Regulates hnRNPA2 Granule Protein Partitioning and Reduces Neurodegeneration. *EMBO J.* 40, e105001. doi:10.15252/embj.2020105001

Saini, A., and Chauhan, V. S. (2011). Delineation of the Core Aggregation Sequences of TDP-43 C-Terminal Fragment. *Chembiochem.* 12, 2495–2501. doi:10.1002/cbic.201100427

Saito, M., Hess, D., Eglinger, J., Fritsch, A. W., Kreysing, M., Weinert, B. T., et al. (2019). Acetylation of Intrinsically Disordered Regions Regulates Phase Separation. *Nat. Chem. Biol.* 15, 51–61. doi:10.1038/s41589-018-0180-7

Schmidt, H. B., and Rohatgi, R. (2016). *In Vivo* Formation of Vacuolated Multi-phase Compartments Lacking Membranes. *Cell Rep.* 16, 1228–1236. doi:10.1016/j.celrep.2016.06.088

Seelaar, H., Klijnsma, K. Y., de Koning, I., van der Lugt, A., Chiu, W. Z., Azmani, A., et al. (2010). Frequency of Ubiquitin and FUS-Positive, TDP-43-Negative Frontotemporal Lobar Degeneration. *J. Neurol.* 257, 747–753. doi:10.1007/s00415-009-5404-z

Shorter, J. (2017). Liquidizing FUS via Prion-like Domain Phosphorylation. *Embo J* 36, 2925–2927. doi:10.15252/embj.201798078

Singatulina, A. S., Hamon, L., Sukhanova, M. V., Desforges, B., Joshi, V., Bouhss, A., et al. (2019). PARP-1 Activation Directs FUS to DNA Damage Sites to Form PARG-Reversible Compartments Enriched in Damaged DNA. *Cell Rep.* 27, 1809–1821.e5. doi:10.1016/j.celrep.2019.04.031

Slade, D., Dunstan, M. S., Barkauskaite, E., Weston, R., Lafite, P., Dixon, N., et al. (2011). The Structure and Catalytic Mechanism of a poly(ADP-Ribose) Glycohydrolase. *Nature* 477, 616–620. doi:10.1038/nature10404

Suárez-Calvet, M., Neumann, M., Arzberger, T., Abou-Ajram, C., Funk, E., Hartmann, H., et al. (2016). Monomethylated and Unmethylated FUS Exhibit Increased Binding to Transportin and Distinguish FTLD-FUS from ALS-FUS. *Acta Neuropathol.* 131, 587–604. doi:10.1007/s00401-016-1544-2

Tanikawa, C., Ueda, K., Suzuki, A., Iida, A., Nakamura, R., Atsuta, N., et al. (2018). Citrullination of RGG Motifs in FET Proteins by PAD4 Regulates Protein Aggregation and ALS Susceptibility. *Cell Rep.* 22, 1473–1483. doi:10.1016/j.celrep.2018.01.031

Thandapani, P., O'Connor, T. R., Bailey, T. L., and Richard, S. (2013). Defining the RGG/RG Motif. *Mol. Cell* 50, 613–623. doi:10.1016/j.molcel.2013.05.021

Toretsky, J. A., and Wright, P. E. (2014). Assemblages: Functional Units Formed by Cellular Phase Separation. *J. Cell Biol* 206, 579–588. doi:10.1083/jcb.201404124

Tsang, B., Arsenault, J., Vernon, R. M., Lin, H., Sonenberg, N., Wang, L.-Y., et al. (2019). Phosphoregulated FMRP Phase Separation Models Activity-dependent Translation through Bidirectional Control of mRNA Granule Formation. *Proc. Natl. Acad. Sci. USA* 116, 4218–4227. doi:10.1073/pnas.1814385116

van der Lee, R., Buljan, M., Lang, B., Weatheritt, R. J., Daughdrill, G. W., Dunker, A. K., et al. (2014). Classification of Intrinsically Disordered Regions and Proteins. *Chem. Rev.* 114, 6589–6631. doi:10.1021/cr400525m

Vashistha, V., Bhardwaj, S., Yadav, B. K., and Yadav, A. K. (2020). Depleting Deubiquitinating Enzymes Promotes Apoptosis in Glioma Cell Line via RNA Binding Proteins SF2/ASF1. *Biochem. Biophys. Rep.* 24, 100846. doi:10.1016/j.bbrep.2020.100846

Walport, L. J., Hopkinson, R. J., Chowdhury, R., Schiller, R., Ge, W., Kawamura, A., et al. (2016). Arginine Demethylation Is Catalysed by a Subset of JmjC Histone Lysine Demethylases. *Nat. Commun.* 7, 11974. doi:10.1038/ncomms11974

Wang, A., Conicella, A. E., Schmidt, H. B., Martin, E. W., Rhoads, S. N., Reeb, A. N., et al. (2018). A Single N-Terminal Phosphomimic Disrupts TDP-43 Polymerization, Phase Separation, and RNA Splicing. *Embo j* 37. doi:10.15252/embj.201797452

Wang, H., Guo, W., Mitra, J., Hegde, P. M., Vandoorne, T., Eckelmann, B. J., et al. (2018). Mutant FUS Causes DNA Ligation Defects to Inhibit Oxidative Damage Repair in Amyotrophic Lateral Sclerosis. *Nat. Commun.* 9, 3683. doi:10.1038/s41467-018-06111-6

Wang, P., Wander, C. M., Yuan, C. X., Bereman, M. S., and Cohen, T. J. (2017). Acetylation-induced TDP-43 Pathology Is Suppressed by an HSF1-dependent Chaperone Program. *Nat. Commun.* 8, 82. doi:10.1038/s41467-017-00088-4

Wang, W.-Y., Pan, L., Su, S. C., Quinn, E. J., Sasaki, M., Jimenez, J. C., et al. (2013). Interaction of FUS and HDAC1 Regulates DNA Damage Response and Repair in Neurons. *Nat. Neurosci.* 16, 1383–1391. doi:10.1038/nn.3514

Wright, P. E., and Dyson, H. J. (2009). Linking Folding and Binding. *Curr. Opin. Struct. Biol.* 19, 31–38. doi:10.1016/j.sbi.2008.12.003

Xie, H., Vucetic, S., Iakoucheva, L. M., Oldfield, C. J., Dunker, A. K., Obradovic, Z., et al. (2007). Functional Anthology of Intrinsic Disorder. 3. Ligands, post-translational Modifications, and Diseases Associated with Intrinsically Disordered Proteins. *J. Proteome Res.* 6, 1917–1932. doi:10.1021/pr060394e

Xie, X., Matsumoto, S., Endo, A., Fukushima, T., Kawahara, H., Saeki, Y., et al. (2018). Deubiquitylases USP5 and USP13 Are Recruited to and Regulate Heat-Induced Stress Granules through Their Deubiquitylating Activities. *J. Cell Sci* 131. doi:10.1242/jcs.210856

Yang, Y., and Bedford, M. T. (2013). Protein Arginine Methyltransferases and Cancer. *Nat. Rev. Cancer* 13, 37–50. doi:10.1038/nrc3409

Zhang, Y.-J., Gendron, T. F., Xu, Y.-F., Ko, L.-W., Yen, S.-H., and Petrucelli, L. (2010). Phosphorylation Regulates Proteasomal-Mediated Degradation and Solubility of TAR DNA Binding Protein-43 C-Terminal Fragments. *Mol. Neurodegeneration* 5, 33. doi:10.1186/1750-1326-5-33

Conflict of Interest: The authors declare that the research was conducted in the absence of any commercial or financial relationships that could be construed as a potential conflict of interest.

frontiers in Molecular Biosciences

ORIGINAL RESEARCH
published: 07 September 2021
doi: 10.3389/fmolb.2021.688973

Systematic Analysis of the Impact of R-Methylation on RBPs-RNA Interactions: A Proteomic Approach

*Marianna Maniaci [1,2], Francesca Ludovica Boffo [1], Enrico Massignani [1,2] and Tiziana Bonaldi [1]**

[1]Laboratory of Nuclear Proteomics to Study Gene Expression Regulation in Cancer, European Institute of Oncology (IEO) IRCSS, Department of Experimental Oncology (DEO), Milan, Italy, [2]European School of Molecular Medicine (SEMM), Milan, Italy

RNA binding proteins (RBPs) bind RNAs through specific RNA-binding domains, generating multi-molecular complexes known as ribonucleoproteins (RNPs). Various post-translational modifications (PTMs) have been described to regulate RBP structure, subcellular localization, and interactions with other proteins or RNAs. Recent proteome-wide experiments showed that RBPs are the most representative group within the class of arginine (R)-methylated proteins. Moreover, emerging evidence suggests that this modification plays a role in the regulation of RBP-RNA interactions. Nevertheless, a systematic analysis of how changes in protein-R-methylation can affect globally RBPs-RNA interactions is still missing. We describe here a quantitative proteomics approach to profile global changes of RBP-RNA interactions upon the modulation of type I and II protein arginine methyltransferases (PRMTs). By coupling the recently described Orthogonal Organic Phase Separation (OOPS) strategy with the Stable Isotope Labelling with Amino acids in Cell culture (SILAC) and pharmacological modulation of PRMTs, we profiled RNA-protein interaction dynamics in dependence of protein-R-methylation. Data are available via ProteomeXchange with identifier PXD024601.

Keywords: proteomics, PTMs, protein-R-methylation, PRMTs, SILAC, OOPS, RBPs, mass spectrometry

OPEN ACCESS

Edited by:
Ewa Anna Grzybowska, Maria Sklodowska-Curie National Research Institute of Oncology, Poland

Reviewed by:
Michael Yu, University at Buffalo, United States
Ubaldo Gioia, IFOM-The FIRC Institute of Molecular Oncology, Italy
Jocelyn Cote, University of Ottawa, Canada

***Correspondence:**
Tiziana Bonaldi
tiziana.bonaldi@ieo.it

Specialty section:
This article was submitted to Protein and RNA Networks, a section of the journal Frontiers in Molecular Biosciences

Received: *31 March 2021*
Accepted: *11 August 2021*
Published: *07 September 2021*

Citation:
Maniaci M, Boffo FL, Massignani E and Bonaldi T (2021) Systematic Analysis of the Impact of R-Methylation on RBPs-RNA Interactions: A Proteomic Approach. Front. Mol. Biosci. 8:688973. doi: 10.3389/fmolb.2021.688973

INTRODUCTION

Arginine (R)-methylation is a widespread post-translational modification (PTM) that occurs on both histones, where it acts as an epigenetic regulator of gene expression, and non-histone proteins, where it modulates protein-protein, protein-RNA and protein-DNA interactions (Blanc and Richard, 2017), emerging as a key modulator of several cellular processes, from translation and splicing to growth factor–receptor signaling, miRNA biogenesis and DNA damage response (Guccione and Richard, 2019; Musiani et al., 2020; Spadotto et al., 2020). In mammals, nine enzymes have been identified and classified as type I, type II and type III protein R-methyltransferases (PRMTs), depending on their ability to transfer to the guanidino group of the arginine residues either two methyl-groups in asymmetric (ADMA) and symmetric (SDMA) manner, or one methyl-group (MMA), respectively (Blanc and Richard, 2017). Arginines located within glycine-arginine-rich regions, the so called "RGG/RG motifs", are preferred sites for methylation by PRMTs (Thandapani et al., 2013). In mammals, PRMT1 and PRMT5 are the most active PRMTs of the type I and II families, respectively, and object of intense investigation in both basic and translational research (Zhang et al., 2019). As a matter of fact, various PRMTs have been found overexpressed in several solid tumors -such as breast, lung, colon, bladder, head, neck cancers- and hematological malignancies, such as leukemia (Smith et al., 2018; Zhang et al., 2018). Hence, various inhibitors

with different selectivity for PRMTs are under development as anti-cancer drugs, some already entering phase-1 and -2 clinical trials (Hu et al., 2016; Kaniskan et al., 2018). In recent years, proteome-wide strategies to study R-methylated proteins have been optimized, thanks to the implementation of efficient biochemical protocols for methyl-peptide enrichment, coupled to off-line high pH (HpH) chromatographic fractionation and high-resolution mass spectrometry (MS) analysis. Recently published evidence (Fedoriw et al., 2019; Fong et al., 2019; Lim et al., 2020; Szewczyk et al., 2020), together with MS-proteomics analyses carried out in our group (Musiani et al., 2019; Musiani et al., 2020; Spadotto et al., 2020), has shown that pharmacological and genetic inhibition of PRMTs coupled with quantitative MS-based analysis are powerful approaches to expand the knowledge about the extent of this modification, its dynamics upon different perturbation and its involvement in different cellular pathways. One interesting piece of information emerging from these studies is that RNA-binding proteins (RBPs) are over-represented among experimentally-annotated R-methylated proteins.

RBPs bind their cognate RNAs either in a sequence-specific manner, through their RNA-binding domains (RBDs), such as the RNA recognition motif (RRM), the hnRNP K homology (KH) domain and the dead/deah box helicase (DDX) domain, or in a structure-dependent fashion, whereby they interact to specific RNA secondary structures rather than nucleotide sequences (Hentze et al., 2018). RBPs are involved in several cellular processes linked to RNA processing, including pre-mRNA splicing, mRNA transport, microRNA biogenesis, and translation; such processes are essential for cell homeostasis and for fine-tuning gene expression in response to perturbations, or during differentiation and developmental transitions, and are frequently dis-regulated in cancer (Yang and Bedford, 2013; Pereira et al., 2017). In addition to the RBDs, these RBPs often contain sequences that have been variously termed as low complexity (LC) region or intrinsically disordered regions (IDRs), which were shown to confer the capability to undergo liquid-liquid phase separation (LLPS) and form membranless organelles (MLOs) (Lin et al., 2015). Notably, these disordered regions very often include RGG/RG motifs, the preferred targets of PRMT enzymes (Chong et al., 2018). This provides strong indication of a mechanistic link between the R-methylation state of RBPs and their capability to undergo LLPS, through a change in their interaction with RNA. In line with this idea, Tsai and colleagues have recently shown that the assembly of stress granules (SGs), a type of cytosolic MLOs, is dependent on the R-methylation level of the SG-nucleating protein G3BP1 (Tsai et al., 2016). Furthermore, FUS protein was shown to undergo phase-separation in the nucleus upon pharmacological inhibition of ADMA by Adenosine Dialdehyde (AdOx), an inhibitor of S-adenosyl-L-homocystein hydrolase that leads to the accumulation of S-adenosyl-L-homocystein (Adoicy), a general inhibitor of methyltransferases (Qamar et al., 2018). This evidence hints towards a more general role of protein-R-methylation in regulating RBP-RNA dynamics and, for some proteins, promoting LLPS. Nevertheless, the mechanistic link between the R-methylation state of a protein and its binding to cognate RNAs has been so far described non-systematically, only for individual cases, while a proteome-wide evaluation is still missing.

To address this question, we carried out the first proteome-wide analysis of global changes of RBP-RNA interactions in dependence of protein R-methylation by applying the Orthogonal Organic Phase Separation (OOPS) strategy (Queiroz et al., 2019) to isolate RBP-RNA complexes and coupling it to Stable Isotope Labelling with Amino acids in Cell culture (SILAC) and pharmacological modulation of PRMTs. The observation that the presence of a subset of RBPs is reproducibly altered in the interface fraction enriched by OOPS upon treatment with PRMT type I (but not type-II) inhibitor suggests that MMA/ADMA levels in these proteins modulate their interaction with RNAs. Moreover, we observed that treatment with the same PRMT inhibitor induces LLPS of some candidate RBPs, whose interaction with RNA was found modulated in the proteomics experiments. Overall, our data confirm that modulation of MMA/ADMA, rather than SDMA, directly impacts on RBP-RNA interactions, with consequent effects on MLO assembly.

RESULTS

Analysis of RNA Binding Protein Dynamics in Dependence of PRMTs by SILAC-Based OOPS Strategy

To evaluate the role of protein-R-methylation in the regulation of RBP-RNA interactions, we took advantage of the OOPS strategy to isolate RBP-RNA complexes, coupling it with triple SILAC-proteomics and the use of PRMT inhibitors, in HeLa cervical cancer cells. The experimental design is illustrated in **Figure 1A**: HeLa cells were grown in light, medium and heavy SILAC culture medium, in order to profile in parallel three conditions: DMSO (as control treatment), PRMT type I and PRMT5 inhibition. The triple SILAC experiment was carried out in two biological replicates, "Forward" and "Reverse", whereby the medium- and heavy-SILAC channels were swapped among the two drug treatments, to increase the confidence in identification of specific alterations in protein-RNA interactions. Efficient inhibition of PRMTs was achieved with a 48 h treatment with the PRMT type I inhibitor MS023 (which - at the IC50 conditions used in the experiment- mainly targets PRMT1, the most active enzyme in the type I family) (Eram et al., 2016) and GSK591, a selective inhibitor of PRMT5 (Sachamitr et al., 2021). Drug efficiency was confirmed by monitoring changes in ADMA and SDMA, both globally (**Supplementary Figure S1**) and on the asymmetric di-methylation of Arginine 3 on histone 4 (H4R3me2a) and on the symmetric di-methylation of Arginine 3 on histone 4 (H4R3me2s), modifications known to be specifically deposed by PRMT1 and PRMT5, respectively (**Figure 1B**). The Western Blot (WB) control of the levels of H3R2me2a, deposed by PRMT6, and of H3R17me2a, set by PRMT4/CARM1, was instead used to confirm the preferential

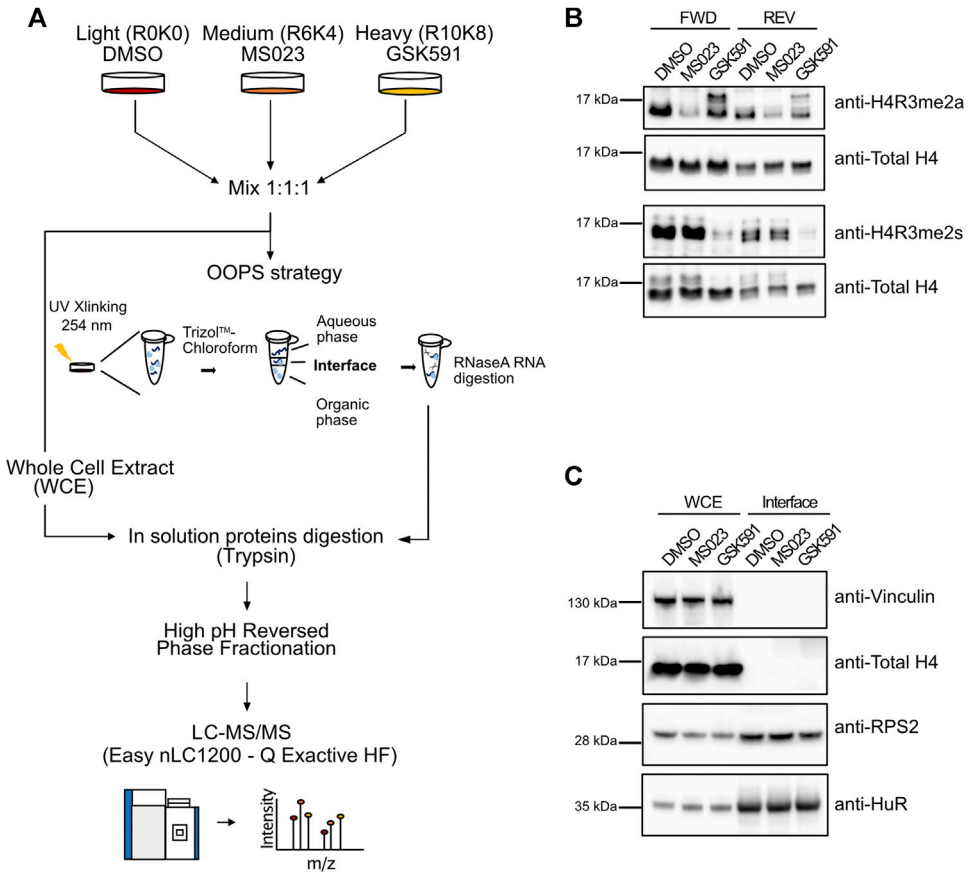

D

Tot n° of identified proteins	4345
Proteins with high confidence identification	2123
Proteins in the WCE	2061
Proteins in the Interface	433
Dynamically regulated proteins in the WCE	563
Dynamically regulated proteins in the Interface	96

FIGURE 1 | Setup of the proteomic approach for the systematic analysis of RNA-protein interactions: the OOPS strategy in combination with PRMT pharmacological inhibition and triple SILAC labelling. **(A)** Representative workflow of the proteomic approach. Cells were grown in light (R0K0), medium (R6K4) and heavy (R10K8) SILAC medium and treated with DMSO, 10 μM MS023 and 5 μM GSK591 for 48h. Aliquots from the light-, medium- and heavy-labelled cells were mixed in 1:1:1 proportion and saved as whole cell extract (WCE), while the remaining cells were UV-crosslinked at 254 nm and phase-partitioned through a Trizol™ - chloroform mixture, as described in (Queiroz et al., 2019). Proteins extracted from the WCE and from the interface fraction were subjected to in-solution digestion with Trypsin and fractionation by off-line HpH-RP chromatography. Tryptic peptides were analyzed by high resolution LC-MS/MS. **(B)** Western Blot (WB) validation of the PRMT pharmacological inhibition. Before mixing in 1:1:1 proportion described in **(A)**, an aliquot of each condition was used to test the methylation state of distinct histone R residues specifically targeted by PRMT1 and PRMT5 by WB, both in the forward (FWD) and in the reversed (REV) experiment. Reduction of asymmetric di-methylation of arginine 3 on histone 4 (H4R3me2a) was observed upon MS023 treatment; total unmodified H4 was used as loading control. Similarly, the reduction of symmetric di-methylation of arginine 3 on histone 4 (H4R3me2s) was observed upon GSK591 treatment (H4 was used as loading control). **(C)** WB validation of RBPs enrichment by OOPS. WB analysis of the RNA binding proteins RPS2 and HuR confirms their enrichment in the interface fraction upon OOPS, while the absence of the non-RBP protein Vinculin and Histone 4 from the same fraction was used to assess the selectivity of the method. **(D)** Summary of the MS-identified proteins by OOPS. Table summarizing the number of proteins identified by MaxQuant from raw MS data, after the application of the indicated filtering criteria: 1) total number of identified proteins, upon removal of reverse hits and contaminants; 2) total number of proteins with Andromeda score ≥25 and at least two peptides, one of which unique, for each experiment (high-confidence identification); 3) total number of proteins identified with high confidence in the WCE; 4) total number of proteins identified at high confidence in the interface fraction from OOPS; 5) number of proteins dynamically regulated by the drugs in the WCE; 6) number of proteins dynamically regulated by the drugs in the interface fraction from OOPS.

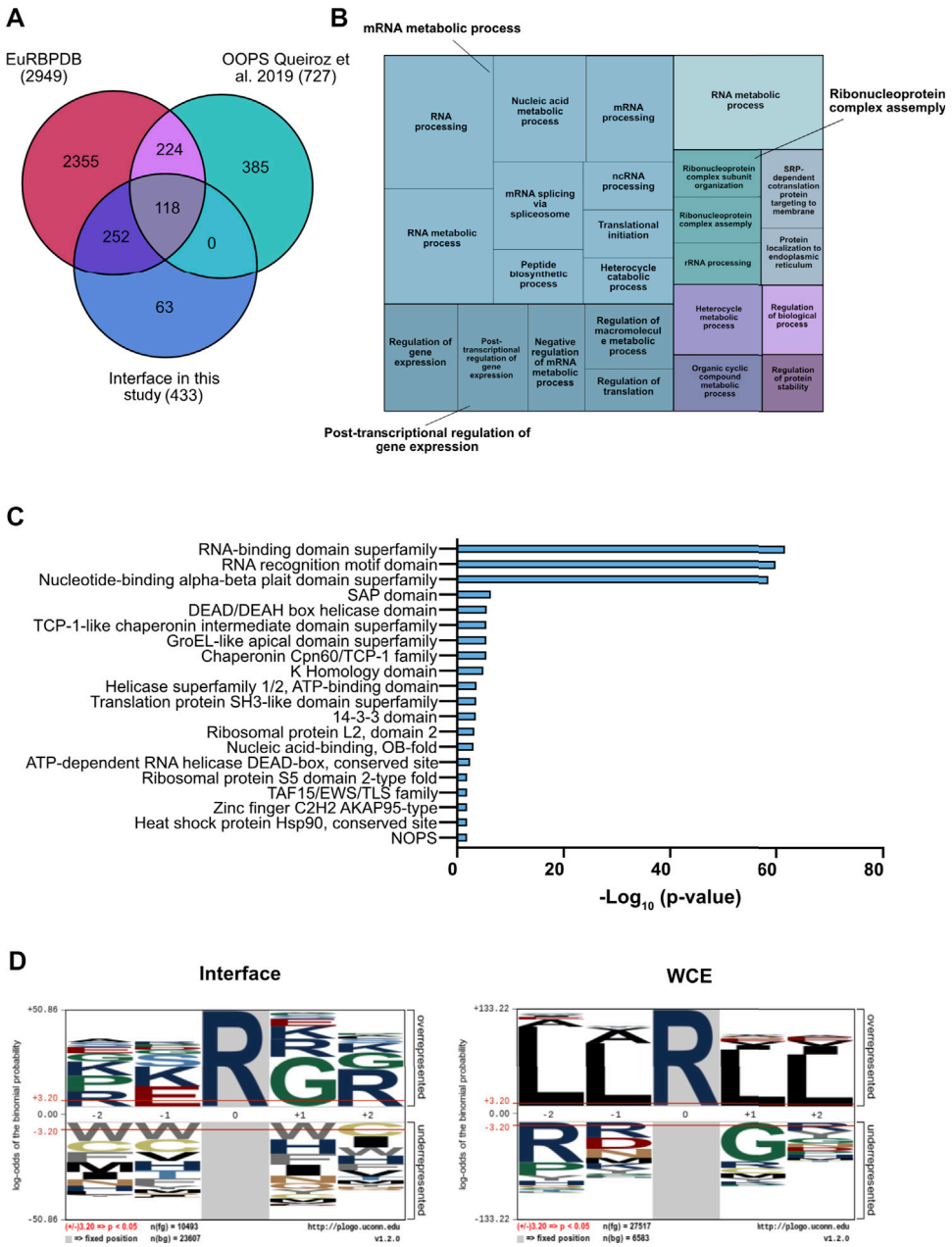

FIGURE 2 | Functional characterization of the interface fraction upon OOPS. **(A)** Comparative validation of RBPs enrichment in the interface fraction. Comparative analysis was performed against the Eukaryotic RNA Binding Proteins Database (EuRBPDB) and the RBPs identified in (Queiroz et al., 2019): 370 out the 433 proteins identified within the interface fraction (85.5%) showed overlap with the other datasets. **(B)** Treemap representation of the GO enriched terms in the interface fraction. GO analysis performed by GOrilla and REVIGO indicates the most enriched GO terms in the interface proteins. **(C)** Domain enrichment analysis of the interface proteins. Analysis was performed by STRING database on the list of the interface proteins **(D)** Over representation analysis of the R-centered sequences. The analysis was performed with the pLogo software, comparing interface and WCE proteins.

selectivity of MS023 towards PRMT1, at least in the experimental conditions used in this study (**Supplementary Figure S1E**). Following drug treatment, fractions (about 20%) from the light-, medium- and heavy-labelled cells were mixed in 1:1:1 proportion and saved as whole cell extract (WCE), while the remaining cells were UV-crosslinked at 254 nm and phase-partitioned through incubation with a Trizol™-chloroform mixture, as described in (Queiroz et al., 2019). This step allows separating three fractions: an upper aqueous part containing free RNAs, an interface that contains the RBP-RNA complexes and a lower organic part containing free proteins. For our purpose, we in-depth analysed the interface fraction. To confirm the expected enrichment of RBPs in the interface fraction, we profiled by WB the levels of known RBPs,

like RPS2 and HuR, in both the WCE and interface fraction: their enrichment in the interface confirmed the efficiency of the OOPS protocol, while the absence in the same fraction of the non-RNA-binding proteins Histone 4 and Vinculin corroborated its selectivity (**Figure 1C**). Both WCE and the interface fractions were then selected for subsequent MS-proteomics analysis: proteins were in solution Trypsin-digested and peptides were separated by off-line HpH Reversed Phase (RP) Chromatography prior to Liquid Chromatography-tandem Mass Spectrometry (LC-MS/MS) analysis (**Figure 1A**). MS analysis on a Q Exactive HF mass spectrometer, followed by data processing for protein identification and quantification with the MaxQuant suite of algorithms (Tyanova et al., 2016), led to the annotation of 2123 proteins identified with at least 2 peptides, one of which unique, and an Andromeda score ≥25. Of them, 2061 were annotated in the WCE and 433 in the interface, respectively (**Figure 1D**). The majority (425, 98%) of the interface proteins were in common with the WCE, with only 8 proteins exclusively found in this fraction (**Supplementary Figure S1H**), among which TIAL1, hnRNPD, NOLC1, SPEN and RALY are well-known RBPs.

Efficiency of the Orthogonal Organic Phase Separation Strategy in Enriching RNA Binding Proteins and Over Representation Analysis of R-Centered Motifs Within the Interface Fraction

To characterize the proteins enriched in the interface fraction upon OOPS, we first compared our experimental list with that annotated by K. Lilley and co-workers, who first optimized the OOPS strategy (Queiroz et al., 2019), and with the EuRBPDB database, a comprehensive repository of eukaryotic RNA-binding proteins (Liao et al., 2020). EuRBPDB includes both "canonical" RBPs containing RBDs and "non-canonical" RBPs that do not contain RBDs but are predicted to bind the secondary structure of cognate RNAs, such as IDRs located in their primary sequences. We found that 370 of the 433 proteins detected in the interface (85%) were validated by the intersection with the two datasets (**Figure 2A**). Gene Ontology (GO) indicated a good representation of the so-called RNA-binding proteome (RBPome) while the same analysis of the non-overlapping 63 proteins (14.5%) showed that 7 have predicted RNA-binding capability and represent putative novel RBPs, whereas the rest are proteins related to extracellular matrix organization, drug response and phosphorylation-related processes. While we cannot exclude that they may be contaminants, it is also possible that such proteins, while not being intrinsic RNA-binders, are enriched in this fraction through association with genuine RBPs.

The smaller number of proteins enriched in the interface fraction compared to Queiroz et al. could reflect the fact that their dataset was obtained by the combination of data from three different cell lines (HEK293, MCF10A and U2OS) comprising both cancer and non-tumor cells. Functional analysis of our protein list showed an almost exclusive enrichment of biological process related to RNA metabolism, such as RNA splicing, RNA metabolic process, RNA processing and translation (**Figure 2B** and **Supplementary Figure S2C**). Moreover, a domain enrichment analysis highlighted the strong over-representation of RBDs and RRMs (p-value = e-60), known to be frequently R-methylated (Blackwell and Ceman, 2012; Bedford and Richard, 2005; Fulton et al., 2019). In addition, we found other domains frequently associated to RBPs, such as the SAP domain (Aravind and Koonin, 2000), the DDX (Gilman et al., 2017) and the KH (Valverde et al., 2008) domains, also known to be R-methylated (**Figure 2C**). The fact that the 14-3-3 protein family was also enriched in the interface fraction is particularly intriguing, because these proteins were the first identified containing a reader motif for phospho-serine/threonine (Espejo et al., 2017); hence this result supports the idea of a possible cross-talk between R-methylation and Ser/Thr-phosphorylation (Chen et al., 2016; Liu et al., 2020; Smith et al., 2020).

Elaborating on the evidence that PRMTs typically recognize and modify arginines located within the glycine-arginine-rich (RG\RGG) domains (Thandapani et al., 2013), we asked whether specific enrichment of such motifs could be observed in an amino acid window around each R located within the proteins annotated in the interface: indeed, the strong enrichment of the RG\RGG domain in the interface proteins, but not in the WCE, corroborates the evidence that RBPs are preferential targets of PRMTs (**Figure 2D**).

Pharmacological Modulation of Protein Arginine Methyltransferases Type I, but Not of Protein Arginine Methyltransferase 5, Affects Protein-RNA Interactions

Since the majority of RBPs identified by OOPS are putative PRMT targets, we next set to investigate the effect of R-methylation modulation on RBP-RNA interaction. We took advantage of the quantitative information included in our SILAC OOPS experiment coupled with MS023 and GSK591 treatment. We performed supervised clustering analysis of the Log_2 SILAC protein ratios of the proteins presenting M\L and H\L SILAC ratios (ratio count >0) in all experimental conditions tested, both in the total proteome and in the RBPome. To better highlight changes exclusively affecting RBP-RNA interactions and not protein expression, for each protein we compared the SILAC ratio measured in the interface fraction with the corresponding ratio in the WCE. From 416 proteins profiled upon filtering, four different clusters emerged (**Figure 3A**), which reflect either the different protein expression or association with cognate RNAs, upon modulation of PRMT type I and PRMT5: Cluster 1, including 53 proteins (red), and Cluster 2, including 85 proteins (blue), represent proteins that show increased levels in the interface fraction (+1 and +1.5 Log_2 SILAC ratio, respectively), but not in the WCE upon MS023 treatment, with no significant changes upon GSK591. This pattern indicates that MS023 has a positive impact on the interaction of these proteins to RNAs and that this increase is not a mere consequence of protein expression up-regulation. Cluster 3,

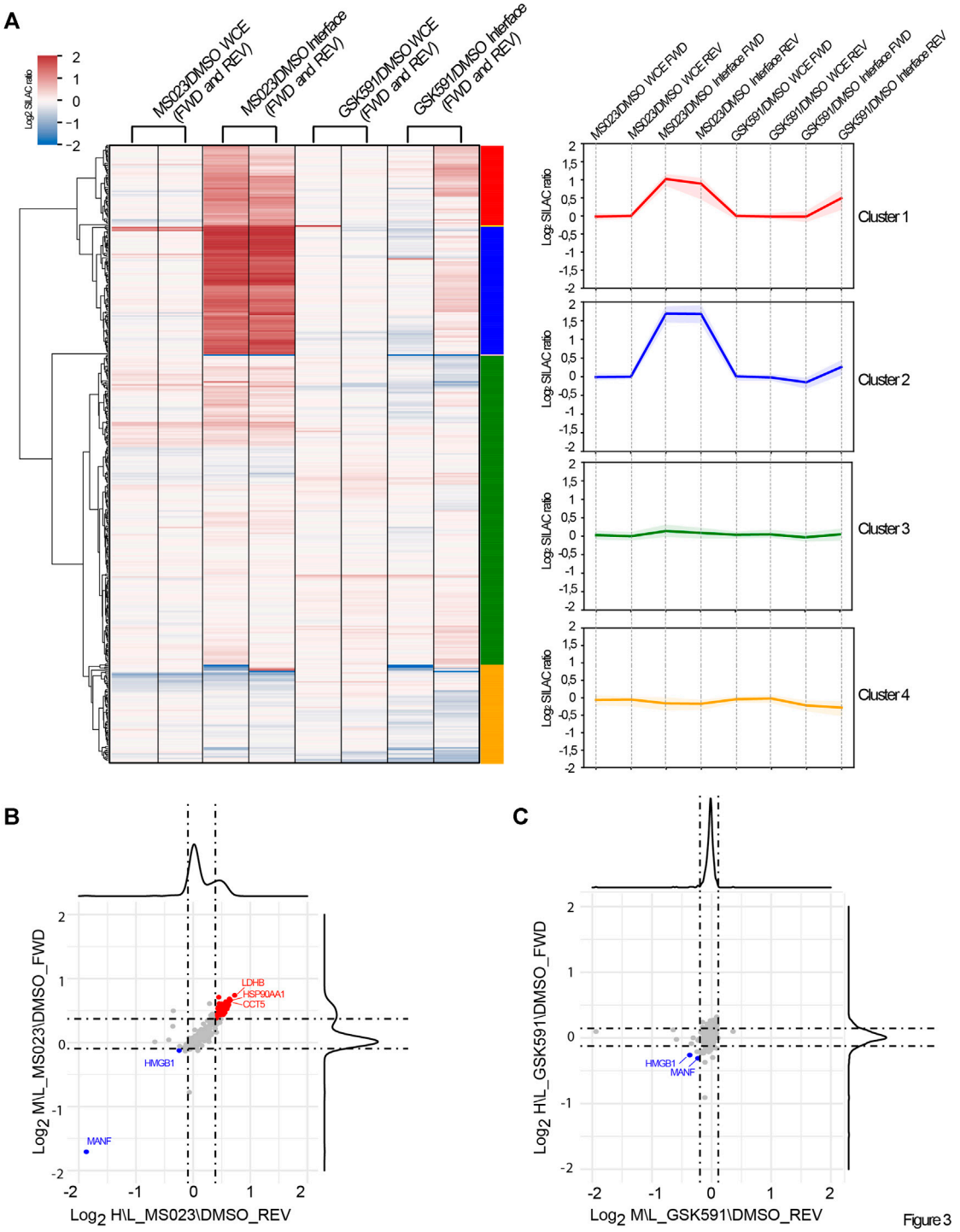

Figure 3

FIGURE 3 | Dynamics of RBP-RNA interactions in dependence of PRMT pharmacological modulation. **(A)** Supervised clustering analysis of the quantitative OOPS proteomics data. Supervised clustering analysis of differential protein expression or differential RNA-binding after MS023 and GSK591 treatment normalized on DMSO led to the identification of four representative clusters: Cluster 1 and Cluster 2 contain proteins with Log_2 SILAC ratio MS023/DMSO +1 and +1.5, respectively, only in the interface fraction; Cluster 3 and Cluster 4 contains proteins overall not significantly modulated in the interface, with Cluster 4 displaying a mild decrease in the interface upon GSK591 (−0.3 Log_2 SILAC ratios). **(B)** Scatter plot representation of the normalized Log_2 SILAC ratio in MS023-treated condition. Scatter plot of the Log_2 MS023/DMSO SILAC ratio of interface proteins, normalized on the respective protein SILAC ratio in the WCE, in FWD versus REV experiment. Dashed lines indicate μ±σ of the respective SILAC protein ratio distributions; proteins up- or down-regulated are displayed in red and blue, respectively. **(C)** Scatter-plot representation of the normalized Log_2 SILAC ratio in GSK591 treated condition. The scatter plot displays the Log_2 GSK591/DMSO SILAC ratio of interface proteins, normalized on the respective SILAC ratio in the WCE in FWD versus REV experiment. Dashed lines indicate μ±σ of the respective SILAC protein ratio distributions; proteins down-regulated are displayed in blue.

A

			WCE				Interface			
Protein ID	Protein Names	Gene Names	MS023/DMSO FWD	MS023/DMSO REV	GSK591/DMSO FWD	GSK591/DMSO REV	MS023/DMSO FWD	MS023/DMSO REV	GSK591/DMSO FWD	GSK591/DMSO REV
P07900	Heat shock protein HSP90-alpha	HSP90AA1	-0.02	0.05	-0.03	0.00	2.05	2.01	0.24	-0.19
P63104	14-3-3 protein zeta/delta	YWHAZ	-0.08	-0.07	-0.06	0.02	1.97	1.97	0.08	-0.21
P62258	14-3-3 protein epsilon	YWHAE	-0.06	0.00	0.04	0.01	1.90	1.90	0.02	-0.22
P27348	14-3-3 protein theta	YWHAQ	0.01	-0.05	0.05	0.03	1.88	1.82	0.27	0.17
P61981	14-3-3 protein gamma	YWHAG	-0.06	-0.03	-0.03	-0.12	1.78	1.72	-0.03	-0.22
A0A5F9Z	L-lactate dehydrogenase B chain	LDHB	-0.07	0.01	-0.03	0.04	2.05	2.27	0.09	-0.36
P48643	T-complex protein 1 (TCP1) subunit epsilon	CCT5	-0.06	0.00	0.07	0.06	1.98	2.06	0.44	0.02
P31942	Heterogeneous nuclear ribonucleoprotein H3	HNRNPH3	0.60	0.54	0.05	-0.12	0.67	0.58	0.02	-0.10
Q15233	Non-POU domain-containing octamer-binding protein	NONO	-0.05	-0.05	0.00	0.00	-0.24	-0.15	-0.10	-0.03
Q15717	ELAV-like protein 1 (HuR)	ELAVL1	-0.11	-0.15	0.16	0.07	-0.17	-0.17	-0.12	0.06
F8W8I6	Nucleolysin TIA-1 isoform p40	TIA1	-0.61	-0.73	0.36	-0.05	-0.94	-0.92	-0.35	-0.22
P09429	High mobility group protein B1	HMGB1	-0.07	-0.01	0.04	0.03	-0.89	-0.53	-0.97	-0.53
A8K878	Mesencephalic astrocyte-derived neurotrophic factor	MANF	-0.04	-0.12	-0.01	-0.18	-6.64	-5.64	-5.06	-6.64

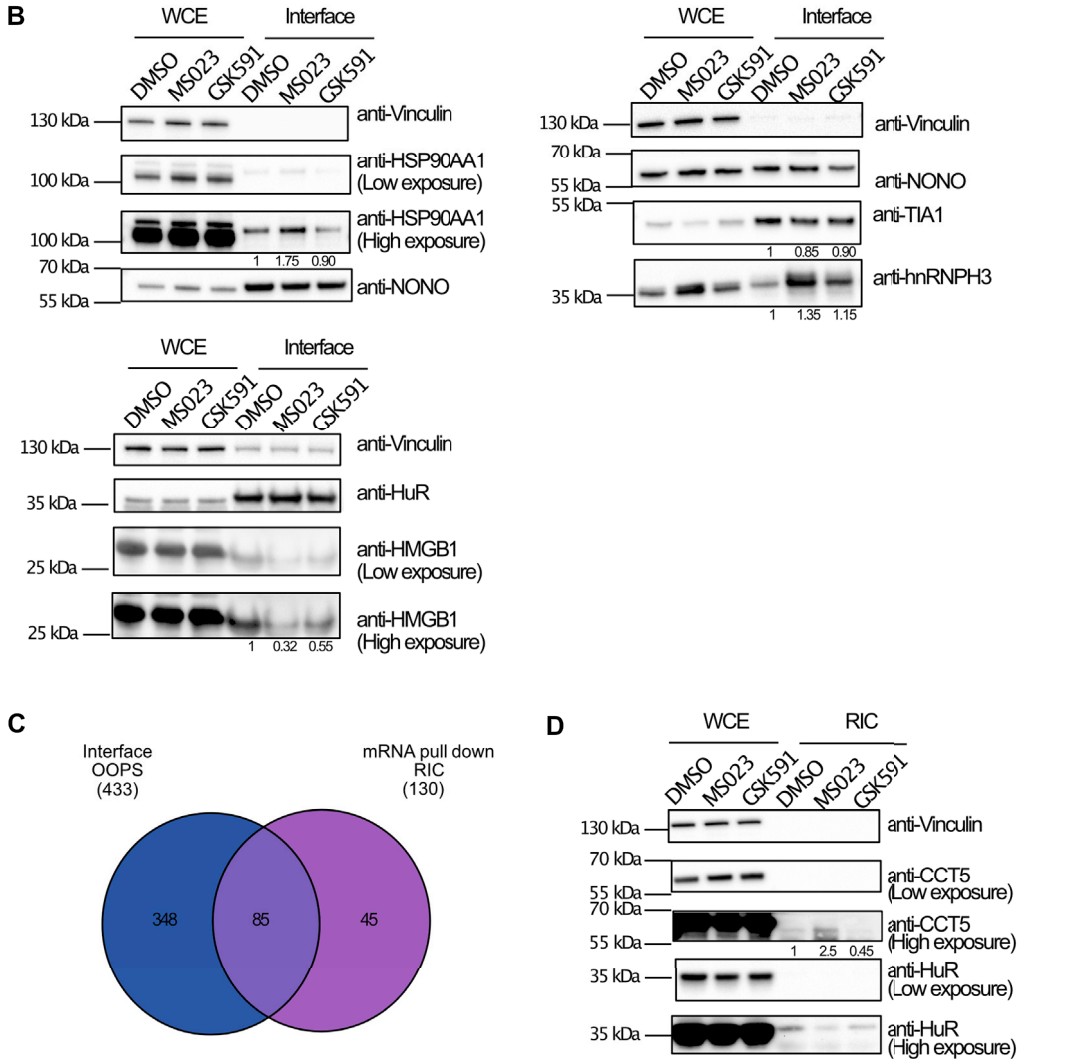

FIGURE 4 | WB validation of the MS-proteomics data. **(A)** Overview of representative RBPs quantified by SILAC OOPS. Table summarizes the MS023/DMSO and GSK591/DMSO SILAC protein ratio of representative proteins, both in the WCE and in the interface fraction, both in FWD and REV experiment. **(B)** WB validation of the differential protein response to PRMT inhibitors upon OOPS. WB profiling of representative proteins, whose MS023/DMSO SILAC protein ratio is summarized in **(A)**, was used to assess the different modulation upon drugs treatment in both WCE and interface fraction: HSP90AA1 and HMGB1 were selected as examples of proteins up-regulated and down-regulated, respectively, in the interface fraction but not in WCE upon MS023; hnRNPH3 was selected as example of protein up-regulated upon MS023 in the interface as consequence of a similar modulation in the WCE; TIA1 was selected as example of protein down-regulated upon MS023 treatment as consequence of a similar modulation in the WCE; NONO and HuR, displaying SILAC protein ratios around 1 in the interface, were selected as loading controls for the interface fraction. Protein abundance in the interface upon different treatments were evaluated upon multiple normalization of band intensities, as described in the

(*Continued*)

FIGURE 4 | Materials and Methods *section.* ***(C)*** *Comparative analysis of proteins identified by OOPS and by RIC-MS experiment. Intersection of the proteins in the interface fraction from OOPS and those identified by RIC-MS allows validating 85 proteins identified in both experiments upon stringent filtering of MS-data (Andromeda score ≥25, at least 2 peptides identified per protein, one of which unique, for each experiment).* ***(D)*** *Western Blot validation of differential protein response to MS023 in the RIC experiment. WB analysis of CCT5 and HMGB1 protein upon MS023 treatment in the RIC experiment confirms their increased and decreased binding to RNA, respectively. Vinculin and HuR were used as loading control for the WCE and the interface, respectively. Protein abundances in the RNA pull-down fraction upon different treatments were evaluated upon multiple normalization of band intensities, as described in the* Materials and Methods *section.*

including 206 proteins (green), and Cluster 4, including 65 proteins (yellow), represent proteins that are overall not changing after pharmacological treatment, with a minor down-regulation observed in Cluster 4. Too few to belong to any specific cluster, we identified MANF and HMGB1, whose level is however significantly down-regulated (-5 and -1 Log_2 SILAC ratio, respectively) in the interface fraction, but not in the WCE, upon both MS023 and GSK591 treatment. This readout suggests that the altered R-methylation level of these two proteins reduces their binding to RNA, with no effect on protein expression. By plotting the MS023\DMSO SILAC ratio of the interface proteins (normalized over the corresponding SILAC ratio in the WCE) in the forward versus the reverse experiment and defining the significant outliers based on the SILAC protein ratio distributions, we identified 76 proteins up-regulated (+1σ) and 4 down-regulated (−1σ) upon MS023 (**Figure 3B**); the same analysis carried out with the GSK591\DMSO SILAC ratio led to the identification of only 4 proteins significantly down-regulated (−1σ), of which 2 were also down-regulated by MS023; no proteins appeared to be up-regulated in the interface fraction with this drug (**Figure 3C**).

Taken together, these results indicate that inhibition of PRMTs type I has a much stronger impact on RBP-RNA interactions than PRMT5 blockage and they corroborate the hypothesis that alteration of ADMA\MMA levels of a set of proteins could be directly involved in the modulation of their interaction with cognate RNAs.

Validation of MS-Proteomics Data Confirms That RNA Interaction of a RBP Subset Is Modulated by Protein Arginine Methyltransferase 1 Inhibition

The proteomics data revealed different protein responses in terms of interaction with RNAs, with more pronounced changes upon PRMT type I inhibition, which affects globally ADMA/MMA balance. We selected some proteins representative of these different responses to validate the SILAC data by WB analysis. NONO and HuR proteins, whose SILAC ratios were unchanged in all fractions upon the two drugs, were profiled as representative of the RBPs whose interaction with cognate RNAs is R-methylation independent (**Figure 4A**); HSP90AA1 and HMGB1 belong to the subset of proteins with significantly modulated (up- and down-regulated, respectively) SILAC ratio in the interface fraction upon treatment with MS023, which was not reflected in the WCE (**Figure 4A**). The WB analysis confirmed their altered levels in the interface fraction when normalized on NONO and HuR levels in the corresponding functional states (**Figure 4B**). On the other hand, hnRNPH3 and TIA1 were selected as examples of proteins whose altered levels in the interface upon drug treatment followed expression changes in the WCE. In particular, hnRNPH3 was up-regulated by MS023 both in WCE and in interface, while TIA1 resulted down-regulated in both fractions (**Figure 4B**). Hence, even if PRMT modulation could partly affect their RNA-protein capability, this change seems mainly a reflecion of their altered expression (**Figure 4B**).

To confirm the more prominent involvement of PRMT1 in governing these dynamics, we used OOPS-WB analysis in HeLa cells which were depleted of PRMT1 upon transfection with two distinct shRNA constructs and a scrambled shRNA, as negative control. OOPS was carried out and selected proteins were WB-profiled in wild-type and PRMT1 KD conditions, both in WCE and interface fraction: the observation of the specific increase of HSP90AA1 and decrease of HMGB1 in the interface when PRMT1 was depleted confirmed the effect observed upon treatment with MS023 and corroborated the OOPS-MS data (**Supplementary Figures S3A,B**).

The OOPS experiment coupled with SILAC and external perturbation allows to enrich for RBPs associated to their cognate RNAs and to assess their dynamic behaviour. This experiment can be used to infer alterations of specific protein-RNA interactions, however, an important limitation is the lack of direct proof of changes in binding of individual proteins with the respective RNA partners. To address this point and corroborate the OOPS-MS data with a complementary method, we performed the RNA Interactome Capture (RIC) experiment, which enables to pull-down poly(A)-RNAs by oligo(dT)-conjugated beads and the co-associated proteins, which are then identified by MS (Castello et al., 2013; Perez-Perri et al., 2018). The RIC approach is complementary to OOPS because it is based on affinity-enrichment and direct protein-mRNA interaction, while OOPS is based on a biochemical fractionation strategy that allows analysing proteins associated also to non-polyadenylated RNAs.

We coupled RIC with triple SILAC labelling upon pharmacological inhibition of PRMT1 and PRMT5. Upon RNA pull-down, protein extraction, digestion, LC-MS/MS analysis and MaxQuant processing of the MS data, we produced a list of 130 RBPs identified in at least one of the two replicates, in the different conditions. Protein SILAC ratios in the RNA-pulldown fraction were normalized over the corresponding SILAC ratios in the WCE used as input, in order to distinguish genuine changes in protein-RNA interactions from mere protein expression alterations (**Supplementary Table S2**).

When the proteins annotated at the interface from OOPS were intersected with the protein list from RIC, we found a rather limited overlap (**Figure 4C**), with 18% of the OOPS proteins also identified in RIC, whose dataset was much smaller. The limited overlap and the dissimilar size of the two proteomes can be

explained in light of the different rationale and biochemical procedure for putative RBP enrichment, whereby RIC enrichement is limited to messenger RNAs while OOPS allow fractionating a broader spectrum of RNAs and the associated proteins, as also reflected by the GO analysis carried out on the two proteomes (**Supplementary Figure S3C**). Despite the limited overlap, we focused on the ratios of the proteins in common: a good proportion of proteins (61 out of 85, corresponding to 71% of the RIC dataset), comprising the hnRNP family proteins, the ribosomal proteins RPS2 and RPS10, NONO and HuR, resulted unchanged both in OOPS and RIC. More interestingly, proteins displaying a reduced level in the OOPS fraction upon MS023, such as MANF and HMGB1, were also found down-regulated in the RIC experiment. Unfortunately, no proteins up-regulated in the OOPS were detected by RIC, so their dynamic behavior could not be validated. To be more explorative and expand the overlap between the OOPS and RIC datasets, we relaxed the filtering criteria applied and considered as valid hits all proteins identified in at least one of the two replicates, removed the Andromeda score>25 and the criterium that, for each protein, the SILAC ratio should be measured both in the interface/RIC and WCE, for normalization. The intersection from these relaxed datasets led to a higher number of proteins in common, from 85 to 108 (**Supplementary Figure S3D**). Among them, the majority (75%) resulted not significantly changed neither in the RIC nor in the OOPS experiments upon drug treatment; the group of significantly down-regulated protein was enriched with 9 proteins (TCEA1, NQO1, HISTH1E, RPL26, RPL7A, RPS27A, RRBP1, H2AFV and FKBP3) in addition to MANF and HMGB1. More importantly, we found the protein RALY, whose dynamic increase upon MS023 was observed in both experiments (**Supplementary Table S2**). As a final confirmation of our results, at least for the protein CCT5 that was up-regulated in the interface upon MS023 but not identified in the RIC-MS experiment, we carried out the WB profiling upon RIC in untreated and drug-treated cells, confirming its increased association with RNA upon type I PRMT inhibition, while the HuR stable behavior served as an additional validation (**Figure 4D**).

Despite the restrains linked to the limited overlap between the two complementary methods, these results support our working hypothesis that -at least for a subset of proteins - the modulation of PRMT1 causes their altered interaction with cognate RNAs, probably through a change of their ADMA\MMA modification level.

RNA Binding Proteins-RNA Dynamics Is Linked to Changes in the Asymmetric-R-Methylation State of RNA Binding Proteins

To understand whether the changes in protein-RNA interactions observed in Cluster 1 and 2 could be linked to possible alteration in the protein R-methylation state, we compared the percentage of protein dynamically modulated by the two inhibitors in the WCE and in the interface fraction: only 12% of the whole proteome is modulated by MS023 while this fraction increases to 21% in the interface fraction (**Figure 5A**). Fisher's exact test applied to these percentages confirmed that the fraction of modulated proteins in the interface is statistically significant ($p < 0.0001$); so, modulation of MMA/ADMA levels seems to affect protein-RNA interactions, beyond mere gene expression effects. Such difference could not be detected when using GSK591, where we even observed a reduction in the proportion of protein modulated by GSK591 in the interface fraction compared to the WCE (2% versus 18%, respectively). Following the same reasoning, we carried out WB profiling of global protein-R-methylation upon MS023 and GSK591 in WCE and interface fraction using pan-antibodies against ADMA, SDMA and MMA. In the WCE, we detected a stronger effect induced by MS023 than by GSK591, measured by an overall stronger reduction of ADMA than SDMA (**Figure 5C**). As previously observed (Eram et al., 2016), inhibition of PRMT type I by MS023 led also to increased MMA (**Figure 5B**) that paralleled ADMA reduction; this can be interpreted as the result of the substrate scavenging effect by other enzymes when PRMT1 is blocked (Dhar et al., 2013) (**Figure 5B**). Interestingly, overall changes in global ADMA, SDMA and MMA upon the two drugs were more marked in the interface fraction than in the WCE, which -in our opinion- indicates that RBPs enriched in this fraction are overall more R-methylated and that their R-methylation state is more modulated.

We then asked how many of the proteins regulated by MS023 in the OOPS experiment are annotated as R-methylated, using as experimental references both the protein post-translational modification database PhosphositePlus (Hornbeck et al., 2015) and our in-house experimentally annotated high-confidence methyl-proteome (*manuscript in preparation*): 51 out of 103 (49.5%) proteins modulated in the WCE and 59 out of 77 proteins (76.6%) modulated in the interface fraction, respectively, are annotated as R-methylated (**Supplementary Figure S3A**). Fisher's exact test calculated on these percentages confirmed that the enrichment of R-methyl-proteins within the interface modulated proteins is statistically significant ($p < 0.0001$), which supports the idea that the changes in the RBP-RNA interaction observed are *bona fide* mechanistically linked to their R-methylation state. To validate the R-methylation state of representative RBPs, we performed the immunoprecipitation (IP) of 14-3-3 and LDHB proteins followed by probing their R-methylation state with pan-antibodies against ADMA, SDMA and MMA. In the PhosphositePlus database, 14-3-3 and LDHB proteins are annotated as R-monomethylated, and indeed MMA of both proteins resulted modulated upon MS023 treatment, in line with our proteomics evidence from OOPS, that was interpreted as an altered interaction with RNA, whereas the detection of asymmetric and symmetric R-di-methylation was ambiguous or unchanging upon drug treatments (**Figures 5D,E**). Overall, these data indicate that, at least for the set of proteins inspected, the observed change in their RNA-interaction is linked to an alteration of their R-methylation, triggered by PRMT pharmacological inhibition.

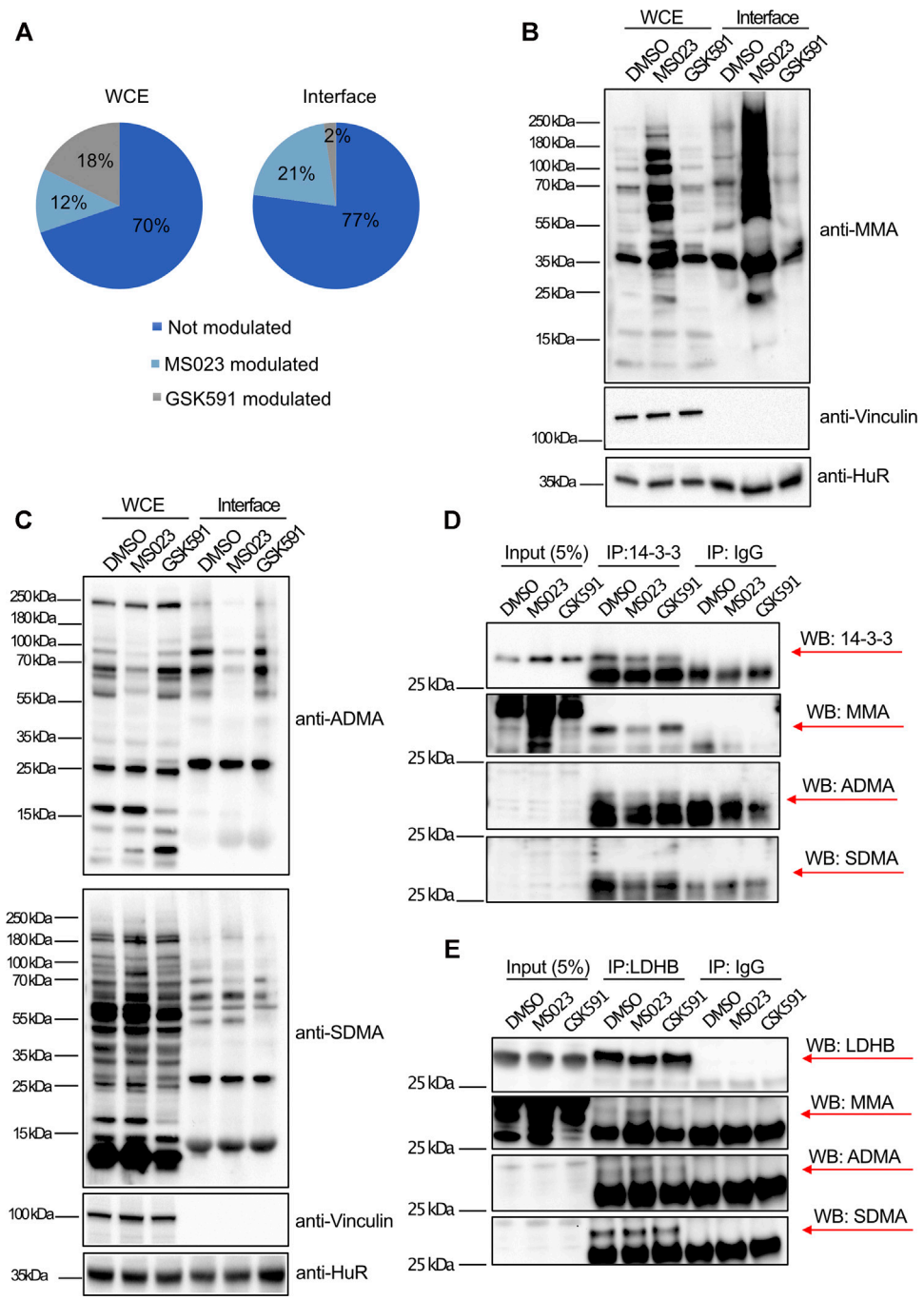

FIGURE 5 | Interface-enriched protein dynamic binding to RNA is associated to their R-methylation state. **(A)** Percentage of protein modulated in response to PRMT inhibitors. Percentage of protein significantly modulated (±1σ) was calculated in dependence of MS023 or GSK591 treatment, both in WCE and interface fraction. In the WCE the two treatments equally modulate protein expression (12% regulated by MS023 and 18% by GSK591, respectively), whereas in the interface fraction, RBP-RNA interactions are almost exclusively regulated by MS023 treatment (21% regulated by MS023 and 2% regulated by GSK591, respectively). **(B)** WB profiling of dynamic regulation of global protein R-mono-methylation (MMA). WB was carried out on aliquots of WCE and interface fraction in control DMSO and upon MS023 and GSK591. Vinculin and HuR protein were used as loading control for WCE and interface, respectively. **(C)** WB profiling of dynamic regulation of protein asymmetric R-di-methylation (ADMA) and symmetric R-di-methylation (SDMA). WB analysis was carried out on aliquots of WCE and interface fraction in control DMSO and upon MS023 and GSK59. The same membrane was first probed with anti-ADMA antibody, then stripped and used to detect SDMA. Vinculin and HuR protein were used as loading control for WCE and interface, respectively. **(D)** Protein immunoprecipitation (IP) followed by WB validation of the R-methylation state of 14-3-3 proteins as representative for MS023-modulated RBPs in the OOPS. The R-methylation states of 14-3-3 protein was assessed upon DMSO, MS023 or GSK591 treatment by protein IP followed by probing with the anti-pan-methyls antibodies against MMA ADMA and SDMA. IgG were used as mock controls for IP. For 14-3-3 proteins MMA is clearly detectable, while ADMA and SDMA signals are ambiguous, due to the cross-contaminating signals of the light chains of denatured antibodies. **(E)** Protein IP

(*Continued*)

FIGURE 5 | followed by WB validation of the R-methylation state of LDHB protein as representative for MS023-modulated RBPs in the OOPS. The R-methylation states of LDHB protein was assessed upon DMSO, MS023 or GSK591 treatment by protein IP followed by probing with anti-pan-methyl antibodies against MMA ADMA and SDMA. IgG was used as mock control for IP. MMA and SDMA are clearly detectable, while the ADMA signal is ambiguous, due to the cross-contaminating signals of the light chains of denatured antibodies.

Modulation of the ADMA/MMA Balance but Not of SDMA Induces Phase-Separation of Candidate RNA Binding Proteins

Based on the data acquired and in light of published evidence that reduction of ADMA can induce changes in the subcellular localization of some RBPs and-in some cases-also their aggregation and LLPS, we intersected the list of proteins dynamically regulated in the interface fraction upon MS023 with two available databases of proteins undergoing LLPS: the Phase Separation Database (PhaSepDB) (You et al., 2020) and the RNA Granule Database (http://rnagranuledb.lunenfeld.ca/). This comparison revealed that 42 out of 77 (54.5%) proteins are indeed annotated as capable to phase-separate (**Figure 6A**). Among them, we selected LDHB, 14-3-3 proteins and CDC37 to verify their capability of undergoing phase-separation in response to MS023 treatment. To do so, we followed their subcellular localization by immuno-fluorescence (IF) analysis and assessed their co-localization with both cognate RNAs and the SGs marker G3BP1 (Yang et al., 2020; Wheeler et al., 2016). While proteins were IF-profiled by antibodies, RNA was labelled using the "click" chemistry strategy to incorporate the uridine analog 5-ethynyluridine (EU) into RNA from differentially treated cells, so that EU-labelled RNA could be detected by IF (Jao and Salic, 2008). IF analysis showed that MS023 treatment induces cytosolic aggregates in which the proteins under investigation co-localize with both G3BP1 and EU-labelled RNA (**Figure 6B** and **Supplementary Figure S4A**, respectively); such aggregates were overall not observed (or detected to a much lower extenet) when cells were treated with either DMSO or GSK591. Remarkably, MS023-induced granules were disassembled upon treatment with 1,6-Hexanediol, an alcohol widely used for solubilisation of MLOs (Duster et al., 2021), which confirms the phase-separation origin of these RNPs. As further control, we also profiled the subcellular localization of LDHB and 14-3-3 proteins upon $NaAsO_2$, a compound well-known to induce SGs formation: as expected, stronger and more numerous G3BP1-stained MLOs were formed upon $NaAsO_2$ treament, which remarkably displayed co-localization with our proteins of interest and RNA. Also in this case, the disassembly of such granules by 1,6-Hexanediol confirmed their nature as MLOs.

Unbiased and automatic quantification analysis of IF images demostrated an increase of the percentage of cells displaying at least one of these RNP granules per cell, both in MS023 and $NaAsO_2$ conditions, and that such granules are completely abolished upon incubation with 1,6-Hexanediol (**Figure 6C** and **Supplementary Figure S4A**). Morevoer, a statistically significant increase of co-localization percentage of the candidate RBPs with G3BP1 in the granules was measured after MS023 and $NaAsO_2$ compared to DMSO; GSK59 instead did not lead to such increase of co-localising granules.

Collectively, these results corroborate our hypothesis that the MS023-triggered alteration of R-methylation state of specific RBPs leads to their increased interaction with cognate RNAs which-in turn-favors their tendency to undergo LLPS and generate MLOs.

DISCUSSION

Through a quantitative proteomics approach, we have described that modulation of protein-R-methylation, and in particular of ADMA/MMA, can affect protein-RNA interactions and that this process is linked to the capability of some RBPs to undergo LLPS. The pharmacological modulation of PRMTs type I was achieved by treating cells with the small molecule MS023, whereas the selective inhibition of PRMT5 was obtained using GSK591 compound. It is generally accepted that PRMT1 is the most active among the type I family and that PRMT1 is the most inhibited enzyme at the concentrations of MS023 used in this study, as also confirmed by the unchanged levels of H3R2me2a and H3R17me2a, known targets of PRMT6 and PRMT4/CARM1, respectively, observed upon drug treatment (**Supplementary Figure S1E**). Obviously, while we cannot completely rule out the involvement in the regulation of RBP-RNA interaction dynamics of other members of the PRMTs type I family-such as PRMT2, PRMT3, and PRMT8- the observation that PRMT1 knock-down recapitulates the molecular effect observed upon MS023 is a futher corroboration of the key role played by this enzyme (**Supplementary Figures S3A,B**). However, substrate scavenging has also been observed among different PRMTs, in particular when PRMT1 is blocked, with consequent release of its preferential target sites (Dhar et al., 2013). Hence, more systematic studies will be needed to understand whether other enzymes of the family are involed in this specific cellular process.

In the last years, several biochemical strategies have been introduced for RBP-RNA complexes enrichment, which can be classified in two main groups: RNA-centric and protein-centric strategies (Ramanathan et al., 2019). The former group of methods includes RNA immunoprecipitation (RIP), RNA interactome capture (RIC) (Perez-Perri et al., 2018), RNA interactome using click chemistry (RICK) (Bao et al., 2018), click chemistry-assisted RNA interactome capture (CARIC) (Huang R. et al., 2018) and cross-linking and immunoprecipitation (CLIP) approach, with its variants (HITS-CLIP, iCLIP, eCLIP and PAR-CLIP) (Ule et al., 2018). The majority of these methods includes a step of poly(A)-RNAs capture via hybridization to oligo(dT) beads under denaturing conditions, with proteins directly bound to poly(A)-RNAs co-enriched and then identified by MS. This

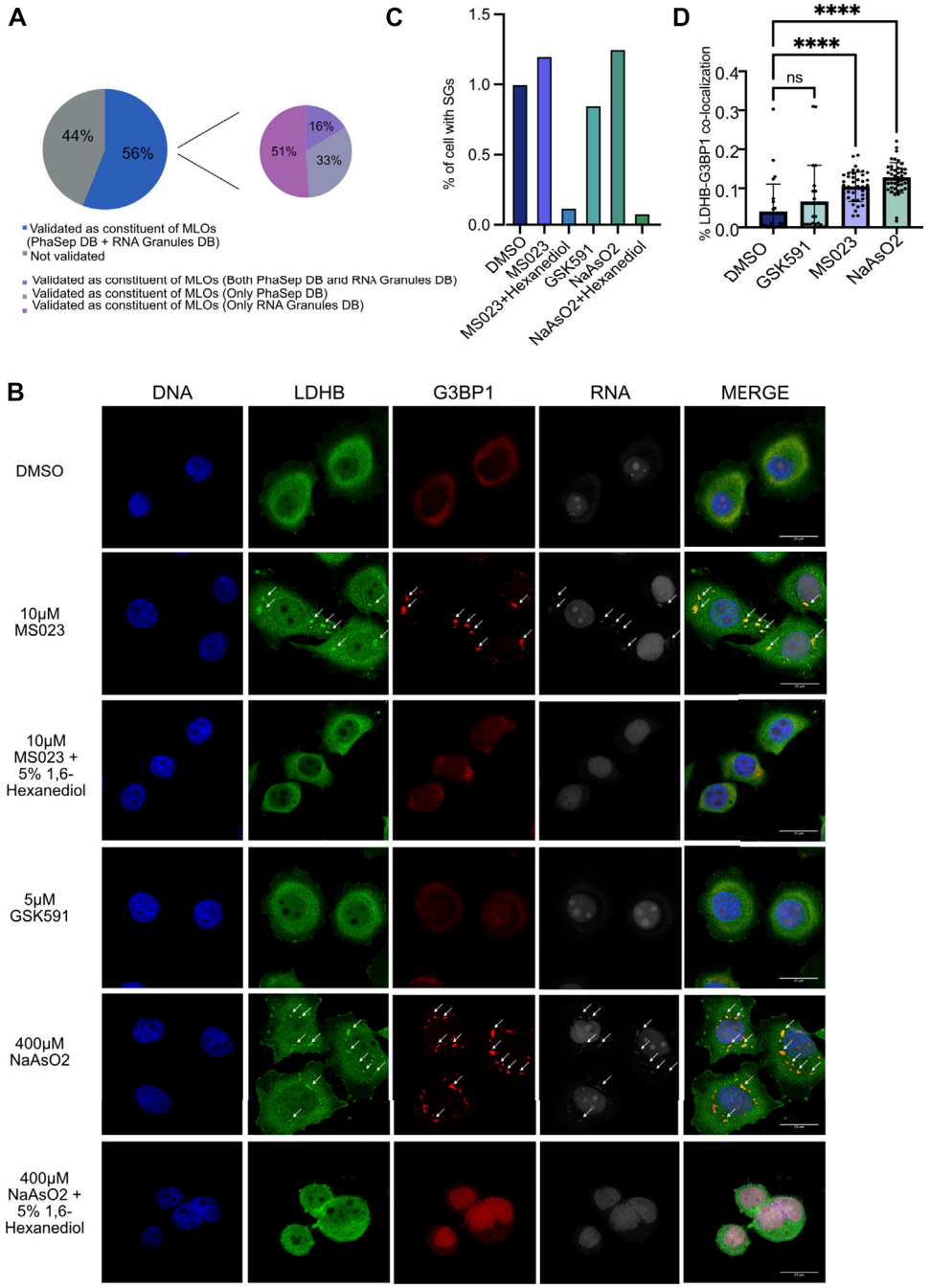

FIGURE 6 | MS023 treatment induces LLPS of candidate RBPs. **(A)** Tendency of MS023-modulated RBPs to undergo LLPS. Among the 77 proteins up-regulated in the interface fraction upon MS023, 43 (56%) were also annotated as proteins undergoing phase separation in at least one of the two PhaSepDB (http://db.phasep.pro/) and RNA Granules DB (http://rnagranuledb.lunenfeld.ca/) databases. Among them, 16% were annotated in both databases, 33% were annotated only in PhaSepDB and 51% were annotated only in RNA Granules DB. **(B)** Immunofluorescence (IF) analysis of LDHB in basal condition (DMSO) and in response to different treatments. Representative IF image shows LDHB protein subcellular localization in HeLa cells treated with the following compounds: DMSO, 10 μM MS023 and 5 μM GSK591 for 48 h; 10 μM MS023 for 48 h, followed by 10 min treatment with 5% 1,6-Hexanediol; 400 μM $NaAsO_2$ for 30 min, or 400 μM $NaAsO_2$ for 30 min followed by 10 min-treatment with 5% 1,6-Hexanediol. Immunostaining of RNA was performed with the Click-iT™ RNA Alexa Fluor™ 594 Imaging Kit. DAPI staining was used for nuclei visualization (DNA). G3BP1 staining was used as positive control for SGs formation. DAPI, LDHB, G3BP1 and RNA staining and the respective merged images are displayed. Images were taken by SP8 confocal microscopy using a 60× oil objective, and a scale bar of 25 μM are included in the merged figure. Arrows indicate co-localization of target RBP, G3BP1 and RNA. **(C)** Bar-graph representation of the percentage of cells with stress granules. The bar-graph shows the percentage of cells with at least 1 G3BP1-positive stress granule (SG) for the different conditions; all the treatments were normalized over DMSO. **(D)** Bar-graph representation of the percentage of LDHB-G3BP1 co-localization. The image describes the percentage of co-localization between G3BP1 and LDHB in the SGs in each condition. All the treatment were normalized over the DMSO. Statistical significance was calculated by Student't Test (* = p <0.05).

limits these approaches to poly(A)-RNAs, excluding bacterial or eukaryotic non-polyadenylated RNAs, as also observed in our study, where we detected a sensibly smaller number of proteins more strongly associated to functional processes linked to mRNAs than what obtained by OOPS (**Figure 4C** and **Supplementary Figure S3C**). Moreover, these strategies are difficult to scale up for system-wide RBPs analyses and for multiplexed profiling in dynamic conditions. The latter group comprises protein-centric methods that are based on the biochemical separation of RNP complexes using the principle of chemical phase partition, where RNAs and proteins are physically co-enriched and then separately analyzed by RNA-seq and LC-MS/MS, respectively. Among them, three very similar methods have been described: XRNAX (Trendel et al., 2019), PTex (Urdaneta et al., 2019) and OOPS; the last one was adopted in this study and coupled with PRMT inhibitor treatment to assess RNPs dynamics in dependence of protein-R-methylation. We slightly modified the published biochemical workflow of the OOPS to include a step of HpH-RP-chromatography after tryptic digestion of the interface-enriched proteins and prior to MS analysis. The efficacy of the HpH-RP-fractionation was assessed during the optimization phase of the experiment, by comparing the number of proteins identified from the interface, with or without the introduction of this step (**Supplementary Figure S1G**). While its introduction led to a significant increase of the protein identification rate, most likely by simply increasing peptide separation prior to MS detection, clearly it did not outcompete the number of proteins identified by (Queiroz et al., 2019), in which multiple experiments were pooled to generate the reference dataset.

The comparison of our experimental list of interface proteins annotated by OOPS with the EuRBPDB (Liao et al., 2020) and the Quieroz et al. datasets indicates 85.5% proteins in common, so that we can *bona fide* state that our dataset is a good representation of the known RBPome. Among the 14.5% non-overlapping proteins, we found essentially three protein categories by GO analysis: 1) a set of proteins recognized as RNA-binding, or somehow related to RNA-based process, such as CDK11A, GNB2L1 and ATP5A1; they are *bona fide* novel RBPs that could be added to the RBPome databases; 2) a group of "structural" and highly abundant proteins -such as TUBB8, LAMB1 and ACTC1- which are probable contaminants; 3) a set of proteins related to protein-phosphorylation which could be functionally linked to R-methylation because of the known crosstalk between these two PTMs (Chen et al., 2016; Liu et al., 2020; Smith et al., 2020). Domain enrichment analysis of the protein found in the interface fraction confirms the over representation of several RBDs: the RRM, the DDX and the KH domains. Sequence analysis of the interface proteins confirmed that RGG motif is enriched in this fraction, in line with data describing RG\RGG domains as preferred substrate recognition motifs for PRMTs and able to promote RNA binding (Castello et al., 2016), which set foundations to the hypothesis underlying this study. Clustering analysis of the experimental proteomics data allow quantifying a protein subset in the interface fraction significantly enriched upon MS023 treatment but with no changes at the expression level: remarkably, >75% of them resulted as R-methylated upon intersection with a datasets of experimentally-validated methyl-proteins (**Supplementary Figure S3A**). While the WB validation confirmed the MS-data, it is important to keep in mind that SILAC-MS analysis provides a much more accurate quantification of proteins than WB; hence, minor variations in proteins levels among different functional states detected by proteomics could be missed by antibody-based approaches.

A protein-protein interaction analysis by Cytoscape (https://cytoscape.org/) carried out on the MS023-regulated RBPs from the interface produced a high-density network in which each protein interacts at least with another partner within the same group (**Supplementary Figure S3B**). Interestingly, the RBPs with higher node degrees, such as HSP90AA1, HSP90AB1, YWHAE or TCP1, were also those displaying the higher SILAC ratios upon MS023 treatment. These results suggest that -by applying the OOPS protocol- we may enrich not only for proteins directly interacting with RNAs, but also for some of their co-interactors: for instance, HSP90AA1, HSP90AB1, and CDC37 are reported to belong to the same pathway and were shown to physically interact (Zuehlke et al., 2015; Haase and Fitze, 2016). Upon proteomics analysis, we experimentally demonstrated that LDHB, CDC37 and 14-3-3 proteins (RBPs whose association with RNA is MS023-dependent) are also capable to form MLOs and co-localize with G3BP1 and RNA into RNPs, under pharmacological treatment. This evidence of a link between protein-R-methylation, RNP dynamics and LLPs is not surprising in light of the fact that the majority of proteins found in the interface are enriched in RGG/RG motifs, which are over-represented in disordered regions and contribute to conferring phase-separating capability (Chau et al., 2016; Huang L. et al., 2018; Chong et al., 2018; Qamar et al., 2018; Mersaoui et al., 2019; Huang et al., 2020; Kawahara et al., 2021). It is however, notable that our proteomics approach suggested novel candidate proteins involved in this physicochemical process. Interestingly, MLOs have been recently suggested to play roles in cancer chemo-resistance (Loll-Krippleber and Brown, 2017; El-Naggar and Sorensen, 2018; Zhan et al., 2020). An attractive perspective is to investigate wether they can be targeted to counteract tumor chemo-resistance, by impairing their capability to undergo LLPs and form MLOs.

MATERIALS AND METHODS

Cell Culturing and Stable Isotope Labelling with Amino acids in Cell Culture Labelling

HeLa cells were cultured in Dulbecco's modified Eagle's medium (DMEM) already including 1% glutamine and supplemented with 10% fetal bovine serum (FBS; Life Technologies), penicillin (100 U/ml), and streptomycin (100 mg/ml). Cells were cultured at 37°C in a 5% CO2 humidified atmosphere. The cells were tested free of mycoplasma contamination. MS023 was purchased from Cayman chemicals; GSK591 was purchased from Sigma Aldrich. Both MS023 (10 μM) and GSK591 (5 μM) were used for 48 h treatment, together with DMSO as control. For triple SILAC, HeLa were grown in "Light", "Medium" and "Heavy" SILAC DMEM (Thermo

Fisher Scientific), supplemented with either L-Arginine, L-Lysine or their medium (Arg6: Sigma-Aldrich; Lys4: Sigma-Aldrich) or heavy (Arg10: Sigma-Aldrich; Lys8: Sigma-Aldrich) isotope-counterparts. Arginine and Lysine were added at a concentration of 84 mg/L and 146 mg/L, respectively. SILAC media were supplemented with 10% dialyzed FBS (GIBCO, Life Technologies), 100 U/ml Penicillin and 100 mg/ml Streptomycin. HeLa cells were grown in the respective heavy-isotopes containing media for at least 9 replication cycles, to ensure full incorporation of isotope-encoded amino acids, with a careful monitoring of growth rate, viability and overall morphology, to guarantee that normal cell physiology was preserved.

Orthogonal Organic Phase Separation Experiment

The OOPS protocol was applied as described in (Queiroz et al., 2019), with adjustments based on the specific biological question to be addressed. Briefly, HeLa cells were exposed to UV (254 nm) at a dose of 40 J/m2 using a Stratalinker 2400 UV cross-linker (Stratagene, La Jolla, CA). Immediately after crosslinking, cells were scraped in 1 ml Trizol™(Fisher Molecular Biology) and transferred to an Eppendorf tube; for biphasic extraction, 200 µl of chloroform (Fisher Scientific) were added, phases were vortexed and centrifuged for 15 min at 12,000 x g at 4°C. The lower organic phase (containing non-crosslinked proteins) was transferred to a new Eppendorf tube and proteins precipitated by addition of 9 volumes of propan-2-ol (Fisher Scientific). The interface fraction (containing the Protein-RNA complexes) was subjected to two additional phase separation cycles and precipitated by addition of 9 volumes of propan-2-ol. The precipitated interface fraction was resuspended in 100 µl of RNA digestion buffer (100 mM TEAB, 1 mM $MgCl_2$, 1% SDS) incubated at 95°C for 20 min, cooled down and digested with 4 µg RNase A, incubating overnight at 37°C. The following day, after a final Trizol™-chloroform phase partition, proteins in the organic phase were precipitated by addition of 9 volumes of propan-2-ol and resuspended in urea lysis buffer (9 M urea, 20 mM Hepes (pH 8.0)).

Protein Sample Preparation Prior to MS and LC-MS/MS Analysis

Two independent SILAC based-proteomics experiments were carried out with swapped SILAC channels (Forward and Reverse experiments), both for the whole cell extracts and the interface fractions. For each SILAC experiment, equal numbers of light-, medium- and heavy-labeled HeLa cells differentially treated with either DMSO or PRMT inhibitors were mixed in a 1:1:1 ratio, pelleted and washed twice with PBS. For preparation of the WCE, cell pellets were lysed in urea lysis buffer (9 M urea, 20 mM Hepes (pH 8.0)) supplemented with 1× protease and phosphatase inhibitors cocktail (Roche), sonicated and cleared by ultracentrifugation (20,000g for 15 min at 15°C). For the RBPome, the protein extract was already resuspended in Urea lysis buffer, following OOPS strategy. For in-solution digestion, 200 µg of proteins were reduced by adding 4.5 mM dithiothreitol (DTT) (Sigma-Aldrich) for 30 min at 55°C, alkylated with 5.5 mM iodoacetamide (10% (v/v) for 15 min at RT in the dark; Sigma-Aldrich), and digested overnight with sequencing-grade trypsin (1:100 (w/w); Promega) after a four-fold dilution in 25 mM ammonium bicarbonate solution. Protease digestion was terminated by the addition of 1% trifluoroacetic acid (TFA) to adjust pH < 3. Debris was removed by centrifugation for 15 min at 1780g at RT. Peptides were dried with a vacuum concentrator, re-suspended into 300 µl of 0.1% TFA and off-line High pH fractionated by Pierce™ High pH Reversed-Phase Peptide Fractionation Kit (Thermo Fisher scientific). Eluted fractions were dried with vacuum concentrator and resuspended in an aqueous 0.1% TFA solution prior to analysis by LC-MS/MS.

Nano-LC-MS/MS Analysis

Peptide mixtures were analyzed by online nano-flow LC-MS/MS using an EASY-nLC 1000 (Thermo Fisher Scientific, Odense, Denmark) connected to a Q Exactive instrument (Thermo Fisher Scientific) through a nano-electrospray ion source. The nano-LC system was operated in one column set-up with a 50-cm analytical column (75 mm inner diameter, 350-mm outer diameter) packed with C18 resin (EasySpray PEPMAP RSLC C18 2M 50 cm × 75 M, Thermo Fisher Scientific) configuration. Solvent A was 0.1% formic acid (FA) and solvent B was 0.1% FA in 80% ACN. Samples were injected in an aqueous 0.1% TFA solution at a flow rate of 500 nl/min. Peptides were separated with a gradient of 5–40% solvent B over 90 min, followed by a gradient of 40–60% for 10 min and 60–80% over 5 min at a flow rate of 250 nl/min in the EASY-nLC 1000 system. The Q Exactive was operated in the data-dependent acquisition (DDA) mode to automatically switch between full scan MS and MS/MS acquisition. Survey full scan MS spectra (from m/z 300-1150) were analyzed in the Orbitrap detector with resolution R = 35,000 at m/z 400. The 15 most intense peptide ions with charge states 2+ were sequentially isolated to a target value of 3×10^6 and fragmented by Higher Energy Collision Dissociation (HCD), with a normalized collision energy setting of 25%. The maximum allowed ion accumulation times were 20 ms for full scans and 50 ms for MS/MS and the target value for MS/MS was set to 10^6. The dynamic exclusion time was set to 20 s.

MS Raw Data Processing for Protein Identification and Quantification

MS raw data were analyzed with the integrated MaxQuant software v1.6.2.10, using the Andromeda search engine (Cox et al., 2011; Tyanova et al., 2016). The 2020_06 version of the UniProt Human sequence database (UP000005640) was used for peptide identification. In MaxQuant, the estimated FDR of all peptide identifications was set to a maximum of 1%. The main search was performed with a mass tolerance of 4.5 parts per million (ppm). Enzyme specificity was set to Trypsin/P. A maximum of three missed cleavages was permitted, and the minimum peptide length was fixed at seven amino acids. Carbamidomethylation of cysteine was set as a fixed modification. To assign and quantify SILAC methyl-peptides, all MS raw data were processed indicating N-terminal acetylation, Methionine oxidation, mono-methyl-K/R, and di-methyl-K/R as variable modifications. The MaxQuant proteinGroups.txt output

file was then filtered: potential contaminants and reverse sequences were removed, and proteins were required to be identified by at least 2 peptides, one of which unique, and to have an Andromeda score ≥25. Last, proteins SILAC H/L and M/L ratios in the interface were normalized on the respective protein SILAC H/L and M/L ratios in WCE, both extracted from the proteinGroups.txt MaxQuant output file. This normalization allowed to discriminate between changes of protein level within the interface fraction (as the hypothetical consequence of a different interaction with cognate RNAs) and the mere protein expression changes following transcriptional changes induced by pharmacological inhibition of PRMTs.

Functional Analysis for Characterization of the Interface

Gene Ontology enrichment analysis was performed with GOrilla and Revigo (Eden et al., 2009; Supek et al., 2011). Analysis of protein-protein interaction network and analysis of protein domains were carried out through the STRING plugin of Cytoscape (Shannon et al., 2003; Szklarczyk et al., 2019).

Motif Analysis

Motif analysis was performed using the pLogo web application (O'Shea et al., 2013). For each R in the human proteome, a 5-amino acid sequence window centered on that R was extracted from the 2020_06 version of the SwissProt human database. Sequence windows from proteins in the interface and in the WCE were then provided to pLogo as foreground sequences, while sequence windows from the remaining proteins were used as background.

Statistical Analysis of the Stable Isotope Labelling with Amino acids in Cell Culture -Based Quantitative Proteomics Data

To define up- or down-regulated proteins by MS023 or GSK591, we used mean (μ) and SD (σ) based on the distribution of the proteins SILAC ratios calculated separately in the forward and reverse experiments for the DMSO condition and applied a μ±1σ cutoff to the protein ratio distributions in each replicate. To determine whether the abundance of the interface proteins was significantly affected by PRMT inhibitors compared to their expression level in the corresponding whole cell extracts, Fisher's exact tests were performed with Python SciPy package. Clusters of regulated proteins were defined with Ward's method (Ward, 1963).

Western Blot Analysis

For Western Blot analysis, protein extracts were lysed in urea lysis buffer (9 M urea, 20 mM Hepes (pH 8.0)), supplemented with 1× cocktail of proteases and phosphatase inhibitors (Roche) from HeLa cells and quantified by BCA assay (Pierce BCA Protein assay kit). Equal protein amounts were separated by SDS-PAGE electrophoresis and transferred on Transfer membrane (Immobilon-P, Merck Millipore) by wet-transfer method. Membrane blocking with 10% BSA/TBS 0.1% Tween-20 for 1 h at RT was followed by overnight incubation with the primary antibodies and subsequently with the HRP-conjugated secondary antibodies, for 1 h (Cell Signaling Technology). Proteins were detected by ECL (Bio-Rad). The following primary antibodies were used: anti-vinculin (V9131, 1:5000) was purchased from Merk Life Science; anti-RPS2 (A303-794A, 1:5000), anti-CCT5 (A300-421A 1:5000), anti-LDHB (A304-7070A 1:5000) and anti-PRMT4 (A300-421A 1:5000) were purchase from Bethyl Laboratories; anti-NONO (SC-376865, 1:500), anti-hnRNPH3 (SC-376416, 1:500) and anti-alpha-tubulin (SC-32293, 1:1000) were purchase from Santa Cruz Biotechnology; anti-HSP90AA1 (AB2928, 1:1000), anti-HuR (AB136542, 1:1000), anti-HMGB1 (AB79823, 1:5000), anti-TIA1 (AB140595, 1:2000), anti-H4R3me2s (AB5923, 1:1000), anti-H3R2me2a (AB9147061:1000), anti-H3R17me2a (AB8284 1:1000), anti-PRMT6 (AB 47244 1:1000) and anti-total histone 4 (AB7311 1:2000) were purchase from Abcam; anti-H4R3me2a (61988, 1:500) was purchase from Active Motifs; anti-ADMA (ASYM24 07-414, 1:1000) and anti-SDMA (SYM10 07-412, 1:2000) were purchase from Millipore; anti-MMA (D5A12; 1:1000) was purchase from Cell Signaling Technology; anti-pan -14-3-3 (MA5-1224, 1:2000) was purchase from Thermo Fisher Scientific.

Protein Arginine Methyltransferase 1 Knock-Down by shRNA

PRMT1 knock-down (KD) in Hela cells was obtained using a second-generation pLKO lentiviral vectors, in which two distinct shRNAs targeting PRMT1 were cloned:

5′-CCGGCAGTACAAAGACTACAA-3′ (sh#1, PRMT1), 5′-GTGTTCCAGTATCTCTGATTA-3′ (sh#2, PRMT1).

The pLKO scamble shRNA was used as negative control. To obtain PRMT1 depletion, HeLa cells were transduced using lentiviruses whose stocks were produced by transient $CaCl_2$ transfection of HEK293 cells with the packaging plasmid pCMV-DR8.74, the envelope plasmid pMD2G-VSVG and the respective transfer gene-carrying vector. After 48 h from transfection, the supernatant containing the virus was ultra-centrifuged and added to the HeLa medium. Transduced Hela cell were then selected by incubation with 1 μg/ml puromycine for 48 h and subsequent used for the downstream applications.

RNA Interactome Capture (RIC) Experiment Followed by Mass Spectrometry Analysis or Western Blot Profiling

The RNA pull-down was performed as described in (Castello et al., 2013). Briefly, SILAC-labelled HeLa cells were treated with DMSO or MS023 10 μM or GSK591 5 μM for 48h and then were harvested and UV-crosslinked at 254 nm at a dose of 40 J/m2 using a Stratalinker 2400 UV cross-linker (Stratagene, La Jolla, CA). A small aliquot (corresponding to about 10%) of sample from each treatment was saved for WB analysis while the remaining was mixed in 1:1:1 proportion with samples from the other conditions. Cell were then lysed and poly(A)-mRNAs were pulled down 3 times (each time using the flow-through from the previous pull-down) using Dynabeads® Oligo $(dT)_{25}$ (Thermo Fisher Scientific).

Poly(A)-mRNA-associated proteins were eluted from the beads following the manufacturer's instruction and subsequently processed by in-solution digestion prior to LC-MS/MS.

WB profiling of candidate proteins from OOPS and RIC were also carried out for validation of the quantitative MS-proteomics data. For the WB analysis each band intensity in each condition was measured with FiJi software (http://www.yorku.ca/yisheng/Internal/Protocols/ImageJ.pdf) and subsequently normalized at four different leves:

1. In the WCE, each band was normalized on the vinculin as loading control;
2. In the interface or RIC fractions, each band was normalized on HuR or NONO, selected as loading controls for the interface/RIC, because they resulted unchanging from quantitative proteomics analyses;
3. For each treatment, the intensity in the interface/RIC was normalized over the corresponding in the WCE, to discern the different abundance within these fractions from mere protein expression changes;
4. After the previous three normalizations, the intensity for each treatment was normalized over DMSO.

Protein Immunoprecipitation

Protein immunoprecipitation (IP) was performed starting from 500 µg of HeLa cell extract, 5% of cell extract was loaded as input. Briefly, 30×10^6 HeLa cells were harvested, washed twice with cold PBS and re-suspended in 2 volumes of RIPA Buffer (10 mM Tris pH 8, 150 nM NaCl, 0.1% SDS, 1% Triton X-100, 1 mM EDTA, 0.1% Na-Deoxycholate,1 mM PMSF,1 mM DTT and 1x Proteases and Phosphatase Inhibitors cocktail (Roche), supplemented with 10K U of Benzonase (Merck Life Science). The suspension was rotated on wheel for 45 min at RT (vortexing every-10 min), centrifuged at 12.000 g for 1 h at 4°C and the supernatant was transferred into a new Eppendorf tube; proteins were quantified by BCA colorimetric assay (Pierce BCA Protein assay kit). The protein lysate was rotated at 4°C overnight with 8 µg of anti-pan -14-3-3 (MA5-1224 Thermo Fisher Scientific) or 5 µg of anti-LDHB (A304-770A Bethyl Laboratories) each for 500 µg of protein extract. In parallel, G-protein-coupled magnetic beads (Dynabeads, Thermo Fisher Scientific) were blocked with a blocking solution (0.5% BSA in TBS supplemented with 1% Triton X-100) and rotated at 4°C overnight. The following day, the beads were added to the lysate in 1:100 proportion with a primary antibodies and incubated for 3 h at 4°C on a wheel; the captured immuno-complexes were washed 4 times with the RIPA Buffer and then incubated for 10 min at 95° with LSD sample Buffer supplemented with 100 mM DTT in order to elute the immunoprecipitated proteins for subsequent analyses.

Confocal Immunofluorescence Experiments

Cells were plated on glass coverslips for 24 h and grown with DMSO or 10 µM MS023 or 5 µM GSK591 for 48 h or 400 µM $NaAsO_2$ for 30 min and 0.8 mM modified uridine (EU) for 48 h. For MS023 and $NaAsO_2$ tretaments, each experiment was carried out in duplicate and one of the two experiments was subsequently treated with 5% 1,6-Hexanediol for 10 min. Then, cells were washed with 1x PSB, fixed in 4% paraformaldehyde for 20 min at RT, permeabilized with 0.1% Triton X-100 in PBS for 5 min on ice and the "click" reaction was carried out to conjugate the incorporated EU with Alexa 594 Fluor according to the manufacture instruction (Click-iT™ RNA Alexa Fluor™ 594 Imaging Kit, Thermo Fisher Scientific). Then, cells were incubated with 2% BSA in PBS for 30 min at RT and subsequently with the primary antibody in PBS containing 2% BSA overnight at 4°C. After being washed, the primary antibodies were removed and cells were incubated with the antibody anti-G3BP1 (BD 611126 1:400) for 3 h at RT. After three additional washes, cells were stained with Rabbit Alexa Fluor 488 secondary antibody (for the protein of interest) or with Mouse Alexa Fluor 647 secondary antibody (for G3BP1) (Molecular Probes, Eugene, OR, United States), both diluted 1:400 in PBS containing 2% BSA for 1 h at RT. Nuclei were stained with DAPI (Invitrogen). Images were acquired with a Leica TCS SP8 confocal microscope (Leica Microsystems, Heerbrugg, Switzerland).

Confocal Imaging and Analysis

To evaluate the percentage of cells with stress granules, samples were acquired with a Nikon CSU-W1 spinning disk using a 60X/1.4NA objective lens, a 50 um-pinhole disk, solid state lasers, a multiband dichroic mirror and a fast-rotating emission filters wheel. Eighty-one fields of view (FOV) were automatically acquired for each sample with an autofocus routine on the DAPI channel. A Z-stack of 7 optical sections with a step size of 0.6 µm together with the emissions from the 4 fluorophores (DAPI, AlexaFluor488, AlexaFluor594 and AlexaFluor647) were acquired in each FOV with a pixel size of 108 × 108 nm (2048 × 2048 pixels per FOV). The acquired images were analysed with a custom-made FiJi/ImageJ (Schindelin et al., 2012) macro. Briefly, the DAPI channel was used to identify the relevant area of each cell (cell area) using the Voronoi filter on the maximum intensity projections. In each cell area the presence of a nucleus was evaluated, and the cell areas without any nucleus or with more than one, were discarded. Then, a band of 12 microns was created around each nucleus (cytoplasmic area), the G3BP1 signal was used to segment the stress granules using a fixed threshold in all samples and the objects inside the cytoplasmic area (stress granules) were counted in each cell. For each sample, the number of cells with at least one stress granule was considered. To evaluate the colocalization between G3BP1 and the RBP signals, single optical sections per sample were acquired with a Leica SP8 laser scanning confocal microscope equipped with a 405 nm and 561 solid state lasers, an Argon and a HeNe lasers, Hybrid detectors and a motorized stage. More than 15 FOV per sample were acquired using a 63X/1.4NA objective lens with a pixel size of 45 nm (2048 × 2048 pixels per FOV). The co-localization indices were calculated in a 10um-thick band around each nucleus (cytoplasmic area) thanks to a custom-made FiJi/ImageJ macro and the JaCoP plug-in (Bolte and Cordelieres, 2006). In all experimental conditions, the M1 coefficient (the

fraction of RBP signal colocalizing with G3BP1 signal) was used as indication of colocalization between RBP and stress granules. The Huang and the Max Entropy algorithms were used to automatically find the thresholds for RBP and G3BP1 signals, respectively.

DATA AVAILABILITY STATEMENT

The datasets presented in this study can be found in online repositories. The mass spectrometry proteomics data have been deposited to the ProteomeXchange Consortium via the PRIDE (Perez-Riverol et al., 2019) partner repository with the dataset identifier PXD024601.

AUTHOR CONTRIBUTIONS

MM designed and carried out the proteomics cell biology and biochemical experiments, wrote a first draft of the manuscript; FB contributed with cell biology and biochemical experiments; EM carried out the data analysis and contributed to writing the computational parts of the manuscript; TB proposed the project, designed and supervised the experiments, critically evaluated the results, defined the manuscript structure, carried out the draft revision and curated manuscript submission. TB also supported financially the project through individual grant supporting this study.

FUNDING

This project is supported by the Italian Association for Cancer Research (IG-grant# 2018-15741). MM is a PhD student within the European School of Molecular Medicine (SEMM); FB is supported by a Fellowship of the European Institute of Oncology foundation (FIEO); EM is supported by a fellowship of the Italian Foundation for Cancer Research (FIRC) and is a PhD student within the European School of Molecular Medicine (SEMM).

ACKNOWLEDGMENTS

We would like to thank A. Cuomo, F. Marini, R. Noberini, M. Mihailovich and F. Iommazzo for critical discussion, S. Rodighiero and C. Soriani of the Imaging Unit of the Dept. Of Experimental Oncology of IEO, for the support with the confocal microscopy and all members of the TB laboratory for support.

SUPPLEMENTARY MATERIAL

The Supplementary Material for this article can be found online at: https://www.frontiersin.org/articles/10.3389/fmolb.2021.688973/full#supplementary-material

REFERENCES

Aravind, L., and Koonin, E. V. (2000). SAP - a Putative DNA-Binding Motif Involved in Chromosomal Organization. *Trends Biochem. Sci.* 25, 112–114. doi:10.1016/s0968-0004(99)01537-6

Bao, X., Guo, X., Yin, M., Tariq, M., Lai, Y., Kanwal, S., et al. (2018). Capturing the Interactome of Newly Transcribed RNA. *Nat. Methods* 15, 213–220. doi:10.1038/nmeth.4595

Bedford, M. T., and Richard, S. (2005). Arginine Methylation. *Mol. Cel* 18, 263–272. doi:10.1016/j.molcel.2005.04.003

Blackwell, E., and Ceman, S. (2012). Arginine Methylation of RNA-Binding Proteins Regulates Cell Function and Differentiation. *Mol. Reprod. Dev.* 79, 163–175. doi:10.1002/mrd.22024

Blanc, R. S., and Richard, S. (2017). Arginine Methylation: The Coming of Age. *Mol. Cel* 65, 8–24. doi:10.1016/j.molcel.2016.11.003

Bolte, S., and Cordelières, F. P. (2006). A Guided Tour into Subcellular Colocalization Analysis in Light Microscopy. *J. Microsc.* 224, 213–232. doi:10.1111/j.1365-2818.2006.01706.x

Castello, A., Fischer, B., Frese, C. K., Horos, R., Alleaume, A.-M., Foehr, S., et al. (2016). Comprehensive Identification of RNA-Binding Domains in Human Cells. *Mol. Cel* 63, 696–710. doi:10.1016/j.molcel.2016.06.029

Castello, A., Horos, R., Strein, C., Fischer, B., Eichelbaum, K., Steinmetz, L. M., et al. (2013). System-wide Identification of RNA-Binding Proteins by Interactome Capture. *Nat. Protoc.* 8, 491–500. doi:10.1038/nprot.2013.020

Chau, B. L., Ng, K. P., Li, K. K. C., and Lee, K. A. W. (2016). RGG Boxes within the TET/FET Family of RNA-Binding Proteins Are Functionally Distinct. *Transcription* 7, 141–151. doi:10.1080/21541264.2016.1183071

Chen, M., Qu, X., Zhang, Z., Wu, H., Qin, X., Li, F., et al. (2016). Cross-talk between Arg Methylation and Ser Phosphorylation Modulates Apoptosis Signal-Regulating Kinase 1 Activation in Endothelial Cells. *MBoC* 27, 1358–1366. doi:10.1091/mbc.e15-10-0738

Chong, P. A., Vernon, R. M., and Forman-Kay, J. D. (2018). RGG/RG Motif Regions in RNA Binding and Phase Separation. *J. Mol. Biol.* 430, 4650–4665. doi:10.1016/j.jmb.2018.06.014

Cox, J., Neuhauser, N., Michalski, A., Scheltema, R. A., Olsen, J. V., and Mann, M. (2011). Andromeda: a Peptide Search Engine Integrated into the MaxQuant Environment. *J. Proteome Res.* 10, 1794–1805. doi:10.1021/pr101065j

Dhar, S., Vemulapalli, V., Patananan, A. N., Huang, G. L., DI Lorenzo, A., Richard, S., et al. (2013). Loss of the Major Type I Arginine Methyltransferase PRMT1 Causes Substrate Scavenging by Other PRMTs. *Sci. Rep.* 3, 1311. doi:10.1038/srep01311

Düster, R., Kaltheuner, I. H., Schmitz, M., and Geyer, M. (2021). 1,6-Hexanediol, Commonly Used to Dissolve Liquid-Liquid Phase Separated Condensates, Directly Impairs Kinase and Phosphatase Activities. *J. Biol. Chem.* 296, 100260. doi:10.1016/j.jbc.2021.100260

Eden, E., Navon, R., Steinfeld, I., Lipson, D., and Yakhini, Z. (2009). GOrilla: a Tool for Discovery and Visualization of Enriched GO Terms in Ranked Gene Lists. *BMC Bioinformatics* 10, 48. doi:10.1186/1471-2105-10-48

El-naggar, A. M., and Sorensen, P. H. (2018). Translational Control of Aberrant Stress Responses as a Hallmark of Cancer. *J. Pathol.* 244, 650–666. doi:10.1002/path.5030

Eram, M. S., Shen, Y., Szewczyk, M. M., Wu, H., Senisterra, G., Li, F., et al. (2016). A Potent, Selective, and Cell-Active Inhibitor of Human Type I Protein Arginine Methyltransferases. *ACS Chem. Biol.* 11, 772–781. doi:10.1021/acschembio.5b00839

Espejo, A. B., Gao, G., Black, K., Gayatri, S., Veland, N., Kim, J., et al. (2017). PRMT5 C-Terminal Phosphorylation Modulates a 14-3-3/PDZ Interaction Switch. *J. Biol. Chem.* 292, 2255–2265. doi:10.1074/jbc.m116.760330

Fedoriw, A., Rajapurkar, S. R., O'Brien, S., Gerhart, S. V., Mitchell, L. H., Adams, N. D., et al. (2019). Anti-tumor Activity of the Type I PRMT Inhibitor, GSK3368715, Synergizes with PRMT5 Inhibition through MTAP Loss. *Cancer Cell* 36, 100–114. doi:10.1016/j.ccell.2019.05.014

Fong, J. Y., Pignata, L., Goy, P.-A., Kawabata, K. C., Lee, S. C.-W., Koh, C. M., et al. (2019). Therapeutic Targeting of RNA Splicing Catalysis through Inhibition of

Protein Arginine Methylation. *Cancer Cell* 36, 194–209. doi:10.1016/j.ccell.2019.07.003

Fulton, M. D., Brown, T., and Zheng, Y. G. (2019). The Biological Axis of Protein Arginine Methylation and Asymmetric Dimethylarginine. *Int. J. Mol. Sci.* 20. doi:10.3390/ijms20133322

Gilman, B., Tijerina, P., and Russell, R. (2017). Distinct RNA-Unwinding Mechanisms of DEAD-Box and DEAH-Box RNA Helicase Proteins in Remodeling Structured RNAs and RNPs. *Biochem. Soc. Trans.* 45, 1313–1321. doi:10.1042/bst20170095

Guccione, E., and Richard, S. (2019). The Regulation, Functions and Clinical Relevance of Arginine Methylation. *Nat. Rev. Mol. Cel. Biol.* 20, 642–657. doi:10.1038/s41580-019-0155-x

Haase, M., and Fitze, G. (2016). HSP90AB1: Helping the Good and the Bad. *Gene* 575, 171–186. doi:10.1016/j.gene.2015.08.063

Hentze, M. W., Castello, A., Schwarzl, T., and Preiss, T. (2018). A Brave New World of RNA-Binding Proteins. *Nat. Rev. Mol. Cel. Biol.* 19, 327–341. doi:10.1038/nrm.2017.130

Hornbeck, P. V., Zhang, B., Murray, B., Kornhauser, J. M., Latham, V., and Skrzypek, E. (2015). PhosphoSitePlus, 2014: Mutations, PTMs and Recalibrations. *Nucleic Acids Res.* 43, D512–D520. doi:10.1093/nar/gku1267

Hu, H., Qian, K., Ho, M.-C., and Zheng, Y. G. (2016). Small Molecule Inhibitors of Protein Arginine Methyltransferases. *Expert Opin. Investig. Drugs* 25, 335–358. doi:10.1517/13543784.2016.1144747

Huang, C., Chen, Y., Dai, H., Zhang, H., Xie, M., Zhang, H., et al. (2020). UBAP2L Arginine Methylation by PRMT1 Modulates Stress Granule Assembly. *Cell Death Differ* 27, 227–241. doi:10.1038/s41418-019-0350-5

Huang, L., Wang, Z., Narayanan, N., and Yang, Y. (2018a). Arginine Methylation of the C-Terminus RGG Motif Promotes TOP3B Topoisomerase Activity and Stress Granule Localization. *Nucleic Acids Res.* 46, 3061–3074. doi:10.1093/nar/gky103

Huang, R., Han, M., Meng, L., and Chen, X. (2018b). Transcriptome-wide Discovery of Coding and Noncoding RNA-Binding Proteins. *Proc. Natl. Acad. Sci. USA* 115, E3879–E3887. doi:10.1073/pnas.1718406115

Jao, C. Y., and Salic, A. (2008). Exploring RNA Transcription and Turnover *In Vivo* by Using Click Chemistry. *Proc. Natl. Acad. Sci.* 105, 15779–15784. doi:10.1073/pnas.0808480105

Kaniskan, H. Ü., Martini, M. L., and Jin, J. (2018). Inhibitors of Protein Methyltransferases and Demethylases. *Chem. Rev.* 118, 989–1068. doi:10.1021/acs.chemrev.6b00801

Kawahara, D., Suzuki, T., and Nakaya, T. (2021). Cytoplasmic Granule Formation by FUS-R495X Is Attributable to Arginine Methylation in All Gly-rich, RGG1 and RGG2 Domains. *Genes Cells* 26, 190–197. doi:10.1111/gtc.12827

Liao, J.-Y., Yang, B., Zhang, Y.-C., Wang, X.-J., Ye, Y., Peng, J.-W., et al. (2020). EuRBPDB: a Comprehensive Resource for Annotation, Functional and Oncological Investigation of Eukaryotic RNA Binding Proteins (RBPs). *Nucleic Acids Res.* 48, D307–D313. doi:10.1093/nar/gkz823

Lim, Y., Lee, J. Y., Ha, S. J., Yu, S., Shin, J. K., and Kim, H. C. (2020). Proteome-wide Identification of Arginine Methylation in Colorectal Cancer Tissues from Patients. *Proteome Sci.* 18, 6. doi:10.1186/s12953-020-00162-8

Lin, Y., Protter, D. S. W., Rosen, M. K., and Parker, R. (2015). Formation and Maturation of Phase-Separated Liquid Droplets by RNA-Binding Proteins. *Mol. Cel.* 60, 208–219. doi:10.1016/j.molcel.2015.08.018

Liu, N., Yang, R., Shi, Y., Chen, L., Liu, Y., Wang, Z., et al. (2020). The Cross-Talk between Methylation and Phosphorylation in Lymphoid-specific Helicase Drives Cancer Stem-like Properties. *Sig. Transduct. Target. Ther.* 5, 197. doi:10.1038/s41392-020-00249-w

Loll-krippleber, R., and Brown, G. W. (2017). P-body Proteins Regulate Transcriptional Rewiring to Promote DNA Replication Stress Resistance. *Nat. Commun.* 8, 558. doi:10.1038/s41467-017-00632-2

Mersaoui, S. Y., Yu, Z., Coulombe, Y., Karam, M., Busatto, F. F., Masson, J. Y., et al. (2019). Arginine Methylation of the DDX5 Helicase RGG/RG Motif by PRMT5 Regulates Resolution of RNA:DNA Hybrids. *EMBO J.* 38, e100986. doi:10.15252/embj.2018100986

Musiani, D., Bok, J., Massignani, E., Wu, L., Tabaglio, T., Ippolito, M. R., et al. (2019). Proteomics Profiling of Arginine Methylation Defines PRMT5 Substrate Specificity. *Sci. Signal.* 12. doi:10.1126/scisignal.aat8388

Musiani, D., Giambruno, R., Massignani, E., Ippolito, M. R., Maniaci, M., Jammula, S., et al. (2020). PRMT1 Is Recruited via DNA-PK to Chromatin where it Sustains the Senescence-Associated Secretory Phenotype in Response to Cisplatin. *Cel. Rep.* 30, 1208–1222. doi:10.1016/j.celrep.2019.12.061

O'shea, J. P., Chou, M. F., Quader, S. A., Ryan, J. K., Church, G. M., and Schwartz, D. (2013). pLogo: a Probabilistic Approach to Visualizing Sequence Motifs. *Nat. Methods* 10, 1211–1212. doi:10.1038/nmeth.2646

Pereira, B., Billaud, M., and Almeida, R. (2017). RNA-binding Proteins in Cancer: Old Players and New Actors. *Trends Cancer* 3, 506–528. doi:10.1016/j.trecan.2017.05.003

Perez-perri, J. I., Rogell, B., Schwarzl, T., Stein, F., Zhou, Y., Rettel, M., et al. (2018). Discovery of RNA-Binding Proteins and Characterization of Their Dynamic Responses by Enhanced RNA Interactome Capture. *Nat. Commun.* 9, 4408. doi:10.1038/s41467-018-06557-8

Perez-riverol, Y., Csordas, A., Bai, J., Bernal-Llinares, M., Hewapathirana, S., Kundu, D. J., et al. (2019). The PRIDE Database and Related Tools and Resources in 2019: Improving Support for Quantification Data. *Nucleic Acids Res.* 47, D442–D450. doi:10.1093/nar/gky1106

Qamar, S., Wang, G., Randle, S. J., Ruggeri, F. S., Varela, J. A., Lin, J. Q., et al. (2018). FUS Phase Separation Is Modulated by a Molecular Chaperone and Methylation of Arginine Cation-π Interactions. *Cell* 173, 720–734. doi:10.1016/j.cell.2018.03.056

Queiroz, R. M. L., Smith, T., Villanueva, E., Marti-Solano, M., Monti, M., Pizzinga, M., et al. (2019). Comprehensive Identification of RNA-Protein Interactions in Any Organism Using Orthogonal Organic Phase Separation (OOPS). *Nat. Biotechnol.* 37, 169–178. doi:10.1038/s41587-018-0001-2

Ramanathan, M., Porter, D. F., and Khavari, P. A. (2019). Methods to Study RNA-Protein Interactions. *Nat. Methods* 16, 225–234. doi:10.1038/s41592-019-0330-1

Sachamitr, P., Ho, J. C., Ciamponi, F. E., Ba-Alawi, W., Coutinho, F. J., Guilhamon, P., et al. (2021). PRMT5 Inhibition Disrupts Splicing and Stemness in Glioblastoma. *Nat. Commun.* 12, 979. doi:10.1038/s41467-021-21204-5

Schindelin, J., Arganda-Carreras, I., Frise, E., Kaynig, V., Longair, M., Pietzsch, T., et al. (2012). Fiji: an Open-Source Platform for Biological-Image Analysis. *Nat. Methods* 9, 676–682. doi:10.1038/nmeth.2019

Shannon, P., Markiel, A., Ozier, O., Baliga, N. S., Wang, J. T., Ramage, D., et al. (2003). Cytoscape: a Software Environment for Integrated Models of Biomolecular Interaction Networks. *Genome Res.* 13, 2498–2504. doi:10.1101/gr.1239303

Smith, D.-L., Erce, M. A., Lai, Y.-W., Tomasetig, F., Hart-Smith, G., Hamey, J. J., et al. (2020). Crosstalk of Phosphorylation and Arginine Methylation in Disordered SRGG Repeats of *Saccharomyces cerevisiae* Fibrillarin and its Association with Nucleolar Localization. *J. Mol. Biol.* 432, 448–466. doi:10.1016/j.jmb.2019.11.006

Smith, E., Zhou, W., Shindiapina, P., Sif, S., Li, C., and Baiocchi, R. A. (2018). Recent Advances in Targeting Protein Arginine Methyltransferase Enzymes in Cancer Therapy. *Expert Opin. Ther. Targets* 22, 527–545. doi:10.1080/14728222.2018.1474203

Spadotto, V., Giambruno, R., Massignani, E., Mihailovich, M., Maniaci, M., Patuzzo, F., et al. (2020). PRMT1-mediated Methylation of the Microprocessor-Associated Proteins Regulates microRNA Biogenesis. *Nucleic Acids Res.* 48, 96–115. doi:10.1093/nar/gkz1051

Supek, F., Bošnjak, M., Škunca, N., and Šmuc, T. (2011). REVIGO Summarizes and Visualizes Long Lists of Gene Ontology Terms. *PLoS One* 6, e21800. doi:10.1371/journal.pone.0021800

Szewczyk, M. M., Ishikawa, Y., Organ, S., Sakai, N., Li, F., Halabelian, L., et al. (2020). Pharmacological Inhibition of PRMT7 Links Arginine Monomethylation to the Cellular Stress Response. *Nat. Commun.* 11, 2396. doi:10.1038/s41467-020-16271-z

Szklarczyk, D., Gable, A. L., Lyon, D., Junge, A., Wyder, S., Huerta-Cepas, J., et al. (2019). STRING V11: Protein-Protein Association Networks with Increased Coverage, Supporting Functional Discovery in Genome-wide Experimental Datasets. *Nucleic Acids Res.* 47, D607–D613. doi:10.1093/nar/gky1131

Thandapani, P., O'Connor, T. R., Bailey, T. L., and Richard, S. (2013). Defining the RGG/RG Motif. *Mol. Cel.* 50, 613–623. doi:10.1016/j.molcel.2013.05.021

Trendel, J., Schwarzl, T., Horos, R., Prakash, A., Bateman, A., Hentze, M. W., et al. (2019). The Human RNA-Binding Proteome and its Dynamics during Translational Arrest. *Cell* 176, 391–403. doi:10.1016/j.cell.2018.11.004

Tsai, W.-C., Gayatri, S., Reineke, L. C., Sbardella, G., Bedford, M. T., and Lloyd, R. E. (2016). Arginine Demethylation of G3BP1 Promotes Stress Granule Assembly. *J. Biol. Chem.* 291, 22671–22685. doi:10.1074/jbc.m116.739573

Tyanova, S., Temu, T., and Cox, J. (2016). The MaxQuant Computational Platform for Mass Spectrometry-Based Shotgun Proteomics. *Nat. Protoc.* 11, 2301–2319. doi:10.1038/nprot.2016.136

Ule, J., Hwang, H. W., and Darnell, R. B. (2018). The Future of Cross-Linking and Immunoprecipitation (CLIP). *Cold Spring Harb Perspect. Biol.* 10. doi:10.1101/cshperspect.a032243

Urdaneta, E. C., Vieira-Vieira, C. H., Hick, T., Wessels, H.-H., Figini, D., Moschall, R., et al. (2019). Purification of Cross-Linked RNA-Protein Complexes by Phenol-Toluol Extraction. *Nat. Commun.* 10, 990. doi:10.1038/s41467-019-08942-3

Valverde, R., Edwards, L., and Regan, L. (2008). Structure and Function of KH Domains. *FEBS J.* 275, 2712–2726. doi:10.1111/j.1742-4658.2008.06411.x

Ward, J. H. (1963). Hierarchical Grouping to Optimize an Objective Function. *J. Am. Stat. Assoc.* 58, 236–244. doi:10.1080/01621459.1963.10500845

Wheeler, J. R., Matheny, T., Jain, S., Abrisch, R., and Parker, R. (2016). Distinct Stages in Stress Granule Assembly and Disassembly. *Elife* 5. doi:10.7554/eLife.18413

Yang, P., Mathieu, C., Kolaitis, R.-M., Zhang, P., Messing, J., Yurtsever, U., et al. (2020). G3BP1 Is a Tunable Switch that Triggers Phase Separation to Assemble Stress Granules. *Cell* 181, 325–345. doi:10.1016/j.cell.2020.03.046

Yang, Y., and Bedford, M. T. (2013). Protein Arginine Methyltransferases and Cancer. *Nat. Rev. Cancer* 13, 37–50. doi:10.1038/nrc3409

You, K., Huang, Q., Yu, C., Shen, B., Sevilla, C., Shi, M., et al. (2020). PhaSepDB: a Database of Liquid-Liquid Phase Separation Related Proteins. *Nucleic Acids Res.* 48, D354–D359. doi:10.1093/nar/gkz847

Zhan, Y., Wang, H., Ning, Y., Zheng, H., Liu, S., Yang, Y., et al. (2020). Understanding the Roles of Stress Granule during Chemotherapy for Patients with Malignant Tumors. *Am. J. Cancer Res.* 10, 2226–2241.

Zhang, J., Jing, L., Li, M., He, L., and Guo, Z. (2019). Regulation of Histone Arginine Methylation/demethylation by Methylase and Demethylase (Review). *Mol. Med. Rep.* 19, 3963–3971. doi:10.3892/mmr.2019.10111

Zhang, X.-P., Jiang, Y.-B., Zhong, C.-Q., Ma, N., Zhang, E.-B., Zhang, F., et al. (2018). PRMT1 Promoted HCC Growth and Metastasis *In Vitro* and *In Vivo* via Activating the STAT3 Signalling Pathway. *Cell Physiol Biochem* 47, 1643–1654. doi:10.1159/000490983

Zuehlke, A. D., Beebe, K., Neckers, L., and Prince, T. (2015). Regulation and Function of the Human HSP90AA1 Gene. *Gene* 570, 8–16. doi:10.1016/j.gene.2015.06.018

Conflict of Interest: The authors declare that the research was conducted in the absence of any commercial or financial relationships that could be construed as a potential conflict of interest.

Publisher's Note: All claims expressed in this article are solely those of the authors and do not necessarily represent those of their affiliated organizations, or those of the publisher, the editors and the reviewers. Any product that may be evaluated in this article, or claim that may be made by its manufacturer, is not guaranteed or endorsed by the publisher.

frontiers in Molecular Biosciences

ORIGINAL RESEARCH
published: 19 October 2021
doi: 10.3389/fmolb.2021.689687

Phosphorylation Regulates CIRBP Arginine Methylation, Transportin-1 Binding and Liquid-Liquid Phase Separation

*Aneta J. Lenard[1], Saskia Hutten[2,3], Qishun Zhou[1], Sinem Usluer[1], Fangrong Zhang[1], Benjamin M. R. Bourgeois[1], Dorothee Dormann[2,3,4,5] and Tobias Madl[1,6]**

[1]Gottfried Schatz Research Center for Cell Signaling, Metabolism and Aging, Molecular Biology and Biochemistry, Medical University of Graz, Graz, Austria, [2]Johannes Gutenberg-Universität (JGU) Mainz, Faculty of Biology, Mainz, Germany, [3]BioMedical Center, Cell Biology, Ludwig-Maximilians-Universität (LMU) München, Martinsried, Germany, [4]Institute of Molecular Biology (IMB), Mainz, Germany, [5]Munich Cluster for Systems Neurology (SyNergy), Munich, Germany, [6]BioTechMed-Graz, Graz, Austria

Arginine-glycine(-glycine) (RG/RGG) regions are highly abundant in RNA-binding proteins and involved in numerous physiological processes. Aberrant liquid-liquid phase separation (LLPS) and stress granule (SGs) association of RG/RGG regions in the cytoplasm have been implicated in several neurodegenerative disorders. LLPS and SG association of these proteins is regulated by the interaction with nuclear import receptors, such as transportin-1 (TNPO1), and by post-translational arginine methylation. Strikingly, many RG/RGG proteins harbour potential phosphorylation sites within or close to their arginine methylated regions, indicating a regulatory role. Here, we studied the role of phosphorylation within RG/RGG regions on arginine methylation, TNPO1-binding and LLPS using the cold-inducible RNA-binding protein (CIRBP) as a paradigm. We show that the RG/RGG region of CIRBP is *in vitro* phosphorylated by serine-arginine protein kinase 1 (SRPK1), and discovered two novel phosphorylation sites in CIRBP. SRPK1-mediated phosphorylation of the CIRBP RG/RGG region impairs LLPS and binding to TNPO1 *in vitro* and interferes with SG association in cells. Furthermore, we uncovered that arginine methylation of the CIRBP RG/RGG region regulates *in vitro* phosphorylation by SRPK1. In conclusion, our findings indicate that LLPS and TNPO1-mediated chaperoning of RG/RGG proteins is regulated through an intricate interplay of post-translational modifications.

Keywords: RNA-binding proteins, CIRBP, SRPK1, phosphorylation, arginine methylation, PTMs, liquid-liquid phase separation, transportin-1

OPEN ACCESS

Edited by:
Sandro Fernandes Ataide, The University of Sydney, Australia

Reviewed by:
Carmen Nussbaum-Krammer, University of Heidelberg, Germany
Graciela Lidia Boccaccio, IIBBA-CONICET Leloir Institute Foundation, Argentina

****Correspondence:***
Tobias Madl
tobias.madl@medunigraz.at

Specialty section:
This article was submitted to Protein and RNA Networks, a section of the journal Frontiers in Molecular Biosciences

Received: *01 April 2021*
Accepted: *01 October 2021*
Published: *19 October 2021*

Citation:
Lenard AJ, Hutten S, Zhou Q, Usluer S, Zhang F, Bourgeois BMR, Dormann D and Madl T (2021) Phosphorylation Regulates CIRBP Arginine Methylation, Transportin-1 Binding and Liquid-Liquid Phase Separation. Front. Mol. Biosci. 8:689687. doi: 10.3389/fmolb.2021.689687

INTRODUCTION

A growing number of evidences has emerged over the last decade implicating that cells organize a plethora of biochemical processes by means of biomolecular condensation, including the formation of membraneless ribonucleoprotein (RNP) granules (Banani et al., 2016; Banani et al., 2017; Shin and Brangwynne, 2017). RNP granules constitute micron-sized, condensed, dynamic assemblies of RNA and RNA-binding proteins (RBPs), exemplified by nucleoli, Cajal bodies, paraspeckles in the nucleus or stress granules (SGs), and P-bodies in the cytoplasm (Hyman et al., 2014; Molliex et al., 2015; Feric et al., 2016). These membraneless organelles are proposed to form through the process of liquid-liquid phase separation (LLPS), by which coexisting protein/RNA-depleted (dilute) and highly

protein/RNA-enriched (condensed) phases emerge and remain in a dynamic equilibrium with the cellular surroundings (Aguzzi and Altmeyer, 2016; Alberti, 2017; Ditlev et al., 2018; Alberti et al., 2019). Multivalent interactions have been recognized as a critical factor driving the assembly of protein/RNA into the condensed phase. They are facilitated by the modular structure of RBPs possessing multiple RNA-binding domains and intrinsically disordered regions with low complexity sequences of amino acids (Li et al., 2012; Banani et al., 2017; Chong et al., 2018; Martin and Holehouse, 2020). Importantly, RNP compartments and missense mutations in RBPs are thought to be central to the pathogenesis of several neuronal disorders such as amyotrophic lateral sclerosis (ALS), frontotemporal dementia (FTD), inclusion body myopathy (IBM) (Li et al., 2013; Ramaswami et al., 2013; Tsang et al., 2020). These diseases are characterized by the presence of mis-localized pathological protein aggregates formed in the cytoplasm of neuronal cells, and till now no effective therapies targeting them have been reported (Harrison and Shorter, 2017).

Proteins containing RG/RGG-regions are highly abundant in the eukaryotic proteome, and have been demonstrated to localize to cellular RNP granules (Thandapani et al., 2013). For example, SGs contain a large number of RG/RGG proteins, e.g. members of FET protein family (including FUS, EWS and TAF15) (Andersson et al., 2008; Dormann et al., 2010), TDP-43 (Bentmann et al., 2012), FMRP (Didiot et al., 2009), G3BP1 (Tourrière et al., 2003) and CAPRIN-1 (Solomon et al., 2007), nucleoli contain nucleolin and fibrillarin (Frottin et al., 2019), the RG-dipeptide repeats containing coilin is a marker for Cajal bodies (Hebert et al., 2002), and Lsm14a can be found in P-bodies (Yang et al., 2006). Purified proteins containing RG/RGG-regions have been shown to undergo LLPS *in vitro* in a reversible and concentration-dependent manner, and that addition of RNA can enhance their propensity for phase separation (Patel et al., 2015; Boeynaems et al., 2017; Chong et al., 2018). Wang *et al.* determined a sequence-encoded "molecular grammar" where the interactions between aromatic and positively charged residues have been identified as critical for phase separation of RBPs (Wang et al., 2018), and various studies showed that arginines are necessary for LLPS of RG/RGG regions- or RG-FG repeats-containing proteins (Elbaum-Garfinkle et al., 2015; Nott et al., 2015; Hofweber et al., 2018; Yang et al., 2020). Moreover, post-translational modifications (PTMs) within RG/RGG regions provide a means of phase separation regulation (Chong et al., 2018; Rhoads et al., 2018; Hofweber and Dormann, 2019). For instance, methylation of arginines in FUS, hnRNP-A2, FMRP, and DDX4 suppresses their LLPS by reducing arginine-(pi) aromatic interactions (Nott et al., 2015; Hofweber et al., 2018; Qamar et al., 2018; Ryan et al., 2018; Tsang et al., 2019). In addition, arginine methylation impairs SG association of RG/RGG proteins, such as G3BP1 (Tsai et al., 2016), FUS (Hofweber et al., 2018), FMRP (Dolzhanskaya et al., 2006), CIRBP (De Leeuw et al., 2007).

Another PTM frequently occurring in RBPs is phosphorylation of serine (in mammals ~90% of phosphorylation events occur on serines), threonine, or tyrosine residues, which introduces a double negative charge via a phosphate group (Bah and Forman-Kay, 2016). In contrast to arginine methylation, phosphorylation can regulate LLPS of RBPs either positively or negatively (Wang et al., 2018; Hofweber and Dormann, 2019). For example, phosphorylation of the low-complexity domain of FUS disrupts *in vitro* phase separation (Monahan et al., 2017), whereas phosphorylation within the low-complexity region of FMRP promotes LLPS *in vitro* (Tsang et al., 2019). Phosphorylation of G3BP1 on serine-149 by casein kinase 2 (CK2) as well as dual specificity tyrosine phosphorylation–regulated kinase 3 (DYRK3) – mediated phosphorylation of multiple RBPs have been shown to disassemble corresponding membraneless organelles (Wippich et al., 2013; Reineke et al., 2018). On the contrary, SG localization of 5′-AMP-activated protein kinase-α2 (AMPK-α2) and mTOR (mechanistic target of rapamycin) effector kinases S6 kinase 1 and 2 (S6K1 and S6K2) are required for SG assembly (Mahboubi et al., 2015; Sfakianos et al., 2018).

RBPs often carry a combination of multiple PTMs, in which modifications can affect one another when located closely in the primary sequence or 3D space (PTM cross-talk). For instance, a recent study conducted a bioinformatic analysis focused on SRGG motifs (overlapping SR and RGG regions, with serine serving as a site for phosphorylation, and arginine as a site for methylation) in the *S. cerevisiae* proteome (Smith et al., 2020). The authors identified 38 yeast proteins harboring the SRGG motif, and only three of them – Nop1p, Npl3p, and Gar1p – possess multiple repeats of the SRGG region. They further demonstrated for Nop1p that the presence of serine phosphorylation within the SRGG motif blocks arginine methylation by a yeast methyltransferase within the same and adjacent motifs, as well as that the presence of arginine methylation in the SRGG region decreases serine phosphorylation. Besides arginine methylation and phosphorylation, many other PTMs appear in RBPs and may affect their LLPS, as exemplified by arginine-to-citrulline conversion (Tanikawa et al., 2018), lysine acetylation (Saito et al., 2019), or *O*-GlcNAcylation (Ohn et al., 2008). Thus, further studies are needed to fill gaps in our knowledge about the crosstalk between PTMs as well as the impact of various modifications on LLPS.

In addition to aberrant arginine methylation, defective nucleocytoplasmic transport of RBPs is a crucial pathological factor driving the onset of ALS/FTD disorders (Dormann et al., 2010). We and others have previously reported that the nuclear import receptor Transportin-1 (TNPO1)/Karyopherin-β2 (Kapβ2) acts as a chaperone for the RBP FUS, and reduces both its phase separation and SG recruitment via direct interaction with the RGG3-PY (proline-tyrosine) region of FUS (Guo et al., 2018; Hofweber et al., 2018; Qamar et al., 2018; Yoshizawa et al., 2018). Nucleocytoplasmic shuttling and chaperoning activity of importins are believed to be dependent on the specific interaction between an importin and a nuclear localization signal (NLS) within its cargo protein (Chook and Blobel, 2001; Soniat and Chook, 2015; Frey et al., 2018). Recently, we have identified the RG/RGG region and an arginine-serine-tyrosine (RSY)–rich region in cold-inducible RNA-binding protein (CIRBP) to serve as NLSs for transportin-1 and

transportin-3 (Bourgeois et al., 2020). CIRBP is a member of the family of cold shock proteins. In response to different cellular stresses, such as mild cold shock, ultraviolet irradiation, osmotic shock, or hypoxia, CIRBP relocalizes from the nucleus to the cytoplasm where it partitions into SGs (Aoki et al., 2002; Pan et al., 2004; De Leeuw et al., 2007). CIRBP plays anti-apoptotic and anti-senescent roles in cells (Sakurai et al., 2006; Lee et al., 2015a), and its mis-regulation is associated with numerous pathologies. CIRBP is involved in the development of brain ischemia (Zhou et al., 2014), and extracellular CIRBP triggers inflammation and tissue injury in sepsis by inducing the formation of neutrophil extracellular traps in patients lungs (Ode et al., 2018; Ode et al., 2019). Furthermore, CIRBP constitutes a promising target for anticancer therapy, as its downregulation was found to inhibit cancer cell survival in patients suffering from liver, breast, brain, and prostate cancers (Zeng et al., 2009; Lujan et al., 2018).

Despite our growing understanding of liquid-liquid phase transition phenomena in living cells, we still lack of a full comprehension of their regulation, for example how LLPS of RBPs is regulated. In this study, we show that the RG/RGG region of CIRBP (CIRBP-RGG) is phosphorylated in cell lysate and identified serine-arginine protein kinase-1 (SRPK1) as a relevant kinase *in vitro*. Phosphorylation of CIRBP-RGG inhibited methylation of adjacent arginines and vice versa. *In vitro*, SRPK1-mediated phosphorylation of CIRBP-RGG suppresses phase separation, and in semi-permeabilized cells, it suppresses SG recruitment of CIRBP. Our study furthermore reveals that phosphorylation of CIRBP-RGG impairs binding to the nuclear import receptor Transportin-1 (TNPO1). Summarizing, our study sheds light on the regulation of membraneless organelles and nuclear translocation of RG/RGG region-containing proteins via an intricate interplay of PTMs.

MATERIALS AND METHODS

Recombinant Protein Expression and Purification

Recombinant His_6-protein A-tagged CIRBP-RGG (amino acids 68–137) containing a Tobacco Etch Virus (TEV) protease cleavage site after protein A was expressed from a codon optimized synthetic gene inserted into a pETM11-based vector (Genscript). A 10 mL overnight preculture of freshly transformed *Escherichia coli* BL21(DE3) Star competent cells was transferred to 1L standard lysogeny broth (LB) media containing kanamycin and grown to an OD_{600} of 0.6–0.8 at 37°C before induction with 1 mM isopropyl β-D-1-thiogalactopyranoside (IPTG), and further expressed for 16 h at 20°C and 160 rpm. For NMR experiments, 10 mL overnight precultures were transferred to minimal media (100 mM KH_2PO_4, 50 mM K_2HPO_4, 60 mM Na_2HPO_4, 14 mM K_2SO_4, 5 mM $MgCl_2$; pH 7.2 adjusted with HCl and NaOH with 0.1 dilution of trace element solution (41 mM $CaCl_2$, 22 mM $FeSO_4$, 6 mM $MnCl_2$, 3 mM $CoCl_2$, 1 mM $ZnSO_4$, 0.1 mM $CuCl_2$, 0.2 mM $(NH_4)_6Mo_7O_{24}$, 17 mM EDTA)) supplemented with 1 g of $^{15}NH_4Cl$ (Sigma), and either with 6 g of $^{12}C_6H_{12}O_6$ or 2 g of $^{13}C_6H_{12}O_6$ (Cambridge Isotope Laboratories), followed by a growth as described for unlabeled protein. Cells were harvested (6,000 rpm for 10 min at 4°C), transferred to a denaturing lysis buffer (50 mM Tris-HCl pH 7.5, 150 mM NaCl, 20 mM imidazole, 6M urea), and sonicated (70% amplitude, 1 s pulse for 12 min on ice bath with Qsonica MC-18 sonicator). His_6-protein A-tagged CIRBP-RGG was purified using nickel-nitrilotriacetic (Ni-NTA) agarose resin (Qiagen) and eluted in buffer containing 50 mM Tris-HCl pH 7.5, 1 M NaCl, 500 mM imidazole, 2 mM tris(2-carboxyethyl) phosphine (TCEP), 0.04% NaN_3. The eluted protein was desalted to buffer 50 mM Tris-HCl pH 7.5, 150 mM NaCl, 20 mM imidazole, 2 mM TCEP, 0.04% NaN_3, and subjected to overnight TEV treatment at 4°C. Cleaved CIRBP-RGG was loaded onto a HiTrap Heparin HP column (GE Healthcare), and eluted with a linear gradient of 0–100% high salt buffer (50 mM Tris-HCl pH 7.5, 1 M NaCl, 20 mM imidazole, 2 mM TCEP, 0.04% NaN_3) over 10 column volumes (CVs). A final size exclusion chromatography purification step was performed in the buffer of interest on a Superdex 75 Increase 10/300 GL column (GE Healthcare) at room temperature.

Codon optimized synthetic His_6-protein A-tagged MBP-CIRBP-EGFP gene was inserted into a pETM11-based vector containing a TEV protease cleavage site after protein A (Genscript). For expression of recombinant protein, the construct was transformed into *E. coli* BL21(DE3) Star cells, and grown in LB medium at 37°C. At an OD_{600} of 0.8, cells were induced with 1 mM IPTG and grown for 16 h at 20°C. Cells were harvested and lysed by sonication in a non-denaturing lysis buffer (50 mM Tris-HCl pH 7.5, 150 mM NaCl, 20 mM imidazole, 2 mM TCEP, 10% (v/v) glycerol). Following sonication, 0.1 mg/mL RNase A and $MgCl_2$ (to a final concentration 20 mM) were added to the mixture and incubated in the dark for 30 min before centrifugation (13,000 g for 45 min at 4°C). His_6-protein A-tagged MBP-CIRBP-EGFP was purified using Ni-NTA beads (Qiagen), and the eluted protein was desalted to buffer 50 mM Tris-HCl pH 7.5, 150 mM NaCl, 20 mM imidazole, 2 mM TCEP, 0.04% NaN_3, and subsequently subjected to overnight TEV treatment at 4°C. Cleaved MBP-CIRBP-EGFP was then isolated by a second affinity purification using Ni-NTA beads. The eluted protein was then buffer exchanged to a phosphorylation buffer (50 mM Tris-HCl pH 6.7, 150 mM NaCl, 20 mM $MgCl_2$, 2 mM TCEP, 0.04% NaN_3) using HiPrep 26/10 Sephadex G-25 desalting column (GE Healthcare).

Recombinant His_6-protein A-tagged SRPK1 containing a TEV protease cleavage site after protein A was expressed from a codon optimized synthetic gene inserted into a pETM11-based vector (Genscript). 10 mL of overnight precultures of freshly transformed *E. coli* BL21(DE3) Star cells were added to and grown in 1L LB media at 37°C until an OD_{600} reached ~0.6–0.8, and the expression was induced with 1 mM IPTG for 16 h at 20°C. Cells were harvested at 6,000 rpm for 10 min at 4°C, and lysed by sonication in the non-denaturing lysis buffer. His_6-protein A-tagged SRPK1 was applied on Ni-NTA beads (Qiagen), eluted to buffer 50 mM Tris-HCl pH 7.5, 1 M NaCl, 500 mM imidazole, 2 mM TCEP, 0.04% NaN_3, desalted to buffer 50 mM Tris-HCl pH 7.5, 150 mM NaCl, 20 mM imidazole, 2 mM TCEP, 0.04% NaN_3 at 4°C, and subjected to overnight TEV treatment at

4°C. Cleaved SRPK1 was applied on a Superdex 200 Increase 10/300 GL (GE Healthcare) size exclusion chromatography column and eluted into the phosphorylation buffer. Fractions corresponding to untagged SRPK1 were identified by SDS PAGE gel, and used immediately for experiments.

Recombinant rat His_6-PRMT1 (amino acids 11–353) was inserted into a pET28b-His_6 vector (Novagen) and the expression has been previously described in (Zhang and Cheng, 2003). The expression construct was transformed into *E. coli* BL21(DE3) Star cells, and 1L expression culture was grown in LB medium at 37°C. Cells were induced at an OD_{600} of 0.6–0.8 with 1 mM IPTG followed by protein expression for 16 h at 20°C. Cell pellets were harvested and sonicated in the non-denaturing lysis buffer. His_6PRMT1 was purified using 5 mL HisTrap HP column (GE Healthcare) at 4°C and eluted over 10 CVs into buffer containing 50 mM Tris-HCl pH 7.5, 1 M NaCl, 500 mM imidazole, 2 mM TCEP, 0.04% NaN_3. As a final polishing step size exclusion chromatography purification step was performed in a methylation buffer (50 mM Na_2HPO_4/NaH_2PO_4 pH 8.0, 150 mM NaCl, 2 mM dithiothreitol (DTT), 0.04% NaN_3) using Superdex 200 Increase 10/300 GL column (GE Healthcare) at 4°C. Fractions corresponding to PRMT1 were identified by SDS PAGE gel, and used immediately for experiments.

For expression of recombinant unlabeled His_6-protein A-tagged TNPO1 containing a TEV protease cleavage site after protein A, a codon optimized synthetic gene was inserted into a pETM11-based vector (Genscript). *E.coli* BL21(DE3) Star strain cells were transformed with the expression vector, and picked one colony was grown in 20 mL LB medium for 16 h at 37°C. 1 mL of pre-culture was grown for 3 days in 1L minimal medium supplemented with 6 g of $^{12}C_6H_{12}O_6$ (Cambridge Isotope Laboratories) and 3 g of $^{14}NH_4Cl$ (Sigma) at 30°C. Cells were diluted to an OD_{600} of 0.8 and induced with 0.5 mM IPTG followed by TNPO1 expression for 6 h at 30°C. Cells pellets corresponding to protein expression of the unlabeled folded protein TNPO1 were harvested and sonicated in the non-denaturing lysis buffer. ZZ-His_6 TNPO1 were then purified using Ni-NTA agarose beads (Qiagen) in 50 mM Tris pH 7.5, 150 mM NaCl, 20 mM imidazole, 2 mM TCEP. The eluted ZZ-His_6 TNPO1 was subjected to TEV protease cleavage overnight at 4°C. TEV-cleaved recombinant protein was separated from the His_6-tag using a second step of Ni-NTA purification. A final size exclusion chromatography purification step was performed in buffer containing 50 mM Tris·HCl pH 7.5, 150 mM NaCl, 2 mM TCEP, 0.04% NaN_3 on a Hiload 16/600 Superdex 200 pg (GE Healthcare) column.

For expression of recombinant His_6-TEV protease, *E. coli* BL21(DE3) Star cells were transformed with the pLIC-His_6 expression plasmid (Cabrita et al., 2007) and grown in standard LB medium. Protein expression was induced at OD_{600} of 0.8 with 1 mM IPTG and left overnight at 20°C to grow. Cells were lysed in TEV lysis buffer (50 mM Tris pH 8.0, 200 mM NaCl, 25 mM imidazole, 10% (v/v) glycerol, supplemented 30 min prior sonication with 2 mM $MgCl_2$, 2 µl benzonase, and 50 µl bacterial protease cocktail inhibitor added per 1L culture) by sonification. Next, His_6-TEV was purified using Ni-NTA beads, washed using TEV lysis buffer containing 1.0 M NaCl, and eluted in TEV lysis buffer (pH 8.5) containing 800 mM imidazole. His_6-TEV was subsequently buffer exchanged using HiPrep 26/10 desalting column (GE Healthcare) against storage buffer (50 mM Tris pH 7.5, 150 mM NaCl, 20% glycerol, 2 mM DTT), and the protein was stored at −80°C until further use.

The concentration of proteins was estimated from their absorbance at 280 nm, using the molar extinction coefficient ε at 280 nm predicted by ProtParam tool (Gasteiger et al., 2005), assuming that the ε at 280 nm was equal to the theoretical ε value.

HEK293T Cell Lysate Phosphorylation

HEK293T cells were grown in Dulbecco's modified Eagle's medium (DMEM) (Sigma-Aldrich) containing 10% fetal bovine serum (FBS) (Gibco; Thermo Fisher Scientific), penicillin (100 U/mL, Gibco), streptomycin (100 µg/mL, Gibco), and amphotericin B (1.25 µg/mL; Gibco) in a humidified incubator (37°C, 5% CO_2/95% air). HEK293T cells were lysed in 50 mM Tris-HCl pH 7.5, 150 mM NaCl, 2 mM TCEP, 1% (v/v) Triton by incubating for 30 min at 4°C with vortexing every 5 min. The HEK293T cell lysate was then centrifuged at 13,000 rpm for 30 min at 4°C, and total protein concentration was estimated using Bradford protein assay (Bradford, 1976). To perform phosphorylation reaction, ^{13}C-^{15}N-labeled 50 µM His_6-protein A-tagged CIRBP-RGG was incubated overnight at room temperature with 15 mg/mL of total protein obtained from HEK293T-whole-cell-lysate in the presence of a protease inhibitor (Roche), phosphatases inhibitor (Roche), 10 mM ATP, and 10 mM $MgCl_2$. On the following day, the His_6-protein A-tagged CIRBP-RGG sample was repurified by applying on Ni-NTA agarose beads (Qiagen) and eluted in 50 mM Tris-HCl pH 7.5, 1.0 M NaCl, 500 mM imidazole, 2 mM TCEP, 0.04% NaN_3. The eluted protein was subjected to overnight TEV treatment at 4°C, and on the next day cleaved CIRBP-RGG was desalted to 50 mM Tris-HCl pH 7.5, 150 mM NaCl, 20 mM imidazole, 2 mM TCEP, 0.04% NaN_3 and isolated by a second affinity purification using Ni-NTA beads. As a final polishing step size exclusion chromatography purification step was performed in 50 mM Tris-HCl pH 6.7, 150 mM NaCl, 2 mM TCEP, 0.04% NaN_3 (Superdex 75 Increase 10/300 GL, GE Healthcare) at room temperature.

In vitro Phosphorylation

Recombinant CIRBP-RGG, CIRBP-EGFP and SRPK1 were equilibrated in the phosphorylation buffer. CIRBP-RGG and CIRBP-EGFP were *in vitro* phosphorylated by incubating overnight at room temperature with SRPK1 and 10 mM adenosine triphosphate (ATP), added just prior the reaction start. SRPK1 was used at a molar ratio of 1:2 for CIRBP-RGG and CIRBP-EGFP, and phosphorylation reaction was analyzed using ^{1}H-^{15}N HSQC spectra. Phosphorylated CIRBP-RGG (pCIRBP-RGG) was then isolated from SRPK1 by heating the sample at 95°C for 10 min and performing a size exclusion chromatography in the buffer of interest (Superdex 75 Increase 10/300 GL, GE Healthcare).

In vitro Methylation

The respective gel filtration fractions of CIRBP-RGG and PRMT1 eluted into the methylation buffer were collected and used for

in vitro methylation. CIRBP-RGG was *in vitro* methylated by incubating with PRMT1 and 2 mM S-adenosyl-L-methionine (SAM) overnight at room temperature. PRMT1 was used at a molar ratio of 1:2 for CIRBP-RGG, and the methylation reaction was analyzed by NMR ^{1}H-^{13}C HSQC spectra. To remove PRMT1, methylated CIRBP-RGG (metCIRBP-RGG) sample was heated for 10 min at 95°C and applied on size exclusion chromatography column in the buffer of interest (Superdex 75 Increase 10/300 GL, GE Healthcare).

Stress Granule Association Assay in Semi-Permeabilized Cells

The SGs association assay was performed as described in Hutten and Dormann (2020). HeLa cells were maintained in DMEM high glucose GlutaMAX (Invitrogen) supplemented with 10% FBS and 50 µg/mL gentamicin at 37°C, 5% CO_2 in a humified incubator. For the SG association assay, cells were grown on high precision, poly-L-lysine (Sigma) coated 12 mm coverslips and SGs induced by 10 µM MG132 treatment for 3h. Cells were then permeabilized 2 times 2 min each with 0.004–0.005% digitonin (Calbiochem) in KPB (20 mM potassium phosphate pH 7.4, 5 mM $Mg(OAc)_2$, 200 mM KOAc, 1 mM EGTA, 2 mM DTT and 1 mg/mL each aprotinin (Roth), pepstatin (Roth) and leupeptin (Roth)). After several washes to remove soluble proteins (4 times 4 min in KPB on ice), nuclear pores were blocked by 15 min incubation with 200 µg/mL wheat germ agglutinin (WGA) on ice. Cells were then incubated for 30 min at room temperature with 200 nM CIRBP-EGFP (non- vs phosphorylated and unmethylated vs arg-methylated, respectively) diluted in KPB buffer. For SG association of phosphorylated CIRBP, protein samples were normalized for concentration of ATP and thus differed only in the presence or absence of SRPK (final conc: 100 nM). Note that unmethylated CIRBP contained the same amount of PRMT1 as methylated CIRBP. Subsequently, cells were washed (3 times 5 min in KPB on ice) to remove unbound CIRBP-EGFP. SGs were subsequently subjected to immunofluorescence for G3BP1 as a marker of SGs. For this, cells were fixed in 3.7% formaldehyde/PBS buffer for 7 min at RT and permeabilized in 0.5% TX-100/PBS for 5 min at room temperature. Cells were blocked for 10 min in blocking buffer (1% donkey serum in PBS/0.1% Tween-20) and incubated with primary antibody (rabbit anti-G3BP1, Proteintech, cat.no.13057-2-AP) in blocking buffer for 45–60 min at RT. Secondary antibodies (Alexa 555 Donkey-anti-Rabbit; Thermo, cat.no. A-31572) were diluted in blocking buffer and incubated for 30 min at room temperature. Washing steps after antibody incubation were performed with PBS/0.1% Tween-20. DNA was stained with DAPI (Sigma) at 0.5 mg/mL in PBS and cells mounted in ProLong Diamond Antifade (Thermo). Cells were imaged by confocal microscopy using identical settings for reactions within the same experiment (Performed as described in Hutten and Dormann (2020)).

Stress Granule Enrichment in Intact Cells

For generation of the CIRBP 3D and 3A constructs, synthetic gBlocks (IDT) harboring either S-to-D or S-to-A mutations at the positions Ser97, Ser115 and Ser130 were cloned into the KpnI and BamHI sites of the GCR_2-GFP_2-CIRBP wt construct (Bourgeois et al., 2020). HeLa cells were grown for at least two passages in DMEM supplemented with 10% dialyzed FCS (Thermo) and transiently transfected with GCR_2-GFP_2-CIRBP wt, 3D or 3A constructs using Lipofectamine 2000 (Thermo). One day after transfection, cytoplasmic condensates formed likely either as a response to transfection stress or by CIRBP overexpression were stained by G3BP1 immunostaining, and enrichment of the GCR_2-GFP_2-CIRBP reporter in those cytoplasmic condensates was analyzed.

Confocal Microscopy

For SG association of phosphorylated CIRBP in semi-permeabilized cells, confocal microscopy was performed at the Bioimaging core facility of the Biomedical Center, LMU Munich with an inverted Leica SP8 microscope, equipped with lasers for 405, 488, 552 and 638 nm excitation. Images were acquired using two-fold frame averaging with a 63x1.4 oil objective, and an image pixel size of 59 nm. The following fluorescence settings were used for detection: DAPI: 419–442 nm, GFP: 498–563 nm, Alexa 555: 562–598 nm. Recording was performed sequentially to avoid bleed-through using a conventional photomultiplier tube. For SG association of methylated CIRBP in semi-permeabilized cells and of phosphomutants of CIRBP in intact cells, confocal microscopy was performed at the Light Microscopy Core Facility of the Biocenter at JGU Mainz with an inverted Leica SP5 microscope using lasers for 405 nm, 488 nm (Argon line) and 561 nm for excitation. Images were acquired with bidirectional scanning using two-fold frame averaging with an 100x/1.3 Oil objective and an image pixel size of 60.6 nm. The following fluorescence settings were used for detection: DAPI: 419–442 nm, GFP: 498–563 nm, Alexa 555: 571–598 nm. Recording was performed using a conventional photomultiplier tube for DAPI and Alexa 555 and a Hybrid Detector (HyD) for GFP signals.

Quantification of CIRBP-EGFP in Stress Granules

For quantitative measurements, equal exposure times and processing conditions for respective channels were applied to all samples within one experiment, and acquired images were quantified using ImageJ/Fiji. For quantification of CIRBP SG association in semi-permeabilized cells (performed as described in Hutten and Dormann (2020)), ROIs corresponding to SGs were identified using the wand tool by G3BP1 staining and mean fluorescence intensity in the EGFP channel was determined. For each condition, at least 10 cells and at least 44 SGs were analyzed. To determine the enrichment of CIRBP wt and phosphomutants in intact cells, the ROI corresponding to ~at least 200 G3BP1-positive cytoplasmic condensates was determined by G3BP1 staining as described above, while a band of 0.98 pixels around the condensate was used as a representative area for the cytoplasm. Fluorescence intensity values obtained for the band around the condensate (cytoplasmic intensity) were used as a proxy for expression levels. All values were background corrected and statistical analyses were performed in GraphPad Prism 8.

NMR Spectroscopy

All NMR experiments were conducted at 25°C on Bruker 600- and 700-MHz spectrometers equipped with TXI or a TCI triple-resonance cryoprobe using between 50 and 500 μM of ^{1}H-^{15}N or ^{1}H-^{15}N-^{13}C – labeled CIRBP-RGG. All spectra were processed using TopSpin 4.0.9. In particular, 1D ^{1}H spectra were processed in Mnova 11, 2D heteronuclear spectra were analyzed with the use of NMRFAM-Sparky 3.114 (Lee et al., 2015b) and CcpNMR 3.0.3 (Skinner et al., 2016) software, and triple resonance assignment was performed using CcpNMR 2.4.2 (Vranken et al., 2005). For assignment of *in vitro* phosphorylated and methylated residues in the CIRBP-RGG, we used the previously deposited data corresponding to the ^{1}H-^{15}N chemical shift backbone assignment of CIRBP-RGG (Biological Magnetic Resonance Data Bank (https://www.bmrb.wisc.edu/) entry: 28027) (Bourgeois et al., 2020). In addition, we acquired the following experiments in order to identify the methylated and phosphorylated residues: ^{1}H-^{15}N HSQC, ^{1}H-^{13}C HSQC, (H)CC(CO)NH, CBCA(CO)NH, HN(CA)NNH(N), and HN(CA)NNH(H). Except *in vitro* methylation, all experiments were performed using protein samples prepared in 50 mM Tris-HCl pH 6.7, 150 mM NaCl, 2 mM TCEP, 0.04% NaN_3 (including 20 mM $MgCl_2$ for *in vitro* phosphorylation experiments), and 10% (v/v) deuterium oxide was added for the lock signal in all samples. Processing and analysis of time-resolved 2D NMR spectra was performed as described in Theillet et al. (2013), and the plotted NMR signal intensities corresponding to modified residues were normalized by the sum of respective signal intensities in the reference and final spectra.

Turbidity Assay

CIRBP-RGG, pCIRBP-RGG and RNA (12 × UG repeats) samples were prepared in 50 mM Tris-HCl, pH 7.5, 150 mM NaCl, 2 mM TCEP, 0.04% NaN_3. Turbidity measurements were conducted at 620 nm in 96-well plates with 90-μL samples using a BioTek Power Wave HT plate reader (BioTek).

Differential Interference Contrast Microscopy

CIRBP-RGG, pCIRBP-RGG and RNA (12 × UG repeats) samples were prepared in 50 mM Tris·HCl, pH 7.5, 150 mM NaCl, 2 mM TCEP, 0.04% NaN_3.The 30-μL sample was plated on a 30-mm No. 1 round glass coverslip and mounted on an Observer D1 microscope with 100×/1.45 oil immersion objective (Zeiss). Protein droplets were viewed using HAL100 halogen lamp, and images were captured with an OrcaD2 camera (Hamamatsu) using VisiView 4.0.0.13 software (Visitron Systems GmbH). Droplet formation was induced by the addition of RNA for all proteins, and pictures were recorded for 30 min after addition of RNA.

Isothermal Titration Calorimetry

All proteins samples were equilibrated in the same buffer containing 50 mM Tris·HCl, pH 7.5, 150 mM NaCl, 5 mM TCEP, 0.04% NaN_3. Isothermal titration calorimetry (ITC) measurements were taken with a MicroCal VP-ITC instrument (Microcal) with 28 rounds of 8-μl injections at 25°C. Integration of peaks corresponding to each injection, subtraction of the contribution of protein dilution, and correction for the baseline were performed using the Origin-based 7.0 software provided by the manufacturer. Curve fitting was done with a standard one-site model and gives the equilibrium binding constant (Ka) and enthalpy of the complex formation (ΔH).

RESULTS

Serine-Arginine Protein Kinase-1 Phosphorylates Multiple Sites Within CIRBP-RGG

Arginine methylation in the RG/RGG regions of RNA-binding proteins (RBPs), such as FUS or CIRBP, has been previously shown to suppress their phase separation and stress granule (SG) recruitment, as well as to modulate binding to nuclear importins (Hofweber et al., 2018; Qamar et al., 2018). As several RBPs have been reported to be phosphorylated (Toyota et al., 2010; Nonaka et al., 2016; Monahan et al., 2017; Reineke et al., 2017), we hypothesized that phosphorylation of their low-complexity region could also regulate their LLPS and membrane-less organelles association.

To investigate how phosphorylation in the RG/RGG region of RBPs regulates their LLPS and membrane-less organelles association, we focused on the RG/RGG region of CIRBP (CIRBP-RGG) as it contains serine residues neighboring the low-complexity arginine/glycine-rich regions in its primary sequence (**Figure 1A**). These serine residues may constitute potential phosphorylation sites. NMR spectroscopy is well-suited to study PTMs providing residue-resolved and kinetic information on the post-translationally modified sites (Theillet et al., 2012). Thus, we investigated the effects of treating recombinant CIRBP-RGG with a cell lysate (containing various kinases) obtained from HEK293T cells by applying solution NMR spectroscopy (**Figure 1B**). As recombinant CIRBP-RGG was purified from bacterial cells, the protein was originally non-phosphorylated. ^{1}H-^{15}N heteronuclear single quantum coherence (HSQC) spectra show that after the incubation of the HEK293T whole-cell lysate with ^{13}C-^{15}N-isotopically labeled CIRBP-RGG, downfield ^{1}H-^{15}N resonance peaks appear. With the use of triple-resonance NMR experiments, the new peaks were assigned to phosphorylated residues Ser97 and Ser115. Both residues are located in the proximity of the CIRBP RG/RGG region (**Figure 1A**). These data indicate the presence of enzymatically active serine kinases in the cell lysate phosphorylating serine residues in CIRBP-RGG. We speculated that serine-arginine (SR) protein kinase-1 (SRPK1) phosphorylates CIRBP, as it is known to exhibit a robust phosphorylation activity of serine residues in serine/arginine (SR)-rich protein regions (Ghosh and Adams, 2011; Bullock and Oltean, 2017; Patel et al., 2019).

To address our hypothesis, we established an *in vitro* phosphorylation protocol where purified SRPK1 was incubated

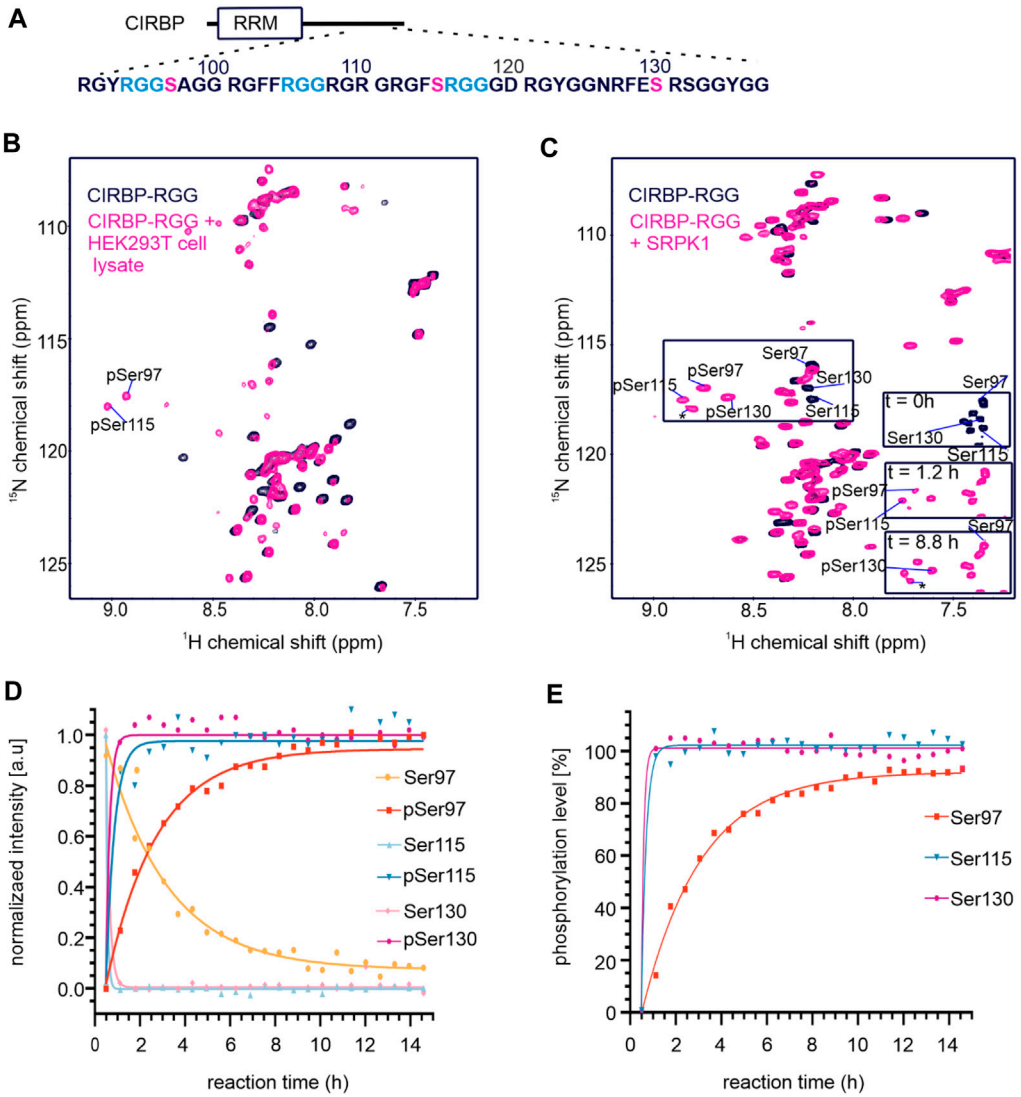

FIGURE 1 | CIRBP-RGG is phosphorylated by SRPK1 *in vitro*. **(A)** Architectural organization of CIRBP showing the RRM (RNA-recognition motif) and the sequence of the CIRBP-RGG containing the three RGGs (blue) with adjacent serine residues (magenta). **(B)** Overlay of ^{1}H-^{15}N HSQC spectra of ^{15}N-labeled CIRBP-RGG (black) with repurified ^{13}C-^{15}N-labeled CIRBP-RGG after incubation with HEK293T whole-cell lysate (magenta). Cross peaks for phosphorylated serine residues assigned by triple resonance experiments are labeled. **(C)** ^{1}H-^{15}N HSQC spectrum of 100 µM ^{15}N-labelled CIRBP-RGG in the absence (black) and presence of 50 µM SRPK1 and 10 mM ATP (magenta). Resonance peaks corresponding to phosphorylated serine residues are marked. Both appearance of phosphoserines and disappearance of the corresponding serine signal are shown at the indicated time points on a bottom right part of the spectrum. The cross peak labeled with an asterisk could not be assigned by triple resonance experiments, and may correspond to either an intermediate phosphorylation state, or to non-assigned phosphosite (e.g. Ser132 is a phosphosite reported in PhosphoSitePlus database, and the shift of its resonance peak was detected in NMR experiments (not shown)). **(D)** Change of NMR cross peak signal intensity of both appearing phosphoserines and disappearing serines is shown over time (sample from **Figure 1C**). **(E)** The graph shows the calculated phosphorylation level for serines 97, 115, and 130 in CIRBP-RGG after incubation with SRPK1 (sample from **Figure 1C**).

with recombinant CIRBP-RGG and adenosine triphosphate (ATP) as a phosphate donor. We examined SRPK1-mediated phosphorylation of ^{15}N-labeled CIRBP-RGG by performing NMR spectroscopy, and monitored the appearance of characteristic downfield ^{1}H-^{15}N NMR cross peaks corresponding to phosphoserine residues (**Figure 1C**). These residues were assigned as pSer97, pSer115 and pSer130. By monitoring the NMR signal intensity of disappearing NMR cross peaks for Ser97, Ser115, Ser130 and appearing resonances for the phospho-residues, we observed that the fully phosphorylated state of serines 115 and 130 is reached within 1 h, whereas the plateau of the maximal NMR intensity for pSer97 is reached after approximately 5 h (**Figures 1D,E**). Both serine residues 115 and 130 are located within the consensus recognition motif for SRPK1 (dipeptide serine-arginine) explaining their faster phosphorylation compared to serine 97, which is separated by two glycine residues from arginine (**Figure 1A**). So far, phosphorylation of serine residues 97 and

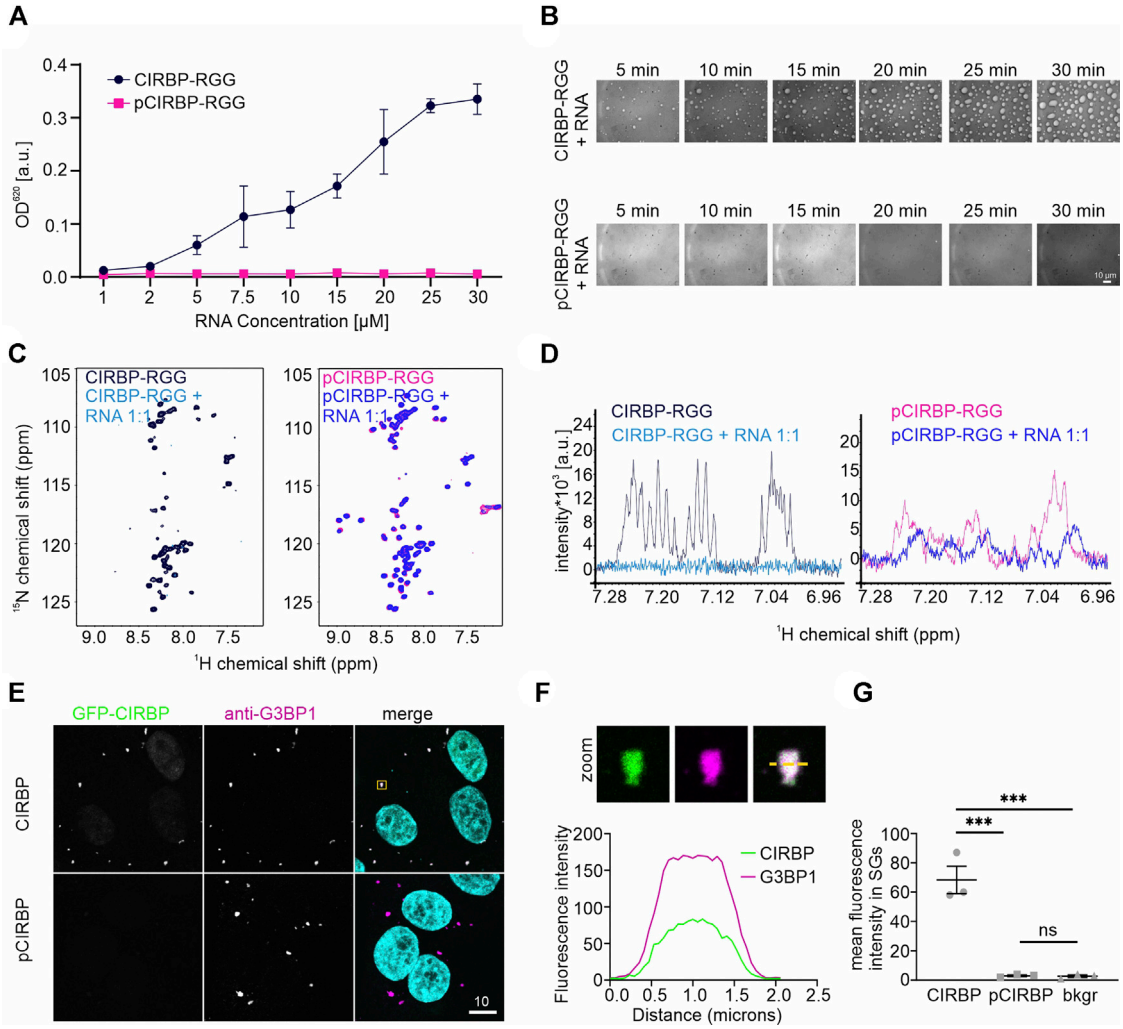

FIGURE 2 | SRPK1-mediated phosphorylation of CIRBP-RGG impairs its phase separation and SGs recruitment. **(A)** Turbidity assay performed at a fixed concentration of CIRBP-RGG and pCIRBP-RGG (both at 30 μM) with an increasing concentration of $(UG)_{12}$ RNA. **(B)** Differential interference contrast microscopy images illustrating CIRBP-RGG **(upper panel)** and pCIRBP-RGG **(bottom panel)** at a concentration 30 μM in the presence of 15 μM $(UG)_{12}$ RNA. Images were recorded over 30 min, scale bar is 10 μm. **(C)** ^{1}H-^{15}N HSQC spectra of 50 μM ^{15}N-labeled CIRBP-RGG **(left panel, in black)** and 50 μM ^{15}N-labeled pCIRBP-RGG **(right panel, in magenta)** in the absence and presence of 50 μM $(UG)_{12}$ RNA (in blue and dark-blue for CIRBP-RGG and pCIRBP-RGG, respectively). **(D)** ^{1}H-NMR spectra of 50 μM ^{15}N-labeled CIRBP-RGG **(left panel, in black)** and 50 μM ^{15}N-labeled pCIRBP-RGG **(right panel, in magenta)** in the absence and presence of $(UG)_{12}$ RNA at a 1:1 stoichiometric ratio (in blue and dark-blue for CIRBP-RGG and pCIRBP-RGG samples, respectively). The spectra were recorded immediately before the corresponding ^{1}H-^{15}N HSQC spectra in **Figure 2C**. **(E)** Association of CIRBP-EGFP **(upper panel)** and phosphorylated CIRBP-EGFP **(lower panel)** with SGs in semi-permeabilized HeLa cells. Scale bar:10 μm. Yellow box indicates the zoomed-in images shown in **Figure 2F**. **(F)** Unmodified CIRBP completely enters the SG as shown by a zoomed-in image of an exemplary SG and plot profiles of fluorescence intensities for G3BP1 and GFP-CIRBP along the yellow line. **(G)** Quantification of the mean fluorescence intensity of CIRBP-EGFP and phosphorylated CIRBP-EGFP in SGs for three independent replicates with ≥44 SGs ± SEM. ***$p <$ 0.0002 by an one-way ANOVA with Tukey's multiple comparison test.

115 has not been reported in databases such as iPTMnet (Huang et al., 2018), PhosphoSitePlus (Hornbeck et al., 2015), qPTM (Yu et al., 2019), or PTMcode (Minguez et al., 2013) implying the discovery of two *de novo* phosphorylation sites in CIRBP-RGG.

In summary, we show that the RG/RGG region of CIRBP can be phosphorylated by SRPK1 *in vitro*, however the manner in which this modification impacts RG/RGG properties on a molecular level remains unknown. Therefore, we subsequently sought to explore the impact of SRPK1-mediated phosphorylation of CIRBP-RGG on its phase separation and SG association.

Phosphorylation Suppresses *in vitro* Phase Separation of CIRBP-RGG and Stress Granules Association of CIRBP in Cells

It has been previously reported that the RG/RGG region of CIRBP phase separates *in vitro* upon addition of RNA in a concentration-dependent manner, and is essential for SG

recruitment in response to cellular stresses (Bourgeois et al., 2020). Furthermore, we and others have shown that asymmetric dimethylation of the RGG3 region in FUS reduces its phase separation propensity (Hofweber et al., 2018; Qamar et al., 2018). Here, we demonstrate that CIRBP-RGG is *in vitro* phosphorylated by SRPK1, but it remains unclear whether CIRBP-RGG phosphorylation could control biologically relevant properties. Therefore, we aimed at deciphering whether SRPK1-mediated *in vitro* phosphorylation of CIRBP-RGG similarly regulates its ability to phase separate and to be recruited into SGs.

In a turbidity assay measuring the optical density (OD) of protein solution at 620 nm, we observed that titration of increasing amounts of $(UG)_{12}$ RNA to a fixed concentration of pCIRBP-RGG yielded no increase in turbidity (**Figure 2A**). In contrast and as expected, the turbidity of CIRBP-RGG in solution increases with rising amounts of added RNA. In line with our turbidity data, differential interference contrast (DIC) microscopy shows the formation of small liquid-like condensates of CIRBP-RGG in the presence of $(UG)_{12}$ RNA, whereas the ability to phase separate was reduced in pCIRBP-RGG (**Figure 2B**). This demonstrates the inhibitory role of *in vitro* phosphorylation on CIRBP-RGG phase separation. To confirm the aforementioned findings, we examined the effects of $(UG)_{12}$ RNA incorporation to a ^{15}N-labeled CIRBP-RGG or pCIRBP-RGG in solution by means of NMR spectroscopy. Addition of 1.0 stoichiometric equivalent of RNA caused a substantial decrease of CIRBP-RGG NMR cross peak signal intensity (**Figure 2C**). This is in line with previous data reporting the formation of high-molecular weight RG/RGG: RNA droplets (Bourgeois et al., 2020). Interestingly, a decrease of NMR signal intensity in the corresponding one-dimensional ^{1}H-NMR spectra after the addition of $(UG)_{12}$ RNA to CIRBP-RGG and pCIRBP-RGG is also observed, suggesting that although pCIRBP-RGG has a reduced propensity to phase separate *in vitro* it still can bind to RNA (**Figure 2D**).

To further confirm our findings in the cellular context, we conducted a SG recruitment assay in cells semi-permeabilized by digitonin (Hutten and Dormann, 2020). We have previously reported that after adding recombinantly purified GFP- and maltose-binding protein (MBP)-tagged full-length CIRBP to semi-permeabilized cells, CIRBP accumulates in G3BP1-positive SGs (Bourgeois et al., 2020). Here, after addition of *in vitro* phosphorylated recombinant CIRBP-EGFP to semi-permeabilized cells, we observed that SG association is significantly reduced compared to the non-phosphorylated protein (**Figures 2E,G**). To analyze localization of CIRBP to cellular, cytoplasmic condensates in dependence of RG/RGG-region phosphorylation in intact cells, we made use of our previously described cytoplasmically anchored CIRBP reporter (GCR_2-GFP_2-CIRBP, (Bourgeois et al., 2020)). In this reporter, CIRBP localizes mainly in the cytoplasm due to fusion with the hormone-binding domain of the glucocorticoid receptor (GCR). When we compared enrichment of a phosphomimetic mutant form of CIRBP, in which Ser 97, 115 and 130 were replaced by aspartate; (CIRBP 3D) with CIRBP wt, we noticed a mild, but significant reduction of the enrichment for the 3D mutant to cytoplasmic condensates that stained positive for the SG protein G3BP1 (**Figure 3A**). Importantly, mutation of the same serines to alanines (CIRBP 3A) did not significantly affect this recruitment compared to the wildtype. While the mean expression levels of the reporters were relatively similar, we noted however, that in some replicates the 3D mutant exhibited a slightly reduced expression level compared to CIRBP wt and 3A, which could also influence the level of SG localization to some extent. Therefore, we binned data with similar expression levels to allow for a direct comparison of cells with comparable expression levels (**Figure 3B**) and confirmed a significant reduction of the enrichment for the 3D mutant to cytoplasmic condensates. These findings suggest that phosphorylation of the RG/RGG region also lessens recruitment of CIRBP to membraneless organelles in intact cells. We cannot exclude that other potential SRPK1 phosphorylation sites contribute to the observed SGs association impairment in the context of full-length CIRBP in our semi-permeabilized cell assay, yet our previous data demonstrated that the RG/RGG region of CIRBP, and not its C-terminal RSY regions, drives SGs association in cells (Bourgeois et al., 2020).

Furthermore, considering our results demonstrating the inhibitory effects of serine phosphorylation of CIRBP-RGG on its phase separation and SGs recruitment, we proceeded to investigate how PRMT1-mediated arginine methylation of CIRBP affects its SGs association. We observe that SG recruitment of *in vitro* methylated CIRBP-EGFP in semi-permeabilized cells is substantially reduced compared to the non-methylated protein (**Figure 4**). Hence, our data remain in agreement with a previous study showing reduction of LLPS and SGs recruitment of methylated FUS, another RG/RGG-region containing protein (Hofweber et al., 2018), and imply that both serine phosphorylation and arginine methylation of CIRBP-RGG weaken its ability to associate with SGs.

Collectively, our data reveal that SRPK1-mediated serine phosphorylation of CIRBP-RGG reduces RNA-driven phase separation *in vitro* and suppresses SGs recruitment of CIRBP. Lastly, we uncover that arginine methylation, similarly to serine phosphorylation, reduces SG recruitment of CIRBP-EGFP, hence the biological implications of the co-existence of these two PTMs and their mutual modulation in CIRBP and other RG/RGG-region containing proteins remains yet to be discovered.

SRPK1-mediated Phosphorylation of CIRBP-RGG Impairs its Binding to the Nuclear Import Receptor Transportin-1

The nuclear import receptor Transportin-1 (TNPO1) binds its cargoes through a proline tyrosine (PY)-NLS and an RG/RGG region to mediate nuclear import (Lee et al., 2006; Dormann et al., 2010; Bourgeois et al., 2020). We and others have shown that TNPO1 binding to RG/RGG proteins, such as FUS or CIRBP, can reduce their phase separation *in vitro* and SGs recruitment in cells, thus exerting a chaperone-like function (Guo et al., 2018; Hofweber et al., 2018; Qamar et al., 2018; Yoshizawa et al., 2018).

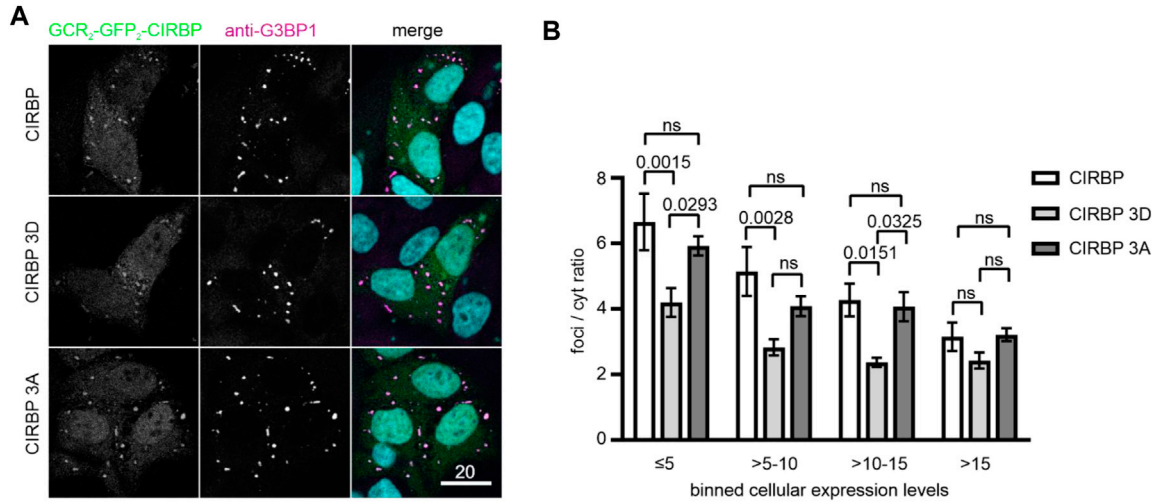

FIGURE 3 | Recruitment of CIRBP into G3BP1-positive condensates in intact cells depends on phosphorylation of the RG/RGG region. **(A)** Association of GCR_2-GFP_2-CIRBP **(upper panel),** GCR_2-GFP_2-CIRBP 3D mutant **(middle panel),** and GCR_2-GFP_2-CIRBP 3A mutant **(bottom panel)** with cytoplasmic condensates positive for G3BP1 in HeLa cells. Scale bar: 20 μm. **(B)** Quantification of enrichment of GCR_2-GFP_2-CIRBP wt, 3D or 3A mutant in G3BP1-positive condensates over the cytoplasm (foci/cyt ratio) as a mean of 4 independent replicates ± SEM depending on the cellular expression levels represented in bins of fluorescence intensity units, adjusted *p*-values by 2-way ANOVA with Tukey's multiple comparisons test; ns, non-significant.

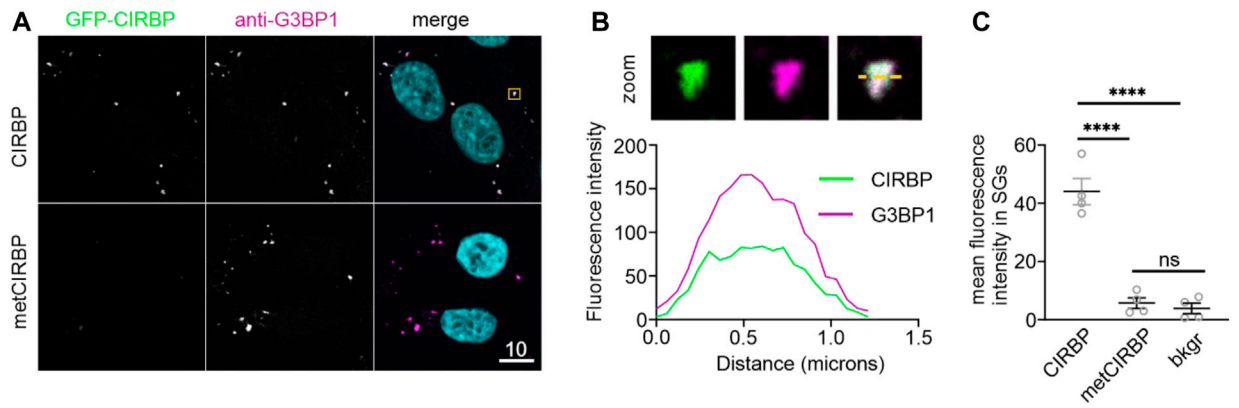

FIGURE 4 | PRMT1-mediated arginine methylation of CIRBP-RGG reduces its SGs recruitment. **(A)** Association of CIRBP-EGFP **(upper panel)** and methylated CIRBP-EGFP **(metCIRBP; lower panel)** with SGs in semi-permeabilized HeLa cells. Scale bar: 10 μm. Yellow box indicates the zoomed-in images shown in **Figure 4B**. **(B)** Unmodified CIRBP completely enters the SG as shown by a zoomed-in image of an exemplary SG and plot profiles of fluorescence intensities for G3BP1 and GFP-CIRBP along the yellow line. **(C)** Quantification of the mean fluorescence intensity of CIRBP-EGFP and methylated CIRBP-EGFP in SGs for 4 independent experiments using CIRBP from 2 independent methylation reactions with ≥44 SGs ± SEM, adjusted *p*-value: ****$p < 0.0001$ by one-way ANOVA with Tukey's multiple comparisons test; ns, non-significant.

Furthermore, arginine methylation of the RG/RGG region in CIRBP weakens its interaction with TNPO1 (Hofweber et al., 2018), but it is still unknown whether and how phosphorylation of CIRBP-RGG affects transportin-1 binding.

To address this question, we utilized isothermal titration calorimetry (ITC) to characterize binding between TNPO1 and pCIRBP-RGG. ITC analysis revealed that *in vitro* phosphorylation of CIRBP-RGG precluded the binding of TNPO1, whereas non-phosphorylated CIRBP-RGG bound TNPO1 with an ITC-derived dissociation constant (Kd) of 124.4 ± 14.8 nM (**Supplementary Figures S1A,B**). These results demonstrate that phosphorylation of CIRBP-RGG substantially reduces binding to TNPO1.

RS/SR Phosphorylation Sites are Found Next to RG/RGG Regions in a Variety of Human Proteins

Given that the primary sequence of CIRBP-RGG contains serine residues located in the proximity to the RG/RGG region with

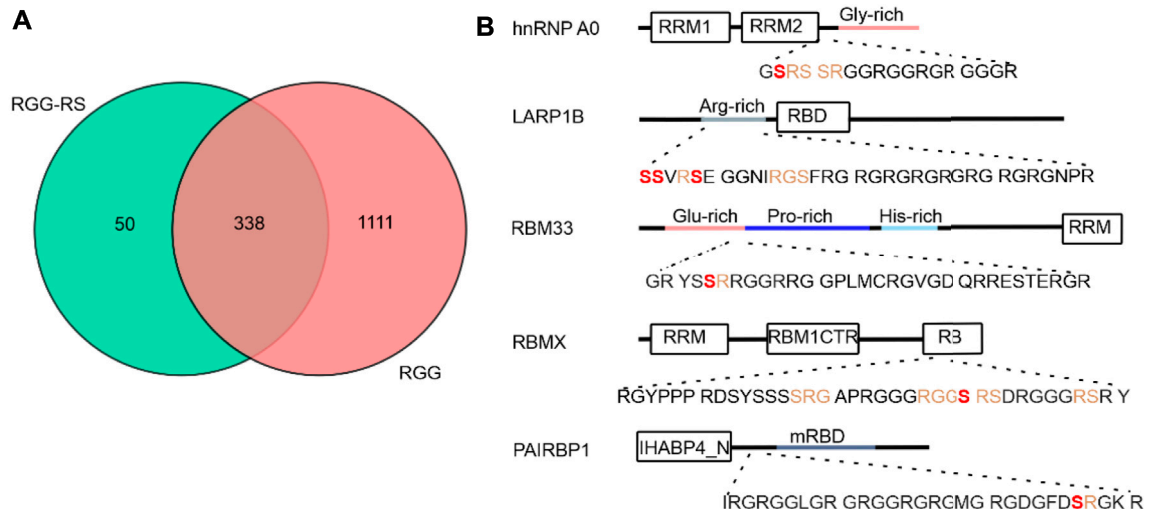

FIGURE 5 | Analysis of distribution of coexisting RG/RGG and RS/SR regions in human proteome. **(A)** Venn diagram corresponding to the PROSITE analysis (https://prosite.expasy.org/scanprosite/) of two motifs from protein sequences database filtered for human proteins (taxid:9606) harboring either 1) a di-RG motif (pink) each spaced by zero to five amino acids [R-G-x(0-5)-R-G] or 2) a di-RG motif in the presence of RS or SR in the middle, after or before di-RG motif(blue) spaced by zero to five residues [R-G-x(0,5)-R-G-x(0,5)-R/S], [R/S-x(0,5)-R-G-x(0,5)-R-G] and [R-G-x(0,5)-R/S-x(0,5)-R-G]. These two groups of proteins were compared with each other in the Venn diagram. **(B)** Domain organization of five putative human proteins possessing RS/SR motifs within or next to the RG/RGG region; architectural representation was performed according to InterPro (https://www.ebi.ac.uk/interpro/protein/) and Uniprot (https://www.uniprot.org/) databases. RS/SR motifs located in the proximity to RG/RGG regions are shown in orange, and serine residues that are reported to carry phosphorylation (according to iPTM and PhosphoSitePlus) are illustrated in bold (red). Abbreviations used: hnRNP A0 - heterogeneous nuclear ribonucleoprotein A0; RRM – RNA recognition motif; LARP1B- La ribonucleoprotein domain family member 1B; RBD - HTH La-type RNA-binding domain; RBM33 - RNA-binding protein 33 (drawn not in a scale); RBMX - RNA-binding motif protein, X chromosome; RBM1CTR - C-terminal region present in RBM1-like RNA binding hnRNPs; RB- region necessary for RNA-binding; PAIRBP1 - plasminogen activator inhibitor 1 RNA-binding protein; IHABP4_N - Intracellular hyaluronan-binding protein 4, N-terminal domain; mRBD - Hyaluronan/mRNA binding family domain.

arginine residues serving as methylation sites (**Figure 1A**), we performed a bioinformatic analysis to address the question of how commonly RS/SR phosphorylation sites can be found within or next to RG/RGG regions in the human proteome. We discovered that 338 out of 1449 proteins containing a di-RG motif possess RS/SR sites located within a distance of 5 residues (**Figure 5A**). Subsequently, we examined whether serine residues that are situated within or near RG/RGG regions can be phosphorylated, and we uncovered that these serines can be modified in a similar manner as in CIRBP-RGG (**Supplementary Datasets S1, S2**). Of interest, we discovered that a number of the identified proteins can carry both arginine methylation and serine phosphorylation sites in their adjacent RG/RGG and RS/SR regions (examples given in **Supplementary Dataset S2**; **Figure 5B**). Taken together, our findings indicate the co-occurrence of RG/RGG and RS/SR regions in a variety of human proteins and the possible crosstalk between phosphorylation and arginine methylation within these regions. We next sought to investigate the interplay between serine phosphorylation and arginine methylation in CIRBP-RGG.

Arginine Methylation of CIRBP-RGG Inhibits its SRPK1-mediated Phosphorylation and *vice versa*

To dissect whether phosphorylation of CIRBP-RGG regulates its arginine methylation and vice versa, we recorded a series of ^{1}H-^{15}N-HSQC or ^{1}H-^{13}C-HSQC spectra over time to follow *in vitro* phosphorylation and methylation reactions, respectively, with measurements starting immediately after reconstitution of the *in vitro* system. To analyze *in vitro* methylation of phosphorylated CIRBP-RGG (pCIRBP-RGG), recombinant ^{13}C,^{15}N-labeled pCIRBP-RGG was applied on a gel filtration column to remove SRPK1 and transfer the protein into methylation buffer. pCIRBP-RGG was then *in vitro* methylated by addition of protein arginine methyltransferase-1 (PRMT1) and S-adenosyl-L-methionine (SAM) as a methyl group donor. Immediately after preparing the *in vitro* methylation reaction, ^{1}H-^{13}C-HSQC and ^{1}H-^{15}N-HSQC spectra were recorded and examined for the appearance of a cross peak indicative for arginine methylation ($^{1}H_{\delta}$ 3.084 ppm,$^{13}C_{\delta}$ 41.554 ppm) (**Figures 6A,B**). The signal intensity of a ^{1}H-^{13}C NMR cross peak corresponding to methylated arginine residues in pCIRBP-RGG reached a plateau within approximately 9 h after the reaction start, whereas for non-phosphorylated CIRBP-RGG the plateau was achieved within 7 h (**Figure 6C**). Consistent with reported methylarginines in iPTM/PhosphoSitePlus, our analysis of ^{1}H-^{13}C-HSQC and HCC(CO)NH spectra revealed that arginine residues 94, 101, 105, 112 and 116 are methylated in non-phosphorylated CIRBP-RGG (**Supplementary Figure S2**). Based on triple resonance assignment of methylated pCIRBP-RGG, the presence of an attached methyl group was detected in arginine residues 101, 105, 108, and 110 (**Supplementary**

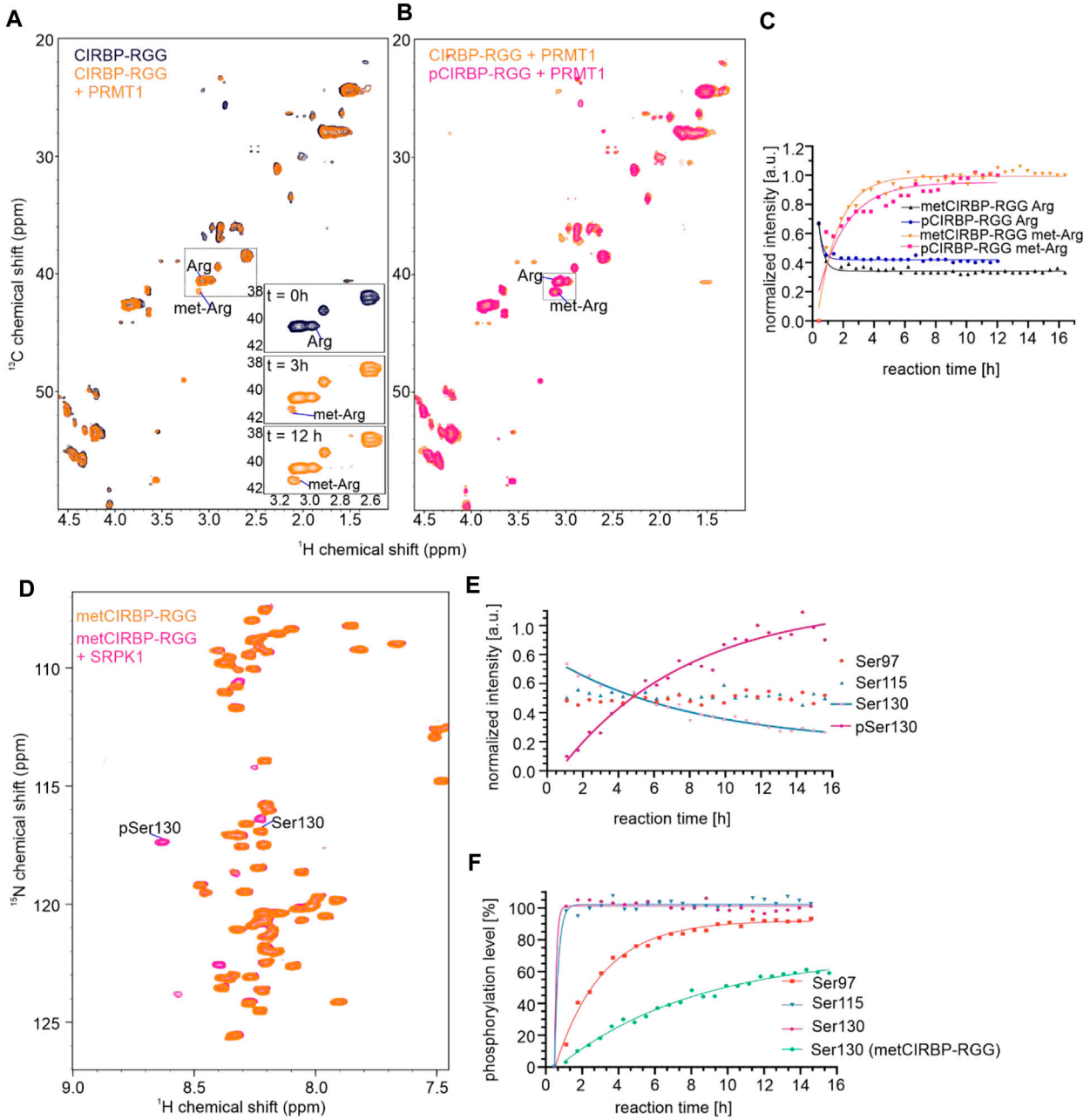

FIGURE 6 | Arginine methylation of CIRBP-RGG modulates its SRPK1-mediated phosphorylation and *vice versa.* **(A)** Overlay of ^{1}H-^{13}C HSQC spectra of 50 μM ^{13}C-^{15}N-labeled CIRBP-RGG in the absence (black) and presence of 10 μM PRMT1 and 2 mM SAM (orange). The region containing a peak corresponding to methylated arginines is indicated by a dotted box, and the rising intensity of methylated arginine cross peak can be followed at the three exemplary time points shown in a bottom right part of the spectrum. **(B)** Overlay of ^{1}H-^{13}C HSQC spectra of ^{13}C-^{15}N-labeled 50 μM metCIRBP-RGG (sample as in **Figure 6A**; in orange) and 100 μM pCIRBP-RGG in the presence of 40 μM PRMT1 and 2 mM SAM (in magenta). The region containing a peak corresponding to methylated arginines is indicated by a dotted box. **(C)** Change of NMR signal intensities of cross peaks corresponding to methylated and non-methylated arginines in metCIRBP-RGG (in orange and black, respectively) and pCIRBP-RGG (in magenta and dark-blue, respectively) over time (samples from **Figure 6B**). **(D)** ^{1}H-^{15}N HSQC spectrum of 50 μM ^{13}C-^{15}N-labeled *in vitro* methylated CIRBP-RGG in the absence (orange) and presence of 25 μM SRPK1 (magenta) **(E)** Change of NMR signal intensity corresponding to cross peaks of SRPK1-phosphorylated metCIRBP-RGG serine residues (sample from **Figure 6D**). **(F)** Comparison of the calculated phosphorylation level of serines 97, 115 and 130 in pCIRBP-RGG (as in **Figure 1E**) with the only phosphoresidue (pSer130) in metCIRBP-RGG after the incubation with SRPK1 (sample from **Figure 6D**).

Figure S2). Resonance peaks allowing to assess the methylation status of arginine 108 and 110 appeared only in the spectrum of methylated pCIRBP-RGG, therefore we cannot draw conclusions about their methylation status in the context of the non-phosphorylated protein. Hence, the presence of a phosphate group on serine residues 97 and 115

prevented methylation of arginines 94, 112 and 116 located in the proximity to the phosphoresidues.

Moreover, we examined how arginine methylation of CIRBP-RGG affected the capacity of SRPK1 to *in vitro* phosphorylate serine residues in CIRBP. To this end, purified ^{13}C-^{15}N-labeled CIRBP-RGG was *in vitro* methylated and subjected to gel filtration to remove PRMT1 (metCIRBP-RGG). After the addition of SRPK1 and ATP to the solution of metCIRBP-RGG, a ^{1}H-^{15}N NMR cross peak ($^{1}H_{\delta}$ 8.620 ppm, $^{15}N_{\delta}$ 117.318 ppm) assigned to pSer130 was detected 1 h after the reaction start (**Figures 6D,E**). For pCIRBP-RGG the final phosphorylation level of pSer130 was estimated to 90%, while in the case of metCIRBP-RGG this value equaled around 60% (**Figure 6F**) and the signal of non-phosphorylated Ser130 could still be detected (**Figures 6D,E**). Resonance peaks for phosphoserines pSer97 and pSer115 were not observed in phosphorylated metCIRBP-RGG (**Figure 6D**), and the intensity of the peaks corresponding to the non-phosphorylated species remained constant during the experiment (**Figure 6E**). Compared to *in vitro* phosphorylation of non-methylated CIRBP-RGG where the maximal signal intensity of the pSer130 resonance peak was achieved within approximately 1 h after the reaction start, for metCIRBP-RGG the pSer130 signal intensity did not reach a plateau after 12 h (**Figures 6E,F**). As serines Ser97 and Ser115 are located in the direct vicinity of arginine residues in the RG/RGG region, we suggest that the presence of methyl groups on these arginines precludes the addition of a phosphate group to a proximal serine presumably via steric effects.

In conclusion, our data show that phosphorylation of CIRBP-RGG precludes methylation of arginine residues in direct proximity to phosphoserines. Our results also indicate that arginine methylation of CIRBP-RGG prevents SRPK1-mediated phosphorylation of serines 97 and 115, and affects kinetics of phosphorylation of serine 130, which is located more distant to the RG/RGG region.

DISCUSSION

Here we show that CIRBP-RGG is a substrate for SRPK1-mediated phosphorylation (**Figure 1**). By applying NMR spectroscopy, we identified two novel phosphorylation sites in CIRBP at positions Ser97 and Ser115, where Ser97 is located outside of the consensus serine-arginine dipeptide recognition motif. Furthermore, we demonstrated that arginine methylation in the RG/RGG region of CIRBP suppresses phosphorylation of serine residues 97 and 115 by SRPK1, and the phosphorylation kinetics of phosphoserine 130 is slower compared to non-methylated CIRBP-RGG (**Figures 6D–F**). The presence of methyl groups on arginines might introduce a sterical hindrance that precludes SRPK1 binding and in turn inhibits phosphorylation of serines 97 and 115. We also found that SRPK1-mediated phosphorylation of CIRBP-RGG prevented methylation of arginines 94, 112 and 116 located in the proximity to phosphoserines (**Figures 6B,C**, **Supplementary Figure S2**). Aside from steric effects, the negatively charged phosphate group could interfere via electrostatic repulsion with the acidic region found in the enzymatic site of PRMTs (Zhang and Cheng, 2003). Thus, we suggest the vicinity of negatively charged phosphate groups to target arginines prevents binding to PRMT1 active site and methylation of arginines 94, 112, and 116 due to the electrostatic repulsion. This is in line with the observation that negatively charged amino acids next to the arginine disfavour methylation (Hamey et al., 2018). Hence, our findings indicate that arginine methylation and serine phosphorylation of CIRBP-RGG directly modulate each other (**Figure 7**).

To our knowledge, the crosstalk between arginine methylation and phosphorylation in the RG/RGG region has not been previously reported for CIRBP. It has been shown that arginine methylation within the RG/RGG region of yeast hnRNP protein Npl3p prevents phosphorylation of Npl3p by Sky1p, which is a yeast orthologue of SRPK1 (Yun and Fu, 2000; Lukasiewicz et al., 2007). Smith *et al.* recently demonstrated that Sky1p-mediated phosphorylation of the SRGG regions in *Saccharomyces cerevisiae* fibrillarin (Nop1p) blocks arginine methylation by Hmt1p (Smith et al., 2020). The authors also reported that a loss of these PTMs results in an atypical nucleolar localization. Of note, authors found that the presence of acidic residues/phosphoserine in Nop1p at positions -1, -2, (and to a smaller extent at -5 and +3) with respect to arginine in the SRGG motif negatively affects Hmt1p-mediated methylation. In contrast, we observed that phosphorylation of CIRBP-RGG did not inhibit PRMT1-methylation of Arg101 (at position +4 from pSer97) and Arg110 (at position -5 from pSer115) suggesting phosphorylation might exert more local inhibiting effects on methylation in human RG/RGG proteins. Moreover, the RG/RGG region of the herpes simplex virus 1 protein ICP27 has been demonstrated to interact with SRPK1 resulting in its translocation from the cytoplasm to the nucleus, and this interaction was decreased when arginine methylation was blocked as demonstrated by co-immunoprecipitation and co-localization studies (Souki and Sandri-Goldin, 2009). Considering the aforementioned examples of the crosstalk between arginine methylation and phosphorylation in RG/RGG proteins, by conducting a bioinformatic analysis we identified 338 di-RG motif-containing proteins that possess RS/SR sites within a five residues distance and some of them were reported to harbour simultaneously arginine methylation and phosphorylation sites. Taken together, these findings corroborate that the interplay between phosphorylation and arginine methylation in RG/RGG regions of proteins may play important roles across the RG/RGG proteome, and remains largely understudied. In this respect, it would be interesting to examine the effects of serine phosphorylation and arginine methylation crosstalk on phase separation, SG recruitment, and the binding to nuclear transport receptors for other (identified) RG/RGG proteins.

We demonstrated that phosphorylation of CIRBP-RGG has profound suppressing effects on its *in vitro* phase separation and SG recruitment (**Figure 2** and **Figure 7**). Phase separation of CIRBP-RGG is induced by the presence of negatively charged RNA, and is driven by multivalent interactions between these

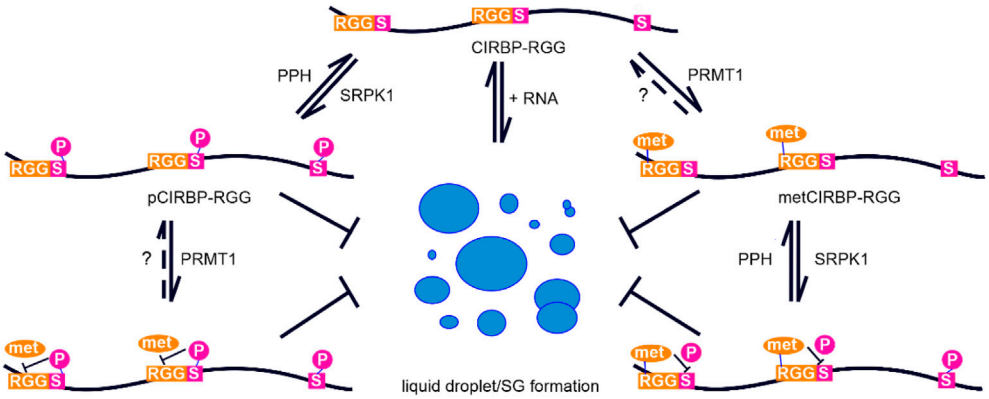

FIGURE 7 | Proposed model depicting arginine methylation and phosphorylation crosstalk in CIRBP-RGG. Graph illustrating the suppression of CIRBP-RGG *in vitro* phase separation by phosphorylation and arginine methylation, as well as the crosstalk between arginine methylation and phosphorylation within CIRBP RG/RGG region. The formation of liquid droplets and biomolecular condensates is shown in a simplified manner as blue circles. Dotted line and the question mark indicate the lack of consensus regarding arginine de-methylation, and PPH represents protein phosphatases.

oppositely charged biomolecules. The positively charged guanidino group of arginine in the RG/RGG region can be involved in the electrostatic interactions, π-stacking, and hydrogen-bonding with RNA molecules, which promote heterogeneous phase separation (Chong et al., 2018). We propose that the interactions of pCIRBP-RGG with RNA, and hence its RNA-driven LLPS *in vitro*, are reduced via the following mechanisms: 1) addition of phosphate groups to serine residues in the proximity of the RG/RGG repeats decreases the overall charge of the RG/RGG region disfavouring its electrostatic interactions with the phosphate backbone of RNA; 2) the incorporation of phosphate group can alter hydrogen bond network of arginine as phosphates can form strong hydrogen bonds with arginines (Mandell et al., 2007). A recent study reported that SRPK1-phosphorylation of a serine/arginine-rich domain in the nucleocapsid protein of severe acute respiratory syndrome coronavirus 2 (SARS-CoV-2) attenuates its RNA-induced phase separation and partitioning into RNA-rich polymerase-containing condensates (Savastano et al., 2020). Furthermore, Shattuck *et al.* revealed that activity of the yeast kinase Sky1 is required for efficient stress granule disassembly, partly through phosphorylation of Npl3 (Shattuck et al., 2019). These findings suggest that SRPK1-mediated phosphorylation may play a "chaperone-like" role in reducing LLPS of certain substrates and the formation of biomolecular condensates for a larger class of proteins containing low-complexity domains enriched in glycine, serine and positively charged arginine residues. Further investigations are required to clarify the role of phosphorylation on the dynamics of membrane-less organelles in cells.

Additionally, our study revealed that SRPK1-mediated phosphorylation of CIRBP-RGG impairs its binding to TNPO1 (**Supplementary Figure S1**). The effects of phosphorylation of cargo proteins on binding to their nuclear import receptors seem to be dependent on the system of interest (Nardozzi et al., 2010). As examples of up-regulation of nuclear import upon phosphorylation can serve 1) phosphorylation of Ser385 in the NLS of Epstein-Barr virus nuclear antigen 1 (EBNA-1) protein that increases the binding affinity for an importin α5, which in turn recruits a receptor importin β1 (Kitamura et al., 2006); 2) the RS region of serine/arginine-rich protein ASF/SF2 that acts as the NLS when phosphorylated, while in an unphosphorylated form the protein localizes to the cytoplasm (Lai et al., 2000); or 3) Sky1p-mediated phosphorylation of Npl3p in *S. cerevisiae* which leads to efficient interaction with the nuclear import receptor Mtr10p (Yun and Fu, 2000). Whereas as examples of down-regulation of nuclear import upon phosphorylation can serve: 1) nuclear factor of activated T-cells (NFAT) which resides in the cytoplasm when its serine-rich region is phosphorylated, and translocates to the nucleus upon calcineurin binding that dephosphorylates certain serine residues causing the exposure of the NLS (Ortega-Pérez et al., 2005); or 2) *S. cerevisiae* transcription factor Swi6, in which the presence of phosphoserine160 or phosphomimetic mutation at this site substantially decreases the binding affinity for importin α1, and the nucleocytoplasmic localization and phosphorylation state of Swi6 are dependent on the cell-cycle state (Harreman et al., 2004). Elucidating how nuclear import is regulated is also crucial for a better understanding of the mechanisms governing the onset of neurodegenerative diseases, such as ALS and FTD (Kwiatkowski et al., 2009; Vance et al., 2009). In this respect, arginine methylation has been demonstrated to affect nucleocytoplasmic transport of FUS (Dormann et al., 2012), PABPN1 (Fronz et al., 2011), SERBP1 (Lee et al., 2012), or CIRBP (Aoki et al., 2002). Mutations in the C-terminal NLS of FUS, consisting of a PY-NLS and a RG/RGG region, can lead to reduced binding to TNPO1 and impaired nuclear import (Dormann et al., 2010; Zhang and Chook, 2012). This causes the formation of pathological cytoplasmic FUS aggregates and motor neuron degeneration, with the most severe TNPO1 binding-disrupting mutations resulting in early onset ALS and a particularly fast progression of disease (Dormann et al.,

2010). Therefore, understanding the regulation of nuclear import of RG/RGG region-containing proteins by means of PTMs might allow the development of effective therapies against neurodegenerative disorders.

It is intriguing to further speculate about possible advantages of serine phosphorylation for CIRBP and other RG/RGG proteins. Protein phosphorylation by kinases and dephosphorylation by phosphatases provide a dynamic control mechanism critical for the regulation of cellular processes, such as signal transduction, protein synthesis, cell growth, development, division, and aging (Ardito et al., 2017; Gelens and Saurin, 2018). Phosphorylation thus acts as a rapid switch, quickly modulating protein function in response to signals (Hofweber and Dormann, 2019). In contrast, transfer of methyl groups to arginine residues catalysed by protein-arginine methyltransferases is a much slower process (Zhang et al., 2021), and whether this modification can be reversed (and which enzyme catalyses demethylation reaction) remains until now poorly understood (Guccione and Richard, 2019). Arginine methylation is therefore significantly more stable and static compared to serine phosphorylation (Zhang et al., 2021), which can be erased within minutes (Gelens and Saurin, 2018). Consequently, we hypothesize that phosphorylation of CIRBP-RGG offers a means of dynamic regulation of its phase separation *in vitro*, SG association, and protein-protein interactions (e.g. with nuclear import receptor TNPO1) in response to cellular signals. Serine phosphorylation, by suppressing *in vitro* LLPS and triggering disassembly of SGs (i.e. exerts similar effects as arginine methylation), might be beneficial for cells when a rapid modulation of protein function is necessary, or when arginine methylation level is decreased, e.g. due to methionine deprivation, aggregation of PRMTs, or in senescent cells (Hong et al., 2012; Tang et al., 2015; Albrecht et al., 2019). Arginine methylation could then rather serve as a "protein quality control" mechanism regulating protein homeostasis and phase separation, and may be especially relevant in modulating function of neurons that require this modification for a proper stress response (Simandi et al., 2018).

Of note, our findings reveal that CIRBP-RGG can carry both phosphorylation and arginine methylation simultaneously (**Figure 6**, **Supplementary Figure S2**). Considering that both modifications play similar roles in regulating phase separation *in vitro* - it remains to be clarified whether they cooperate or interfere with each other. Our bioinformatic analysis suggest that serine phosphorylation within RG/RGG regions might constitute a general mechanism for the dynamic regulation of phase separation of RG/RGG proteins. Still, the manner in which serine phosphorylation affects protein-protein interactions and subcellular localization can be protein specific.

In conclusion, our results imply that PTMs should be seen as key regulators of RBPs phase separation and nucleocytoplasmic transport, and the intricate crosstalk between multiple PTMs serves to fine-tune to changing cellular conditions. As exemplified here for the RG/RGG region of CIRBP, it is essential to study intrinsically disordered regions carrying PTMs when one intends to investigate the regulation of phase separation *in vitro* and the formation of protein aggregates.

DATA AVAILABILITY STATEMENT

The datasets generated for this study are available on request to the corresponding author. The previous original contributions presented in the study are publicly available. This data can be found here: https://bmrb.io/data_library/summary/index.php?bmrbId=28027.

AUTHOR CONTRIBUTIONS

BB and TM conceived the concept and project. TM and DD acquired funding for this project and supervised research. AL, QZ, and SU expressed and purified different proteins. AL established protocols for *in vitro* phosphorylation and methylation of CIRBP-RGG. AL, QZ, SU, FZ, and BB performed NMR experiments. AL, QZ, SU, FZ, BB, and TM analyzed NMR data. SU conducted turbidity assays, DIC microscopy and ITC experiments. SH performed stress granules recruitment assays, and analyzed data. AL and SU prepared figures. AL and TM wrote the manuscript with input from all authors. All authors contributed to manuscript revision, read, and approved the submitted version.

FUNDING

The work was supported by Austrian Science Fund (FWF) grants P28854, I3792, doc.fund BioMolStruct DOC130. and DK-MCD W1226 to TM, the Deutsche Forschungsgemeinschaft (DFG, German Research Foundation) through projects DO1804/2-1 and DO1804/3-1 to DD; TM was supported by the Austrian Research Promotion Agency (FFG) Grants 864690 and 870454; the Integrative Metabolism Research Center Graz; Austrian Infrastructure Program 2016/2017, the Styrian Government (Zukunftsfonds), and BioTechMed-Graz (Flagship project DYNIMO). AL, QZ, and SU were trained within the frame of the PhD program Metabolic and Cardiovascular Disease, and FZ was trained within the frame of the PhD program in Molecular Medicine. DD also acknowledges support by the Munich Cluster for Systems Neurology (EXC2145 SyNergy – ID 390857198), ReALity – Resilience, Adaptation and Longevity (Forschungsinitiative des Landes Rheinland-Pfalz) and the Gutenberg Forschungskolleg (GFK) of JGU Mainz.

ACKNOWLEDGMENTS

We acknowledge support by the core facilities Bioimaging of the Biomedical Center Munich and Light Microscopy Core Facility of the Biocenter at JGU Mainz. We would like to thank Emil Spreitzer for discussions and skilled assistance with NMR spectroscopy.

SUPPLEMENTARY MATERIAL

The Supplementary Material for this article can be found online at: https://www.frontiersin.org/articles/10.3389/fmolb.2021.689687/full#supplementary-material

REFERENCES

Aguzzi, A., and Altmeyer, M. (2016). Phase Separation: Linking Cellular Compartmentalization to Disease. *Trends Cel Biol.* 26, 547–558. doi:10.1016/j.tcb.2016.03.004

Alberti, S., Gladfelter, A., and Mittag, T. (2019). Considerations and Challenges in Studying Liquid-Liquid Phase Separation and Biomolecular Condensates. *Cell* 176, 419–434. doi:10.1016/j.cell.2018.12.035

Alberti, S. (2017). Phase Separation in Biology. *Curr. Biol.* 27, R1097–R1102. doi:10.1016/j.cub.2017.08.069

Albrecht, L. V., Bui, M. H., and De Robertis, E. M. (2019). Canonical Wnt Is Inhibited by Targeting One-Carbon Metabolism through Methotrexate or Methionine Deprivation. *Proc. Natl. Acad. Sci. USA.* 116, 2987–2995. doi:10.1073/pnas.1820161116

Andersson, M. K., Ståhlberg, A., Arvidsson, Y., Olofsson, A., Semb, H., Stenman, G., et al. (2008). The Multifunctional FUS, EWS and TAF15 Proto-Oncoproteins Show Cell Type-specific Expression Patterns and Involvement in Cell Spreading and Stress Response. *BMC Cel Biol.* 9, 37. doi:10.1186/1471-2121-9-37

Aoki, K., Ishii, Y., Matsumoto, K., and Tsujimoto, M. (2002). Methylation of Xenopus CIRP2 Regulates its Arginine- and Glycine-Rich Region-Mediated Nucleocytoplasmic Distribution. *Nucleic Acids Res.* 30, 5182–5192. doi:10.1093/nar/gkf638

Ardito, F., Giuliani, M., Perrone, D., Troiano, G., and Muzio, L. L. (2017). The Crucial Role of Protein Phosphorylation in Cell Signaling and its Use as Targeted Therapy (Review). *Int. J. Mol. Med.* 40, 271–280. doi:10.3892/ijmm.2017.3036

Bah, A., and Forman-Kay, J. D. (2016). Modulation of Intrinsically Disordered Protein Function by Post-translational Modifications. *J. Biol. Chem.* 291, 6696–6705. doi:10.1074/jbc.r115.695056

Banani, S. F., Lee, H. O., Hyman, A. A., and Rosen, M. K. (2017). Biomolecular Condensates: Organizers of Cellular Biochemistry. *Nat. Rev. Mol. Cel Biol.* 18, 285–298. doi:10.1038/nrm.2017.7

Banani, S. F., Rice, A. M., Peeples, W. B., Lin, Y., Jain, S., Parker, R., et al. (2016). Compositional Control of Phase-Separated Cellular Bodies. *Cell* 166, 651–663. doi:10.1016/j.cell.2016.06.010

Bentmann, E., Neumann, M., Tahirovic, S., Rodde, R., Dormann, D., and Haass, C. (2012). Requirements for Stress Granule Recruitment of Fused in Sarcoma (FUS) and TAR DNA-Binding Protein of 43 kDa (TDP-43). *J. Biol. Chem.* 287, 23079–23094. doi:10.1074/jbc.m111.328757

Boeynaems, S., Bogaert, E., Kovacs, D., Konijnenberg, A., Timmerman, E., Volkov, A., et al. (2017). Phase Separation of C9orf72 Dipeptide Repeats Perturbs Stress Granule Dynamics. *Mol. Cel.* 65, 1044–1055. doi:10.1016/j.molcel.2017.02.013

Bourgeois, B., Hutten, S., Gottschalk, B., Hofweber, M., Richter, G., Sternat, J., et al. (2020). Nonclassical Nuclear Localization Signals Mediate Nuclear Import of CIRBP. *Proc. Natl. Acad. Sci. USA.* 117, 8503–8514. doi:10.1073/pnas.1918944117

Bradford, M. M. (1976). A Rapid and Sensitive Method for the Quantitation of Microgram Quantities of Protein Utilizing the Principle of Protein-Dye Binding. *Anal. Biochem.* 72, 248–254. doi:10.1016/0003-2697(76)90527-3

Bullock, N., and Oltean, S. (2017). The many Faces of SRPK1. *J. Pathol.* 241, 437–440. doi:10.1002/path.4846

Cabrita, L. D., Gilis, D., Robertson, A. L., Dehouck, Y., Rooman, M., and Bottomley, S. P. (2007). Enhancing the Stability and Solubility of TEV Protease Using In Silico Design. *Protein Sci.* 16, 2360–2367. doi:10.1110/ps.072822507

Chong, P. A., Vernon, R. M., and Forman-Kay, J. D. (2018). RGG/RG Motif Regions in RNA Binding and Phase Separation. *J. Mol. Biol.* 430, 4650–4665. doi:10.1016/j.jmb.2018.06.014

Chook, Y., and Blobel, G. (2001). Karyopherins and Nuclear Import. *Curr. Opin. Struct. Biol.* 11, 703–715. doi:10.1016/s0959-440x(01)00264-0

De Leeuw, F., Zhang, T., Wauquier, C., Huez, G., Kruys, V., and Gueydan, C. (2007). The Cold-Inducible RNA-Binding Protein Migrates from the Nucleus to Cytoplasmic Stress Granules by a Methylation-dependent Mechanism and Acts as a Translational Repressor. *Exp. Cel Res.* 313, 4130–4144. doi:10.1016/j.yexcr.2007.09.017

Didiot, M.-C., Subramanian, M., Flatter, E., Mandel, J.-L., and Moine, H. (2009). Cells Lacking the Fragile X Mental Retardation Protein (FMRP) Have normal RISC Activity but Exhibit Altered Stress Granule Assembly. *MBoC* 20, 428–437. doi:10.1091/mbc.e08-07-0737

Ditlev, J. A., Case, L. B., and Rosen, M. K. (2018). Who's in and Who's Out-Compositional Control of Biomolecular Condensates. *J. Mol. Biol.* 430, 4666–4684. doi:10.1016/j.jmb.2018.08.003

Dolzhanskaya, N., Merz, G., Aletta, J. M., and Denman, R. B. (2006). Methylation Regulates the Intracellular Protein-Protein and Protein-RNA Interactions of FMRP. *J. Cel Sci.* 119, 1933–1946. doi:10.1242/jcs.02882

Dormann, D., Madl, T., Valori, C. F., Bentmann, E., Tahirovic, S., Abou-Ajram, C., et al. (2012). Arginine Methylation Next to the PY-NLS Modulates Transportin Binding and Nuclear Import of FUS. *EMBO J.* 31, 4258–4275. doi:10.1038/emboj.2012.261

Dormann, D., Rodde, R., Edbauer, D., Bentmann, E., Fischer, I., Hruscha, A., et al. (2010). ALS-associated Fused in Sarcoma (FUS) Mutations Disrupt Transportin-Mediated Nuclear Import. *EMBO J.* 29, 2841–2857. doi:10.1038/emboj.2010.143

Elbaum-Garfinkle, S., Kim, Y., Szczepaniak, K., Chen, C. C.-H., Eckmann, C. R., Myong, S., et al. (2015). The Disordered P Granule Protein LAF-1 Drives Phase Separation into Droplets with Tunable Viscosity and Dynamics. *Proc. Natl. Acad. Sci. USA.* 112, 7189–7194. doi:10.1073/pnas.1504822112

Feric, M., Vaidya, N., Harmon, T. S., Mitrea, D. M., Zhu, L., Richardson, T. M., et al. (2016). Coexisting Liquid Phases Underlie Nucleolar Subcompartments. *Cell* 165, 1686–1697. doi:10.1016/j.cell.2016.04.047

Frey, S., Rees, R., Schünemann, J., Ng, S. C., Fünfgeld, K., Huyton, T., et al. (2018). Surface Properties Determining Passage Rates of Proteins through Nuclear Pores. *Cell* 174, 202–217. doi:10.1016/j.cell.2018.05.045

Fronz, K., Güttinger, S., Burkert, K., Kühn, U., Stöhr, N., Schierhorn, A., et al. (2011). Arginine Methylation of the Nuclear Poly(a) Binding Protein Weakens the Interaction with its Nuclear Import Receptor, Transportin. *J. Biol. Chem.* 286, 32986–32994. doi:10.1074/jbc.m111.273912

Frottin, F., Schueder, F., Tiwary, S., Gupta, R., Körner, R., Schlichthaerle, T., et al. (2019). The Nucleolus Functions as a Phase-Separated Protein Quality Control Compartment. *Science* 365, 342–347. doi:10.1126/science.aaw9157

Gasteiger, E., Hoogland, C., Duvaud, S. e., Wilkins, M. R., and Appel, R. D. (2005, Protein Identification and Analysis Tools on the ExPASy Server *Protein Identification and Analysis Tools on the ExPASy Server in* the Proteomics Protocols Handbook (J. M. Walker, ed) pp. 571–607. Totowa: Humana Press. doi:10.1385/1-59259-890-0:571

Gelens, L., and Saurin, A. T. (2018). Exploring the Function of Dynamic Phosphorylation-Dephosphorylation Cycles. *Dev. Cel.* 44, 659–663. doi:10.1016/j.devcel.2018.03.002

Ghosh, G., and Adams, J. A. (2011). Phosphorylation Mechanism and Structure of Serine-Arginine Protein Kinases. *FEBS J.* 278, 587–597. doi:10.1111/j.1742-4658.2010.07992.x

Guccione, E., and Richard, S. (2019). The Regulation, Functions and Clinical Relevance of Arginine Methylation. *Nat. Rev. Mol. Cel Biol.* 20, 642–657. doi:10.1038/s41580-019-0155-x

Guo, L., Kim, H. J., Wang, H., Monaghan, J., Freyermuth, F., Sung, J. C., et al. (2018). Nuclear-Import Receptors Reverse Aberrant Phase Transitions of RNA-Binding Proteins with Prion-like Domains. *Cell* 173, 677–692. doi:10.1016/j.cell.2018.03.002

Hamey, J. J., Separovich, R. J., and Wilkins, M. R. (2018). MT-MAMS: Protein Methyltransferase Motif Analysis by Mass Spectrometry. *J. Proteome Res.* 17, 3485–3491. doi:10.1021/acs.jproteome.8b00396

Harreman, M. T., Kline, T. M., Milford, H. G., Harben, M. B., Hodel, A. E., and Corbett, A. H. (2004). Regulation of Nuclear Import by Phosphorylation Adjacent to Nuclear Localization Signals. *J. Biol. Chem.* 279, 20613–20621. doi:10.1074/jbc.m401720200

Harrison, A. F., and Shorter, J. (2017). RNA-binding Proteins with Prion-like Domains in Health and Disease. *Biochem. J.* 474, 1417–1438. doi:10.1042/bcj20160499

Hebert, M. D., Shpargel, K. B., Ospina, J. K., Tucker, K. E., and Matera, A. G. (2002). Coilin Methylation Regulates Nuclear Body Formation. *Dev. Cel.* 3, 329–337. doi:10.1016/s1534-5807(02)00222-8

Hofweber, M., and Dormann, D. (2019). Friend or foe-Post-translational Modifications as Regulators of Phase Separation and RNP Granule Dynamics. *J. Biol. Chem.* 294, 7137–7150. doi:10.1074/jbc.tm118.001189

Hofweber, M., Hutten, S., Bourgeois, B., Spreitzer, E., Niedner-Boblenz, A., Schifferer, M., et al. (2018). Phase Separation of FUS Is Suppressed by its Nuclear Import Receptor and Arginine Methylation. *Cell* 173, 706–719. doi:10.1016/j.cell.2018.03.004

Hong, E., Lim, Y., Lee, E., Oh, M., and Kwon, D. (2012). Tissue-specific and Age-dependent Expression of Protein Arginine Methyltransferases (PRMTs) in Male Rat Tissues. *Biogerontology* 13, 329–336. doi:10.1007/s10522-012-9379-2

Hornbeck, P. V., Zhang, B., Murray, B., Kornhauser, J. M., Latham, V., and Skrzypek, E. (2015). PhosphoSitePlus, 2014: Mutations, PTMs and Recalibrations. *Nucleic Acids Res.* 43, D512–D520. doi:10.1093/nar/gku1267

Huang, H., Arighi, C. N., Ross, K. E., Ren, J., Li, G., Chen, S.-C., et al. (2018). iPTMnet: an Integrated Resource for Protein post-translational Modification Network Discovery. *Nucleic Acids Res.* 46, D542–D550. doi:10.1093/nar/gkx1104

Hutten, S., and Dormann, D. (2020). A Quantitative Assay to Measure Stress Granule Association of Proteins and Peptides in Semi-permeabilized Human Cells. *Bio-Protocol* 10. doi:10.21769/bioprotoc.3846

Hyman, A. A., Weber, C. A., and Jülicher, F. (2014). Liquid-liquid Phase Separation in Biology. *Annu. Rev. Cel Dev. Biol.* 30, 39–58. doi:10.1146/annurev-cellbio-100913-013325

Kitamura, R., Sekimoto, T., Ito, S., Harada, S., Yamagata, H., Masai, H., et al. (2006). Nuclear Import of Epstein-Barr Virus Nuclear Antigen 1 Mediated by NPI-1 (Importin α5) Is up- and Down-Regulated by Phosphorylation of the Nuclear Localization Signal for Which Lys379 and Arg380 Are Essential. *J. Virol.* 80, 1979–1991. doi:10.1128/jvi.80.4.1979-1991.2006

Kwiatkowski, T. J., Jr., Bosco, D. A., Leclerc, A. L., Tamrazian, E., Vanderburg, C. R., Russ, C., et al. (2009). Mutations in the FUS/TLS Gene on Chromosome 16 Cause Familial Amyotrophic Lateral Sclerosis. *Science* 323, 1205–1208. doi:10.1126/science.1166066

Lai, M.-C., Lin, R.-I., Huang, S.-Y., Tsai, C.-W., and Tarn, W.-Y. (2000). A Human Importin-β Family Protein, Transportin-SR2, Interacts with the Phosphorylated RS Domain of SR Proteins. *J. Biol. Chem.* 275, 7950–7957. doi:10.1074/jbc.275.11.7950

Lee, B. J., Cansizoglu, A. E., Süel, K. E., Louis, T. H., Zhang, Z., and Chook, Y. M. (2006). Rules for Nuclear Localization Sequence Recognition by Karyopherinβ2. *Cell* 126, 543–558. doi:10.1016/j.cell.2006.05.049

Lee, H. N., Ahn, S.-M., and Jang, H. H. (2015). Cold-inducible RNA-Binding Protein, CIRP, Inhibits DNA Damage-Induced Apoptosis by Regulating P53. *Biochem. Biophysical Res. Commun.* 464, 916–921. doi:10.1016/j.bbrc.2015.07.066

Lee, W., Tonelli, M., and Markley, J. L. (2015). NMRFAM-SPARKY: Enhanced Software for Biomolecular NMR Spectroscopy. *Bioinformatics* 31, 1325–1327. doi:10.1093/bioinformatics/btu830

Lee, Y.-J., Hsieh, W.-Y., Chen, L.-Y., and Li, C. (2012). Protein Arginine Methylation of SERBP1 by Protein Arginine Methyltransferase 1 Affects Cytoplasmic/nuclear Distribution. *J. Cel. Biochem.* 113, 2721–2728. doi:10.1002/jcb.24151

Li, P., Banjade, S., Cheng, H.-C., Kim, S., Chen, B., Guo, L., et al. (2012). Phase Transitions in the Assembly of Multivalent Signalling Proteins. *Nature* 483, 336–340. doi:10.1038/nature10879

Li, Y. R., King, O. D., Shorter, J., and Gitler, A. D. (2013). Stress Granules as Crucibles of ALS Pathogenesis. *J. Cel Biol.* 201, 361–372. doi:10.1083/jcb.201302044

Lujan, D. A., Ochoa, J. L., and Hartley, R. S. (2018). *Cold-inducible RNA Binding Protein in Cancer and Inflammation*, 9. Wiley Interdiscip Rev RNA. doi:10.1002/wrna.1462

Lukasiewicz, R., Nolen, B., Adams, J. A., and Ghosh, G. (2007). The RGG Domain of Npl3p Recruits Sky1p through Docking Interactions. *J. Mol. Biol.* 367, 249–261. doi:10.1016/j.jmb.2006.12.031

Mahboubi, H., Barisé, R., and Stochaj, U. (2015). 5′-AMP-activated Protein Kinase Alpha Regulates Stress Granule Biogenesis. *Biochim. Biophys. Acta (Bba) - Mol. Cel Res.* 1853, 1725–1737. doi:10.1016/j.bbamcr.2015.03.015

Mandell, D. J., Chorny, I., Groban, E. S., Wong, S. E., Levine, E., Rapp, C. S., et al. (2007). Strengths of Hydrogen Bonds Involving Phosphorylated Amino Acid Side Chains. *J. Am. Chem. Soc.* 129, 820–827. doi:10.1021/ja063019w

Martin, E. W., and Holehouse, A. S. (2020). Intrinsically Disordered Protein Regions and Phase Separation: Sequence Determinants of Assembly or Lack Thereof. *Emerg. Top. Life Sci.* 4, 307–329. doi:10.1042/etls20190164

Minguez, P., Letunic, I., Parca, L., and Bork, P. (2013). PTMcode: a Database of Known and Predicted Functional Associations between post-translational Modifications in Proteins. *Nucleic Acids Res.* 41, D306–D311. doi:10.1093/nar/gks1230

Molliex, A., Temirov, J., Lee, J., Coughlin, M., Kanagaraj, A. P., Kim, H. J., et al. (2015). Phase Separation by Low Complexity Domains Promotes Stress Granule Assembly and Drives Pathological Fibrillization. *Cell* 163, 123–133. doi:10.1016/j.cell.2015.09.015

Monahan, Z., Ryan, V. H., Janke, A. M., Burke, K. A., Rhoads, S. N., Zerze, G. H., et al. (2017). Phosphorylation of the FUS Low-complexity Domain Disrupts Phase Separation, Aggregation, and Toxicity. *EMBO J.* 36, 2951–2967. doi:10.15252/embj.201696394

Nardozzi, J. D., Lott, K., and Cingolani, G. (2010). Phosphorylation Meets Nuclear Import: a Review. *Cell Commun Signal* 8, 32. doi:10.1186/1478-811x-8-32

Nonaka, T., Suzuki, G., Tanaka, Y., Kametani, F., Hirai, S., Okado, H., et al. (2016). Phosphorylation of TAR DNA-Binding Protein of 43 kDa (TDP-43) by Truncated Casein Kinase 1δ Triggers Mislocalization and Accumulation of TDP-43. *J. Biol. Chem.* 291, 5473–5483. doi:10.1074/jbc.m115.695379

Nott, T. J., Petsalaki, E., Farber, P., Jervis, D., Fussner, E., Plochowietz, A., et al. (2015). Phase Transition of a Disordered Nuage Protein Generates Environmentally Responsive Membraneless Organelles. *Mol. Cel.* 57, 936–947. doi:10.1016/j.molcel.2015.01.013

Ode, Y., Aziz, M., Jin, H., Arif, A., Nicastro, J. G., and Wang, P. (2019). Cold-inducible RNA-Binding Protein Induces Neutrophil Extracellular Traps in the Lungs during Sepsis. *Sci. Rep.* 9, 6252. doi:10.1038/s41598-019-42762-1

Ode, Y., Aziz, M., and Wang, P. (2018). CIRP Increases ICAM-1 + Phenotype of Neutrophils Exhibiting Elevated iNOS and NETs in Sepsis. *J. Leukoc. Biol.* 103, 693–707. doi:10.1002/jlb.3a0817-327rr

Ohn, T., Kedersha, N., Hickman, T., Tisdale, S., and Anderson, P. (2008). A Functional RNAi Screen Links O-GlcNAc Modification of Ribosomal Proteins to Stress Granule and Processing Body Assembly. *Nat. Cel Biol.* 10, 1224–1231. doi:10.1038/ncb1783

Ortega-Pérez, I., Cano, E., Were, F., Villar, M., Vázquez, J., and Redondo, J. M. (2005). c-Jun N-Terminal Kinase (JNK) Positively Regulates NFATc2 Transactivation through Phosphorylation within the N-Terminal Regulatory Domain. *J. Biol. Chem.* 280, 20867–20878. doi:10.1074/jbc.m501898200

Pan, F., Zarate, J., Choudhury, A., Rupprecht, R., and Bradley, T. M. (2004). Osmotic Stress of salmon Stimulates Upregulation of a Cold Inducible RNA Binding Protein (CIRP) Similar to that of Mammals and Amphibians. *Biochimie* 86, 451–461. doi:10.1016/j.biochi.2004.06.006

Patel, A., Lee, H. O., Jawerth, L., Maharana, S., Jahnel, M., Hein, M. Y., et al. (2015). A Liquid-To-Solid Phase Transition of the ALS Protein FUS Accelerated by Disease Mutation. *Cell* 162, 1066–1077. doi:10.1016/j.cell.2015.07.047

Patel, M., Sachidanandan, M., and Adnan, M. (2019). Serine Arginine Protein Kinase 1 (SRPK1): a Moonlighting Protein with Theranostic Ability in Cancer Prevention. *Mol. Biol. Rep.* 46, 1487–1497. doi:10.1007/s11033-018-4545-5

Qamar, S., Wang, G., Randle, S. J., Ruggeri, F. S., Varela, J. A., Lin, J. Q., et al. (2018). FUS Phase Separation Is Modulated by a Molecular Chaperone and Methylation of Arginine Cation-π Interactions. *Cell* 173, 720–734. doi:10.1016/j.cell.2018.03.056

Ramaswami, M., Taylor, J. P., and Parker, R. (2013). Altered Ribostasis: RNA-Protein Granules in Degenerative Disorders. *Cell* 154, 727–736. doi:10.1016/j.cell.2013.07.038

Reineke, L. C., Cheema, S. A., Dubrulle, J., and Neilson, J. R. (2018). Chronic Starvation Induces Noncanonical Pro-death Stress Granules. *J. Cel Sci.* 131. doi:10.1242/jcs.220244

Reineke, L. C., Tsai, W. C., Jain, A., Kaelber, J. T., Jung, S. Y., and Lloyd, R. E. (2017). Casein Kinase 2 Is Linked to Stress Granule Dynamics through Phosphorylation of the Stress Granule Nucleating Protein G3BP1. *Mol. Cel Biol.* 37. doi:10.1128/MCB.00596-16

Rhoads, S. N., Monahan, Z. T., Yee, D. S., and Shewmaker, F. P. (2018). The Role of Post-Translational Modifications on Prion-like Aggregation and Liquid-phase Separation of FUS. *Int. J. Mol. Sci.* 19. doi:10.3390/ijms19030886

Ryan, V. H., Dignon, G. L., Zerze, G. H., Chabata, C. V., Silva, R., Conicella, A. E., et al. (2018). Mechanistic View of hnRNPA2 Low-Complexity Domain Structure, Interactions, and Phase Separation Altered by Mutation and Arginine Methylation. *Mol. Cel.* 69, 465–479. doi:10.1016/j.molcel.2017.12.022

Saito, M., Hess, D., Eglinger, J., Fritsch, A. W., Kreysing, M., Weinert, B. T., et al. (2019). Acetylation of Intrinsically Disordered Regions Regulates Phase Separation. *Nat. Chem. Biol.* 15, 51–61. doi:10.1038/s41589-018-0180-7

Sakurai, T., Itoh, K., Higashitsuji, H., Nonoguchi, K., Liu, Y., Watanabe, H., et al. (2006). Cirp Protects against Tumor Necrosis Factor-α-Induced Apoptosis via Activation of Extracellular Signal-Regulated Kinase. *Biochim. Biophys. Acta (Bba) - Mol. Cel Res.* 1763, 290–295. doi:10.1016/j.bbamcr.2006.02.007

Savastano, A., Ibáñez de Opakua, A., Rankovic, M., and Zweckstetter, M. (2020). Nucleocapsid Protein of SARS-CoV-2 Phase Separates into RNA-Rich Polymerase-Containing Condensates. *Nat. Commun.* 11, 6041. doi:10.1038/s41467-020-19843-1

Sfakianos, A. P., Mellor, L. E., Pang, Y. F., Kritsiligkou, P., Needs, H., Abou-Hamdan, H., et al. (2018). The mTOR-S6 Kinase Pathway Promotes Stress Granule Assembly. *Cell Death Differ.* 25, 1766–1780. doi:10.1038/s41418-018-0076-9

Shattuck, J. E., Paul, K. R., Cascarina, S. M., and Ross, E. D. (2019). The Prion-like Protein Kinase Sky1 Is Required for Efficient Stress Granule Disassembly. *Nat. Commun.* 10, 3614. doi:10.1038/s41467-019-11550-w

Shin, Y., and Brangwynne, C. P. (2017). Liquid Phase Condensation in Cell Physiology and Disease. *Science* 357. doi:10.1126/science.aaf4382

Simandi, Z., Pajer, K., Karolyi, K., Sieler, T., Jiang, L.-L., Kolostyak, Z., et al. (2018). Arginine Methyltransferase PRMT8 Provides Cellular Stress Tolerance in Aging Motoneurons. *J. Neurosci.* 38, 7683–7700. doi:10.1523/jneurosci.3389-17.2018

Skinner, S. P., Fogh, R. H., Boucher, W., Ragan, T. J., Mureddu, L. G., and Vuister, G. W. (2016). CcpNmr AnalysisAssign: a Flexible Platform for Integrated NMR Analysis. *J. Biomol. NMR* 66, 111–124. doi:10.1007/s10858-016-0060-y

Smith, D.-L., Erce, M. A., Lai, Y.-W., Tomasetig, F., Hart-Smith, G., Hamey, J. J., et al. (2020). Crosstalk of Phosphorylation and Arginine Methylation in Disordered SRGG Repeats of *Saccharomyces cerevisiae* Fibrillarin and its Association with Nucleolar Localization. *J. Mol. Biol.* 432, 448–466. doi:10.1016/j.jmb.2019.11.006

Solomon, S., Xu, Y., Wang, B., David, M. D., Schubert, P., Kennedy, D., et al. (2007). Distinct Structural Features ofCaprin-1 Mediate its Interaction with G3BP-1 and its Induction of Phosphorylation of Eukaryotic Translation InitiationFactor 2α, Entry to Cytoplasmic Stress Granules, and Selective Interaction with a Subset of mRNAs. *Mol. Cel Biol.* 27, 2324–2342. doi:10.1128/mcb.02300-06

Soniat, M., and Chook, Y. M. (2015). Nuclear Localization Signals for Four Distinct Karyopherin-β Nuclear Import Systems. *Biochem. J.* 468, 353–362. doi:10.1042/bj20150368

Souki, S. K., and Sandri-Goldin, R. M. (2009). Arginine Methylation of the ICP27 RGG Box Regulates the Functional Interactions of ICP27 with SRPK1 and Aly/REF during Herpes Simplex Virus 1 Infection. *J. Virol.* 83, 8970–8975. doi:10.1128/jvi.00801-09

Tang, X., Keenan, M. M., Wu, J., Lin, C.-A., Dubois, L., Thompson, J. W., et al. (2015). Comprehensive Profiling of Amino Acid Response Uncovers Unique Methionine-Deprived Response Dependent on Intact Creatine Biosynthesis. *Plos Genet.* 11, e1005158. doi:10.1371/journal.pgen.1005158

Tanikawa, C., Ueda, K., Suzuki, A., Iida, A., Nakamura, R., Atsuta, N., et al. (2018). Citrullination of RGG Motifs in FET Proteins by PAD4 Regulates Protein Aggregation and ALS Susceptibility. *Cel Rep.* 22, 1473–1483. doi:10.1016/j.celrep.2018.01.031

Thandapani, P., O'Connor, T. R., Bailey, T. L., and Richard, S. (2013). Defining the RGG/RG Motif. *Mol. Cel.* 50, 613–623. doi:10.1016/j.molcel.2013.05.021

Theillet, F.-X., Rose, H. M., Liokatis, S., Binolfi, A., Thongwichian, R., Stuiver, M., et al. (2013). Site-specific NMR Mapping and Time-Resolved Monitoring of Serine and Threonine Phosphorylation in Reconstituted Kinase Reactions and Mammalian Cell Extracts. *Nat. Protoc.* 8, 1416–1432. doi:10.1038/nprot.2013.083

Theillet, F.-X., Smet-Nocca, C., Liokatis, S., Thongwichian, R., Kosten, J., Yoon, M.-K., et al. (2012). Cell Signaling, post-translational Protein Modifications and NMR Spectroscopy. *J. Biomol. NMR* 54, 217–236. doi:10.1007/s10858-012-9674-x

Tourrière, H., Chebli, K., Zekri, L., Courselaud, B., Blanchard, J. M., Bertrand, E., et al. (2003). The RasGAP-Associated Endoribonuclease G3BP Assembles Stress Granules. *J. Cel Biol.* 160, 823–831. doi:10.1083/jcb.200212128

Toyota, C. G., Davis, M. D., Cosman, A. M., and Hebert, M. D. (2010). Coilin Phosphorylation Mediates Interaction with SMN and SmB′. *Chromosoma* 119, 205–215. doi:10.1007/s00412-009-0249-x

Tsai, W.-C., Gayatri, S., Reineke, L. C., Sbardella, G., Bedford, M. T., and Lloyd, R. E. (2016). Arginine Demethylation of G3BP1 Promotes Stress Granule Assembly. *J. Biol. Chem.* 291, 22671–22685. doi:10.1074/jbc.m116.739573

Tsang, B., Arsenault, J., Vernon, R. M., Lin, H., Sonenberg, N., Wang, L.-Y., et al. (2019). Phosphoregulated FMRP Phase Separation Models Activity-dependent Translation through Bidirectional Control of mRNA Granule Formation. *Proc. Natl. Acad. Sci. USA.* 116, 4218–4227. doi:10.1073/pnas.1814385116

Tsang, B., Pritišanac, I., Scherer, S. W., Moses, A. M., and Forman-Kay, J. D. (2020). Phase Separation as a Missing Mechanism for Interpretation of Disease Mutations. *Cell* 183, 1742–1756. doi:10.1016/j.cell.2020.11.050

Vance, C., Rogelj, B., Hortobagyi, T., De Vos, K. J., Nishimura, A. L., Sreedharan, J., et al. (2009). Mutations in FUS, an RNA Processing Protein, Cause Familial Amyotrophic Lateral Sclerosis Type 6. *Science* 323, 1208–1211. doi:10.1126/science.1165942

Vranken, W. F., Boucher, W., Stevens, T. J., Fogh, R. H., Pajon, A., Llinas, M., et al. (2005). The CCPN Data Model for NMR Spectroscopy: Development of a Software Pipeline. *Proteins* 59, 687–696. doi:10.1002/prot.20449

Wang, J., Choi, J.-M., Holehouse, A. S., Lee, H. O., Zhang, X., Jahnel, M., et al. (2018). A Molecular Grammar Governing the Driving Forces for Phase Separation of Prion-like RNA Binding Proteins. *Cell* 174, 688–699. doi:10.1016/j.cell.2018.06.006

Wippich, F., Bodenmiller, B., Trajkovska, M. G., Wanka, S., Aebersold, R., and Pelkmans, L. (2013). Dual Specificity Kinase DYRK3 Couples Stress Granule Condensation/dissolution to mTORC1 Signaling. *Cell* 152, 791–805. doi:10.1016/j.cell.2013.01.033

Yang, P., Mathieu, C., Kolaitis, R.-M., Zhang, P., Messing, J., Yurtsever, U., et al. (2020). G3BP1 Is a Tunable Switch that Triggers Phase Separation to Assemble Stress Granules. *Cell* 181, 325–345. doi:10.1016/j.cell.2020.03.046

Yang, W.-H., Yu, J. H., Gulick, T., Bloch, K. D., and Bloch, D. B. (2006). RNA-associated Protein 55 (RAP55) Localizes to mRNA Processing Bodies and Stress Granules. *RNA* 12, 547–554. doi:10.1261/rna.2302706

Yoshizawa, T., Ali, R., Jiou, J., Fung, H. Y. J., Burke, K. A., Kim, S. J., et al. (2018). Nuclear Import Receptor Inhibits Phase Separation of FUS through Binding to Multiple Sites. *Cell* 173, 693–705. doi:10.1016/j.cell.2018.03.003

Yu, K., Zhang, Q., Liu, Z., Zhao, Q., Zhang, X., Wang, Y., et al. (2019). qPhos: a Database of Protein Phosphorylation Dynamics in Humans. *Nucleic Acids Res.* 47, D451–D458. doi:10.1093/nar/gky1052

Yun, C. Y., and Fu, X.-D. (2000). Conserved SR Protein Kinase Functions in Nuclear Import and its Action Is Counteracted by Arginine Methylation in *Saccharomyces cerevisiae*. *J. Cel Biol.* 150, 707–718. doi:10.1083/jcb.150.4.707

Zeng, Y., Kulkarni, P., Inoue, T., and Getzenberg, R. H. (2009). Down-regulating Cold Shock Protein Genes Impairs Cancer Cell Survival and Enhances Chemosensitivity. *J. Cel. Biochem.* 107, 179–188. doi:10.1002/jcb.22114

Zhang, F., Kerbl-Knapp, J., Rodriguez Colman, M. J., Meinitzer, A., Macher, T., Vujić, N., et al. (2021). Global Analysis of Protein Arginine Methylation. *Cel Rep. Methods* 1, 100016. doi:10.1016/j.crmeth.2021.100016

Zhang, X., and Cheng, X. (2003). Structure of the Predominant Protein Arginine Methyltransferase PRMT1 and Analysis of its Binding to Substrate Peptides. *Structure* 11, 509–520. doi:10.1016/s0969-2126(03)00071-6

Zhang, Z. C., and Chook, Y. M. (2012). Structural and Energetic Basis of ALS-Causing Mutations in the Atypical Proline-Tyrosine Nuclear Localization Signal of the Fused in Sarcoma Protein (FUS). *Proc. Natl. Acad. Sci. USA.* 109, 12017–12021. doi:10.1073/pnas.1207247109

Zhou, M., Yang, W.-L., Ji, Y., Qiang, X., and Wang, P. (2014). Cold-inducible RNA-Binding Protein Mediates Neuroinflammation in Cerebral Ischemia. *Biochim. Biophys. Acta (Bba) - Gen. Subjects* 1840, 2253–2261. doi:10.1016/j.bbagen.2014.02.027

Conflict of Interest: The authors declare that the research was conducted in the absence of any commercial or financial relationships that could be construed as a potential conflict of interest.

Publisher's Note: All claims expressed in this article are solely those of the authors and do not necessarily represent those of their affiliated organizations, or those of the publisher, the editors and the reviewers. Any product that may be evaluated in this article, or claim that may be made by its manufacturer, is not guaranteed or endorsed by the publisher.

Advantages of publishing in Frontiers

OPEN ACCESS
Articles are free to read for greatest visibility and readership

FAST PUBLICATION
Around 90 days from submission to decision

HIGH QUALITY PEER-REVIEW
Rigorous, collaborative, and constructive peer-review

TRANSPARENT PEER-REVIEW
Editors and reviewers acknowledged by name on published articles

Frontiers
Avenue du Tribunal-Fédéral 34
1005 Lausanne | Switzerland

Visit us: www.frontiersin.org
Contact us: frontiersin.org/about/contact

REPRODUCIBILITY OF RESEARCH
Support open data and methods to enhance research reproducibility

DIGITAL PUBLISHING
Articles designed for optimal readership across devices

FOLLOW US
@frontiersin

IMPACT METRICS
Advanced article metrics track visibility across digital media

EXTENSIVE PROMOTION
Marketing and promotion of impactful research

LOOP RESEARCH NETWORK
Our network increases your article's readership